CRANFIELD UNIVERSITY

FAYE ANDREWS

DESIGN OF A COTS MST DISTRIBUTED SENSOR SUITE SYSTEM FOR PLANETARY SURFACE EXPLORATION.

SCHOOL OF ENGINEERING

EngD. THESIS

CRANFIELD UNIVERSITY

SCHOOL OF ENGINEERING

EngD. THESIS

Academic Year 2005

FAYE ANDREWS

Design of a COTS MST distributed Sensor Suite System for planetary surface exploration.

Supervisors: Dr. Stephen Hobbs
Dr. Ian Honstvet
Dr. Robin Lane

This thesis is submitted in partial fulfilment of the requirements for the degree of Engineering Doctorate.

ABSTRACT

The aim of this project is

To bring together current commercially available technology and relevant Microsystems Technology (MST) into a small, standardised spacecraft primary systems architecture, multiple units of which can demonstrate collaboration…

Distributed "lab-on-a-chip" sensor networks are a possible option for the surface exploration of both Earth and Mars, and as such have been chosen as a model small spacecraft architecture. This project presents a systems approach to the design of a collection of collaborative MST sensor suites for use in a variety of environments.

Based on a set of derived objectives, the main features of the study are:

- What are the fundamental limits to miniaturisation?
- What are the hardware issues raised using both standard and MST components?
- What is the optimum deployment pattern of the network to locate various shaped targets?
- What are the strategic and economic challenges of MST and the development of a sensor suite network?

In general, there are few fundamental physical laws that limit the size of the sensor system. Limits tend to be driven by other factors including user requirements and the external environment.

A simple breadboard model of the sensor suite consisting current COTS MST components raised practical issues such as circuit layouts, power requirements and packaging.

A grid illustrating features of the Martian surface was created. Various patterns of target and sensor clusters were simulated. Overall, for larger target areas, clusters of sensors produced the best "hit rate".

The overall system utilises both wired and wireless communications methods. The I2C protocol has been investigated for intersuite communications.

A link has been made between bacteria pools found on Glaciers (Cryoconites) and the possible conditions for life at the Polar Ice Caps of Mars. The investigation of Arctic Cryoconites has been selected as a representative case study that will incorporate all aspects of the project and demonstrate the system design. A comprehensive mission baseline based on this application has been produced, however the system has been designed to enable its use in a variety of situations whilst requiring only minimal modification to the overall design.

Acknowledgements

I wish to thank all the people who have supported and encouraged me throughout this project and my time at Cranfield.

Particular thanks goes to Dr Steve Hobbs and the staff at Cranfield Space Research Centre for their continuing guidance, understanding and valued friendship. I would also like to thank those at Astrium who have helped me during this project, especially Ian Honstvet, Martyn Snelling Arnaud Lecuyot and Steve Eckersley, and the staff at the School of Management, in particular Robin Lane.

Many people have touched my life during my research period. I'd like to offer my heartfelt thanks to the friends I have made, especially my fellow Research students with whom I have shared many memorable experiences, both good and not so good. In particular, huge thanks goes to Angie for always being there when I needed a walk and a friendly ear, to Patrick for being a Paint master, a great friend and for brightening my life and Jenny, my writing-up buddy.

I would also like to thank Red 1 (Pete, Peter, Linda, Sam and Mayan), my Learning team during my MBA year. Without them I never would have known what a balanced score card is or how badly a group of project managers could manage a simulated warehouse exercise!

Finally and most importantly, I would like to thank my family – in particular my Mum and Dad. Their love and encouragement have helped me realise my dreams and I will always be thankful for that.

I dedicate this Thesis to the memory of my Father, James Andrews. I hope I make him proud.

TABLE OF CONTENTS

TABLE OF FIGURES

Chapter 8

Chapter 9

TABLE OF TABLES

Definition of Acronyms

MST - Microsystems Technology
MNT - Micro - NanoTechnology
MEMS - MicroElectroMechanical Systems
ESA - European Space Agency
NASA -National Aeronautics and Space Administration
NASDA - National Space Development Agency (Japan)
PESTLE - Political, Economic, Social, Technological, Legal and Environmental
R & D - Research and Development
EADS - European Aeronautic Defence and Space company
KT - Knowledge Transfer
DTI - Department of Trade and Industry
COTS - Commercial of the Shelf
I2C - Inter Integrated Circuit
UAV - Unmanned Aerial Vehicle
LED - Light Emitting Diode
VBA - Visual Basic Applications
JPL - Jet Propulsion Laboratory
ADC - Analogue to Digital Converter
RTD - Resistance Temperature Detector
CMOS - Complementary Metal-Oxide Semiconductor
SDA - Serial Data Line
SCL - Serial Clock Line
EEPROM - Electrically Erasable Programmable Read Only Memory

1. Introduction

1.1 Introduction

This chapter introduces the aims and objectives of this project.

Six objectives are identified and the approach to achieving these objectives is presented in section 1.4 Section 1.5 includes an overview of the rationale behind this research project. Finally the structure of the Thesis, which follows the order of the objectives, is detailed in section 1.6.

1.2 Project Aim

The overall aim of this project is:

To bring together current commercially available technology and relevant Microsystems Technology (MST) into a small, standardized, spacecraft "primary systems" architecture, multiple units of which can demonstrate collaboration. This is to be studied by means of a hardware prototype and simulated deployment strategies that address survivability and reliability issues in a planetary or Space environment.

There were several small spacecraft primary systems architectures that could have been investigated as part of this project, including Nanosatellites and Micro-Rovers. The focus of this investigation, however, is a collaborative network of planetary surface sensing suites.

Standardisation will be demonstrated by designing a sensor suite system that has a generic nature. This means that one design can be used for multiple applications. The specified commercially available technology is taken to refer to Commercial-Off-The-Shelf (COTS) components, which also leads to a low cost system compared to the use of bespoke components.

Microsystems Technology is a relatively new technology which enables the miniaturisation of systems through micro-scale components. Its potential for Space applications has been recognised, however it has yet to be adopted as a proven Space-qualified technology. This technology will form a key part of the sensor suite system investigated here.

From this overall aim, six distinct project objectives were derived.

1.3 Project Objectives

The aim as stated above can be divided into several different aspects that address various issues related to a deployed sensor suite system. As such, each derived objective relates to one key idea. This can be illustrated as a series of related yet parallel strands that are linked together through a final application study.

The project objectives can be stated as:

1. To investigate the fundamental physical limits which determine the minimum size of a spacecraft and compare it to nature and existing spacecraft.

2. To investigate the Space Industry and its related strategic issues, identify possible future markets and scenarios for MST and the proposed sensor devices and investigate the importance of innovation and technology transfer in the adoption of MST for Space.

3. To design and build several basic sensor suites using current technology, including commercially available MST, and demonstrate collaborative working between them.

4. To investigate future full integration to "lab-on-a-chip", resulting in the eventual adaptation and miniaturisation of the suites to "matchbox" size.

5. To create a computer simulated environment, e.g. Mars, and simulate deployment and search strategies for a range of scenarios to establish deployment patterns, communications architectures and the impact of performance parameters, such as reliability, on the overall system and the individual miniaturised suites.

6. To bring together the theoretical limits, the practical hardware design and simulation results from the previous steps to refine the design and link it to the technological, industrial and future "bigger picture".

Each objective represents a different aspect of the project. Objectives 1 and 2 establish the feasibility of the proposed miniaturised system from a physical and industrial perspective. Objectives 3 and 4 focus on the hardware and technological issues to be addressed, whereas objective 5 relates to other system design issues. The final objective is to create a synthesis between all the aspects of the project.

1.4 Approach for Achieving Objectives

As described in section 1.3, Figure 1-1 shows a flowchart that illustrates the relationships between the above objectives.

The objectives present the need for an overall systems approach to this project, since they imply the investigation of not only the design of a sensor suite node, but also its deployment, communications architecture and industrial potential. Therefore, a number of strategies have been employed to achieve these objectives.

Objective 1, or the "Fundamentals" objective is achieved by reviewing and correlating previously accepted examples of the fundamental physical principles that define the primary and secondary functions of any spacecraft system. These relationships are then

used to determine the minimum size of a sensor system from a simple example. Finally, this example is compared to other existing spacecraft architectures and conclusions as to the nature of the fundamental physical limits to miniaturisation are made.

Objective 2 investigates the overall strategy of the Space industry using recognised managements tools. This sets the project in an industrial context. The sensor suite concept is also investigated in terms of the adoption of the technology within the industry and the economic issues surrounding the integration of the suites in-house or by an external contractor.

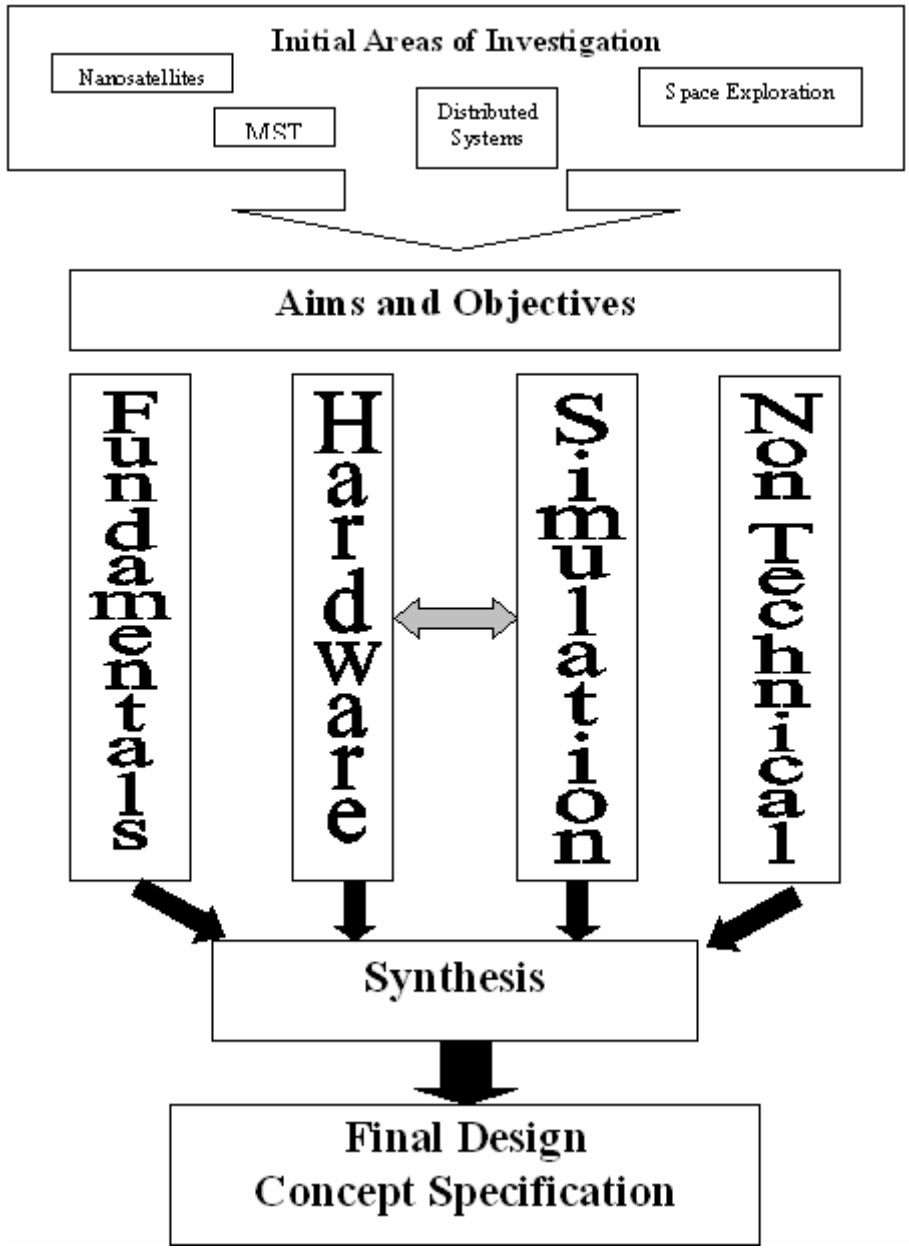

Figure 1-1 Flow chart illustration of project objectives

Objective 3 is the "Hardware" objective. To achieve this, standard and MST components are to be procured and a breadboard model of a basic sensor suite is to be produced. The appropriate processing hardware will also be investigated. The collaboration aspect will be achieved through the use of the Philips I2C bus protocol.

Objective 4 can be divided into two separate bodies of work. The first investigates future full integration and miniaturisation of the suite. This is achieved through a paper study of MST and its associated challenges. The second aspect of this objective concerns the adaptation of the design to a "matchbox". Appropriate sensors and components will be chosen based on a set of criteria, and a circuit diagram will be produced. Finally the packaging options available that allow the required reduced dimensions of the suite are examined.

For the satisfaction of objective 5, a simple Visual Basic computer simulation will be produced. This program will run a series of possible sensor suite deployment scenarios to establish the preferred pattern, based on the ability to locate a given target in an environment that represents the hazards of the Martian surface.

A representative application is proposed that will combine the findings from the previous objectives, and a refined system design is presented that will satisfy the final objective. This scenario is based on a realistic environmental sensing application in the Arctic, which is analogous to a potential planetary surface exploration mission. Although a similar system has not yet been proposed for this application, data from other traditional sensing experiments is used to influence the design of the sensor suite system. It is then compared to the equivalent application on Mars, which leads to conclusions over the generic nature of the proposed system.

1.5 Research Rationale

Microsystems technology (MST) is a relatively new technology that has been identified by many industries as having considerable future potential. MST components are designed to have the same capability as standard components but at greatly reduced dimensions and power consumption. These components are being researched and designed by a number of different companies and institutions around the world, and public bodies such as the European Union are heavily funding their development. It has been recognised that this technology will have significant benefits in areas such as biomedical and military applications, and several prototype model sensors are beginning to be developed. However, the considerable potential of this technology has yet to be fully demonstrated or exploited.

As with most industries, cost has become one of the main drivers for the global Space industry. As a result, the industry is beginning to move towards smaller spacecraft and systems, which reduce production costs and, due to the mass reduction, reduce launch costs. The low mass and low power consumption of MST components makes them ideal for use in Space where these two factors are critical. EADS Astrium, as the sponsors of this project, amongst others, have identified this as a key technology for the future and has started to investigate its potential. EADS Astrium is a member of several partnerships involved in the promotion and development of MST in the UK and

Europe. This EngD project is the second Doctoral project where EADS Astrium has collaborated with Cranfield University – which itself has many interests in MST and its own Nanotechnology Department – on the investigation and integration of this new technology and future Space applications. This low cost drive has also increased the use of readily available, mass produced COTS components in an attempt to reduce production costs and enable rapid prototyping.

The initial project proposed by the sponsors was for a generic system that could "go anywhere, do anything". The initial constraints were that it used off-the-shelf MST components that were commercially available and low cost. The system would demonstrate a Space-related application but should be able to adapted for other purposes. In order to define a realistic scope for the project, both from a time perspective and that of providing representative systems requirements, a variety of missions and applications were discussed.

The initial proposal was to investigate Nanosatellites, however from the nature of the applications and their related payload sensors suggested by the project supervisors, it became evident that an *in-situ* sensor network would be more suitable than a system where readings were taken from orbit. Hence, it was determined that the focus of this EngD project would be Distributed Sensor Networks and their deployment issues. The investigation into the use of MST for the "primary subsystems" architecture and payload sensors for a simple "planet" based system will address many of the issues raised by this technology as well as by the system itself. Investigations into this type of architecture can be the basis for many other examples of MST distributed systems.

In order to fulfil the original research requirement of the Doctoral project, the application chosen had to contain different elements to previously published work, but still be relevant to Space and follow suggested departmental interests. Hence, the application chosen is that of monitoring Cryoconites on Arctic Glaciers. Sensor networks have not yet been used for this purpose, and it has been proposed that similar phenomena occur in the Martian Polar regions and other planetary environments. Another requirement specific to the EngD is that of the "non-technical" aspect based around the Management studies carried out as part of the programme. This is fulfilled through the analysis of the current Space Industry and of the strategic implications of the adoption of MST for Space.

1.6 Thesis Overview

The structure of the Thesis approximately follows the order of the list of project objectives.

Chapter 2 presents a selection of relevant background subjects principally associated with Distributed Sensor Networks.

Chapter 3 relates to the "Fundamentals" objective and discusses the minimum size of a system related to it fundamental physical principles.

Chapter 4 discusses the strategic issues of the Space industry.

Chapter 5 details the hardware design and lessons learnt from investigations into sensor components, I2C bus protocols and PIC microcontrollers.

Chapter 6 presents the study of Microsystems Technology in relation to potential sensor suite components.

Chapter 7 contains the program development and results from the deployment pattern simulations.

Chapter 8 contains the final sensor suite design in terms of selected sensors and components. It also discusses the different Multichip Module (MCM) packing options for the suite, with particular attention on 3D methods. Various potential space-related applications are also discussed.

The final chapter (9) draws together the conclusions from the previous chapters and applies them to the research into the monitoring of Cryoconites in the Arctic. This is an environmental sensing application, and as well as providing the basis for a full systems baseline design, it can be used as an analogy to Martian surface sensing.

Overall conclusions and recommendations for further work are then presented.

2 Background and Review of Literature

2.1 Introduction

The subjects discussed in this chapter provide background to the main themes of this project. These themes reflect the methodology chosen to satisfy the project objectives, which are predominantly related to Microsystems Technology (MST) and Sensor Networks.

Section 2.2 introduces the concept of the Distributed Sensor Network and the related issues, challenges and potential applications. Continuing this theme, section 2.3 examines six examples of existing Sensor Networks, many of which utilise MST.

Microsystems Technology is a relatively new technology which has the potential to miniaturise many systems in many applications. This technology is discussed extensively in chapter 6, however, its relation to Space applications is presented in section 2.4

Another important part of the project methodology is the use of the I2C bus for communications. Section 2.5 introduces this bus in terms of its use in a Nanosatellite project, thereby illustrating that it has potential for space use.

Finally, Section 2.6 positions this project in terms of existing concepts and the background presented here.

2.2 Distributed Sensor Networks

This section discusses several of the issues related to Distributed Sensor Networks. The networks consist of a collection of miniature, intercommunicating sensor nodes. These networks can be wired or, more commonly, wireless Section 2.2.1 presents the basic features of sensor networks including wireless operation, the types of sensors typically included and the classifications that describe the network traits.

Examples of communications architectures for the wireless options are presented in section 2.2.2. The issues that concern the sensor nodes themselves, and examples are given in section 2.2.3. An often overlooked topic in relation to sensor networks is that of the deployments strategies. The four methods of deployment are discussed in section 2.2.4. Finally, Distributed Sensor Networks have great potential for use in many applications including military, environmental sensing and health care. These are listed in section 2.2.5.

2.2.1 What is a Distributed Sensor Network?

As microtechnology has progressed, the focus for sensor hardware has began to move away from limited, large and expensive macrosensors communicating with a single base

station to networks of microsensors that can provide complex, multi-dimensional data of an environment (Min, Bhardwaj, Cho, Sinha, Shih, Wang, and Chandrakasan, 2001).

Distributed Sensor Networks consist of many small, low cost, spatially dispersed, intercommunication sensing nodes (Agre and Clare, 2000). There are two possibilities for node communication; transmission through a conduit or through the air wirelessly (Nagel, 2002). The conduits can either be in the form of electrical wires or optical fibres. In both cases the cables could be used to transfer data and power to the nodes providing the frequencies were sufficiently separated. The wireless option is an attractive option in many cases, as demonstrated by the range of different research programmes and various literature has been produced on the subject. The growing interest is also visible by the number of webpages, workshops and conference sessions that have been dedicated to Distributed Sensor Networks, particularly wireless sensor networks (Haenggi, 2005).

The basic features of a sensor network are (Haenggi, 2005):

- Self organising capabilities
- Short range broadcast communications
- Dense deployment and cooperative efforts between nodes
- Frequently changing topology due to node failure
- Limitations in energy, transmit power, memory and computing power

Several of the features of a sensor network differ from a standard ad-hoc wireless network (Su, Akan, and Cayirci, 2004). The most notable differences are the greater number of densely deployed sensors present in a sensor network and the broadcast communication paradigms used instead of point-to point communication. The principle difference is that sensing networks tend to be deployed for a specific application, whereas ad-hoc networks are usually formed for communications purposes only.

Compared to conventional macrosensors, a network of microsensors offers greater flexibility as to the location and timing of the data gathering exercise. Macrosensors are limited to sensing certain types of environment due to the cost and need for manual deployment. A sensor network is designed to be low cost and does not require any human interaction resulting in its potential use in hazardous regions, extreme climates and in all seasons. Where a large macrosensor can only collect data in a limited range, the network can extend its coverage by employing simultaneous collaboration, and the correlation of data from neighbouring nodes can result in improved accuracy and anomalous reading and fault detection. A network also has greater fault tolerance than a larger single sensor due to its dense deployment. The loss of one node will generally not lead to the failure of the network and subsequent loss of the data collection capability in that region. The networks have the flexibility to reconfigure so no loss in overall coverage is experienced following the expiration of one node.

With traditional larger sensors, measurements often had to be taken at a distance from the target then use complex techniques to extract the relevant data from the environmental noise. With a microsensor network, the nodes can be deployed inside

the target or in very close proximately to it, requiring less data processing and reporting a more accurate picture of the subject under investigation (Su et al, 2004). Miniaturised sensor nodes provide readings on the scale of the microclimate rather than at the scale of the investigator (Polastre, Szewczyk, Mainwaring, Culler, and Anderson, 2004). A sensor network can be equipped with sensors that can monitor features such as:

- Temperature
- Humidity
- Light
- Pressure
- Motion
- Soil compression
- Noise levels
- Detection of the presence of a given object
- Identification of the subject's characteristics, for example its mass, size, speed, direction and position.

The above only identifies a selection of the potential integrated sensors. A sensor network can be beneficial to a wide range of applications.

Due to the requirements of many of these applications and technology constraints, there are several design and architectural objectives that should be addressed when designing a sensor network (Feng, Koushanfer, and Potkonjak, 2005). These include: maintaining a reasonable compact node whilst providing the most powerful processor, radio, memory and components possible; ensuring low power consumption as this impacts the lifetime of the node; concurrency-intensive operation which allows capture, processing and communication of data simultaneously; robust operations including self test and calibration and fault tolerant in hostile terrains; have the flexibility to accommodate functional and timing changes and demonstrate compatibility with existing hardware and software reducing development costs. Many of these design requirements however are not exclusive to sensor networks and can be applied to many examples of micro-scale technology.

The issue of security and privacy is raised several times in the literature ((Hac, 2003), (Feng et al, 2005), (Wang, Hassanein, and Xu, 2005)). Especially with reference to military applications, protocols and mechanisms for preventing unauthorised access to data and damage from attack appears to be a critical design requirement. Because of the broadcasting nature of the network, encryption protocols and authentication of sensitive data are used to address this issue.

Although the sensor networks tend to be application-specific, the can be classified by various common critera (Wang et al, 2005). Depending on the distance of sensor nodes to the base station, wireless networks can be classified as single-hop or multihop. This architecture is discussed further in section 2.2.2. Networks can also be classified as aggregating or nonaggregating. In a nonaggregating network, all the raw data is reported, reducing the computational load on the node itself. However, the total communications traffic load increases considerably as the scale of the network

increases, leading to increased risk of data collisions and higher system latency. A nonaggregating scheme is therefore suitable for a low density network. In densely distributed networks, closely neighbouring nodes are likely to provide highly correlated information. Aggregating functions at intermediate nodes can eliminate data redundancy and reduce the communications load. This can however lead to a reduction of accuracy and minimisation of total scientific data, which may be deemed unacceptable for some applications.

Another classification is related to the distribution method of the network. Where the positions of the nodes are fixed or preplanned, the system can be considered to be deterministic. In contrast, a dynamic system is more scaleable and flexible, for example where the nodes are randomly distributed, however they can require more complex control and position determination algorithms. The networks can also be described as either self-configurable or non-self configurable. In the non-self configurable category, the networks cannot organise themselves and rely on a central controller to collect the information gathered. Examples of this type are common in wired and small-scale networks. However most wireless networks are designed to be self-configurable, where connectivity is established and maintained autonomously and sensing and control tasks are performed collaboratively. These systems are more complex to implement, however for large-scale deployment, this can be the more practical option.

The network can also be classified according to the variety of functions performed by its nodes. In a homogenous network, the nodes have identical capability and functionality in terms of their sensing abilities, communications and resource constraints (Papavassiliou and Zhu, 2005). In contrast, a heterogeneous network contains nodes that have different capabilities and can execute different functions. For example, some of the nodes may have a larger battery capacity for increased lifetime or be able to perform more powerful processing. Some nodes in the network may be designed for sensing only, whilst others in the network contain the data aggregation or communications relay functionality. There are certain functions such as long-range communication or GPS that do not need to be implemented by every node in order for the network to have absolute positioning and timing functions. However, limiting the number of crucial functions to a fraction of the total network density can result in reduced reliability (Pottie, 1998). A Homogeneous network is relatively simple and easier to deploy than the heterogeneous network, which is more complex to produce and be deployed in a way to ensure that the different types of node are dispersed into specific areas of the network.

Although these are general classifications, most sensor networks can be classified under several categories. For example, depending on the application the network could be described as self-configurable, deterministic and nonaggregating or any combination of the above.

As previously stated, the reduced dimensions of the nodes within the networks provide many benefits. Microsystems Technology and Microelectromechanical Systems (MEMS) components are being investigated to facilitate the reduction of size without decreasing the node's functionality (Warneke, 2005). Many examples of MEMS

sensors exist or are in development as well of RF and optical communications components required in any wireless network. Several sensor network projects have been undertaken which utilise this technology and are discussed in section 2.3.

2.2.2 Communications Architectures for Sensor Networks

The communications architecture of the wireless sensor network has been the subject of much literature (including (Hong, Gerla, Wang, and Clare, 2002), (Akyildiz, Su, Sankarasubramaniam, and Cayirci, 2002), (Qi, Iyengar, and Chakrabarty, 2001), (Pottie, 1998), (Arnon, 2000)). Various proposals have been made for the most suitable and energy efficient protocols and designs.

Typically, wireless communication is made directly or via a multihop process (Papavassiliou and Zhu, 2005). Direct communication from each node to the collector requires each node to have sufficient power for transmission. Since the nodes are energy limited, over a large range this becomes impractical. Also for a substantial size network, the amount of data traffic to the collector becomes prohibitively large.

A multihop architecture if generally more energy efficient as only short range communication is required. Two versions of the multihop architecture are the flat ad-hoc and the cluster-based multihop (Papavassiliou and Zhu, 2005). The flat ad-hoc routes data between nodes to the node located nearest to the collector, which acts as a relay. While this is more flexible and energy efficient than direct communication, it does not scale well and larger networks can soon produce a large amount of data.

With a cluster-based multihop architecture, the nodes form groups or clusters and transmit their data to a selected cluster head, which communicates with the collector. Localised data fusion could be performed by the cluster head to reduce the volume of data to be transmitted, which in turn reduces the overall transmission energy required. However, communications then rely on the cluster heads. To increase reliability and to ensure even energy depletion between the nodes, the function of the cluster head could be rotated. A multiple level hierarchy could also be used with several layers of cluster heads between the nodes and the collector.

From a model which relates the power consumed by the multihop transmission to the distance of transmission, it becomes advantageous to increase the number of hops. This assumes ideal communication with no overheads. However, contrary to the conclusions by Papavassiliou and Zhu (2005), Hac (2003) suggests that there is a range of distances where direct transmission can be more energy efficient. The energy characterisation must account for the protocol and access overheads, suboptimal node spacing and the occasional need to poll packets of data that arrive. These sources introduce an additional power overhead that for large networks can become substantial. Hac concludes that the transmission distance where a multihop architecture becomes advantageous over direct transmission is much greater than 30m.

These examples assume that the collector is stationary, however mobile collectors such as UAVs or mobile hubs could be present around the region of interest.

2.2.3 Sensor Nodes

Each sensor network generally consists of a collection of sensor nodes. These contain both the sensors and the subsystems needed to process the data and communicate with the others in the network.

Within the literature, there appears to be inconsistency in the number of components considered to be required within each sensor node. Feng et al. (2005) state that sensor nodes consist of six components: a processor, radio, local storage, sensors and/or actuators and a power supply. However Wang et al. (2005) propose that only four are necessary: a power supply, sensing unit, computing/processing unit and a communications unit. Papavassiliou and Zhu (2005) suggest a typical architecture comprising seven components: a power unit, sensing module, analogue to digital converter, processor, memory, storage and a radio module. Nagel (2002) also states that seven items are required, however in additional to the power source, processor, sensors and communications unit that are common between these examples, he also highlights the need for interface electronics, and printed circuit board and exterior housing.

Although overall there is a general agreement in the types of components required, the difference in the number appears to be a product of whether the authors have considered individual components or collective units based on subsystems.

For example, where Feng separates the need for a processor and local storage, Wang and colleagues have combined this to form their computing unit. They also combine the sensors and A/D converter into one sensing unit. The examples here are all given for a wireless sensor node, however the radio could be replaced by another communications component for other network architectures.

Figure 2-1 shows a typical sensor node architecture which incorporates details from all four approaches discussed.

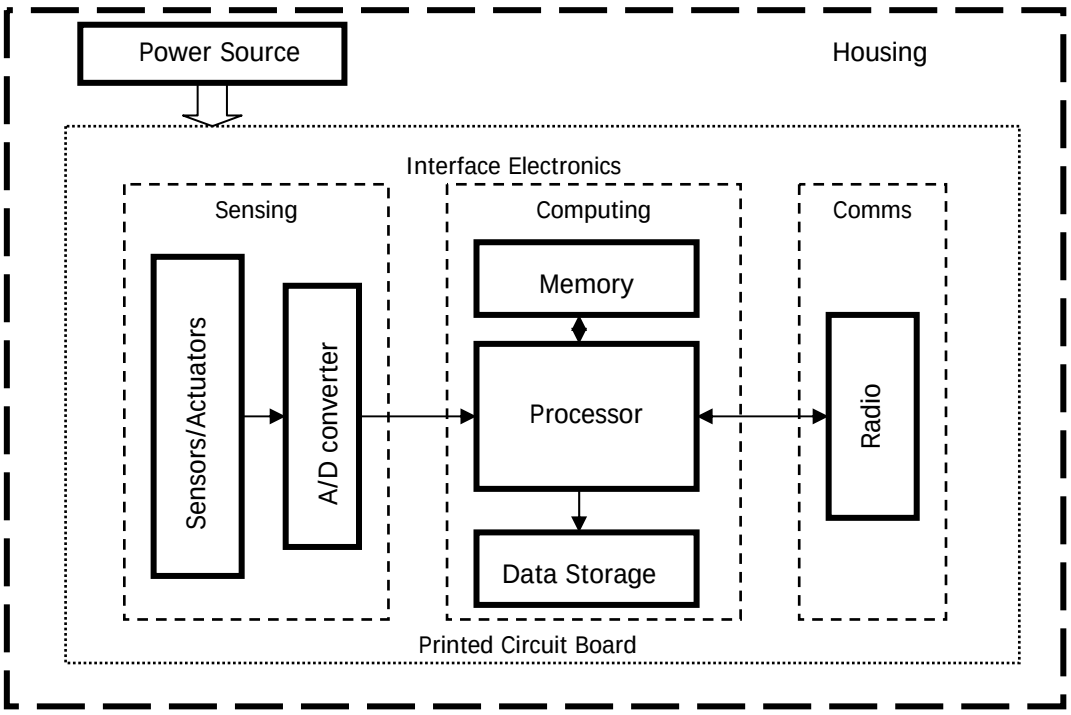

Figure 2-1 Block diagram of a typical sensor node architecture

A node can also be seen as a collection of functional layers that are supported by the components discussed above. Each node contains four layers or subsystems: the sensing layer, communications layer, data fusion layer and user layer (Papavassiliou and Zhu, 2005). This model assumes that on-board data processing is performed. The function of the sensing layer is data acquisition. The communications layer comprises data correlating, compression, dissemination and routing. This layer delivers the statistically observed results to a collecting centre and determines what kind of data should be transmitted and which route to follow. The data fusion layer processes the data received from the communications layer using a combination of signal processing, decision-making techniques and prior knowledge of sensor performance. The calculation and an analysis performed by this layer produces the final results that are transmitted to the network. The final user layer represents the man/machine interface which presents the final results in the desired format. The layers are supported by two other functions: topology and coverage control also resource management.

Some other forms of sensor node employ a tiered architecture. The following are examples of Motes which contain a processor, memory and a short range radio for wireless applications (Yarvis and Ye, 2005). These Motes are general purpose platforms to which sensors boards can be attached. By using a standard Mote to provide the processing and communications functions, rapid prototyping of multi-sensor nodes can be achieved since the networking capability of the node does not have to be designed separately. The examples in Table 2-1 are from both university-based project and industry developments. In general, the research programmes focus on developing the technology, whereas the industry designers focus on real world applications (Yarvis and Ye, 2005).

		Processor	Memory	Radio	Notes
Mica	Crossbow	ATMega128L 8-bit RISC core. 4MHz clock	128kB flash, 4kB SRAM	RFM TR1000 or TR3000 916MHz or 433 MHz	Extension boards for: Light, IR, Temperature, Humidity, Pressure, acoustic, acceleration, magnetometer, windspeed.
Mica 2		ATMega128L 7.37MHz clock	128 kB flash, 4kB SRAM	ChipCon CC1000 Tunable 300MHz to 1GHz	
Berkeley Mote	Berkeley	8-bit Amtel 90LS8535 4MHz	8kB flash, 512 SRAM	RFM 916.50 transceiver, 19.2 kbps	can have up to 8 sensors
Nymph	University of Colorado MANTIS project	Amtel ATMega128L		ChipCon CC1000	1st node to directly support GPS
Imotes	Intel	32 bit ARM 12MHz clock	512kB flash, 64kB SRAM	Bluetooth	Stackable module boards for sensing, 3 x 3 cm
Medusa mk2	UCLA	Includes 2nd controller. ATMega128L plus 32 bit RISC ARM THUMB 40MHz	1st as Mica, 2nd: 1MB flash, 136kB SRAM	TR1000	ATMega processor and TR radio for low level comms and simple sensors, THUMB for more extensive computations.

Table 2-1 Examples of tiered architecture Motes (Yarvis and Ye, 2005)

The Berkeley Mote (Feng et al, 2005) also contains an 8-bit microcontroller and low power radio. It also includes various sensors and was developed during the Smart Dust project. During the project, an operating system for the microcontroller was developed called TinyOS. This has become widely used, and the Berkeley Mote is the most widely used platforms by the research community (Yarvis and Ye, 2005). Berkeley have also developed the SPEC Mote, which includes a RISC processor, 3kB of memory, an 8-bit ADC, 4-bit input/output channels and an integrated radio, with a footprint area of 2 x 2.5mm. This system reduces the size, cost and power of the node,

which is the goal in many research programmes, but at a cost of reduced capability (Yarvis and Ye, 2005).

As yet there is little standardisation between the different nodes regarding the interface between the sensors, processor and networks. IEEE 1451 is a proposed standard that aims to reduce the complexity in establishing communication with the sensors by developing a modular block approach to systems design (Hac, 2003). Figure 2-2 illustrates this proposed standard as a functional block diagram.

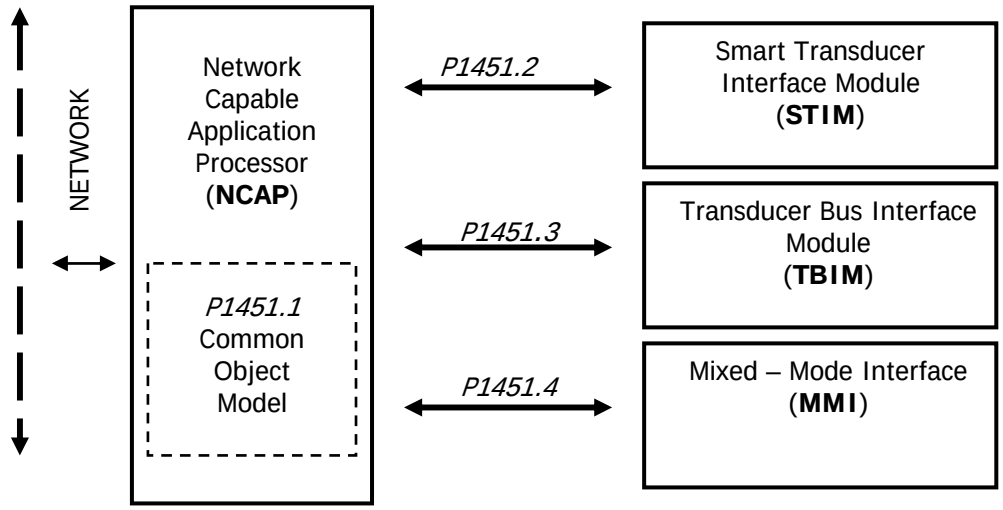

Figure 2-2 Illustration of IEEE 1451 standard as a functional block diagram (Hac, 2003)

The standard defines the bus architecture, addressing protocols, wiring, calibration and error correction. There are four subsections to the standard (Hac, 2003). P1451.1 defines the Network Capable Application Processor (NCAP) – a processor with embedded operating system, sense of time and communication stack for networking. P1451.2 relates to the Smart Transducer Interface Module (STIM) – a digital interface and serial communication protocol that allows a transducer to send and receive data using a common interface. P1451.3 defines the Transducer Bus Interface Module which provides a standard physical interface for connecting multiple separate sensors. Finally the Mixed Mode Interface (MMI) is a communication protocol that allows analogue transducers to communicate digital information for self identification and configuration.

Although this standard will be beneficial as guidelines to designers wishing to develop a standardised sensor node with "plug and play" capability, it has yet to be implemented within the sensor network programmes investigated.

2.2.4 Deployment strategies

The deployment strategy adopted for the distribution of the sensor nodes, particularly in a wireless sensor network, aims to achieve the desired surface coverage with a minimum number of sensor nodes whilst complying with the constrains of cost, quality of service, reliability and scalability (Wang et al, 2005). In this case, coverage refers to

both the area of the sensing mission and the relative space between the sensor nodes and the target to enable accurate measurements.

The majority of the literature produced concerning wireless sensor networks focuses on issues such as the communications or sensor data fusion, however the issue of sensor placement appears to be largely overlooked (Dhillon, Chakrabarty, and Iyengar, 2002). However Wang, Hassanein and Xu (2005) have compiled a useful review of the types of sensor distribution strategies. They have identified four methods of deployment: predetermined, self-regulated, randomly undetermined or biased distribution.

A predetermined strategy can be applied when sufficient knowledge about the targets or environment is known or the nodes can be uniformly in a grid-based topology. The granularity of the grid is determined by the desired accuracy of the sensing network. In general, a predetermined strategy can provide an optimal solution in terms of coverage, quality and cost efficiency, however it is often impractical as prior knowledge of the targets is unavailable. The grid strategy is a better approach, however due to computational complexity, it is not scalable over large networks.

Two examples of a self-regulated approach are given. The first is where the sensor nodes are deployed automatically over an unknown environment. The node is repelled by obstacles and other nodes thereby spreading the network. Another scheme suggests deploying the nodes sequentially in various size steps. These self-regulating strategies can achieve the desirable coverage, are scalable and minimise the cost of deployment. However the computational expense may become prohibitive.

A more realistic strategy for the large scale deployment of sensor nodes over an unknown environment is the randomly undetermined strategy. The ease of placement compared with a deterministic approach therefore means that the cost of deployment is low. However, the random spread may not be uniform due to obstacles or other environmental factors. For some applications a random deployment of sensors may not satisfy the design requirements, which may result in the need for a biased deployment. Biased placement means that a greater proportion of the sensors are deployed in certain areas, such as deploying more around the edges of a room than in the centre.

Tilak and colleagues (Tilak, Abu-Ghazaleh, and Heinzelman, 2002) performed simulations of a grid-based structure, a random distribution and a biased deployment. Their findings showed that there was no appreciable difference in performance between the grid and the random strategies, however biasing the deployment density to the pattern of the phenomena under investigation results in significantly higher accuracy.

Another typical purpose for a sensor network is target location (Qi et al, 2001). If the field is considered to be a grid, then target location refers to finding a target point at any one time. One way of achieving the goal is to deploy large numbers of sensors and if the target is located within the overlapping coverage zones, its precise location can be determined by the positions of the sensors. In some cases it may be virtually impossible to locate the target using this method.

The examples discussed generally assume 100% reliability. However, this is not always true in reality. Dhillon et al. (2002) and others have presented optimisation frameworks, where for a given detection probability, the optimum position and number of sensors can be calculated to achieve sufficient area coverage.

Another aspect to the strategy is the physical method of deployment. Again there appears to be relatively little published that considers this aspect in detail. However, Delin and Jackson (2000) have considered this in terms of their Sensor Webs project and have looked to nature to suggest various schemes. These schemes appear to be based on methods of seed distribution. They suggest dropping their pods from altitude with each pod equipped with a parachute or rotor to lessen the impact; ballistically firing the pods from a central point, which would enable the pods to be driven into steep crater walls for example; dropped from a moving ground vehicle or attached to the central craft with cable links like streamers or runners. They also briefly consider secondary deployment, for example if the pods should be designed with aerodynamic cups to assist movement by the wind, or whether to attach stickers so that they remain stationary during high winds. As yet, no conclusions to this investigation have been published.

Overall the deployment strategies for distributed sensor networks appear to be largely determined by the application and the related cost.

2.2.5 Applications

As demonstrated by the previous discussions, the application of the sensor network is important in determining many aspects of its design and deployment. There are many existing and proposed applications that can be divided in a variety of categories. These applications are referenced from several sources ((Su et al, 2004), (Haenggi, 2005), (Wang et al, 2005), (Akyildiz et al, 2002)) , however each one has arranged them differently under widely varying headings. The categories chosen here reflect the main trends between them.

2.2.5.1 Military

Although the categories varied between papers, the discussion of military applications was consistent throughout, and usually appeared first in the section.

Sensor Networks can be an integral part of the military command, control, communications, computing, intelligence, surveillance, reconnaissance and targeting (C4ISRT) systems. Typical military applications include:

- Data collection of enemy targets
- Asset monitoring and battle damage assessment – positioning and status of tank, missiles and personnel.
- Guidance for missiles, tanks and torpedoes.
- Surveillance and Battle Space monitoring – critical paths covered in sensors to detect enemy activity.

- ❖ Urban Warfare – positioning and identifying "friends" through streets and buildings
- ❖ Protection – detection of intruders and chemical/biological/nuclear attacks.

Sensor networks are considered to be preferable in battlefield situations to traditional sensors, as the destruction of a low-cost disposable node in a dense distributed network has less affect on military operations than the destruction of one traditional sensor.

2.2.5.2 Environmental and Ecosystem Monitoring

This is a broad category, and some applications that have appeared under this heading in the literature have been redistributed to other sections. This category features traditional environmental monitoring applications and examples in agriculture.

Typical applications include:

- ❖ Habitat monitoring
- ❖ Plant and animal population and behaviour monitoring – including Great Duck Island and Zebra tracking with Zebranet
- ❖ Biodiversity and Biocomplexity mapping
- ❖ Water quality and sewerage assessment
- ❖ Air quality assessment
- ❖ Soil chemistry and composition
- ❖ Pollution studying
- ❖ Geophysical monitoring – including seismic activity
- ❖ Meteorological research
- ❖ Exploration of mineral reserves
- ❖ Crop and livestock management and precision agriculture
- ❖ Control of fertilizer concentrates
- ❖ Irrigation control
- ❖ Chemical and Biological detection

Sensor networks have enormous potential benefit in environmental monitoring. Large scale distribution of traditional sensors on probes are intrusive and can prove expensive and involves large amounts of cabling to the large data loggers. Examples where scientists are currently investigating the ecosystems redwood canopies, vineyards, climate and occupancy patterns of seabirds and animal tracking (Polastre et al, 2004). Miniaturised sensors can be inconspicuously deployed on the surface, in burrows or in trees with minimal disturbance to the environment, whereas teams of researchers could have a damaging impact on the population in question particularly during sensitive periods like the breeding season. Sensor networks are also more economical than a traditional personnel-rich long term study.

The example of the research carried out using sensor networks on Great Duck Island (Polastre et al, 2004) is given in several papers. The research was an investigation into the environmental changes and nesting burrow patterns of Storm Petrels on an island in Maine. The investigation was designed to be carried out over the 7 month

breeding season. This was the first long-term example of sensor node use and so the performance of the node was as much interest as the environmental data. Mica motes were used combined with a photoresistive sensor, digital temperature sensor, capacitive humidity sensor and digital pressure sensor, with an additional passive infrared detector to monitor burrow occupancy. This was integrated into a single package, and 43 nodes were deployed in total, both within burrows and on the surface. After 123 days, over 1.1 million readings were logged. Unfortunately, the deployment exhibited a very high node failure rate and failed to produce any meaningful scientific data. It did yield a valuable insight into the operation of a wireless sensor network that could not have been achieved by simulation.

2.2.5.3 Space Applications

The Space environment is one example where the application of a Sensor Network potentially has many benefits. This environment has its own challenges relating to the unique conditions, however there are a range of possible applications, both platform-related and as part of a scientific payload, including:

- Planetary environment sensing
- Spacecraft internal sensors
- Landing area targets
- Launch site monitoring
- Rover path tracing

Planetary environmental sensing is a recognised application of great potential benefit especially due to the low mass, low cost and relatively autonomous operation. Mars has been identified as a potential candidate for this type of network investigation. The Sensor Webs team at NASA JPL and Hong and colleagues at UCLA (2002) have presented concepts of wireless sensor networks for use on the Martian surface. In their 2002 paper, Hong et al focused on the communications architecture for such as network, concluding that "a multipath routing scheme with energy aware, load balanced route selection based on the poll-reply communication model" would be most appropriate in this environment. A rover or lander would act as a base collector and poll the nodes periodically for data creating paths of minimal hop distance to the collector. Discussion of the Sensor Webs project will appear in a later section and further discussion of Space-related applications and mission scenarios is featured in section 5.2.2.

2.2.5.4 Health Care

Sensor networks can be used in a variety of ways under the general heading of health care. These include:

- Interfaces for disabled patients
- Integrated patient monitoring
- Diagnostics
- Drug administration and tracking
- Tracking doctors and patients, including babies, within hospitals

- Collection of human physiological data over time
- Smart bandages
- Microsurgery
- Remote virus monitoring

As with the environmental monitoring, these applications principally rely on the network's low cost and unobtrusive nature for their potential success.

2.2.5.5 Disaster Monitoring

Examples in this category have been placed under several different headings in other papers, however this is an extreme form of environmental monitoring and also has potential benefits that should be highlighted separately.

Applications include:

- Forest Fire detection
- Flood warnings
- Contaminate transportation detection – including gas and toxic waste
- Detecting material fatigue in buildings
- Location of sunken vessels to aid rescue and salvage
- Disaster recovery – identification of trapped personnel

Many of these applications require long term deployment, therefore the nodes must be energy efficient or scavenge power from the external environment.

2.2.5.6 Commercial

The commercial category combines retail, office, factory and warehouse management applications. These include:

- Smart office spaces and environmental controls – including heating, lights and air conditioning.
- Virtual keyboards
- Managing inventory and warehouse inventory tracking
- Monitoring product quality
- Robotic control in automatic manufacturing environments
- Factory process control
- Machine diagnosis and maintenance
- Vehicle tracking
- Tracking goods containers
- Tagging retail goods in stores for inventory and security

2.2.5.7 Home Intelligence, Automation and Security

While the applications above are related to the work environment, those listed here are of benefit in the home including:

- Home automation and smart environments – interactive networks of appliances including vacuums cleaners, ovens and refrigerators allowing remote household management
- Remote metering – readings of gas, water and electricity meters. Parking meter expiry alerts.
- Detection of car thefts
- Intruder surveillance
- Networked smoke detectors

2.2.5.8 Other Applications

These are other potential applications that cannot be obviously included in any of the above categories. These include:

- Interactive toys and learning environments
- Interactive museums
- Traffic monitoring
- Aircraft drag reduction research
- Social interaction studies
- Urban planning

As identified in these sections, there are many potential uses for miniaturised sensor networks in a variety of situations. The following section gives details of several existing research projects into distributed sensor networks.

2.3 Existing Distributed Sensor Network Programmes

Throughout the literature reviewed on the subject of distributed sensor networks, five projects were referred to frequently. They are predominantly US university or NASA developed programmes and several utilise MEMS components.

Each programme is reviewed here. In addition, a section is dedicated to the European EADS Astrium Micropack project as a further example of a potential MST sensor networks.

2.3.1.1 Sensor web

The Sensor Web project is being conducted on behalf of NASA at JPL. It consists of a system of wireless, intra-communicating, spatially distributed sensor pods designed for environmental monitoring over a large area (Delin and Jackson, 2001). Each pod includes two primary modules. The first module contains the sensors and the second represents the Sensor web infrastructure. This module contains the communication subsystem, power and energy harvesting devices and computation subsystems. One of the goals of the project is that the pods extract "knowledge" from the data and adapt and react accordingly (Delin and Jackson, 2001).

The wireless communication is omnidirectional. Each pod obtains information by two methods. Firstly, by its own direct measurements, and secondly by information

received from other pods. The information is treated equally and rebroadcast to any sensor pod within range. Any information received by the Mother pod from the Daughter pods in not rebroadcast, but can be accessed by a user. The unique feature of JPL's Sensor Web is that the information gathered is shared and used by other pods. They then react and modify their behaviour on the basis of that collected data. As the pods fail, additional pods can be deployed that will automatically be included in the network.

A series of experiments have been carried out using the Sensor Web concept. Sensor Web 1 was an initial test consisting of 4 pods, each containing a transceiver, microcontroller, 3V battery and light and temperature sensors. This test allowed the testing of the multihop shared information communication protocol.

Sensor Web 2 was a larger system deployed in a greenhouse environment. This used larger prototype pods measuring 5 x 10 x 16 cm, and containing 7 environmental sensors. All sensors were micropowered except one of the gas sensors and were driven by a rechargeable 8V battery with solar cells. Commercial 916MHz transceiver boards provided the communications subsystem. The Web contained 12 pods and data was collected in five minute intervals. Sensor Web 2 was proved to be fairly robust, as it collected data continuously for 22 weeks, even though it was initially a 2 week study.

Since then other Sensor Webs have been deployed in several environments including around the Kennedy Space Centre (Delin, 2002), various agricultural sites and even in the Antarctic (Delin, Harvey, Chabot, Jackson, Adams, Johnson, and Britton, 2003). Another successful demonstration used the Sensor Web to monitor biogenic gases produced by algal mats in California. The Sensor Web concept was ideal for this application as the nature of the dispersion of the gases meant that a large area coverage *in situ* system was required. Similarly, a potential application that the Sensor Web has been suggested for is locating gaseous biosignatures on the surface of Mars.

2.3.1.2 Microcluster

The University of Michigan's Microcluster (μCluster) is a "Multiparameter sensing system that supports a variety of MEMS sensors within each sensing node of a macrosystem." (Helvajian, 1999). The system was designed to demonstrate how the generic architecture could be used to build a microsystem that is small, low power, uses wireless communication and provides highly accurate sensor data (Mason, Yazdi, Chavan, Najafi, and Wise, 1998).

The system, that has been designed for general environmental monitoring, included an open architecture so that any one aspect or sensor can be changed without affecting the entire system. Each node consisted of interfaces for wired and wireless communication, a microcontroller, power supply, power management circuitry and a collection of sensors. The sensors included were a temperature, barometric pressure, relative humidity and acceleration sensors. Periodic scans of these transducers were made. Between scans a low power sleep mode was used to maximise battery life.

This concept has been packaged to include a wriststrap to make it a wearable system, and has been subject to field trials. Versions of Microcluster have been used in several military applications, including artillery exercises with the US Marine Corps and on modified ocean buoys with the US Navy.

2.3.1.3 μAMPs

The μAMPS project was carried out by MIT and stands for Microadaptive Multidomain Power-aware Sensors (Min, Bhardwaj, Cho, Sinha, Shih, Wang, and Chandrakasan, 2000).

The first prototype was designed using COTS components for rapid prototyping and modularity. However the overall aim is to achieve a microsensor system on a chip of $1cm^3$ with the integration of MEMS sensors and other components on a single die (Wang et al, 2005).

The prototype demonstrated the effectiveness of a power aware system design methodology. The inefficiencies of a low duty cycle and variation in processor workload were exploited by dynamic voltage scaling. The variations in data rate were also exploited by energy agile algorithms. Close collaboration between hardware and software also results in energy savings. Also demonstrated were the systems ability to adapt to changing environmental conditions, as well as its versatility to prioritise between lifetime or output quality as required.

2.3.1.4 Smart Dust

The Smart Dust project has been developed by Berkeley Sensor and Actuator Centre and aims to explore the limits of system miniaturisation by packing a sensing computing and communication node into a $1mm^3$ mote which will form part of a larger sensor network (Warneke, Scott, Leibowitz, Zhou, Bellow, Chediak, Boser, Khan, and Pister, 2002).

A system has been developed that includes 2 sensors, an analogue to digital converter, a controller, solar cells for power and an optical communication device.

The Corner Cube Retroreflector is a passive optical transmission device and has been the subject of much literature due to its unusual nature, as most sensor networks use radio communication.

Although $1mm^3$ is their ultimate goal the current published device has a volume of $16mm^3$, however research on this project is still underway.

2.3.1.5 WINS

WINS stands for Wireless Integrated Network Sensors and was a project run by UCLA. This system also integrates many functions including sensing, processing and network communication in a single compact low power device. These sensors form a self organising network.

This programme has since spawned a spin-off company called Sensoria (www.sensoria.com) (Nagel, 2002).

2.3.1.6 Astrium micropack

EADS Astrium have created a cross disciplinary research project called Micropacks. The objective of the project was to demonstrate complete Microsystems and combine them into other high performance space systems (Eckersley, Schalk, and Koppenhagen, 2005). The micropacks can have different functions that can be integrated together.

An initial 2 micropacks were developed. The atmospheric micropack contained pressure, temperature, humidity and acceleration sensors as well as processor, memory, battery and blue tooth communication system. The inertial measure unit micropack contains 3 gyros and 3 accelerometers. The size of the atmospheric pack was 78 x 53 x 18.5mm.

The latest version of the micropack uses 3D packaging and LTCC ceramic module packages. Each subsystem is represented by a layer in the packaging. The package now has a volume of 20 x 25 x 25mm and a mass of 25g. These packs could potentially be used as the core of a nanosatellite or micro-lander.

2.4 MST for Space

Microsystems Technology (MST) and MEMS devices have the potential to be of great benefit to the Space industry. Many believe their integration into space systems is inevitable as they exhibit many qualities that are highly desirable in the Space environment (Goetz, 1997).

Due to the increasing cost of launches and overall reduction in Space budgets, new technologies and approaches are under investigation which will enable the current volume of Space projects but at reduced costs. One method considered is the use of MST devices to reduce the overall size and mass of the spacecraft, and hence reduce its cost of launch.

Many of the subsystems can become significantly smaller by using MEMS in place of the conventional components (Helvajian, 1999). The power and thermal requirements are also considerably lower with MEMS. Because of their mechanical nature, the components are robust to the vibration environments of a launch and are more resistant to radiation than conventional semiconductor components (Cass, 2001). The can withstand greater shocks mainly because the mass of each moving component is extremely small which are therefore subject to much smaller internal force that may cause damage (Cass, 2001). Because many incorporate integrated processors, an MST device can perform several functions including data processing and calibration from within the device itself (Goetz, 1997). Due to their small mass and power requirements, MEMS components can also be used to provide redundancy for subsystem for only a small penalty.

However, since reliability is important in space systems, MST devices are still a long way from being used on mission critical subsystems. The technology must demonstrate that it can maintain a high degree of capability under the severe constraints of mass, power and size, and many spacecraft developer will not be satisfied of this until each subsystem has been demonstrated in practice and a large volume of engineering evidence is produced. Demonstrator missions such as the picosats aboard the OPAL project (Cass, 2001) are underway to achieve this.

Further discussions on the potential benefits and challenges of MST in general and in space applications are presented throughout this thesis.

2.5 Other Relevant Background

Part of this project investigates the potential use of the Philips Semiconductors I2C bus communication protocol. A previous example of an I2C bus in relation to a space environment is as part of the distributed data handling system in Stanford University's Emerald Nanosatellite project (Townsend, Palmintier, and Allison, 2000).

The Emerald team chose the I2C bus as their main data handling system because it offered simplicity, reduced wiring, speed and was supported by many commercially available components. It also allows for subsystems to be added as they became available and for subsystems to be removed without affecting the systems still attached to the bus.

They showed that the I2C bus is a useful development tool for investigating a distributed system and that it has the potential to be used in real space hardware.

The I2C bus was also demonstrated as an internal chip-to-chip interface between the digital temperature sensor and the microcontroller the initial Berkeley Mote design (Hill, Szewczyk, Woo, Hollar, Culler, and Pister, 2000).

2.6 Positioning of this project

After reviewing the literature currently available in the fields of Sensor Networks and Microsystems Technology, the position of this project can be established.

Currently the architecture of Distributed Sensor Networks tends to be application-specific. One of the main aims of this project is to investigate a more generic system that can be used for a variety of applications with only minimal modification. In this case, the sensor suite will be a combination of a sensor node and sensor mote as described above. This system also demonstrates both wired and wireless communications.

The potential benefits of MST and Sensor Networks for use in Space, terrestrial environment and planetary surface sensing applications have been recognised and form an integral part of this project.

The existing programmes investigated have demonstrated many innovative features including the use of MST and the potential for Sensor Networks in space environments. However, in many cases, the overall system has not been fully explored.

This project aims to produce a whole systems approach, which includes suite design, communications consideration and deployment strategies for a generic system that addresses both terrestrial and planetary sensing using commercially available MST-based Distributed Sensor Networks.

3 Fundamental Physical limits to the size of a Space sensing system

3.1 Introduction

The first objective of this project has been defined as:

To investigate the fundamental physical limits which determine the minimum size of a spacecraft or planetary exploration system and compare it to nature and existing spacecraft.

This study considers the broad spectrum of generic sensor systems – the focus of this project – with the intention of establishing the feasibility of potential size reduction without being bound by the limitations of current technology, and motivated by the current interest in the application of MST and Nanotechnology in Space.

Advances in MST and Nanotechnology are continually driving down the size of individual components and systems. However, technology is only a temporary constraint.

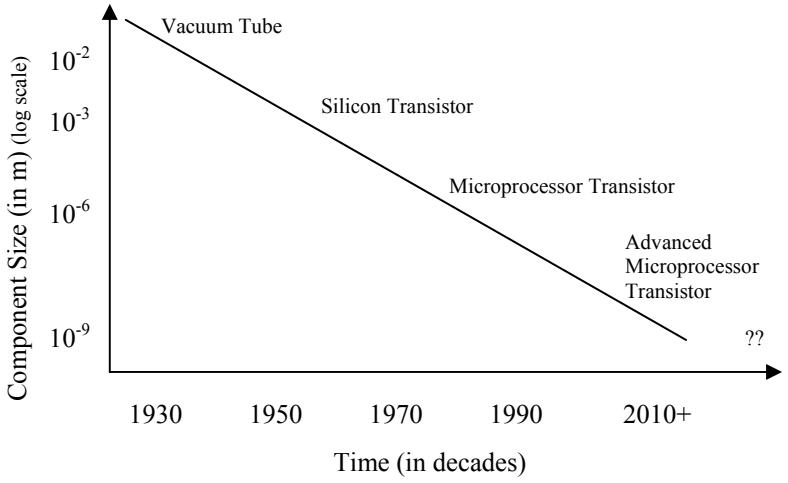

Figure 3-1 A Chronology of technology - Relative size vs time

This chapter is looking at the "Fundamental Limits to Miniaturisation" based on physical laws rather than today's engineering capability. When these limits have been identified, the gap between today's technology and what may be possible in the future can be quantified. Such knowledge is of primarily of use to the planners of future missions where such miniaturisation may enable previously impossible ventures, and will create a benchmark for the further investigations of this project.

This body of work identifies and investigates the physical laws that determine the smallest possible size for the core sensor system functions and then applies these findings to an example of a space borne sensor to support planetary surface exploration.

Section 3.2 outlines the spacecraft systems functions investigated. Section 3.3 then discusses the limiting factors of those primary sensor system functions. The other constraints and drivers that determine the minimum possible size for a sensor system are discussed in section 3.4. Section 3.5 shows a simple example system and a comparison with current systems, followed by a discussion section and concluding remarks.

3.2 Spacecraft systems functions

In order to investigate the fundamental laws of Physics, and their related equations, which govern how a sensor system works and limit its size, a review of the existing literature was initially undertaken.

Previous papers written on this subject have tended to focus on a particular function, Computing or Communication for example, or a specific technology, such as Silicon and Semiconductors. As this study concerns sensor systems for space exploration techniques, it was decided to identify those functions that were key to these techniques and to investigate the limits relating to them.

Virtually any form of exploration system, from remote sensing satellites and *in situ* environmental sensor suites to even a Human explorer, requires the same basic functions in order to evaluate the environment and report its findings.

These primary functions: Sensing, Information Processing and Communication, have their own laws and limits that govern them, although in some cases there is some commonality.

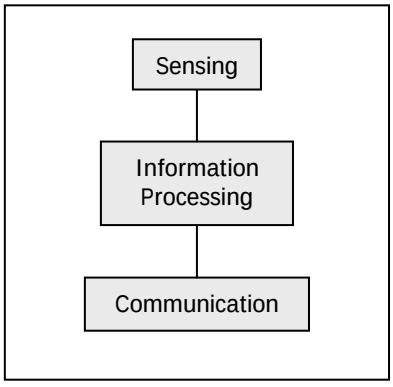

Figure 3-2 Primary functions of a spacecraft or sensing device

3.3 Limiting factors of functions

Each of the aforementioned functions is discussed below in terms of their physical laws.

3.3.1 Sensing

The generic term Sensing is applied to any function that interacts with, and interrogates, its external environment. As such, the limiting laws and equations depend on the type of sensor involved.

Many MST sensors are capacitive, and so their capacitance, which is related to plate separation distance and plate area, its dielectric properties, and the amount of energy needed to be collected in order to get an unambiguous identification of that which is under investigation, are key in determining the size of the sensor. In a similar way, any sensor that uses or measures an electric or magnetic field will be limited by Maxwell's equations.

Sensors that measure effects related to angular momentum, torques and gravity gradients are generally dependant on the inertial properties, which in turn is related to the size, shape and mass of an object. Optical sensing, in particular the angular resolution of the instrument, will be limited by diffraction.

If environmental measurement is the primary purpose of the spacecraft system, the minimum size of the sensor, depending on user-defined specifications such as the desired minimum measurable quantity, may become the dominant factor in determining the overall minimum size of the spacecraft.

Two common sensors are the accelerometer and the pressure sensor. The fundamental principles behind these two sensors are described in the following sections.

3.3.1.1 Physical principles behind the operation of an accelerometer

An accelerometer is essentially a mass-spring-damper system attached to a casing. As acceleration is applied to the casing, the resulting motion of the mass can be used to determine the magnitude of the acceleration. This principle is illustrated in Figure 3-3.

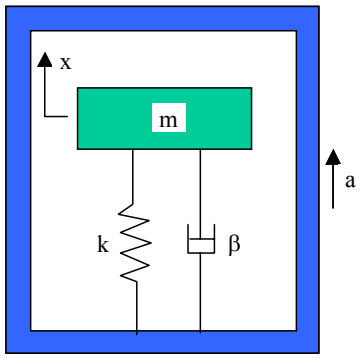

Figure 3-3 Fundamental principle of the Accelerometer(Lin, 2001)

The fundamental equation behind this principle is the equation of motion for the mass, m, given by:

$$m\ddot{x} + \beta\dot{x} + kx = -ma$$

where β is the damping coefficient and k is the spring constant. Using this equation, the acceleration, a, can be determined by measuring the displacement, x, of the mass.

There are two key parameters of the system; the natural frequency ω_n, and the damping ratio ζ. These parameters are given by:

$$\omega_n = \sqrt{\frac{k}{m}}$$

and

$$\zeta = \frac{\beta}{\sqrt{4mk}}$$

The equation of motion then becomes:

$$\ddot{x} + 2\zeta\omega_n\dot{x} + \omega_n{}^2 x = -a$$

The solution to this equation comprises a transient response and a steady-state response. The transient response is the effect on the system that depends on the initial conditions and is damped out over time. While the transient effects are an important part of the systems characteristics, they can be ignored if the response of the system is sufficiently fast. The steady-state response, which is independent on initial conditions, is the final condition of the system from which the minimum detectable acceleration a_{min} and the bandwidth within which the accelerometer is useful can be calculated. These performance parameters are important in determining the useful minimum size of the accelerometer.

A common configuration for a micromachined accelerometer is a truncated pyramid shaped mass, shown in Figure 3-4, suspended by eight beams above an air gap. The beams have integrated strain gauges that are used to measure the deflection of the beam and therefore the acceleration. This is shown in Figure 3-5 below.

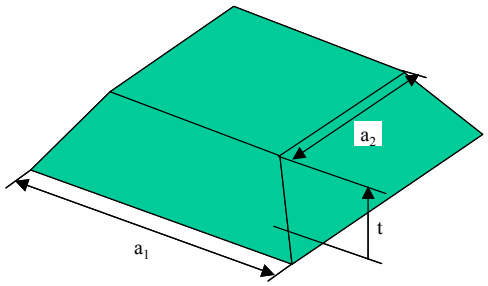

Figure 3-4 The shape of silicon mass in the micro accelerometer (shown upside down)(Lin, 2001)

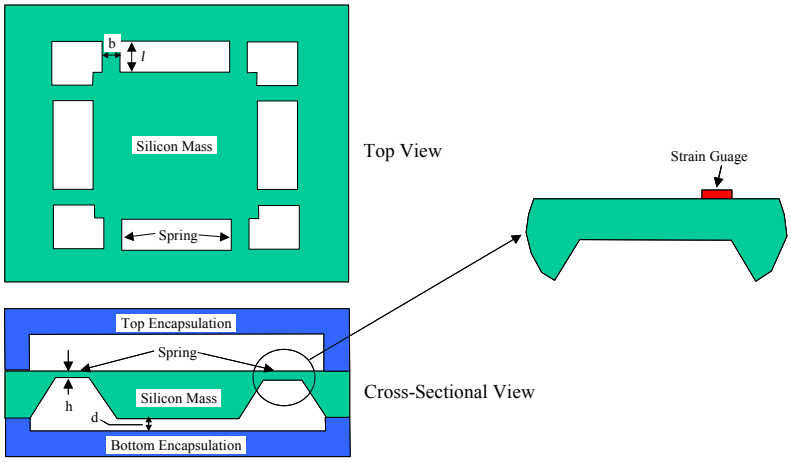

Figure 3-5 Schematic of a micromachined accelerometer (top and cross-sectional views).(Lin, 2001)

The lengths shown in the diagrams as a_1, l, b, h and d are the dimensions that have to be selected in order to produce an accelerometer that performs to the desired levels.

The mass, m, is related to the silicon mass horizontal edge lengths a_1 and a_2. The longer of the two lengths, a_1, is a specified design parameter and from this a_2 can be calculated using the formula:

$$a_2 = \frac{a_1 - t}{\sqrt{2}}$$

where t is the thickness of the mass, and is generally given as the thickness of the silicon wafer that the mass is machined from. An typical value for this is 525 μm. The mass itself can then be calculated using the equation:

$$m = \frac{1}{3}\rho t \frac{(a_1^3 - a_2^3)}{(a_1 - a_2)}$$

where $\rho = 2300\ \text{kgm}^{-3}$, the density of silicon.

The dimensions of the beams, l, h and b (as shown in Figure 3-4 and 3-5) in this case determine the spring constant k. These dimensions are also specified design parameters. From Beam theory, the spring constant is given by:

$$k = \frac{E(bh^3)}{l^3}$$

where $E = 190 \times 10^9\ \text{Nm}^{-2}$, the Young's Modulus of silicon (Lin, 2001).

Once the mass and the spring constant have been determined, the natural frequency ω_n can be calculated. This parameter, the natural resonance frequency of the system without damping, is the basis of calculating the minimum detectable acceleration and the bandwidth.

The damping coefficient β corresponds to the "squeeze film" effect between the silicon mass and the air film trapped in the gap between the mass and the bottom of the casing.

β is related to the area, A, of the air film, given by a_2^2, and the depth of the gap, labelled d in Figure 3.5. From this, the damping coefficient is given by:

$$\beta = \frac{0.42\mu A^2}{d^3}$$

where $\mu = 1.85 \times 10^{-5}$ $Nm^{-2}s^{-1}$, the dynamic viscosity of air (at standard temperature/pressure).

Following the determination of β, the other important parameter, the damping ratio ζ can be calculated. This damping ratio defines the transient response that gives the accelerometer the desired characteristics. As stated above, the damping ratio is given by:

$$\zeta = \frac{\beta}{\sqrt{4mk}}$$

If ζ = 1, the system is described as critically damped, where oscillatory motion is prevented and the system returns to the steady-state equilibrium as quickly as possible. If ζ < 1, the system is underdamped and oscillation occurs before reaching equilibrium. Conversely if ζ > 1 the system is overdamped, resulting in a system where there is no oscillation but where the time taken for the system to return to equilibrium is longer than of it is critically damped. This is illustrated in Figure 3-6. For an accelerometer, it is desirable to have ζ between 0.6 and 1.1 to give a suitable transient response.

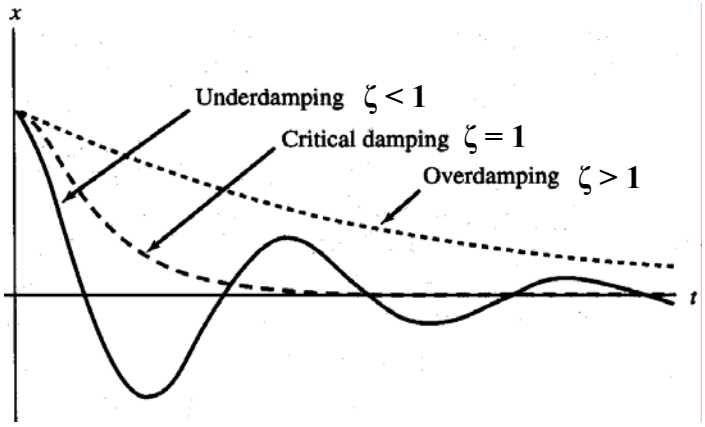

Figure 3-6 Graph depicting damped oscillations (Marion and Thornton, 1995)

As the applied acceleration can be described as sinusoidal with an angular frequency ω, the bandwidth of frequencies that can be detected by the accelerometer is defined by the cutoff frequency ω_c. The deflection x that measures the acceleration becomes diminishingly small at large frequencies, which means that the accelerometer becomes ineffective above the given frequency, ω_c. This cutoff frequency is defined as:

$$\omega_c = \gamma\omega_n$$

where

$$\gamma = \sqrt{1 - 2\zeta^2 + \sqrt{(1 - 2\zeta^2)^2 + 1}}$$

Common values for the accelerometer's bandwidth, given by the cutoff frequency, are approximately 4 kHz to 5 kHz.
Finally, as the steady-state spring deflection x is directly proportional to the applied acceleration a, the minimum acceleration detectable by the system is related to the minimum measurable spring deflection as:

$$a_{\min} = x_{\min}\omega_n^2$$

A value for the minimum acceleration can be set by the user, which thereby defines the minimum spring deflection, or vice versa. (Lin, 2001) x_{min} is also related to the beam length l as:

$$x_{\min} = l\varepsilon_{\min}$$

where ε_{min} is the minimum measurable strain allowable by the strain gauges, which is assumed to be a typical value, $\varepsilon_{min} = 5 \times 10^{-7}$ (Lin, 2001).

These relationships can be used to determine or specify the minimum size of the accelerometer. As stated previously, the design of the accelerometer is defined by the selection of the lengths a_1, l, b, h and d. The ultimate limit for any size has to be the diameter of the atom of the material it is made from. If the diameter of the silicon atom, 0.234 nm, is taken for a_2, l, b, h and d, ($a_1 = 3a_2$ in this case), and m is given as 10 times the mass of the silicon atom, 4.7×10^{-25} kg, it can be calculated that ω_c = 15.1 THz and $\zeta = 0.000199$. The bandwidth is very wide, which could be useful for certain applications, however the damping ratio is extremely small, resulting in a large amount of oscillation in the system, and is unacceptable for an accelerometer. This does, however, assume that these equations hold at such low values, however it is likely that should an atomic accelerometer be developed it would not use this particular principle as its basis.

Current micromachining technology allows the design parameters to be chosen from the following ranges (Lin, 2001):

$$1\text{ mm} \le a_1 \le 5\text{ mm}$$
$$300\ \mu\text{m} \le l \le 600\ \mu\text{m}$$
$$100\ \mu\text{m} \le b \le 300\ \mu\text{m}$$
$$2\ \mu\text{m} \le h \le 10\ \mu\text{m}$$
$$5\ \mu\text{m} \le d \le 40\ \mu\text{m}$$

Substituting values within these ranges into the equations defined above, values of minimum acceleration, a_{min}, damping coefficient, ζ and the bandwidth can be obtained that meet the user-defined specifications.

3.3.1.2 Fundamental principles behind a pressure sensor

In general, pressure sensors work on the principle of detecting a force that results from an applied pressure, usually by measuring the deflection of a diaphragm (Shown in

Figure 3-7 as Y_0) (Kenny, 2002). A thin diaphragm will maximise the amount of deflection that can be detected, and silicon diaphragms are now common as they allow thickness below 1mm and allow integration with electronics.

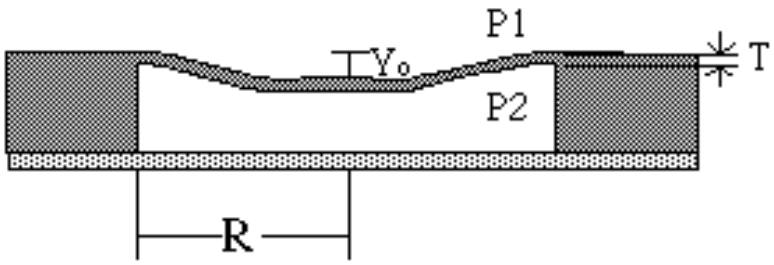

Figure 3-7 Deflection of a Pressure sensor diaphragm (Kenny, 2002)

A common form of a micromachined pressure sensor is a piezoresistive sensor. This uses strain gauges in a Wheatstone bridge embedded into the silicon diaphragm. (Figure 3-8) These strain gauges are typically a p-type dopant, such as boron, diffused into the silicon to form a resistor (Webster, 1999). As the pressure deforms the membrane, the strain causes the bridge to become unbalanced, and causes a change in resistance. This then gives a differential change in voltage across the sensor, which gives an output signal that can be measured.

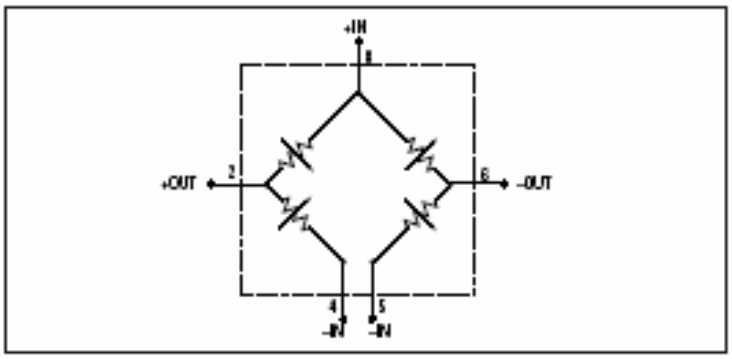

Figure 3-8 Wheatstone Bridge configuration of Strain Gauges(GE Novasensor, 2003)

Figure 3-9 shows the typical construction of a piezoresistive pressure sensor, including the sensor housing and a glass carrier chip that reinforces the sensor die.

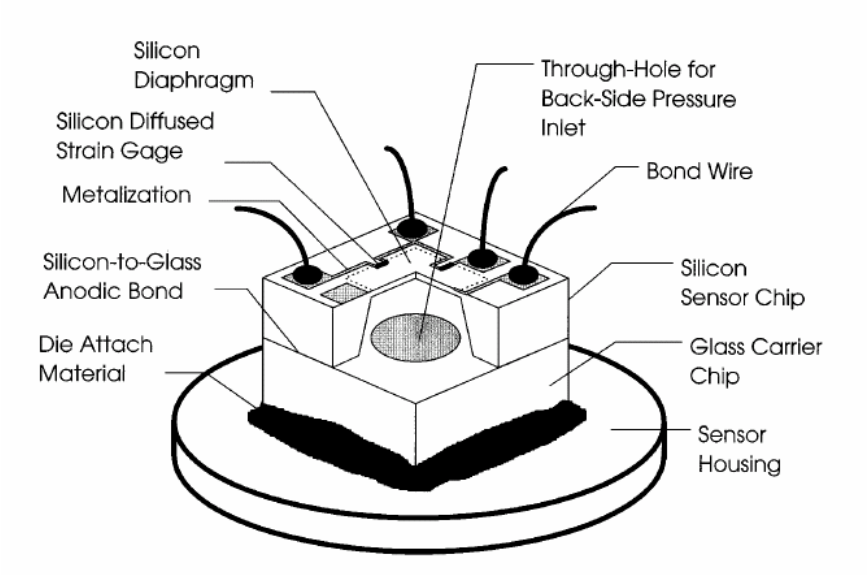

Figure 3-9 Cut away view of the typical construction of a piezoresistive pressure sensor(Webster, 1999)

In order to determine the change in resistance, first the stress σ induced in the diaphragm due to pressure P is calculated. This is given by:

$$\sigma(x) = \frac{3R^2}{8T^2}\left[(3+\nu)\frac{x^2}{R^2} - (1+\nu)\right]P$$

where R is the radius of the diaphragm, T is the diaphragm thickness and v is the Poisson ratio for silicon, which can be taken to be 0.25. x is the position on the diaphragm where the stress is measured. This is greatest where x = R, and so the edges are optimum position for the strain gauges (Webster, 1999).

The strain ε is related to the induced stress σ as:

$$\varepsilon = \frac{\sigma}{E}$$

where E is the Young's modulus of silicon as previously stated and is given as 190×10^9 Nm^{-2}. This in turn can be used to calculate the change in resistance R as:

$$\frac{\Delta R}{R} = K\varepsilon$$

K is the gauge factor and for semiconductor materials is approximately 100. If this change in resistance is too small, it follows that the change in the output signal cannot be detected.

Using the minimum measurable strain ε_{min} stated in the previous section, the minimum change in resistance can be found. If $\varepsilon_{min} = 5 \times 10^{-7}$, the minimum measurable resistance change can be calculated to be 0.005%. If a single silicon atom is used as the diaphragm, at a pressure of 100 kPa, with the radius R taken as the radius of the atom, 0.117 nm and the thickness T taken as the diameter of the atom, 0.234 nm, using the above equations the change in resistance is calculated as 0.00395%. This is lower than

the minimum measurable change discussed above. If the thickness is doubled to 0.468 nm and the radius multiplied by a factor of 6 to 0.7 nm, the resistance change then becomes 0.0088% - this is equivalent to a diaphragm that is 3 atoms wide and 2 atoms thick. It is likely that this is the minimum size allowable for a diaphragm to give a detectable signal, although it appears that this model is inappropriate at very small dimensions.

There is also a maximum limit to the diameter of the diaphragm set by the yield strain of the material. For a silicon diaphragm, the maximum fractional change in resistance caused by the maximum strain allowable is in the order of 1 – 2 % (Gad-el-Hak, 2002). For a typical pressure range of 2.5 kPa and with a diaphragm thickness of 20 μm, the maximum radius is calculated to be 2.8mm. For the same pressure range and a thickness of 2 μm,(paper) this maximum becomes 0.285 mm (or 285 μm). At a range of 100kPa, the maximum for a thickness of 2μm is 45μm.

The resistors that form the strain gauge also limit the minimum size that the sensor can be, however these are also subject to user specifications. Reducing the length of the resistors lowers the resistance and therefore increases power consumption, which would be undesirable for a low power application. Also if the resistor covers too much of the diaphragm between the two maximum strain points at the centre and at the edge, the output is subject to averaging effects, and this compromises the sensitivity of the sensor. (Gad-el-Hak, 2002) Again, it is the user's choice as to whether a reduction in sensitivity is worth a small reduction in dimensions.

3.3.2 Information Processing

Information processing is the part of the system that takes the sensors' findings and performs some function on them. This ranges from a simple analogue to digital conversion using a capacitor to complicated calculations made on a supercomputer. The fundamental limits of information processing rely on thermodynamics, quantum mechanics and electromagnetism. Thermodynamics dictates that the minimum energy required per binary operation or bit of information, or the Entropy of the system, is given by

$$E = \Delta S = k_B T \ln 2 \qquad (1)$$

where ΔS = change in Entropy
E = Energy
k_B is Boltzmann's Constant
and T is Temperature.

This relates the energy dissipated as heat as the entropy of the system increases per bit of information processed. As the energy of the input is different from the energy of the output, this is then known as irreversible computing (Frank, 2002).

The Shannon Limit (cited in Keyes, 2001) for the capacity of bits in a channel implies that the minimum energy per bit must be much greater than the noise power per unit bandwidth. In the case of thermal noise, this means it must be greater than $k_B T \ln 2$.

This and the Heisenberg uncertainty principle can be used to calculate the minimum size of a component element or switch which comprises the processor (Zhirnov, Cavin, Hutchby, and Bourianoff, 2003). The uncertainty principle states that the minimum size x_{min} is given by:

$$x_{\min} = \frac{\hbar}{\Delta p}$$

where p is defined by $\sqrt{2m_e E_{\min}}$

Therefore x_{min} can be defined as:

$$x_{\min} = \frac{\hbar}{\sqrt{2m_e k_B T \ln 2}}$$

where $m_e = 9.10939 \times 10^{-31}$ kg, $k_B = 1.38066 \times 10^{-23}$ JK^{-1}, and $\hbar = \frac{6.63 \times 10^{-34}}{2\pi}$ Js.
This means that the minimum component size is between 1.4 nm and 1.6 nm for a range of temperatures between 250K and 330K. Using this minimum size, the maximum density of switches n_{max} that can be integrated per unit area can be calculated.

$$n_{\max} = \frac{1}{x_{\min}^2}$$

For a minimum switch size of 1.5 nm, $n_{max} = 4.7 \times 10^{13}$ devices per cm^2.

Another parameter that can be determined from the uncertainty principle is the minimum switching time. The uncertainty principle can also be written as:

$$t_{\min} = \frac{\hbar}{\Delta E_{\min}} = \frac{\hbar}{k_B T \ln 2}$$

At a temperature of 300K, $t_{min} = 0.04 \times 10^{-12}$ s. Using these values, the power dissipation per unit area can also be calculated. This is given by:

$$P = \frac{n_{\max} E_{bit}}{t_{\min}} = 3.7 \times 10^6 \text{ W cm}^{-2}.$$

This power dissipation is extremely large, especially when compared to a macroscopic object e.g. a light bulb that has a power dissipation of approximately 100 W cm^{-2}. However as a light bulb is on continuously for long periods of time, the power dissipation creates large amounts of heat. If this were the case with the switches, the density of the devices would be limited by the ability to remove heat from the system rather than on the fundamental physics. However as the switches are only active for short intermittent periods and not all switches are active simultaneously, the power dissipation is high, but the heat produced is not and therefore heat removal is less of an issue.

Also, in practice, the processor contains others elements such as interconnects in addition to the switches. This means that the density of devices cannot be as high as the theoretical maximum.

The laws of electromagnetism effect the lengths of the interconnects between switches. As the velocity of a pulse through the interconnect must be less than the speed of light, this means that the length of the interconnect, L must be less than the product of the speed of light and the transit time of the pulse (Meindl, 1995). For example, if the transit time is 1 x 10^{-12} s, the interconnect length must be less than 0.3 mm.

3.3.3 Communication

This is the function of the system that transfers the processed data to another external system.

As with information processing, the signal to noise ratio is important for the clarity of the information received by the external system. The limit for this, the Shannon Limit, is –1.6dB, below which no error-free communication can occur (Wertz and Larson, 1999).

Communication can be made in a variety of ways. Perhaps the simplest way is to use a wire to connect the two systems. The size limit here then depends on the resistance of that wire, which is a function of the cross-sectional area of the wire and the length, or distance over which the information must be communicated. The resistance of a wire is given by:

$$R = \frac{\rho l}{A} \ \Omega\text{m}$$

where ρ is the resistivity of the material, l is the length and A is the cross sectional area. This means that the resistance increases for longer lengths and smaller areas, which in turn increases the amount of energy lost as heat and creates more noise on the signal. Therefore, wires with large area and short length are desirable.

Another important factor in using wires for communications is the wire's capacitance. The wire obeys the same trends in its capacitance as a parallel plate capacitor (Aziz, 2004). The governing equation is:

$$C = \frac{\varepsilon A}{d} \ \text{F}$$

where A again is the cross sectional area and d is the distance between two layers of wires. ε is the dielectric constant and is given by $k\varepsilon_0$, where $\varepsilon_0 = 8.85 \times 10^{-14}$ F cm^{-1} and k for $SiO_2 = 3.9$. In order for the capacitance to be low, a small area is needed and a large distance between wires. There must therefore be a trade off between resistance and capacitance in determining the ideal area of the wire. A greater distance between two wires will reduce the likelihood of crosstalk. This is when a switch from low to high in a wire of higher capacitance will cause its neighbour to switch also, creating a false reading. As with the resistance, the shorter the wire, the less capacitance it has.

Other communication options include RF and optical systems. In general terms, RF communications depend on the power and wavelength being transmitted, the area of the antenna and the distance over which it is to be transmitted (Wertz and Larson, 1999). The minimum antenna size is determined by the wavelength, the desired gain and bandwidth. The fundamental relationship for both the Quality factor Q of the antenna and its gain include the terms ka. k is the wavenumber and is related to the wavelength as $k = \frac{2\pi}{\lambda}$ and a is the radius of the sphere enclosing the maximum dimensions of the antenna (Bancroft, 2004). For example, an octave bandwidth requires $Q = \sqrt{2}$ (Hanson, 1981). Using an example frequency of 15 GHz (wavelength λ= 2cm), the relationship $Q = \frac{1}{k^3 a^3}$ (Mclean, 1996) gives the radius of the sphere as 2.83mm. However, Hansen also states that the minimum antenna length required is 0.365λ. From the example, this gives a minimum length of 7.3mm.

Another limit on the size of communications systems is that of diffraction. The diffraction limit determines the minimum antenna diameter needed to resolve transmitted signals from two points, such as satellites, at a given angular separation. The limit can be expressed as:

$$\sin\theta = 1.22\frac{\lambda}{D}$$

Where θ is the angular separation, λ is the wavelength and D is the aperture or dish diameter in metres. This equation is known as the Rayleigh criterion. For example, if two signals 5° apart broadcast on a 2cm wavelength, the minimum antenna diameter needed to resolve the signals is 30cm. The required diameter is reduced as the wavelength is increased. It is clear that the choice of wavelength is an important factor in determining the size of the communications system.

However, in reality, there are other important factors that are user defined such as the amount of power available, the distance over which the signal is travelling and the acceptable amount of free space loss that will reduce the received signal. Waveguides limit the free space losses, however this adds to the overall size of the system.

With optical systems, many of the same laws as RF apply, however the gain of the optical transmitter tends to be larger. Thermal and broadband noise place a limit on the performance of the system, as does the "quantum limit", which is the required number of received photons per pulse for a given error rate (Personick, 1981). If the system contains an optical fibre, the capacity of the fibre is, as with RF communications, dependant on the bandwidth and the power of the signal being transmitted.

3.3.4 Secondary Functions

The three functions described above can be considered to be the three primary functions. Other functions, such as the provision of power and, to some extent, the physical structure of the system can be seen as secondary functions, in that they only become necessary because of the primary functions. For example, if the system did not

need to process information or communicate that information, it would not need power. There are cases where it does not need external power to do so. Where these systems are necessary, there are additional size limits, and these can prove to be the dominant factor.

Any photovoltaic sensor could also be used as an energy converter, as in a solar cell. However if power is required, some form of energy storage will be necessary for times when solar energy is not available. The principles behind this are related to electron flow between a positive anode and a negative cathode that is immersed in an electrolyte solution. When the two electrodes are connected through an external resistor, chemical reactions occur at each electrode that release electrons and allow a current to flow, thus converting chemical energy to electrical energy. The most common characteristic quoted when defining the performance of a battery cell is the Energy Density. This is the product of the cells potential and its capacity. The capacity is given by:

$$Capacity = \frac{26.8ne}{MW}$$

where ne is the number of electrons involved in the chemical reaction and MW is the molecular weight of the material (Helvajian, 1999). The capacity is given in ampere hours per gram. Lithium, for example, has a capacity of 3.8 Ah/g. If it is assumed that a minimum of two atoms are required for the reaction, it can be calculated that this would have a mass of 2.3×10^{-23} g and would have a capacity of 8.76×10^{-23} Ah. The energy density = $Ah\ V$ and is expressed in Watt hours, which can then be expressed either in terms of mass or volume (Helvajian, 1999). Hence, the required current and voltage of the system is directly related to the size and mass of the battery which may well be the largest feature of the system.

As discussed above, the change in the entropy of the system can mean that a proportion of the energy is dissipated as heat. This can heat up the system and cause the amount of thermal noise to rise. This can cause significant problems as the density of circuits in a system, for example, increases as the size of the individual circuit is reduced. In order to compensate for this effect, a thermal regulation function becomes important to remove or redistribute this heat. Again, these "secondary" parts of the system, such as radiators may prove to be a critical factor in the determination of the size of the system.

3.4 Other Constraints and Drivers

There are other limiting factors and drivers that are not related to one function in particular, but are more general. Perhaps the most general fundamental limit is that of the speed of light. This is not only a limit in terms of optical communication, but also, for example, that it is the fastest that information can travel, and so limits rate of computation (Feynman, 2001). Other more general limits can be grouped as either material properties or environmental factors.

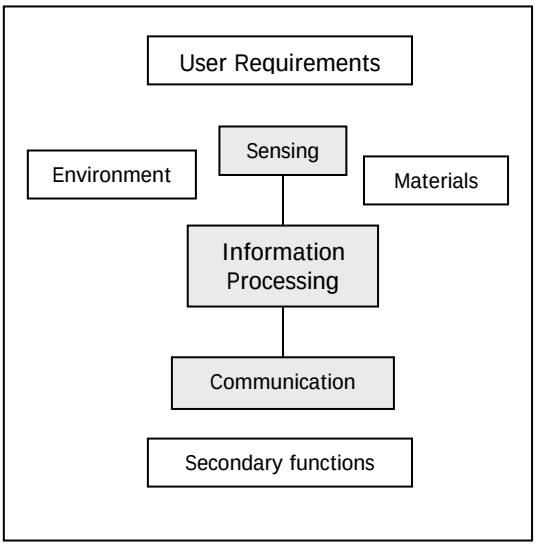

Figure 3-10 System functions with constraints and drivers

3.4.1 Material properties

A critical constraint on the system is the material that it is made from and the properties of that material. Thermal, electrical and mechanical properties, such as its conductivity and melting point, all affect how the material behaves, and how it will react as the size of the system is reduced. This is especially true for semiconductors, which have significantly different properties to that of metals.

In the wire example in the previous section, the resistance, and therefore the effectiveness of the wire as a communications system, depends on the resistivity of the material as well as the wire's area and length. Hence, the choice of material will directly affect the performance and will influence the acceptable minimum size. Just a few years ago, the use of wire would have been considered impractical for communications, however with superconductors, and especially "High T_c" superconductors, it now may look particularly attractive for missions where there is a low temperature environment.

One fundamental material property that clearly limits the size of any system is that of atomic radius. The atomic radius of Hydrogen, and thus the limit to atomic size, is 0.046nm (Shackleford and Alexander, 2001). The radius of a silicon atom, the most common material for semiconductors, is 0.117nm. It is difficult to conceive of a system smaller than that of a single atom.

3.4.2 Environmental

The external environment provides other constraints on the system. One of the most significant is that of the temperature. For example, the temperature drives the amount

of thermal Johnson noise, as well as having an effect on the material properties of the system. A number of fundamental thermal limits involve the relationship k_BT, and so are related to Thermodynamics.

Other constraints from the environment include the effect of background EM radiation as a noise limit for RF receivers and certain sensors, and how the environment acts as a baseline for all sensor readings, and will therefore determine the sensitivity of the sensor needed with respect to the background noise. Other effects will also be caused by particle radiation. There is also man-made noise in the EM Spectrum that may be present in the environment. Any system will need to look carefully at potential interference sources.

The magnitude of these constraints differs depending on which environment is under investigation. This is where sensors for planetary exploration will show significant differences from their terrestrial counterparts. The baseline for which the sensors must be calibrated for the Martian surface or for a Deep Space mission, for example, will differ from those sensing on Earth, as will the nature of the environmental features being investigated. This may affect the choice of material used or determine whether a thermal regulation system is required, as well as affecting the thermodynamics of the system and influencing the choice of sensor. Also, the destination will determine the maximum allowable mass for the system, especially where the mass allocated for the payload at launch is critical. Although not a fundamental limit, planetary exploration sensors are likely to be required to limit their mass, and this provides an additional constraint on the size of the sensing system.

The limitations on the size of a system on Mars are expected to be mostly related to the extreme thermal environment. Although low temperatures such as those experienced on Mars reduce the effects of thermal noise, at low temperatures the thermodynamic effects on electrons mean that electronic systems fail. Therefore addition insulation may be required which will increase the size of the system. Other system size requirements that may be influenced by the Martian environment include the communications system, which will have to have a larger antenna or use more power due to the increased distance of transmission.

3.4.3 User requirements

A driver that greatly influences the minimum size of the system is that of the user requirements and what is defined as acceptable performance.

These requirements can be part of the mission design, such as the mission lifetime or the architecture of the communications system. An extended lifetime will ultimately mean that the reliability of the system as a whole must be high. This could mean that redundancy for critical systems would be necessary, which will increase the overall size. Additional consumables may also be required, which will require storage space. If the sensor systems are small enough and could be organised into a network, many systems could be deployed for the same mass limit. In this case, the individual reliability could be lower, as long as the overall reliability of the system, and its ability to perform over the desired lifetime, remains at the required level. This concept of a network would

also have an effect on the communications architecture and over the distance of which the information must be transmitted. This distance is decided by the user, whether it is a short distance to another sensor system or for transmission from the planetary surface to an orbiting spacecraft, and will impact system parameters such as the transmitter size and the minimum acceptable received power, which may require some form of additional amplification equipment.

Another key limit, which is related to reliability, is that of statistics and the acceptable probability of error. In many cases, the smallest size or the minimum energy depends on the probability of an error occurring. For example, if memory is a form of charge stored on a capacitor, the minimum charge must then be a multiple of the charge caused by a soft-error. Soft errors are non-reproducible and are generally caused by stray energetic radiation (Keyes, 2001). This minimum would probably need to be higher in a space environment, which would impact on the minimum size of the capacitor, or would require shielding, again adding to the overall size. However, if the acceptable error rate, or the frequency of which this effect occurs, is high, then the corresponding minimum size can be much lower. Another example is that of a photon detector. The detector could be as small as one atom, however the probability of the desired photon hitting this target is very small. As the required probability increases, the size of detector must also increase. Smaller systems are also more likely to be subject to other forms of noise, the effects of which are negligible at larger sizes. Overall, the higher the acceptable probability of error, the smaller the system size can become. The acceptable resolution, be it spatial, temporal or measurand, of the system is another user defined limit

The functionality of the individual system is another user defined requirement that can impact the minimum size of the system. If the system only includes one form of simple sensor, or is not required to actively communicate, then the minimum size naturally becomes reduced. This desired functionality must therefore be traded off against the systems dimensions. The next section discusses this idea in context of one of the smallest possible sensors – the molecule.

3.5 Examples

This section shows examples of systems created based solely on the fundamental relationships. This first example considers a molecule as an example of small sensing device. The second is the example of a simple sensing system containing a sensor, an information processing device and a way of communicating its findings. This example is then compared with examples of real spacecraft and planetary sensing systems.

3.5.1 The Molecular sensor system

Perhaps the smallest sensor system can be considered to be a molecule. Although a single atom would be smaller, it would be much harder to measure and monitor, but a molecule may be detectable.

If the properties of the molecule were well known, for example the way it reacted to other elements or to temperature or radiation, it could be used to monitor certain features of a given environment. Any chemical reactions could be considered to be a method of information processing. The molecule itself would not be able to actively communicate, however if its reactions could be monitored or the molecule was interrogated, this could be a form of passive communication. Although the molecule appears to have all the functions necessary to perform as a sensing system, its functionality, and the data that could be taken regarding its environment, would be extremely limited.

In order to avoid false readings and random fluctuations in the data, a great number of the sensing molecules would have to be deployed. The number again would be determined by the acceptable probability of error set by the user.

However, if the molecule was one that was not naturally occurring in that environment, the release of vast amounts of an unnatural chemical into a planetary environment is likely to have a serious impact on that environment and could lead to problems with contamination. The acceptable limit of this contamination could be defined as another potential user requirement. This could make the molecular sensing system an unattractive option.

3.5.2 A Simple Sensing System Example

The following is an example of a simple sensing system, which will be used to demonstrate the minimum size a system could be based on physical principles.

The sensing element comprises a photovoltaic cell that will act as a photon counter. The cell produces a flow of electrons, which in turn charges the top plate of the capacitor. This plate is attached to a spring, so as the charge increases, the two plates are forced together. At a predetermined point, which corresponds to a certain number of photons, the plate reaches a switch and the capacitor is discharged. This part of the system acts as a digitiser and is therefore regarded as a form of information processing. This packet of information is then passed to a transmitter to be communicated. In this case, the example shows an LED. This could be used on its own or be a part of an optical fibre system.

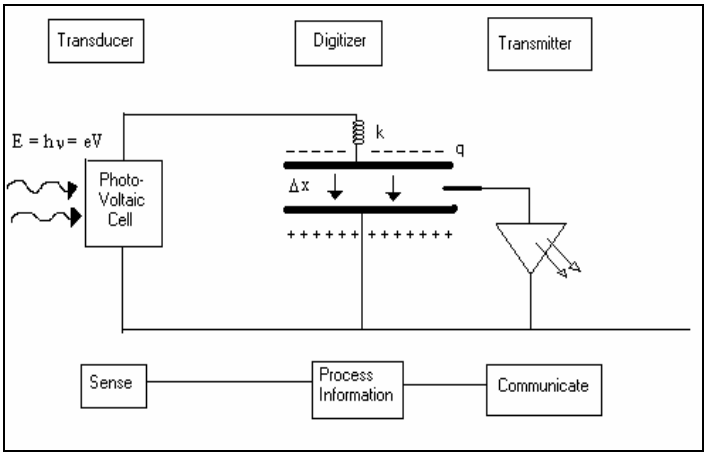

Figure 3-11 A schematic of a simple sensing system

3.5.2.1 Transducer – Photovoltaic cell photon detector

The minimum size for the photovoltaic cell photon detector is related to the wavelength of the radiation it is measuring. This is to capture the incident energy efficiently: the minimum dimensions for a cell to detect visible light would be 400nm, since this is the lower limit on the wavelength of visible light.

This photon detector is essentially an illuminated pn-junction. A photon is absorbed and transfers energy to an electron within the junction, creating an electron hole pair (EHP). The energy in the photon is dependant on its wavelength and is given by

$$E = \frac{hc}{\lambda}$$

where h is planck's constant, c is the speed of light and λ is wavelength.

The energy in the photon must exceed the Bandgap energy E_g of the semiconductor material to be absorbed. Even if the energy greatly exceeds E_g, only one EHP will be produced. The remaining energy is lost as heat and other losses.

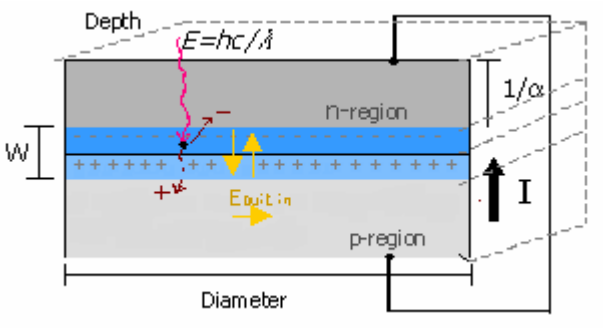

Figure 3-12 The principles behind a photodiode

When an EHP is generated inside the junction – coloured blue in the diagram above, both charge carriers (electron and hole) will be acted upon by the Electric field, E, built into the junction. As the field runs from the n-side to the p-side, the field causes the

electrons to move towards the n-region and the holes towards the p-region. Although carriers are present in each region, excess concentrations of charge carriers appear at each side of the junction. The addition of charge carriers to each side results in a flow of current in an external circuit. This flow of photocurrent, I, is proportional to the number of EHPs generated in the junction, which in turn is proportional to the number of photons absorbed. The upper limit for this photocurrent is given by:

$$\Delta I = -qAF_{ph}$$

where F_{ph} = number of photons per unit area per unit time per unit wavelength incident on the cell.

Since the thickness of the cell must be such that the incident light is absorbed, the thickness of each region must be related to the absorption constant, in this case its inverse ($1/\alpha$), for that material. This constant depends on the material and the wavelength of the incident light. A graph showing the relationship between the absorption constant and wavelength for Silicon is shown below.

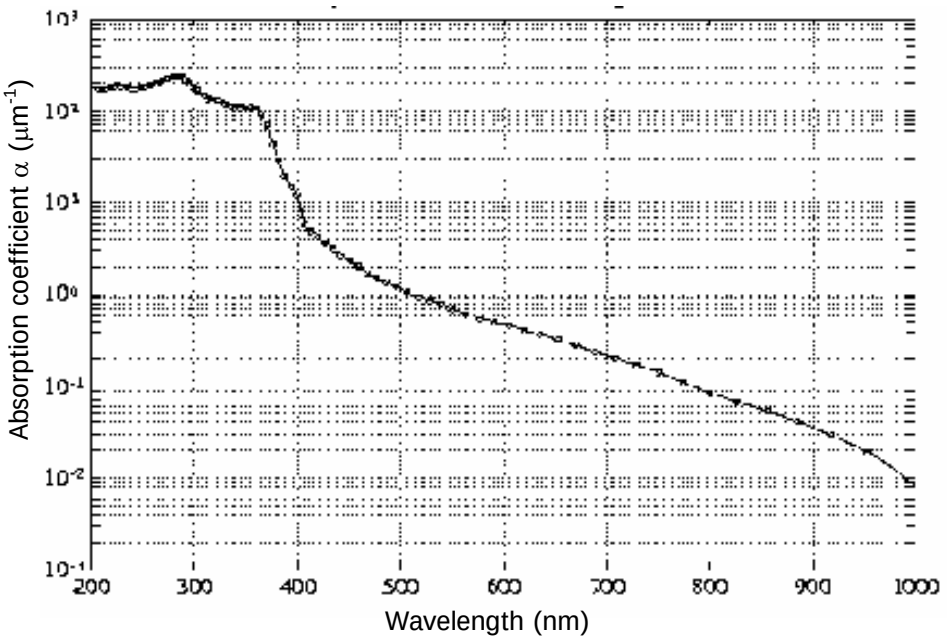

Figure 3-13 Absorption coefficient vs Wavelength for Silicon (Moini, 1997)

From this graph, it can be shown that for a wavelength of 400nm, $\alpha = 10\mu m^{-1}$, meaning that the minimum thickness for each region, excluding the junction, must be at least $1/\alpha$ = 0.1 μm or 100nm. For a wavelength of 700nm, this minimum thickness of the region increases to 5 μm.

The width of the junction itself is related to Gauss's Law, as the junction is a region that contains electric charge (Messenger and Ventre, 2000). Since the junction must have an equal number of charges on either side, it can extend further into the n-region or p-region depending on the relative doping of each side. For example, if the number of donor ions (N_d) in the n-region is higher, and so is greater doped, than the number of

acceptors in the p-region (N_a), then the junction extends further into the p material to cover the same amount of charge as in the n material (Streetman, 1980). The total width of the junction is therefore the sum of the penetration into n (x_{n0}) and the penetration into p (x_{p0}). Using Gauss's Law, the maximum value of the electric field E, in the junction can be found in relation to the charge, the permittivity, ε, of the material, the doping (N_a and N_d) and the relative penetrations (x_{n0} and x_{p0}).

$$E = -\frac{q}{\varepsilon} N_d x_{n0} = \frac{q}{\varepsilon} N_a x_{p0}$$

The contact potential of the junction, V_0, is related to the integral of the Electric field over the width of the junction (W), so it can be shown that:

$$V_0 = -\frac{1}{2}\varepsilon_0 W$$

Therefore, the total width W (Streetman, 1980) can be given by

$$W = \left[\frac{2\varepsilon V_0}{q} \left(\frac{1}{N_a} + \frac{1}{N_d} \right)^{1/2} \right]$$

For example, if an n-type silicon sample ($N_d = 10^{16}$ cm^{-3}) is alloyed with Aluminium ($N_a = 4 \times 10^{18}$ cm^{-3}) to form a junction, and if the temperature T is assumed to be 300K, the contact potential V_0 is calculated (Streetman, 1980) as:

$$V_0 = \frac{kT}{q} \ln \frac{N_a N_d}{n_i^2} = \frac{1.38 \times 10^{-23} \cdot 300}{1.6 \times 10^{-19}} \ln \frac{10^{16} \cdot 4 \times 10^{18}}{\left(1.5 \times 10^{10}\right)^2}$$

$$= 0.85\text{V}$$

where n_i represents the intrinsic carrier concentration, in this case of silicon.

From this the width of the junction can be calculated:

$$W = \left[\frac{2\varepsilon V_0}{q} \left(\frac{1}{N_a} + \frac{1}{N_d} \right) \right]^{1/2} = \left[\frac{2\left(11.8 \cdot 8.85 \times 10^{-14}\right) \cdot 0.85}{1.6 \times 10^{-19}} \left(\frac{1}{4 \times 10^{18}} + \frac{1}{10^{16}} \right) \right]^{1/2}$$

$$= 0.334\ \mu\text{m}$$

where ε = permittivity of silicon = $\varepsilon_0 \varepsilon_{rsilicon}$

It can also be shown that the penetration into each material is:

$x_{p0} = 3.3267 \times 10^{-5}$ cm
$x_{n0} = 8.3 \times 10^{-8}$ cm

Given the calculated width of the junction and the absorption coefficient of the material, the minimum size of the photodiode to measure photons of wavelength of 400nm is:

100nm + 334nm + 100nm (minimum)

≈ 600nm.

However, for 700nm wavelength, this rises is approximately 10μm.

For use in photon detectors, the current produced in these diodes is largely dependent on the optical generation rate and therefore, the speed of the response of the diode. In order for this to be at its most efficient, W must be wide enough so that most of the photons are absorbed within the junction rather than in the neutral n and p regions. However if W is too wide, the time required for the generated carriers to drift to the edges of the junction becomes excessive and the sensitivity is lost.

The Photocell can be viewed in terms of an equivalent circuit. This circuit comprises a current source, resistors and a capacitor.

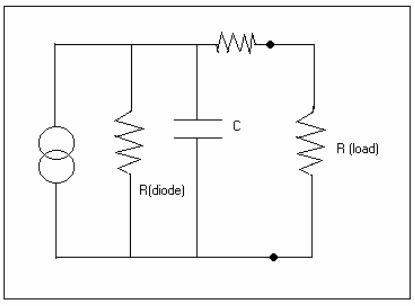

Figure 3-14 Equivalent circuit for a photovoltaic cell

The detector has two types of capacitance associated with it. The junction capacitance C_j is due to the dipole within the junction. The voltage lagging behind the changing current caused by charge storage effects results in the second type of capacitance, the charge storage capacitance C_s. Although both are important, the first becomes dominant if the junction is reversed-biased and the second if it is forward-biased (Streetman, 1980). The formula for calculating the junction capacitance can be seen to be comparable with that of a parallel plate capacitor:

$$C_j = \frac{\varepsilon A}{W}$$

where the junction width W is equivalent to the separation of the plates. It can be seen that a wide W would then result in a small junction capacitance, which would in turn reduce the RC time constant of the circuit and increase the speed of response.

The charge storage capacitance C_s is time-dependant. Any change in current, I, must lead to a change to the charge stored in the carriers. The time-dependence is due to the time taken to build up or deplete this charge. This can be calculated using

$$C_s = \frac{q}{kT} I\tau_p$$

where τ_p is the recombination lifetime for the holes in an n-type material.

From this example, it appears that the minimum size for the photon detector is 400nm x 400nm x 600nm. The photocurrent, I is related to the number of photons detected and the time taken to detect them. Both of these are user-defined requirements.

3.5.2.2 Digitiser - Capacitor System

If the capacitance of this capacitor is less than that of the junction capacitance, less charge will be passed from the photocell to the digitiser. If it is greater, then digitiser sensitivity will be lost. Thus, it can be assumed that these must have approximately the same capacitance. The formula for calculating the junction capacitance has been shown to be

$$C_j = \frac{\varepsilon A}{W}$$

This is the equivalent to the formula for the parallel plate $C = \frac{\varepsilon A}{d}$, and so therefore the plate separation d must be equal to the junction width W, which in this case is 0.334μm.

In order to perform the information processing function on the system, ideally the effect of the background radiation must be subtracted from the data readings. This could be done in several ways including using a resistor to leak away the excess charge caused by this effect.

At these small dimensions, the effect of thermal noise becomes important. The spring system will be prone to this form of noise. The average extension of the spring system can be calculated in relation to the equilibrium point of the kinetic and potential energies. The potential energy of the spring is given by

$$E_p = \frac{1}{2} kx^2$$

where k is the spring constant.

The kinetic energy of the spring can be equated to $E_k = k_B T$, or the thermal energy, where k_B is Boltzmann's constant. If the two are in equilibrium, then

$$\sqrt{x^2} = \sqrt{\frac{2k_B T}{k}}$$

This will result in additional movement of the suspended capacitor plate, which if it is too much will cause the plates to discharge in error. The collected energy required for a discharge pulse must therefore be greater than the thermal energy, which at 300K is 4.14×10^{-21}J. The key factors in minimizing this noise are therefore the choice of spring constant for the system and the external temperature, which again are user requirements.

There will be some heat dissipated in the system, due to resistance. This energy needs to be removed from the system, by radiation or conduction for example, to avoid

excessive temperatures and therefore increased noise and reduced reliability. The user requirements will determine the acceptable error rate and thus the cooling requirement. The external temperature, which is a parameter of the environment, will also play a significant role.

The minimum size of the spring is dependent on the number of coils and its material properties, in particular the modulus of rigidity G. The equation for the spring constant k (Engineers Edge, 2000) can be rearranged to give an equation relating the mean spring diameter D and the diameter of the wire d,

$$D^3 = \frac{Gd^4}{8kn}$$

These two variables can be plotted against each other. The minimum must be the point where diameter of the wire exceeds that of the spring. This point varies for different spring constants and number of coils, however in general this point appears to be at approximately 100nm.

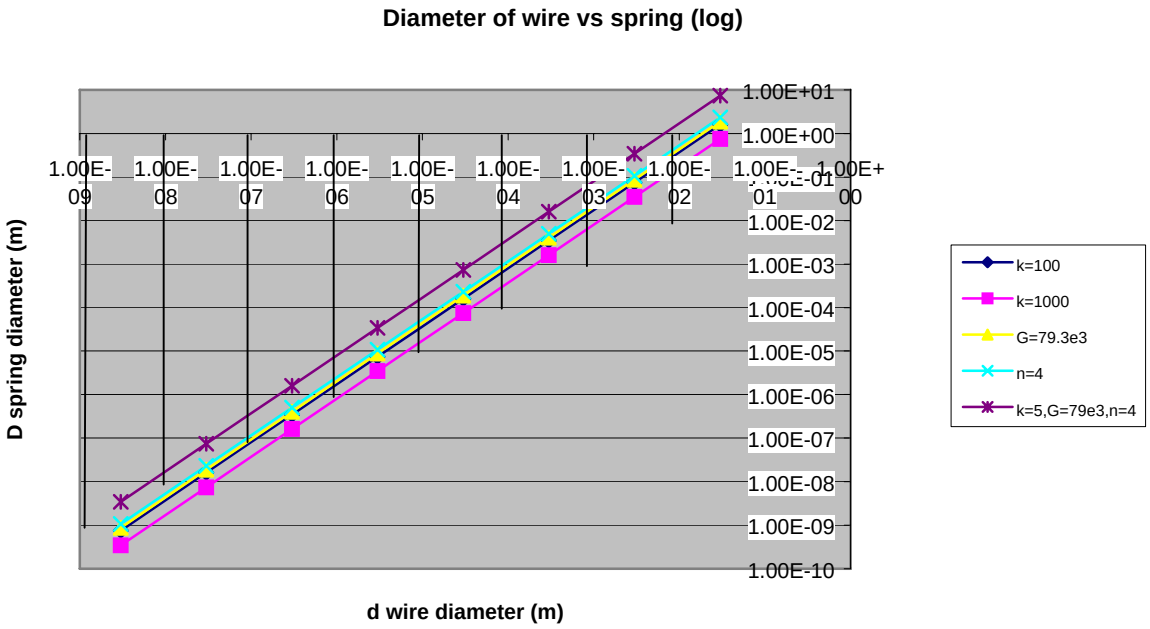

Figure 3-15 Graph showing the diameter of wire versus the diameter of the spring

As charge is collected on the plate, the spring extends and the distance between the plates varies as

$$\Delta d = \frac{q^2}{2k\varepsilon_0 A}$$

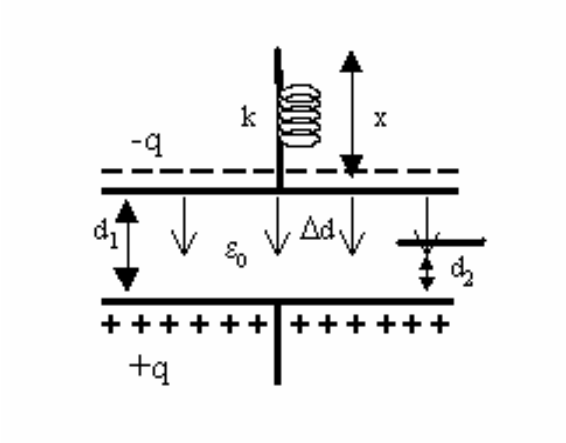

Figure 3-16 A spring/capacitor system

The rate of plate discharge can be considered to be the processing speed or data rate of the system. Assuming the distance between the two plates has to decrease to half its initial value to discharge, $\Delta d = 0.167$ μm and the spring constant k=100, the charge required to retract the plates can be calculated as:

$$q^2 = \Delta d \cdot 2k\varepsilon_0 A = 4.73 \times 10^{-29}$$

$$q = 6.88 \times 10^{-15}\,\text{C}$$

where the area A is given as 400nm x 400nm, $\varepsilon_0 = 8.85 \times 10^{-12} \text{C}^2\,\text{N}^{-1}\text{m}^2$.

As each photon arriving at the photodiode produces an electron with a charge of 1.6×10^{-19} C, 42982 electrons will be needed to discharge the capacitor system. Assuming a photon arrival rate of 6.02×10^{17} photons $\text{m}^{-2}\,\text{s}^{-1}$, for this detector approximately 96000 photons arrive per second. This means that the capacitor is discharged 2.2 times per second. If 1 discharge is regarded as 1 bit of data, this means a data rate of 2.2 bps.

The capacitance changes with the separation of the plates. As the distance decreases from d_1 to d_2, the capacitance increases. Since the energy of a capacitor system is given as

$$E = \frac{q^2}{2C}$$

and the charge q is assumed to be constant at the point of discharge, the energy therefore decreases as the capacitance increases. If the method of communication is an LED, the energy of the system must be at least equal to the bandgap energy of the LED in order to illuminate it, which in the case of silicon is 1.107eV. This limits the capacitance, and therefore the area and separation distance of the capacitor. In this case, assuming a final separation capacitance of

$$C = \frac{\varepsilon A}{d} = \frac{8.85 \times 10^{-12} \times 400 \times 10^{-9} \times 400 \times 10^{-9}}{0.167 \times 10^{-6}} = 8.48 \times 10^{-18}\,\text{F}$$

The energy of the system is calculated as

$$E = \frac{q^2}{2C} = \frac{4.73 \times 10^{-29}}{2 \times 8.48 \times 10^{-18}} = 2.79 \times 10^{-12}\,\text{J}$$

which is many times greater than the required bandgap energy.

3.5.2.3 Transmitter – LED

An LED represents the communication part of the system here. In order to release photons, the energy must be greater than that of the bandgap of the material. As previously stated, this places another limit on the minimum energy that can be passed for the digitiser. An LED as part of an optical communication system that includes an optical fibre, could prove to be a fairly efficient system. Again the size limit of the fibre would be related to the wavelength of the light sent along it. This, however adds additional mass to the system. If the LED were to be used without such a waveguide, a significant portion of the energy will be diffused, and would make this a very lossy system. The receiver would have to be very close by in order to detect a sufficient amount of photons.

This example shows that the size of this system is closely related to the wavelength of the radiation it is detecting, the chose of materials, the external temperature and the error that is acceptable to the user. Overall the minimum size of this system is in the order of microns (10^{-6}m). It can be assumed that the system described is a silicon cube of 1.5µm x 1.5µm x 1.5µm, with mass of 7.86×10^{-15} kg (assuming the density of silicon = 2330 kgm^{-3}.)

3.5.3 Comparison to existing spacecraft

There are many possible directions that future planetary exploration could take. Concepts currently under investigation include Autonomous Rovers and sophisticated networks of landers, both designed to explore and examine specific areas of a planetary surface, as well as the more traditional remote sensing satellites. Another option that is being investigated to monitor Earth environments is that of distributed “lab-on-a-chip” sensor networks – a concept that is also currently being adapted for use on other planetary surface environments.

The following is a size comparison of various forms of planetary exploration spacecraft including satellites, landers, rovers and the microsystem examples given below.

Name	Type	Dimensions	Mass	Power	Data Rate	
SNAP-1[a]	Nanosat	33x45x50 cm	8.3 kg	9.1W	76.8 kbps	User specified platform
Artemis / Opal [b]	Picosat	20.3x7.6x2.5 cm	1 kg	6.9W	1200 bps	Demonstrator
Beagle 2[c]	European Mars Lander (2003)	64 cm diameter, 23 cm height	33.2 kg	87W	128 kbps	inc camera and spectrograph
Sojourner[d]	NASA Mars Rover (97)	63cm x 48cm x 28cm	11.5 kg	16W	9600 bps	
Sensor Web[e]	Sensor network for Mars (JPL)	volume $20cm^3$ per node	50g per pod	50μW	20 kbps	temperature and light sensors plus processor
Fundamentals example	theoretical example	≈ 1.5 μm x 1.5 μm x 1.5μm	7.86×10^{-15} kg	5.58×10^{-12} W	2.2 bps	simple photon detector and capacitor system. One sensor only.

a (SSTL, 2000), b (Valdez, Hu, Kitts, Breiling, Slaughterbeck, Ota, Hadi, Kuhlman, and Lyons, 1999), c (Open University, 2002), d (JPL, 1996), e (Delin and Jackson, 2000)

Table 3-1 Comparison of example Planetary Exploration devices and satellites

In order to compare the systems, three figures of merit were derived. Since mass and size are the key points under discussion, the first figure of merit compares the density. Both the communications and power subsystems can also have significant influence on the overall size of the hardware. Figures of merit comparing the power per unit volume and data rate per unit mass are calculated. These values are reported in the table.

	Density ($g\ cm^{-3}$)	Power per volume ($mW\ cm^{-3}$)	Data Rate per unit mass ($kb\ s^{-1}\ kg^{-1}$)
SNAP 1	0.11	0.12	9.25
Artemis	2.63	18.2	1.17
Beagle 2	0.45	1.18	3.86
Sojourner	0.14	0.19	0.815
Sensor Web	2.5	0.0025	4000
Example	2.3	1.65	2.8×10^{14}

Table 3-2 Derived figures of merit comparing various spacecraft

In general for the practical systems, the smaller devices such as the picosat and sensor web node have a higher density. This is expected as they have same functionality as their larger counterparts but in a much smaller volume. A low power per unit volume could be interpreted as a higher proportion of the device does not require power, for

example the wheels on the rover. The highest data rate per unit mass is for the sensor web node, which uses MST components for its transmitters, but only has to transmit over small distances. For its size, the sensor web node gives the overall best results of low power and high performance.

From this simple comparison, it can be seen that there is a considerable size difference between the theoretical example shown here and existing or proposed spacecraft. As discussed these differences are likely to be due to current technology and the defined user requirements rather than the theoretical principles governing the size of each part of the system.

3.6 Discussion

In general there are very few physical laws that fundamentally limit the size of the sensor system. However, applying these laws blindly to identify the smallest possible size could lead to a sensor system whose lifespan is a few microseconds and whose communication capability is a few bits per second, which although it is physically possible, is practically unattractive. The governing factor then becomes the user requirements e.g. data rate, reliability, resolution and required communication distance. These can be regarded as a necessary overhead on top of the minimum size dictated by the Laws of Physics.

The minimum practical size will also vary according to the environment in which the sensor system has to operate. The thermal noise limit will be vastly different for a detector close to the Sun to one at the outer reaches of the Solar System. The necessary power of a communication system will also depend on interference from man-made sources.

It is clear that there is no single answer to the question – what are the limits to miniaturisation? The example in this paper showed that a simple sensor system could be $<10^{-6}$m compared to current systems in the mm scale or greater. The application of user requirements and environments is likely to increase this size significantly to give a range that spans many orders of magnitude.

However, as the scale of individual devices is reduced to the sub 50nm level, the effectiveness of the traditional CMOS designs beings to break down as the fundamental limits are approached. Therefore new devices are under development that are better suited for operation at smaller dimensions and also utilise the quantum mechanical effects that become significant at this level. Single-electron devices maintain their scalability even at atomic level and are designed to control the flow of single electrons. It is proposed that if these devices are used as part of a larger integrated circuit, a higher level of integration will be achieved, as well as lower power consumption, since power is proportional to the number of electrons transferred for a voltage source to the ground (Waser, 2003).

The smallest single-electron device, called a single electron box, comprises of a quantum dot connected with two electrodes. One electrode is connected through a tunnelling junction and the other via an insulator through which an electron cannot pass

by quantum tunnelling. This takes advantage of Coulomb's law and the uncertainty principle. Single-electron switching devices are also essential parts of any larger circuit. Single-electron transistors are three terminal switching devices which transfer electrons from the source to the drain individually. These transistors have tunnelling junctions instead of the traditional pn junctions. Tarucha *et al*. (cited in Waser, 2003) have produced a vertical Single-electron transistor, where the quantum dot is in the centre of a pillar. The dot is a few hundred nanometres in diameter by 10 nm deep. This is separated from the conducting material of the pillar by two non-conducting heterostructure barrier layers. The negative voltage is applied to a side gate around the pillar and squeezes the diameter of the dot, reducing its number of electrons until empty. Although the single-electron transistor has good scalability and low power consumption it does have its disadvantages. The operation is currently limited to low temperatures. At room temperature, the quantum dot must be less than 10 nm, which is difficult for current technology. The transistors also have a high output impedance due to the high resistance of the tunnel junctions. Finally the source-to-drain voltage must be lower than the gate voltage swing since the source-to-drain voltage easily affects the potential of the dot, and this affects its use as a gate controlled switching device. These transistors also cannot control the timing of the single-electron tunnelling. For this a single-electron turnstile or a single-electron pump is required. These devices are also under development. These devices are considered to be the future of nanoscale technology.

Nanotechnology has been identified as a significant technology for use in future planetary exploration missions. However in a business context, this is only a small and specialised part of the overall space market, and may not be able to justify the investment needed to develop this technology. The advances that will need to be made in the field of Nanotechnology are unlikely to be driven by the space industry, which makes up a tiny proportion of the emerging Nanotechnology market when compared to industries such as Automotive, Biomedical and Military. It is likely that significant advances will be made in these areas, so the space industry may have to adapt systems that are developed by others in order to utilise this technology in the near future.

3.7 Conclusions

Although the Laws of Physics can be used to determine a minimum size for a sensor system, in the practical world, it is factors other than the laws of physics that drive these limits and are highly significant in the determination of the actual size of the system. Factors such as the user requirements and environment are critical. The effect of these appears to be greater the smaller the system becomes, and as such may prove to be the actual limit to miniaturisation. The smallest existing system investigated was still substantially larger than the theoretical minimum size.

Factors such as the operational environment, the required functionality of the device and the eventual application will have to be taken into account when designing the deployment simulations and the final prototype systems design. Since this system is to use COTS technology, the current state of the art regarding miniaturisation provides another design constraint, rather than any of the fundamental governing laws.

4. Management and Strategic Issues of the Space Industry

4.1 Introduction

Objective 2 of this project is:

"*To investigate the Space Industry and its related strategic issues, identify possible future markets and scenarios for MST and these sensor devices and investigate the importance of innovation and technology transfer in the adoption of MST for Space*."

The Global Space Industry can be described as being characterised by fierce technology driven competition, the need for very high reliability and timeliness of its deliverables and being subject to cyclical developments influenced by external factors.

The aim of this chapter is to introduce the industrial context in which this project is situated and relate it to the bigger picture rather than being an isolated design exercise. The first section of this chapter analyses the current state of the Space Industry in terms of the strategic challenges it faces using recognised Strategic Management models. These models will also be used to investigate a number of scenarios that have or could affect the industry and makes suggestions as to the consequences of these events.

The second section of the chapter examines the factors that will be important in the adoption of Microsystems Technology for widespread use within the industry. One key element in the acceptance of this relatively new technology is that of Knowledge Transfer through the communication of ideas both within the industry and looking to developments made in other fields. This section also examines the possible barriers and facilitators to the adoption of MST.

4.2 Strategic Outline of the Space Industry

The strategic issues faced by the space industry are principally related to its primary customers – the government agencies, and the effect of external factors such as political and social opinion on funding and the distribution of contracts. These issues are examined by using the static Porter's five forces model and a more dynamic PESTLE analysis. Possible scenarios and the effects of past, current and future situations on strategic space issues are also discussed.

4.2.1 Background to the Space industry

The Space industry is unusual. Its main customers tend to be Government agencies, such as the European Space Agency (ESA) or NASA in the USA, in addition to a few commercial customers in the communications satellite market. The agencies have different classes of mission, which range in size, budget and importance. Opportunities are announced for these missions and collaborations of universities and companies bid to be the Prime Contractor to design and build the spacecraft, its instruments and experiments. There are companies that specialise in producing components for

spacecraft, however much of the expertise is contained in-house or sourced from others within the bid consortium.

During the “Glory Days” of the Space industry, at the height of the “Space Race” between the USA and the USSR, funding for space related projects was extravagant, as winning this “race” was considered a top priority by the Governments of the day. Since the majority of the funding available to the Space industry is still government controlled, it is subject to the effects of public opinion and is in competition with other projects and industries that rely on State money. The effect of shrinking budgets is forcing the industry to look for cheaper alternatives to the current way that spacecraft are built, including adopting technologies not specially developed for use in Space and reducing the scope and development time of missions.

In general, it is a fragmented industry with only limited global communication and cooperation. The Space Agencies distribute contracts so that European missions tend to be led by European companies and the prime contractors for US missions are predominantly US based. The European Space Agency operates a system called "Juste Retour". European nations that belong to ESA pay a subscription, plus a contribution of additional funds to various projects. As a result, the contracts resulting from those projects will be distributed proportionally between member nations depending on their financial contribution This system of geographical return also has implications on the composition of the bid consortiums. Those who include members from preferred nations are more likely to win the contract over an equal proposal made by a consortium composed of less financially generous countries. Hence, the Space industry is a well protected industry with a large amount of national pride.

One example of an ESA programme is Aurora, Europe’s planetary exploration programme. In October 2004, it was reported (Amos, 2004) that the Science Minister, Lord Sainsbury, had committed the interim funds to maintain the UK’s place within the programme. The precise details of the programme are still under discussion, however the UK may be asked to pay around £25 million a year to lead some of the missions. The programme still has to be approved by European ministers, and it is still in its very early stages, however by committing this value of funds, the return to UK based companies is likely to be around 17% of the total project budget, expected to be £150 million a year.

The geopolitical preferences of customers such as ESA also influence other aspects of a project, including component selection. Practical implications of this are the independent development of components within the European Union that may already be available in other countries or changes to the initial design selections imposed by the client.

Another example of political influence is the US International Traffic in Arms Regulations (ITAR). (US Department of State, 1992) This is a federal legislation restricting the export of any defence-related articles and services. This means that any component or technical data, specifically those relating to intelligence and sensing, that have been developed for, or have primary use by, the US military, regardless of its civilian uses, cannot be exported or used by a “foreign person”. This again means that

component selection will be limited to those available or developed within a specific country or area and that, in many cases, independent development of components and other competing technologies by different nations is necessary. This is an example of a potential barrier to the transfer of knowledge regarding new technologies. This concept is discussed further in a later section.

The key national players in the Space industry are the USA and Europe. It is these agencies that are principally involved with space exploration. Russia has a great past reputation for designing robust and reliable hardware, however since the demise of the MIR spacestation, funding issues have reduced Russian space activities, and they now are key providers of satellite launchers. The Japanese Space agency JAXA also has its own launchers and funds research.

Relatively new but growing entrants in the industry are China and India. China has developed its own satellites and launchers and is the third nation to launch a man into Space. India has also developed a launcher and communications satellites and has the largest Space budget of all the developing nations. Other nations are much smaller players. In all there are 30 Space agencies, although 95% of the expenditure in the industry comes from the USA, Europe and Japan (as at 2002). Commercial customers are players in this industry whose importance is growing on a yearly basis. The key players are summarised in Figure 4-1. This information was gathered at the World Space Congress, Houston, 2002.

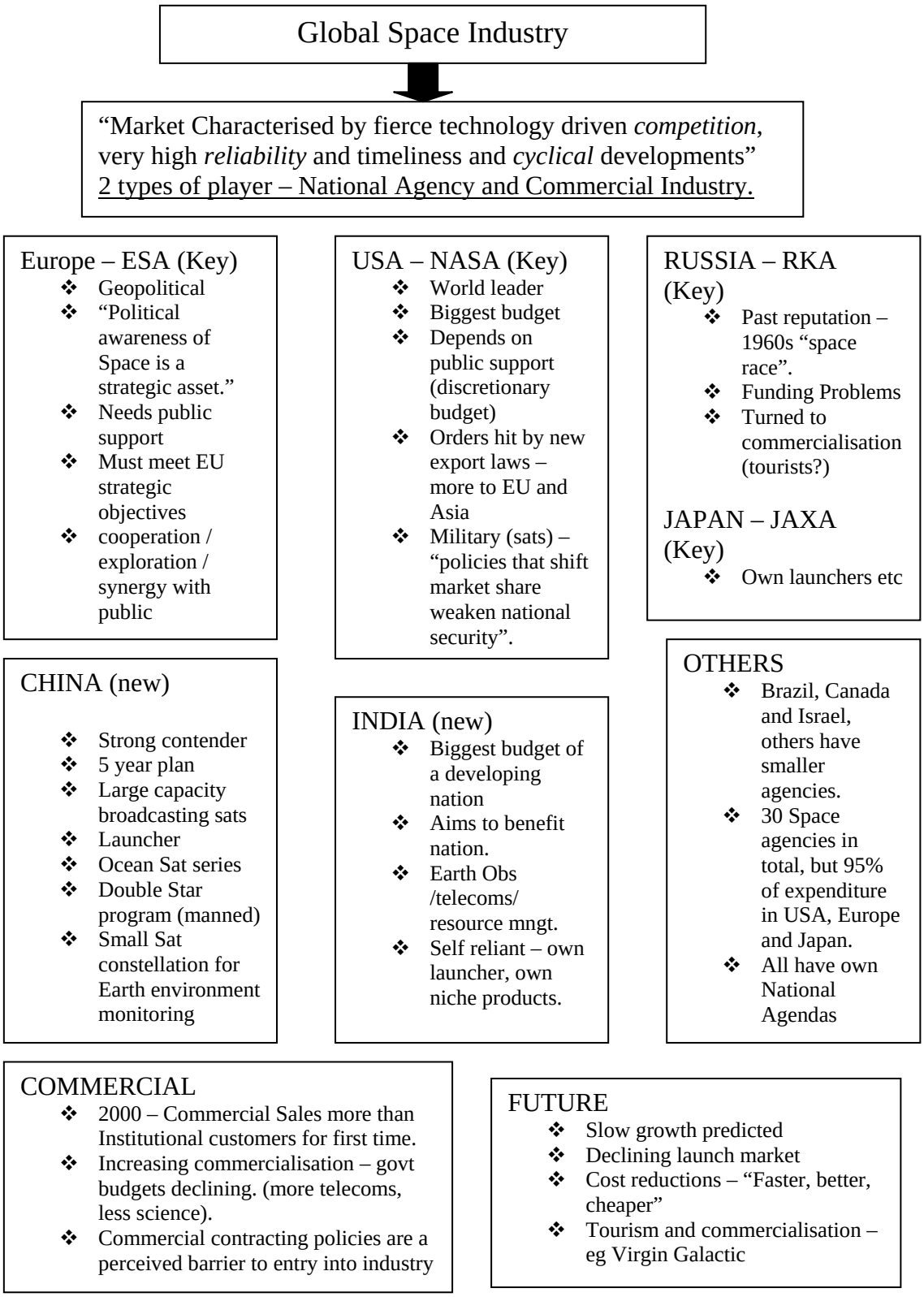

Figure 4-1 Key Players in the Global Space Industry

4.2.2 Porter's 5 Forces

The Space Industry can be divided into several market Sectors. These include Space Sciences, Launch vehicles and commercial Communication Satellites. The Space Sciences Sector includes planetary exploration missions and the telescope programmes such as Hubble, and is where this project is positioned.

A Five forces analysis (Porter, 1979) on the companies that participate in the Space Science Sector of the Space Industry, illustrated in Figure 4-2, gives:

Bargaining power of Suppliers: Low – Many large companies have their own in house capability to produce the components they need, however more specialised components are supplied by small specialist companies.

Bargaining power of customers: High –. With the cyclical nature of the industry, there is no guarantee of major contracts. Without these contracts, layoffs can be the result. The Government Agencies, like ESA, do attempt to ensure that a steady stream of work is available to the Sciences Sector, but the extent of this generally depends on which country in which you are based. In some case, however, combinations of Space companies can join together, resulting in little choice for the customer

Competitive rivalry within the Industry: High – Contracts for Prime Contractor are competed for so therefore new technology leaders for example will have an advantage.

Threat of New Entrants: Low – The companies in the Space Industry tend to be well established, as much capital and specialist expertise is an entrance requirement. Some of the smaller companies are able to merge to become more competitive.

Threat of Substitutes: Low - Although there are ground based telescopes, high resolution imaging is better done from space, and planetary work has to be done from space, either from orbit or on the surface.

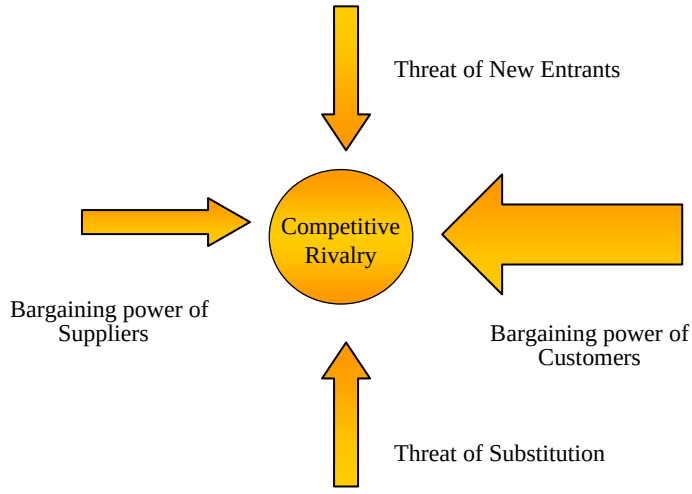

Figure 4-2 Porter's five forces analysis of the Space Sciences Sector of the Space Industry

The forces acting on the other sectors are similar, however for the Launch Vehicle sector, the power of suppliers is medium, since consumables are procured externally. In this sector the power of customers is lower since there is less choice in potential launchers, and most missions are designed around specific vehicles. For the communications satellite sector, the power of the customer is high, as they specify the payload.

This analysis looks at a "snapshot" of the sector at any one moment in time. This is subject to change as other external factors influence the industry.

4.2.3 PESTLE Analysis

The Space Industry is very susceptible to *Political* and *Economic* pressure as well as from new *Technologies*, which can be demonstrated using a PESTLE analysis. (Verity, 1999) This model is dynamic and shows the Political, Economic, Social, Technological, Legal and Environmental effects on each of the Sector's five Forces over time. A general analysis is shown in Table 4-1 overleaf.

	Industry	**Suppliers**	**Customers**	**New Entrants**	**Substitutes**
	High	*Low*	*High*	*Low*	*Low/Medium*
Political	Interest in Science fluctuates as political agendas change	Stricter regulations.	Varying Government support affects number and size of missions	Another Nation enters the Industry. Could lead to contracts or more competition	Backing of alternate ventures.
Economic	Contracts and Funding reliant on favourable economic conditions	Smaller companies may go out of business	Agency budgets dependant on National Economy	A good Economy could encourage new ventures	Lower cost alternatives to expensive Space launches and missions.
Social	Industry depends on public opinion. Is Space still interesting?		Public opinion affects type of mission proposed		Space Science out of favour.
Technology	New technology gives competitive advantage and could make more cost-effective	Need to keep up with new advances and be a better alternative to in-house production.	New technology = bigger risk. Will the customer accept that risk?	Cheaper technology and R & D opportunities open up the Industry	Technology for alternatives becomes better (eg more powerful telescopes)
Legal	Stricter regulations	Regulations may cause use of a material to be restricted	Agencies must abide by own national laws regarding launches etc	Regulation regarding the number of competitors in a market	Changes in laws may make substitutes a more attractive option.
Environmental	Environmental awareness may result in changes to designs	Production of certain components may be deemed "unfriendly"	Pressure to become more aware may influence choice of supplier		"Greener" alternatives may be preferred.

Table 4-1 PESTLE analysis for the general Space industry

This analysis begins to highlight some of the strategic issues faced by participants in the Space Industry. Overall, the inertia of the Industry is strongly influenced by external factors, such as the political climate and fluctuations in public opinion. Analysis was carried out by Roy *et al*. (2000)on space-related opinion poll questions since 1945. Since 1965 the survey analysed has included a question on the level of funding of NASA. The public attitude to this funding has remained relatively stable, except during the early 1970s where responses favouring less NASA funding peaked. This is when public interest in Space was at its lowest since "winning" the "Space race" and moon landings were seen as routine. This attitude shift led to a decline in the US national Space budget and the cancellation of the Apollo programme.

A more recent shift in opinion is towards more "environmentally-friendly" subjects. One way in which this has affected the Space industry is the unpopularity of radioactive materials used for long-term mission power supplies. Although cases have been made to persuade the public that this material is safe, the strength of opinion is such that these materials now have limited use.

4.2.4 Scenario planning and the implications of recent and future events

The PESTLE analysis is a dynamic model and can be used to analyse the effects of recent events on an industry. It can also be used as a forecasting tool to analyse the possible effects of future scenarios. By analysing the scenario in terms of each of the six factors, the tool can assist the forecaster by ensuring that a crucial implication is not overlooked.

One use for this model is to assess the implications of a major event in an industry, for example the failure of an important mission or piece of hardware. The loss of the Space Shuttle Columbia in February 2003 was significant for the global Space industry. Examples of these implications are discussed in Table 4-2.

	Implications
Political	❖ Raises questions for Government customers about their Space Policy, especially continuing the manned programme. ❖ Industry and possible New Entrants subject to changes in political agendas.
Economic	❖ Industry experienced loss of revenue from cancelled launches. ❖ Re-evaluation of Space budget for both Industry and Customers. Extra funds allocated for redevelopment of the Shuttle. ❖ Possible loss or gain of contracts for new and existing Suppliers. ❖ New funding opportunities for New Entrants and Substitutes wishing to replace the Shuttle.
Social	❖ Media coverage and heightened public awareness of the dangers of manned Space flight. Public began to question both the Industry and government Customers about the validity of further manned missions. ❖ Raised awareness of potential Substitutes such as Robotic probes.
Technological	❖ Investigations into the design and technology of the Shuttle affected both the Industry and the Suppliers trying to establish what went wrong. ❖ Replacement Shuttle – possible new developments for the Industry, Suppliers, and New Entrants and other Substitutes.
Legal	❖ Legal Enquires to establish blame – affects Industry, Suppliers and Customers.
Environmental	❖ Location of debris before degradation and contamination of environment – responsibility of Industry and Customers.

Table 4-2. PESTLE Analysis of Columbia Shuttle loss in 2003.

This type of analysis can also be performed to assess successful missions as well as failures. Successes can have just as many implications and can lead to more public awareness of Space programmes and increased funding. An analysis of the successful landing of the Huygens probe on Titan in January 2005 appears in Table 4-3.

	Implications
Political	❖ Example of successful long-term collaboration between Industry, Suppliers and Customers. Good grounding for further cooperation.
Economic	❖ Large long-term mission with large, predominantly government-funded budget. (Customers) ❖ One successful mission could lead to increased funding for further projects from the Customers for both Industry and Suppliers. ❖ Increased reputation for reliable components may lead to increased orders for Suppliers.
Social	❖ Raised profile and public awareness of both the Industry and the Customers, especially ESA. ❖ Positive public interest in Space exploration could have adverse effects on Substitutes like Earth-bound observations.
Technological	❖ Both Industry and Suppliers demonstrated a range of successful technologies.
Legal	❖ Rights to the data and images established between Customers and Industry.
Environmental	❖ Possible contamination of Titan surface recognised and prevented by Industry and Suppliers.

Table 4-3 PESTLE analysis of successful Huygens probe landing on Titan in 2005.

The PESTLE analysis can also be used to assess the future long-term implications of a recent development and predict whether a situation is of benefit or a potential threat to an industry. The future commercialisation of Space and the developments in the X prize competition could have a major effect on the players in the Space industry and is discussed in Table 4-4.

	Implications
Political	❖ Industry no longer reliant on government Space policy for orders. ❖ Encouragement of new enterprise and New Entrants.
Economic	❖ Industry experiences larger markets and competition from New Entrants. ❖ Increased commercial funding for Industry and New Entrants. ❖ Broadening of potential contracts for Suppliers. ❖ New public Customers, cost of Space becomes high but accessible.
Social	❖ Raise profile and generate interest in Space from both established Industry and New Entrants. ❖ Eventual public access to Space - new Customers.
Technological	❖ X Prize inspired new developments and innovation from New Entrants, Suppliers and the Industry.
Legal	❖ Increased commercialisation encourages new legislation for the Industry and New Entrants, especially concerning public Customers.
Environmental	❖ Recognition of possible environmental effects of increased number of Space launches (Industry, Suppliers and New Entrants). ❖ New innovations must not be harmful to the environment.

Table 4-4 PESTLE analysis of future commercialisation of Space travel

The final application of this analysis is forecasting the implications of what if some of science's big questions were answered. An example of this is what if Life were found on Mars. This could have profound effects on the Space industry and is discussed in Table 4-5.

	Implications
Political	❖ Changes in Space Policy to allow further investigation and more Mars missions (Industry and Customers). ❖ Possible negative changes if public opinion changes, as in Apollo programme.
Economical	❖ Extra funding for further Mars missions – more Customer contracts for Industry, Suppliers and possible New Entrants. ❖ Substitutes may experience drop in funding.
Social	❖ Media coverage and general increase in public interest in Mars missions and other Space work. Positive effects felt by Industry, Suppliers and Customers. ❖ Mars missions may become considered routine and Industry becomes out of favour.
Technological	❖ More missions mean further technology innovations by Industry and Supplier are encouraged. ❖ Specific biological technology developed for further investigations.
Legal	❖ Rights to data, landing sites and legislation against possible exploitation. (Industry, Suppliers, Customers and New Entrants) ❖ Possible limitations on the numbers of missions. (Industry, Customers and New Entrants)
Environmental	❖ Industry aware of prevention of contamination of Mars environment.

Table 4-5 PESTLE analysis of the implications of finding Life on Mars

This is a useful strategic tool when considering past and future events, however it is a subjective tool and is open to interpretation. Although this highlights many influential factors, a company's future strategy should not be based solely on this tool alone, as there are many variables that may not have been considered which could have an important impact on the industry.

4.3 Capabilities of companies within the industry

In terms of the participating companies in the Space industry, there are several main players at Prime Contractor level within Europe and worldwide. The UK's main representative is EADS Astrium (2004), which is part of a larger European parent company which also has operations in France, Germany and Spain. They have Prime Contracts in Earth Observation and Science missions, however a significant part of their business comes from the manufacture of large Telecommunications satellites. Other major players in Europe are Alcatel Space (2004), which focuses on Earth Observation and communications missions and Alenia (2004), which is the Prime Contractor for the programmes managed through the Italian Space Agency. Boeing (2004) and Lockheed Martin (2004) are major worldwide players and are both large contractors for NASA missions. There are also many smaller specialist players within the industry. The strategies of the larger companies are relatively similar, and all are searching for some competitive advantage to allow them to win contracts.

In general the technology used onboard space missions is relatively old and well tested. New technologies are considered too risky to be used as mission critical systems. However, the industry is now moving towards the concept of "faster, better, cheaper", one solution of which is smaller spacecraft with miniaturised technologies. Any company that can harness and prove a new technology will have a competitive advantage. In order to win as many prime contracts as possible and to maintain technical leadership in subsystems work, it is aimed to be a centre of excellence for a particular technology or for a particular type of mission. This then leads to a very resourced based strategy.

In a highly resourced based company, two of the main sources of success are a company's *Knowledge Assets* and their *Network Assets* (Jenkins, 2001). One of the main assets is the people within the company and the knowledge that they possess. The employees tend to have a great deal of experience as well as skill and technical knowledge and it is these that the companies work hard to retain. Their Network Assets are the contracts, and the reputation that allows a company to bid for a Prime Contractor contract. The switching costs between them and one of their competitors, however, are not very high, since many science contracts are "one-offs". If the company's strategy is customer focused, especially as the customer tends to specify their requirements and have the end product tailored to their needs, this gives some competitive advantage. However, in order to increase this advantage, a company should be looking towards new technologies and processes to differentiate themselves from their competitors.

A key part of any company's strategy is to develop relationships with suppliers and customers. This develops their own part of the value chain, and looks to extend it to integrate with the suppliers' value chains (Porter, 1985). A value chain looks at how the company adds value to the service or goods it is providing the customer. This is done by not only developing excellent cost effective Space hardware, but also working with the customer to meet their specifications and providing the knowledge, expertise, reputation and support so that the customer feels confident that they are getting the best service possible. Companies also offer the customer end-to-end services, from feasibility studies to the delivery and operation of the space system. By developing relationships with their suppliers, who are likely to be more efficient manufacturers of components and materials, they are looking to add further value to this process.

Since the lack of a steady flow of work has caused problems in the past, a part of the strategy should include expanding their customer base. As described by the Ansoff matrix framework, shown in Figure 4-3, New Product Development is a priority, using new technologies and methods in the existing Space markets. Other ways of increasing business could be Market Penetration (Existing products, Existing markets) by offering more services and seeking more customers in that market. This could be achieved by approaching other government agencies in different parts of the world, such as the new Space players China and India. Another option could be looking to more commercial companies for private satellite use, especially if the price of commissioning a satellite comes down due to new technology and more standardised processes. By increasing the numbers of customers and contracts, there could be more stability in the workload.

If these options are exhausted, other options are Market Extension (Existing Products, New markets) or to Diversify (New products, New markets).

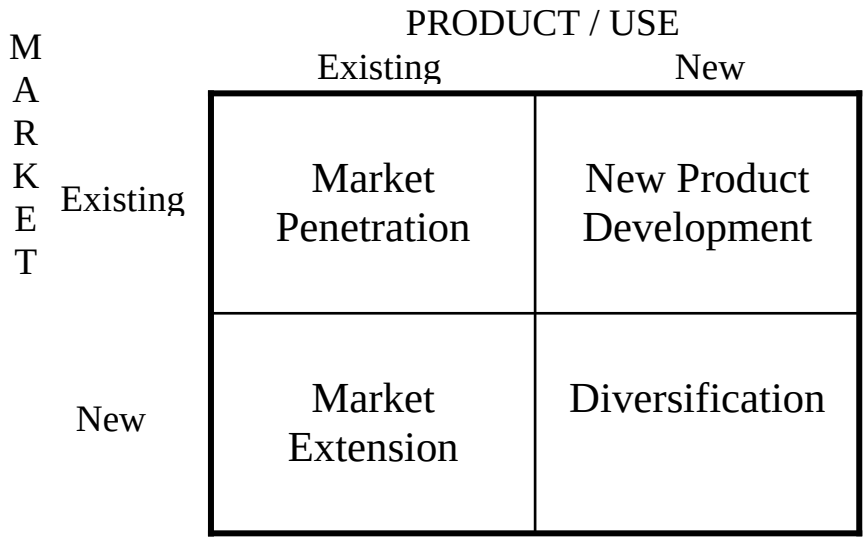

Figure 4-3 The Ansoff Matrix framework

There have been several examples of companies that produce specialist products for the Space industry employing the Market Extension principle to increase business. The Space Certification Program established by The Space Foundation(The Space Foundation, 2004) details companies that have modified their existing products for use in commercial applications. Many of the companies that have developed materials for use in Space have recognised that these have more terrestrial applications, such as home insulation or outdoor extreme weather apparel. Tempur originally developed a material used in Spacecraft seats that moulded to the Astronaut's bodies to absorb g-forces during launch and landing. They have now taken these properties and developed very sophisticated mattresses. Another example of Market Extension is a laser tracking device developed to aid the docking of spacecraft with satellites which is now used in the Lader vision laser eye surgery system. This shift in strategy has been successful for these companies, where the Space market is not broad enough to sustain them.

Part of the resource based strategy is the recognition that people are a key strategic asset. Whilst this enhances the reputation of the company, it could lead to drawbacks. Innovation is important, new ideas are crucial. However the more experience the people have, the more likely they are to develop and maintain one style of operation. This means that the company has to bring in "new blood" with new ideas that are not bound by convention. This is a good strategy to encourage new thinking, however as fewer students are taking specialist physics and engineering degrees that pool of new talent is starting to shrink. Although student sponsorships and summer placements exist, the industry as a whole needs to encourage children at school age to become interested in Space and Engineering or establish development and retraining programs as a new source of skilled people. Successful missions provide good publicity for the Space industry and hopefully this will inspire the next generation of Space Engineers.

4.4 Knowledge and Technology Transfer and the adoption of MST for Space

Any company that can harness and prove a new technology like Microsystems Technology (MST) will have a competitive advantage over the other key players. Although MST is being researched and is having success in the biological and computing fields, it is yet to be fully qualified for Space. The knowledge gained by researchers in other fields will need to be adapted for the specialist Space environment, however the basic knowledge should be exploited. This knowledge can be gathered by means of Knowledge Transfer.

4.4.1 What is Knowledge Transfer?

Innovation is more than just the invention of a new product or process. It involves the conception of a new idea and the invention of a new product combined with the development and exploitation of a new market (Myers and Marquis, 1969). One definition of innovation is "The development and implementation of new ideas by people who over time engage in transactions with others within an institutional context" (Davies and Koza, 2001). This means that it is important not only to design and use new technologies and processes, but to get them accepted by others in a particular field, industry or market through the transfer of knowledge. This idea of knowledge transfer through communication of ideas is therefore a central aspect in innovation.

Using an analogy with physical transfer mechanisms, it has been proposed that there are four mechanisms for knowledge transfer (KT) (Nicolau, Phillimore, Cross, and Nicolau, 2000). These are diffusional, convectional, turbulent and radiative. Diffusional KT describes random verbal and other informal communication in the form of newsletters, workshops or conferences. Convectional KT refers to either large focused R & D projects or the movement of highly educated people or "knowledge carriers" to different locations. Turbulent KT includes "spin-off" knowledge that is being used for other applications than that is was originally intended for. Radiative KT describes "long range" or delayed KT such as that done through reading articles in journals or over the Internet. This means that the most common forms of KT would be diffusional and radiative.

Knowledge transfer is a key to the successful adoption of MST for use in Space. More knowledge on how to design and manufacture these components and their uses needs to filter into the industry. This is being done primarily through the scanning of articles in specialist Microtechnology and Space engineering journals. There are also several conferences held dealing with MST across many fields. The papers presented at these conferences tend to be academic and in many cases components are being developed with no specific commercial or industrial use in mind. While this is a good way of transferring information about new developments to an industrial audience and a way of getting new ideas and processes accepted by peers, there seems to be a lack of information filtering into the academic world that could focus this research. Several companies are now commissioning university-based projects to develop and use this technology with their own applications in mind. This also brings fresh "knowledge carriers" into their companies who bring different perspectives to existing problems and

so transfer their knowledge to the incumbent engineers, who in turn teach their skills to the newcomers.

MST is by nature an interdisciplinary technology. This means that in order to achieve success there had to be "cross-talk" between disciplines such as solid state physics and electrical engineering. Each field has knowledge on a specific part of the process, but were not well versed in others, such as the limitations of microlithography which is a key part of the manufacture of the components. This sort of knowledge transfer needs to spread to include other disciplines. It may be the case that a component designed for use in biotechnology can be adapted for use in the Space environment, but until members of these different fields discuss their work, some opportunities may be missed.

4.4.2 Barriers and facilitation to the adoption of MST

There are, however, barriers to knowledge and technology transfer. In the Space industry one of the biggest is that of risk. Many in the industry are reluctant to use a new technology until it has been well tried and tested, as one component's failure could mean the end of a mission, since it is unlikely that a faulty component can be fixed once in Space, and the loss of millions of dollars. Not enough is known about these components for the industry and their customers to have enough confidence in them to approve their full use. NASA have started an investigation into the failure points of MST components and will come up with a set of standards that a new component must comply with in order to be used. This is likely to be several years away. Until then it is unlikely that full use of MST will be made. Microsensors are beginning to be used in some subsystems, such as the Attitude and Orientation Control Systems (AOCS) and for some failure detection applications, however use in other mission critical systems is still experimental.

Another barrier is that of the "not invented here" mentality. Since the world Space industry is very fragmented, it is unlikely that a technology perfected by one company will be adopted by others in the industry, because their own engineers did not invent it. Although there may be knowledge and technology transferred internally, it is often the case that the knowledge does not reach the outside world. In some cases, the same piece of technology may be being researched in several places, but no collaboration that may increase the wealth of knowledge or accelerate the process will occur. This knowledge barrier is also due to of the competition faced by companies for contracts, and a company that develops a new technology or new process could gain significant competitive advantage, so is unlikely to share results.

Related to this is the issue of Intellectual Property Rights. This is legislation that allows a person or company to own their inventions and innovations to stay competitive against the market. As this usually applies to discrete devices that can be licensed for use by others. However, as one of the primary concepts behind MST is their use in integrated systems, or System-on-a-chip, the ownership of the Intellectual Property (IP) of these systems where many different COTS components from many different providers are used, becomes complicated (Greguras, 1998). Proposed solutions to this include the outright acquisition of the owner of the IP by a larger company, drafting of

complex licensing agreements and careful negotiations. However this does create a large barrier to the sharing of new technology knowledge.

These barriers are being recognised and have started to be addressed. In Europe, networks of institutions and companies are forming to gather their combined knowledge about the uses and availability of MST for Space, and reports are starting to be written and conference held on that subject. There are also similar groups looking into general MST, which are discussed in Chapter 6, and there is some overlap in the members of these two groups. The department of Trade and Industry (DTI) have established an MNT directory (Dept of Trade and Industry, 2004) in order to establish contact between groups with similar interests in the UK. MST seems to be agreed on as one of the possible ways forward for the Space industry, as the use of smaller components would ultimately reduce the mass and therefore cost of launch. Using standardised components should again reduce manufacturing costs. MST also has the potential to be used inside the spacecraft to monitor health, which will lead to better performance, and to be used for a range of different applications that size and cost may have prohibited in the past. However, still more interdisciplinary knowledge needs to be shared before it will be adopted as standard.

4.5 Conclusions

Traditionally, Space is a risk-adverse, technology-driven industry which is subject to many external influences. With several large companies offering similar end-to-end services, any form of competitive advantage is crucial to maintaining a steady supply of contracts won. One way to gain this advantage is by creating a technological edge over the others in the industry and offering added value to the customers.

MST is a new technology that is gaining popularity in many industries, however it is yet to be accepted fully into the Space industry. A new technology must gain acceptance within a field by the transfer and combination of knowledge. Once increased knowledge of MST is gained and the products are well tested, some of the elements of risk are removed and an industry beings to feel more confident in its use. If a company within the Space industry can successfully implement this knowledge to produce reliable, cost-effective hardware, that company will have the advantage. Possibilities for further market penetration present themselves, and new opportunities for market extensions from this new technology also become evident.

The company will increase its knowledge assets from the assimilation of the new technology and will also increase its network assets not only from the increase in potential contracts, but by gaining a reputation for innovation. This reputation will be crucial in an industry where customer and public opinion are vital for continuing success. Unfortunately, there are still several barriers to knowledge transfer between parties, however networks are being formed to share the knowledge gained in many different fields. Utilising this wealth of knowledge is important in creating the strategic advantages in the adoption of MST by the Space industry.

5. Hardware

5.1 Introduction

The third project objective is:

"*To design and build several basic sensor suites using current technology, including commercially available MST, and demonstrate collaborative working between them.*"

The hardware aspect of the project will be used to demonstrate the basic sensor suite concept and a potential method of intersuite collaboration. It will also identify the practical issues involved in hardware design.

This chapter includes the investigation of several types of commercially available sensors and the production of a sensor suite breadboard model consisting of four basic environmental sensors. The I2C data bus is investigated as a method of passing data between the suites and PIC microcontrollers are considered as the suite's internal processor.

5.2 Top Level requirements and selection criteria

In order to establish a focus for the type of sensor suite and the hardware design, firstly a list of top level engineering requirements for the final design was derived. In addition a list of sensor and component selection criteria, based on a variety of proposed scenarios, was composed to find suitable components to build a basic version of the sensor suite.

5.2.1 Overall sensor suite top level requirements

The concept of a sensor suite covers a broad range of possible configurations and designs. A set of basic requirements was established to direct the design study. The end product should:

- be suitable for use in Space applications, but must also have the ability to be adapted for use in a range of environments.
- demonstrate the use of Microsystems Technology in its sensor and systems.
- use COTS components and generally be a low cost system.
- have low mass.
- use standard interfaces and protocols, as well as being "user friendly".
- demonstrate material compatibility for future integration.
- demonstrate collaboration between suites.
- show survivability in extreme conditions.

Some of these requirements, such as using MST and COTS devices, reflect the overall project brief. The remainder begin to define the sensor suite concept in terms of its general abilities.

One proposed aspect of the system is that it can be used for a variety of Space and environmental applications. The following section proposes several Space-related and terrestrial scenarios that the sensor suite concept could be applied to. These include possible additions to Mars missions, Earth environmental sensing and other space-related applications. All these applications have similar traits, which will be identified and discussed.

5.2.2 Proposed mission scenarios

This section proposes 8 space-related scenarios where the sensor suite concept could be a beneficial inclusion to the mission. They are grouped under three headings; Mars, Earth and Other Space applications.

5.2.2.1 Mars Applications

The idea that this concept has possible uses as part of a Mars mission is a common theme throughout this project. The initial deployment scenarios were based around the features of the Martian surface and the low temperature operation criterion for the components is also influenced by the extreme environmental conditions on the planet's surface. The exploration of Mars is a popular target for potential Lander and Orbiter missions, with further programmes under development for the future.

Here, four scenarios are discussed that could find a place amongst those future missions. The landing area targets, Rover path tracers and Dust Devil trackers are based on current or near future applications, however a permanent structure site reconnaissance mission discusses a longer term future application.

- ❖ Landing Area Targets

In this scenario, the sensor suite system is deployed from orbit or from an aerial vehicle in order to determine the suitability of a possible landing site for a main Lander or exploration path for a Rover.

Multiple groups of sensors would be scattered over several different areas. The data gathered could then be used to select a preferred landing site based on nearby features of interest or landing terrain suitability. The sensors could be used to provide a topographical map of the surface in that area detailing hazards such as large rocks, steep gradients or craters which would affect the landing. These readings would also be part of the surface exploration data especially if other mission specific sensors were added to the systems.

As these sensors would be predeployed, the inclusion of a "homing beacon" or visual aid could enable the Lander to locate the chosen site autonomously.

Another related application is deploying the systems from an aerial vehicle as an additional sensing feature of this type of mission. During the flight, the systems could be dropped as markers detailing the path of the vehicle. This could also provide in-situ ground measurements that could be gathered by the UAV overhead in addition to it own remote readings of the surface.

The small nature of the suites means that many can be deployed over one large area or several smaller areas for a limited mass penalty.

- ❖ Rover path tracing

This scenario proposes using a mobile surface vehicle or Rover to deploy the suites using a "breadcrumb" method. The rover drops a suite or collection of suites at specified intervals as it travels across the surface terrain. The path of the Rover can then be traced through the sensors.

The Rover only travels through a particular area for a limited period of time. The sensors can remain in those areas longer, resulting in data that monitors how the conditions in that area change over time. These include for example day/night variations, temperature changes, cumulative radiation effects and rate of dust coverage. The sensors can provide a map of how the terrain differs over the distance travelled. Any areas that then record unexpected results or results of particular interest can be highlighted and returned to at a later date for further investigation. The system provides the mission with greater potential surface coverage and can aid the planning of subsequent Rover activity. In addition, the suites can also be used to provide position data for the Rover should its navigation subsystem fail.

The Rover can deploy the sensors in a uniform pattern that would be difficult to achieve otherwise on the Martian surface. This pattern enables the position of the suites to be determined more easily than if the sensors are randomly deployed, which can reduce the complexity of the system overall.

- ❖ Dust Devil tracking

The research that has been conducted into the Martian Dust Devil phenomena has previously used remote surface observation methods. A sensor suite system could provide subtle *in-situ* measurements that remote sensing cannot detect.

The suites could be deployed in areas that are known to be prone to the formation of these vortices. If the suites were light and flexible enough, as those proposed in the Smart Dust project, they could be picked up by the vortex and monitor the internal conditions. Alternatively, the suites could be anchored to the surface and gather data as the Dust Devil passes overhead. A hybrid system combining both methods would provide comprehensive data on the necessary conditions for their formation, how far they travel, how do they disperse and environment within the vortex which would be difficult to achieve with remote methods.

Issues concerning how to make the suites immovable, such as pins, adhesive or weighting would have to be considered, as well as providing the mobile suites with a method determining their final position.

- Potential permanent structure or Human colonisation site reconnaissance.

The previous scenarios focus on sample missions similar to those that have already occurred or have been proposed for the near future. This scenario suggests applying the sensor suite concept to the preparation for prospective Human colonisation of Mars.

The sensor suite systems would be deployed over the site of a potential permanent structure to monitor the environment. The principle benefits of *in-situ* sensing here are the ability to detect potentially harmful substances or conditions, such as radiation from rocks or toxic gases, that cannot be detected remotely and ability to monitor the environmental changes over time. Although in order to be operational for years the suites will have to be extremely energy efficient, the long term deployment of the sensors would assess the suitability of a site for a permanent structure by observing the changes in the environment and their long term effects. For example, the effect of long term exposure to radiation on materials and electronics, highlighting seasonal and diurnal climate differences or monitoring the area for seismic activity that could be missed if readings were made infrequently. The suites could also be configured to detect conditions that would be harmful to Humans. Deployment would be made at a number of sites to establish a suitable candidate site for colonisation.

5.2.2.2 Earth Applications

The following two examples discuss environmental monitoring applications on Earth, however both have connections with space-based applications.

- Polar Region environmental monitoring

This scenario demonstrates the potential for the concept to be used in extreme Earth environments such as the Polar Regions. The system could be used for general environmental sensing similar to the type performed by unmanned weather stations but on a much wider scale, or be used to investigate a more specific feature. Again *in-situ* sensors could monitor environmental changes over time, such as the rate of ice melting or increases in radiation levels due to the depletion of the Ozone layer.

The investigation of a glacier feature called Cryoconites is an application where a sensor network would be beneficial. Cryoconites are small pools of melted ice which harbour microbes and bacteria. They can grow up to 50cm in diameter and appear to have a random distribution across the glacier. A network of sensor suites could be used to map the distribution patterns of the holes as they form and monitor their growth over a season as well as investigating the holes' internal environments. Using miniaturised sensors could also provide measurements from the holes where a conventional instrument cannot be used due to the diameter of the hole being less than the size of the probe. The system could be combined with an aerial section, such as a UAV, for

compiling an aerial map as well as being the collection point for the sensor's communications subsystem.

It has been proposed by Hoover and Pikuta in their 2004 paper that similar cryoconites holes may be formed in the Martian Polar Regions or on the surface of Comets or Asteroids. As in the glacier regions, these could be areas that contain life. The deployment of a sensor system in these regions could investigate whether cryoconites form and whether they also contain bacteria.

- Launch site monitoring

Sensor suite systems could be spread around existing or potential launch sites. Readings would be taken before and during a launch to determine what effects the launch has had on the surrounding environment.

Vibrations, sound levels and pollution in these areas are subjects of environmental concern and as such should be monitored closely. The sensors deployed prelaunch could then remain in place during and after launch to enable a comparison to be made. During this time, the sensors will not require any human interaction which could disrupt the reading or be hazardous to the person involved. The suites could also be used as person or animal detectors to alert the launch site of any potential threats.

The systems could also be deployed during planetary missions around the site where a returning vehicle is to be launched from. A record could then be made on the effects of that launch on its environment, whether it has damaged the area significantly and how these compare with launches on Earth.

The NASA Sensor Webs team is currently investigating a similar programme around the Kennedy launch site in Florida (Delin, 2005).

5.2.2.3 Other Space Applications

In addition to potential Martian applications, the sensor suite concept would be suitable to fulfil other space-related sensing requirements.

- Comet or Asteroid surface investigation

Lander missions to other bodies such as Comets or Asteroids could also benefit from the addition of a sensor suite system. The main Lander can only survey a portion of the surface, whereas an additional system of sensors would increase the total surface coverage. The suites could be deployed during descent or projected from the Lander on the surface. They would then communicate directly with the Lander, which would combine this data with its own and assume responsibility for communication back to Earth. Depending on the size of the body and the efficiency of the system, the network of sensors could conceivably encompass the entire body.

This system enables a wider area to be studied for limited extra mass and cost, which are critical factors in any space mission.

- Spacecraft internal sensors

Whilst the previous scenarios have suggested applications where the sensor suite is in additional to, or in replacement of, a main spacecraft, this scenario proposes the use of sensors within the main spacecraft to monitor its internal environment.

The suites could be distributed over the inside of the spacecraft or satellite, either on the surface or integrated within the structural material. These could monitor environmental conditions such as temperature or radiation that may be hazardous to the health of spacecraft. Another application would be to distribute the sensor suites on the external surface of the spacecraft to detect micrometeor impact damage.

The network would report to a central system via several smaller hubs, which limits the distance each suite has to send its data reducing the likelihood of interference either to the data or to the surrounding systems. Miniaturised suites will not encroach on other subsystem structures or require a significant increase in the overall size of the spacecraft to house them.

Each of the scenarios discussed above have commonalities that highlight the similarities in each of the required sensor suite systems. They are all examples of environmental monitoring where the measurement of changes over time is important and where the reduced size of the suites is key to minimising external influence of the environment that may result in contaminated data.

Based on these scenarios and the initial requirements, a set of selection criteria for the suite's components and sensors were derived.

5.2.3 Selection criteria for components

There is a wide range of components and sensors that could be selected for use in the suite design. Based on the overall requirements, the components should meet a set of more specific conditions. Many of these are similar to the overall requirements previously listed. Each sensor or component should:

- be an existing example of MST, or likely to be in the near future.
- have small physical dimensions (preferably in the order of mm) and low mass.
- have low power consumption.
- be commercially available and low cost.
- be able to survive a range of environmental conditions, such as low temperatures.
- produce a standard form of output (eg volts, millivolts).
- be made from a material that can be fully integrated, such as silicon.

There are a variety of sensors which measure a range of different environmental conditions. These include:

- Temperature sensors for both surface and air temperature.
- Air pressure sensors.
- Accelerometers for measuring impact acceleration or by measuring the acceleration due to gravity, the tilt angle of a device.
- Photodetectors.
- Ultra Violet radiation sensors.
- Anemometers.
- Chemical detectors.
- Seismometers .
- Magnetometers.
- Humidity sensors.
- Vibration detectors.
- Cameras to record visible phenomena.

Many of these sensors are available in miniaturised formats for use in small remote weather stations as well as other environmental sensing applications. Their availability as COTS devices however varies.

Table 5-1 suggests typical sensors required for each of the proposed scenarios, although this is not an exhaustive list.

Scenario		Sensors	
Mars	Landing targets	Accelerometer Temperature Light LEDs or Homing beacons Scientific payload	- for surface topography -shadows or landed in craters - for landing targets - optional
	Rover path trace	Temperature Pressure Accelerometer Radiation Dust detector Wind speed Position Optional scientific payload	Standard weather station sensors
	Dust Devil tracking	Pressure Motion detection Position Accelerometer Gyroscope	 -for impacts - angular rotation
	Colonisation site recon.	Temperature Pressure Accelerometer Radiation Gas and chemical analyser Seismometer	
Earth	Polar regions	Temperature Accelerometer Pressure UV radiation Gas and chemical analyser	 -tilt sensing -from cryoconites
	Launch sites	Temperature Pressure Accelerometer Vibration Chemical analyser	 -Shock sensing
Space	Comets and Asteroids	Standard environmental sensors Scientific payload depending on mission	
	Spacecraft health	Temperature Radiation Stress	

Table 5-1 Example sensors required for various space-related sensor suite scenarios

The table shows that there are several basic sensors that are common throughout the list, and should therefore form the initial basic sensor suite.

The four sensors chosen were: a temperature sensor, pressure sensor, accelerometer and light detector. The data recorded by these devices is useful in any monitoring situation and forms the basis of many sensing devices because they provide an overall picture of the environment in which they are located.

Accelerometers are examples of commonly available MST devices that have a well tested history and are mass produced for the automotive industry. This means that as well as being relatively inexpensive and easily obtainable, they are reliable and their responses are well documented.

Pressure sensors are also examples of sensors that are widely used in automotives. Again they are mass produced and relatively inexpensive as well as having suitably compact packaging.

The temperature of an environment not only influences that environment, but also has an effect on the measuring device itself due to the temperature sensitive nature of many materials used in the construction of electronic and mechanical devices. Therefore a temperature sensor should be a key part of the sensor suite to monitor the performance of the sensors as well as its surroundings.

A photodetector is included because it too can give simple information about the environment which could affect other systems, such as whether it is day or night or if the suite has landed in shade, both of which are important factors if solar panels for example are used in the power subsystem. Both of these sensors are available in a range of formats from simple variable resistors to complex integrated circuits.

It is envisaged that the final sensor suite will have modular capabilities allowing additional sensors to be included with minimal modification. This means that although only basic sensors are discussed, more complex sensors can be included depending on the specific application or advances in technology.

Examples of the four basic sensors were selected in order to produce a breadboard model of a sensor suite. This will be used to examine the practical issues involved in using sensor hardware and collecting the data.

5.3 Basic Environmental Sensor Suite Version 1

Breadboard circuits of the basic sensors were constructed and preliminary calibration readings taken. Readings were taken to verify the manufacturers' calibration curves and a set of data was collected by a PC through an analogue to digital converter. The lessons learnt from the sensor boards are discussed in this section.

5.3.1 Initially selected sensors

The four example sensors were all COTS devices procured from standard electronics stores. A Manufacturers datasheet was available with each device detailing its electrical characteristics and specifications.

5.3.1.1 Temperature

Temperature sensors are available in a variety of formats including thermistors and integrated circuits. A simple form of sensor however was chosen for the initial investigations. A thin film Pt100 platinum resistance temperature detector (RTD) uses the properties of its material to sense changes in temperature. As the temperature increases, the resistance increases. As the resistance in known at 0˚C, this resistor can be used in a wheatstone bridge arrangement balanced at 0˚C. As the temperature increases, this bridge becomes unbalanced causing an output voltage.

The RTD used for this investigation measures 2mm x 5mm x 1.1mm and has a resistance at 0˚C of 100Ω. It has a fast thermal response time and can detect a range of temperatures from –50˚C to 500˚C. Whilst this is not an example of MST, it is a low mass, low power, low cost solution.

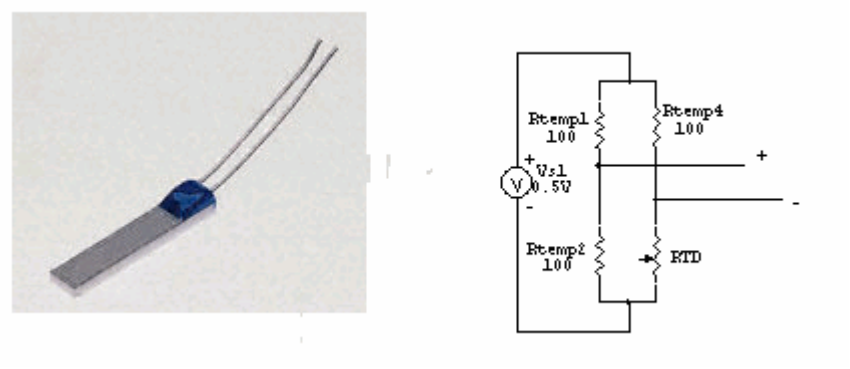

Figure 5-1 Platinum Resistance Temperature Detector and Wheatstone Bridge schematic

The graph in figure shows the resistance change with respect to temperature as specified by the manufacturer (Labfacility Ltd, 2004). This curve can be used for calibration and will be verified experimentally at room temperature.

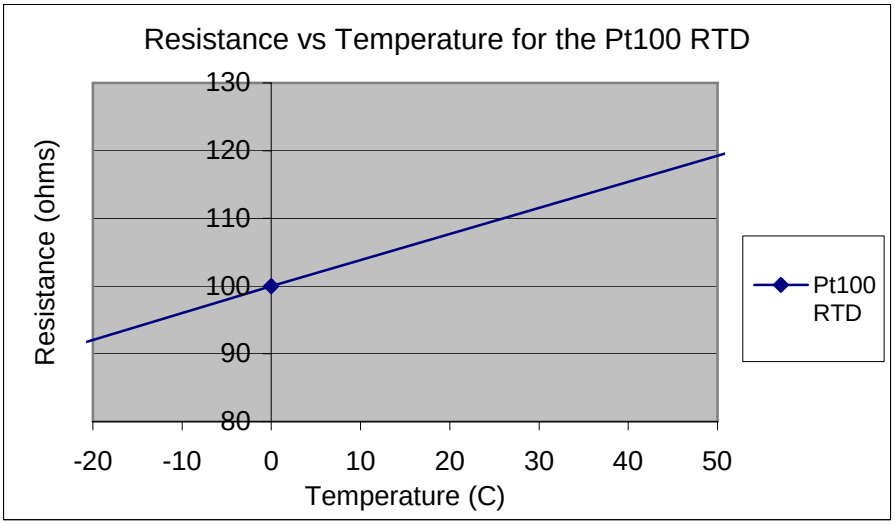

Figure 5-2 Graph showing the change in resistance with respect to temperature for a Pt100 RTD (Labfacility Ltd, 2004)

One disadvantage of the RTD shown by the experiment is that the element becomes hot if a voltage of above 2V is passed through it. This can create noise in the system and affect the measurement. Therefore, between 0.3V and 0.5V was used in this circuit. The output was then amplified using an operational amplifier.

The operational amplifier circuit was produced using a National Semiconductor LP324 Micropower Quad Opamp (2001). This comprises four opamps in one chip. This circuit is used for several of the sensors since a larger output could be detected more accurately than the millivolt output of the system. Figure 5-3 shows the pin configuration for the quad chip and a schematic of the opamp circuit used in this system. This circuit is repeated for each of the opamps. The 150Ω and 300kΩ resistors used produce a gain of 200.

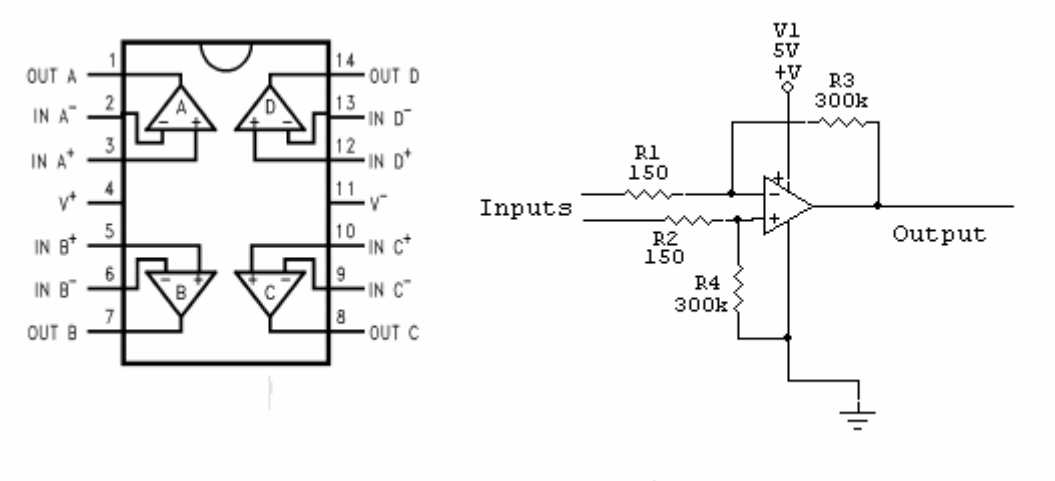

Figure 5-3 Pin configuration for the LP324 quad Opamp (National Semiconductor, 2001) and schematic of the Opamp circuit produced

At room temperature of approximately 20˚C, the resistance of the RTD should be 106Ω from the manufacturer's specifications. If the other resistors in the bridge all have a value of 100Ω, this means that for an input voltage of 0.3V, the output when multiplied by the 200 gain should be approximately 0.87V. Using the circuits described above, the value recorded was approximately 0.9V. Care must be taken if connecting the RTD to extra wire to change the position of the sensor, as this adds further resistance to the system and may cause a discrepancy in the results.

5.3.1.2 Pressure

The pressure sensor chosen was the Honeywell 40PC series (2002). This is a miniature piezoresistive sensor that incorporates its own amplifier. The model used had a range from 0 to 15 psi. The package measured 13mm x 11mm x 9.6mm plus a 10mm funnel. The devices required a 5V and 10mA and has an operating temperature range of between –45˚C and 125˚C. It has a given accuracy of 0.2% and gives a linear output between 0.5V and 4.5V.

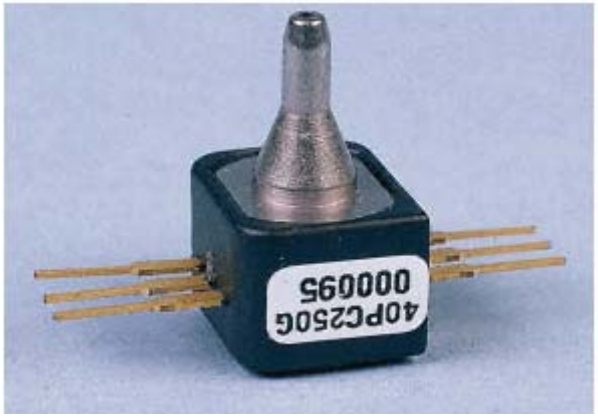

Figure 5-4 Honeywell 40PC Series Miniature Pressure sensor (2002)

As this is a piezoresistive sensor, higher pressure equates to a higher resistance which produces a lower output value. The highest pressure measurable by this sensor is 15psi or 103.4 kPa. Atmospheric pressure is given as approximately 101 kPa, so it is expected that the output at one atmosphere is approximately 0.5V. The circuit produced an output of 0.52V which verifies this figure.

5.3.1.3 Accelerometer

The example accelerometer chosen was the ADXL150 single axis accelerometer from Analog Devices (1998).

This sensor uses iMEMS® technology and as such is an example of an MST device. This is a low power device, requiring an input voltage of between 4V and 6V and drawing a current of 1.8mA. This device has a given mass of 5g and dimensions of 9.9mm x 10.6mm x 5.4mm. This particular model is designed to be surface mounted. The nominal sensitivity is 38mV/g, which can be increased using an external amplifier. The typical signal to noise ratio is given as 80dB to allow a resolution as low as 10mg.

The full range of the sensor extends to ±50g. As with many electronic components, the given operating temperature range is –40˚C to 85˚C.

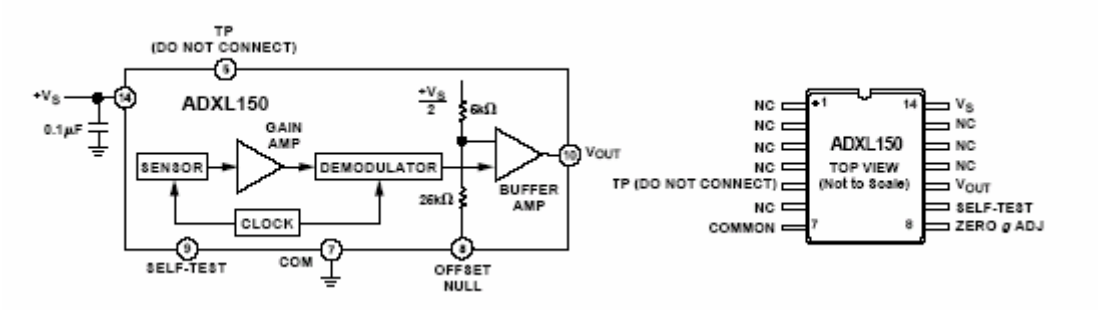

Figure 5-5 Functional block diagram and pin connection diagram for the ADXL150 accelerometer (Analog Devices, 1998)

This sensor will primarily be used to measure the orientation of the suite. The ADXL150 measures acceleration in one plane and should measure 1g when oriented vertically. When held horizontally, no acceleration is measured and the output should be 0V. This is illustrated in Figure 5-6.

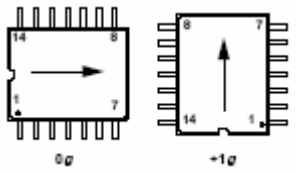

Figure 5-6 Accelerometer used as a tilt sensor - axes of orientation (Analog Devices, 1998)

An input voltage of 5V was supplied to the accelerometer and the output passed through the quad opamp circuit. Held vertically an output of 2.2V was recorded. As the angle of the sensor to the vertical plane was increased, the voltage output drops until as expected, 0V were recorded with the sensor held at 90˚.

5.3.1.4 Light

The light sensor chosen was an NSL19-M51 light dependant resistor (RS, 1997). This comprises two photoconductive cells that have a spectral response similar to the human eye and therefore are designed to detect visible light. The package has a 13mm diameter and a height of 6.6mm. The operating temperature range is from –60˚C to 75˚C. Again this sensor will be part of a wheatstone bridge configuration with an input voltage of 3V.

Figure 5-7 shows the change in resistance with respect to the illumination levels, in Lux. It can be seen that as the light level increases, the resistance decreases resulting in a higher output voltage. This curve is provided by the manufacturer. The bridge has been balanced at 150kΩ, which is equivalent to approximately 1 Lux.

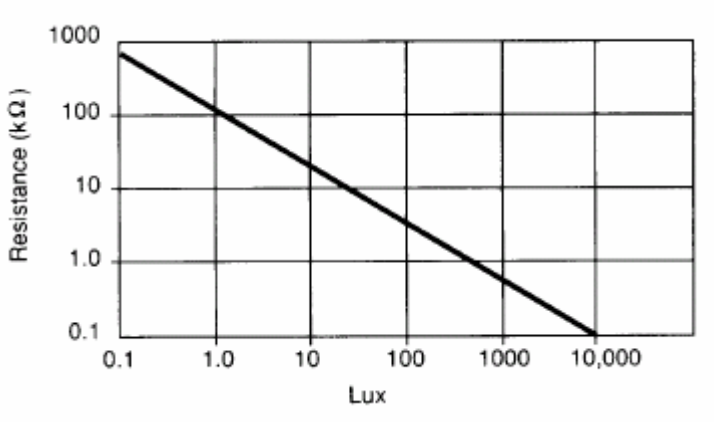

Figure 5-7 Resistance with respect to illumination levels for the light dependant resistor (RS, 1997)

For a light intensity of 40 Lux, the graph shows that the resistance of the sensor reduces to approximately 30kΩ. If the other resistors have 150kΩ and an input voltage of 3V, the output should be approximately 1V. This output was recorded from tests with the sensor a distance away from a 40W bulb, which should be approximately 40 Lux. When the sensor was placed in diffuse natural light, the oscilloscope reading became unfocused. This noise would have to be taken into account when passing the data digitally.

5.3.2 Combined circuit diagram

To simulate a sensor suite, the breadboard models were connected and their data passed to a PC via an analogue to digital converter. In a real sensor suite the analogue data would also need to be digitised before it could be processed by a microcontroller and communicated externally. A schematic of the basic sensor suite is shown in Figure 5-8.

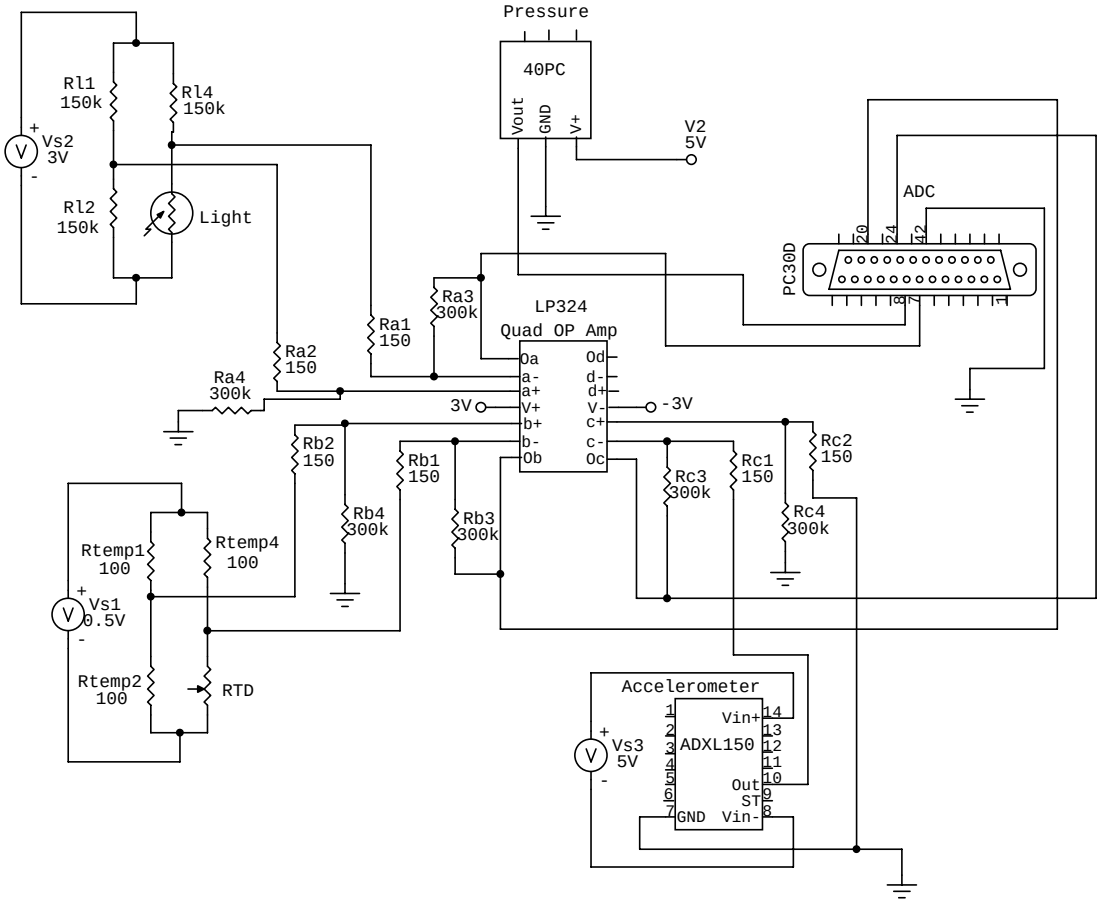

Figure 5-8 Schematic of initial sensors breadboard circuit

The ADC converts the analogue data into an 8 bit digital number. Since the converter cannot process floating point numbers, i.e. those that include a decimal point, the data output is reported in millivolts. This should be noted for post-processing work.

Figure 5-9 shows the completed basic sensor suite boards excluding the power and data processing subsystems. A 50p piece is shown for scale.

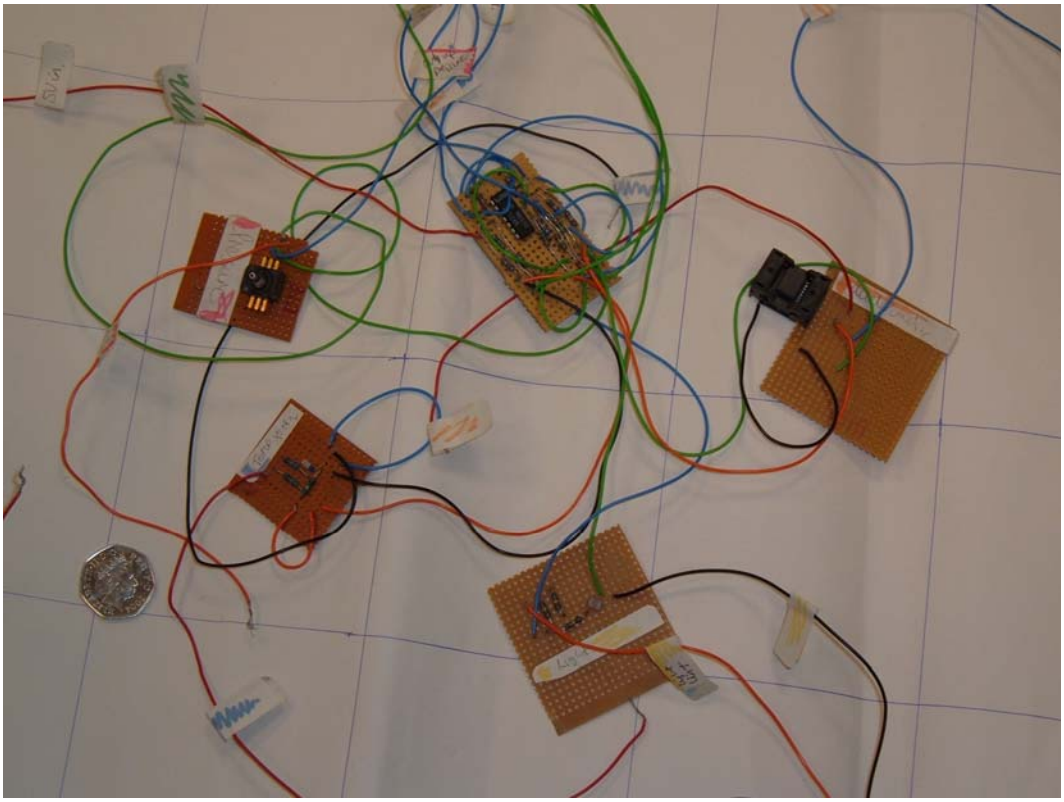

Figure 5-9 Basic sensor suite breadboard model

5.3.3 Lessons from sensor board construction

A number of lessons can be learnt from the construction of the sensor suite circuits. Most importantly it gives an insight into how the sensors work, their size, shape and the type of output data that can be expected. Other valuable conclusions are listed below.

- The sensors that require additional amplifiers have been identified and a suitable gain selected. Also any other necessary components such as resistors and capacitors have been recognised.
- If a common power source is to be used, there should be a standard voltage for the sensors to avoid additional regulation.
- If a common ground wire is used, care must be taken to avoid coupling and crosstalk of the sensor outputs.
- The sample rates are determined by the ADC. The sensor response times and these sample rates must be compatible.
- The orientation and position of some of the sensors within the suite directly affects their measurements. For example, the orientation of the accelerometer determines which axis is measured.

One of the aims of the project is to produce a miniaturised sensor suite. Whilst the breadboard models have not been spatially optimised and smaller sensors can be found, the physical boards could be fitted into a small box approximately 10cm x 6cm x 4cm. This assumes that the boards have been stacked rather than having them all on the same

board. If the power was supplied by batteries and the processing made using a microcontroller, a miniature COTS sensor suite would be feasible.

5.4 Intersuite Communication (I2C)

As one of the criteria for the sensor suite concept is that they demonstrate collaboration, a method of intersuite communication is required. The I2C protocol developed by Philips Semiconductors is a well established standard protocol which uses two wires to connect and communicate between compatible devices. An I2C bus connecting two PCs was investigated and the key issues raised over the use of this protocol noted.

5.4.1 What is I2C?

The I2C bus was developed by Philips Semiconductor in the 1980s and is still widely used today. The bus uses two wires, the serial data line (SDA) and serial clock line (SCL), and a software based protocol to connect two integrated circuits (spec) (Philips Semiconductors, 2000).

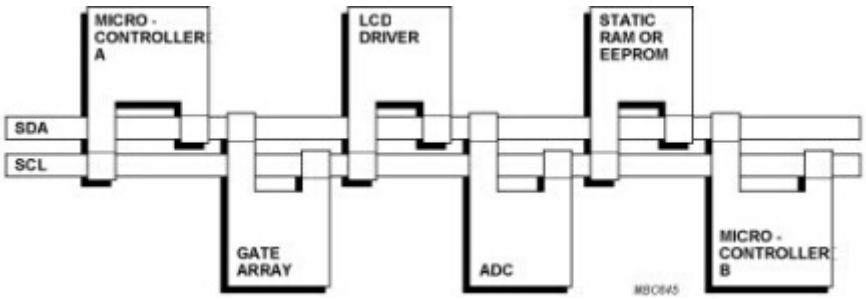

Figure 5-10 Block diagram of an I2C bus (Philips, 2004)

When transferring data, one device is designated as the Master and the other is the Slave. The Master device initiates the data transfer and generates the clock signal. Any I2C compatible device can be connected to the bus and can pass information to the Master. There has to be at least one Master per bus, but multiple Masters are permitted. All Masters have equal priority and are subject to arbitration if two initiate transfer simultaneously. The bus is designed so that extra devices can be added or removed easily. One limiting factor on the number of devices per bus is the total bus capacitance. This is required to be less than 400pF. (Philips Semiconductors, 2000) This limitation is discussed further in Chapter 9.

Each device on the bus has a unique 7-bit address. In general the first four bits are fixed and are specific to the type of device, for example microcontollers or EEPROMs. The last three bits can be programmed allowing up to 8 different address combinations. This means that up to 8 of the same type of device can be connected to the bus and approximately 120 devices in total (Philips, 2004). Therefore the addressing also provides a limiting factor to the number of sensor suites per bus.

Data can be transferred up to 100 kbit/s in Normal mode, increasing to 400 kbit/s in Fast mode and 3.4Mbit/s in High Speed mode (spec). The protocol is based around six

states: START, ADDRESS, ACKNOWLEDGE, NOT ACKNOWLEDGE, DATA and STOP. To transfer data, the Master must (cited in (Quirke, 2003)):

- Wait until both the SDA and SCL are high. This indicates that bus is free.
- Initiate a START condition to claim control of the bus. The other devices LISTEN to the bus to determine if they are to be addressed.
- Provide a clock signal on the SCL. This is used as the reference time for which each bit of data on the SDA wire is valid and can be used.
- Send out the ADDRESS of the selected Slave device.
- Place a READ or WRITE bit on the bus.
- Ask the Slave to ACKNOWLEDGE that it has recognised the address and is ready to communicate.
- Sends or receives 8-bit words of DATA. After every word, the sender expects the receiver to send an ACKNOWLEDGE bit to confirm the transfer is proceeding correctly.
- When the transfer is complete, a STOP condition is sent to free the bus.

This procedure is illustrated in Figure 5-11.

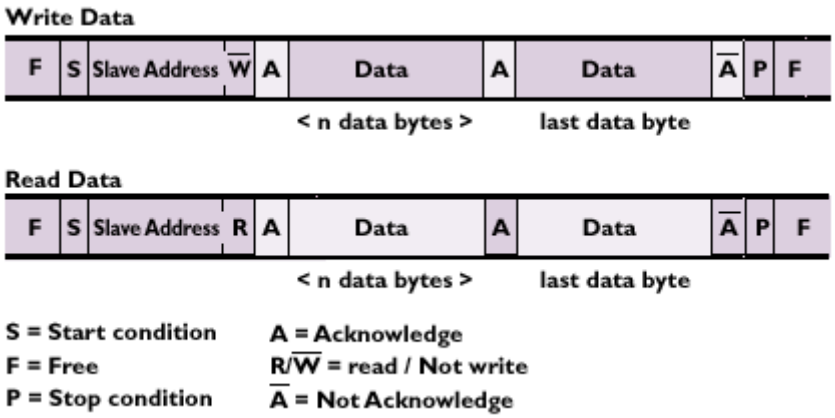

Figure 5-11 Illustration of I2C data transfer procedure (Philips, 2004)

In the case of the sensor suites, the I2C bus will be used to transfer the collected sensor data to the designated Master suite. This will result in the need for only one device to have external communication capabilities such as an RF link. This also means that less memory will be used on each suite since the data is passed and stored elsewhere on the bus.

5.4.2 Practical I2C work

To investigate the practicalities of the I2C bus, a simple bus was established by connecting two PCs via two I2C adapter boards. The boards installed were PC193LV I2C Communications Adapters from Calibre UK (2003). The boards act as an interface between the computer and the peripheral I2C components. In this case, the card contains a Philips PCF854 I2C bus controller chip. The connection is made through a

9-way D socket and uses three wires: the SDA, SCL and a wire connecting five shorted 0V pins between the PCs.

The hardware is controlled by a software interface. The boards are supplied with an application program called WINI2C. This is a development tool with a user friendly interface to allow non-specialist use of the I2C bus. A screenshot of the software interface in shown in Figure 5-12.

The software configures the board to be a Master Reader, Master Writer, Slave Sender or Slave Receiver. As one PC is designated as the Master, the Slave must be configured to perform the opposite function. The addresses of both can be set via the software and the Master told the address of the Slave it is to communicate with. The clock speed can also be set, although in most cases it was set to the fastest of the four possible speeds, 90kHz. The interface includes a table where the data to be sent is entered and where the received data appears. This data can then be saved to a text file.

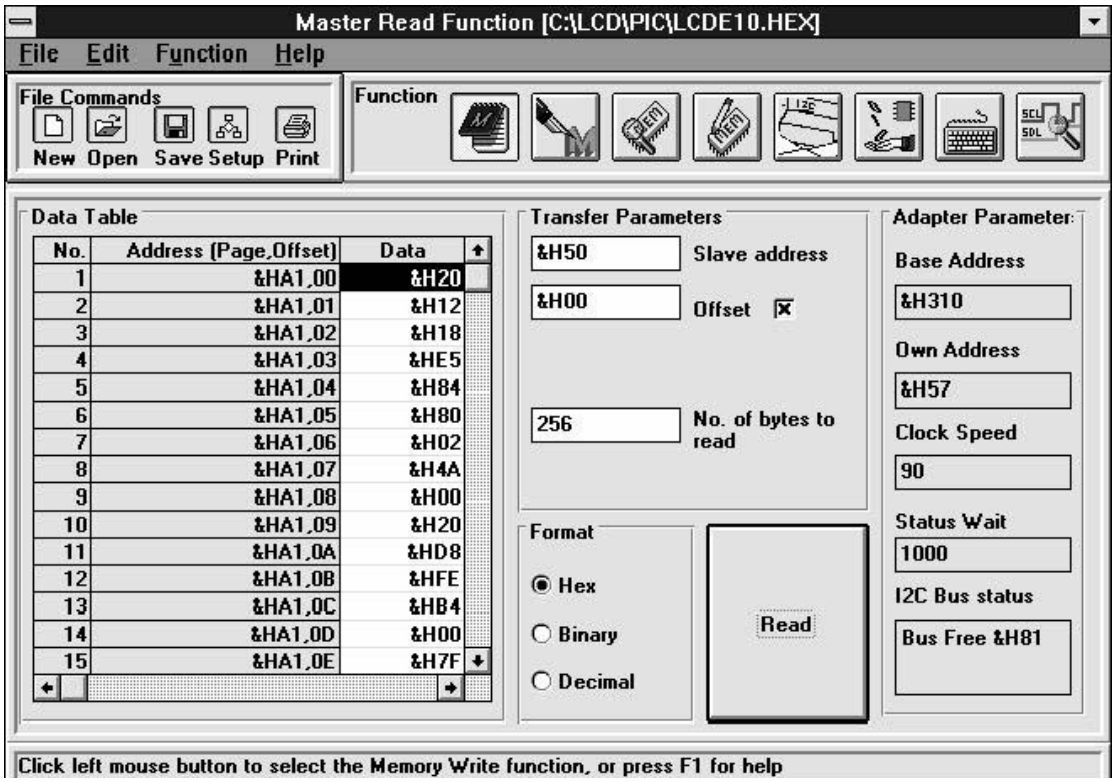

Figure 5-12 Screenshot of the WINI2C software interface (Calibre uk, 2000)

Although this software was sufficient for the purposes of this investigation, the WINI2C program is a demonstration tool and is limited in scope. For more control of the data transfer and sophisticated applications, an initial C++ program was developed by Quirke (2003) as part of an ongoing project investigating the Onboard Data Handling system of a small spacecraft.

5.4.3 Key lessons.

The I2C protocol is robust, well established and commercially available. It also meets many of the sensor suite criteria. From the investigations made the following points have been noted:

- The bus connection is made using three cables, the SDA and SCL wires plus either a 0V wire or a power wire if the device is not internally powered.
- Any device such as a microcontroller can be a Master and more than one Master per bus is permitted. This means that the system can have redundancy in case the Master is lost.
- The cable plus devices must have a capacitance of less than 400pF. This limits the length of the bus and the number of devices.
- Each device has a unique address which is required so that it can be identified by the Master. Due to the 7-bit nature of the address, only 8 devices of any one type can be used per bus, and up to 120 devices in total. This also limits the number of suites per system.
- The address means that the identity of the suite each set of data is sent from can be recorded.
- The clock speed and data transfer rate must be set. For the sensor suites, 100kbit/s is likely to be adequate.
- Pull up resistors are required to regulate the current through the bus.
- Data is passed in 8-bit words so only numbers between 0 and 255 can be transferred. To transfer sensor data, it must first be passed through an ADC.

A suitable method of including I2C capability to the sensor suite has to be selected which also meets the initial criteria. This facility can be provided by the suite's processing subsystem.

5.5 Processing – PIC Microcontroller

The processing functions for the demonstration sensor boards are performed through an ADC to a PC. In the miniaturised sensor suite, this function should be carried out by a microcontroller. The PIC range of microcontrollers from Microchip were investigated as typical devices which can provide the sensor suite with the necessary functionality. Once again the practical issues for using these chips are noted.

5.5.1 What is a PIC?

A microcontroller is essentially a computer control system on a single chip. It houses many electrical circuits which convert programmed instructions into electrical signals. The chips control the input data and produce an output that can be communicated.

The PIC microcontroller is a typical set of devices produced by Microchip Inc (2000) which are well recognised in the field of electronic systems. The range includes devices that are suitable for different applications depending on the amount of memory required or the complexity of the task. The chips are available in four formats with between 4 and 80 pins depending on the device.

The PIC microcontroller requires certain additional hardware in order to function. This is common throughout the range. A typical circuit is shown in Figure 5-13.

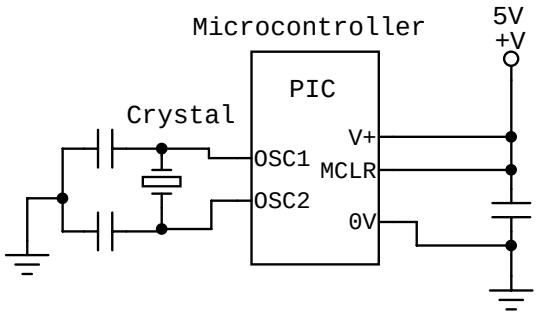

Figure 5-13 Typical Microcontroller circuit (Smith, 2002)

The speed at which the instructions are executed is determined by the clock frequency. This is provided by an oscillator crystal or RC circuit. The PIC generally requires between 2V and 6V.

In choosing a PIC suitable for the application, the minimum number of analogue and digital inputs has to be considered. Other considerations are the number of outputs, whether an internal ADC is required, the amount of program and additional memory and the extra functionality to be provided.

5.5.2 Choice of PIC for the sensor suite application

For the sensor suite, the requirements for the microcontroller are:

- At least 4 analogue inputs for the sensor data, with additional digital inputs for certain sensors.
- An internal ADC to convert the data.
- I2C bus compatibility.
- Low power, preferably with a power save option.
- Available in physically small packaging with wide operating temperature range as per the sensor criteria.

The device chosen was the PIC16LF877A (Microchip Inc, 2003). This device include 8 analogue input channels, an internal ADC, I2C compatible serial communication, 8K program memory with 368 bytes of data memory and 256 bytes of EEPROM. The LF device is a low frequency version which uses a clock frequency of 4MHz and a voltage of 3V. It draws a current of 0.6mA and has a standard operating temperature range of between –40˚C and 85˚C.

The preferred packaging option is the 44 pin QFN package. Its dimensions are given as 8mm x 8mm x 0.65mm. This is currently the smallest packaging option for this version. The pin configuration is shown in Figure 5-14.

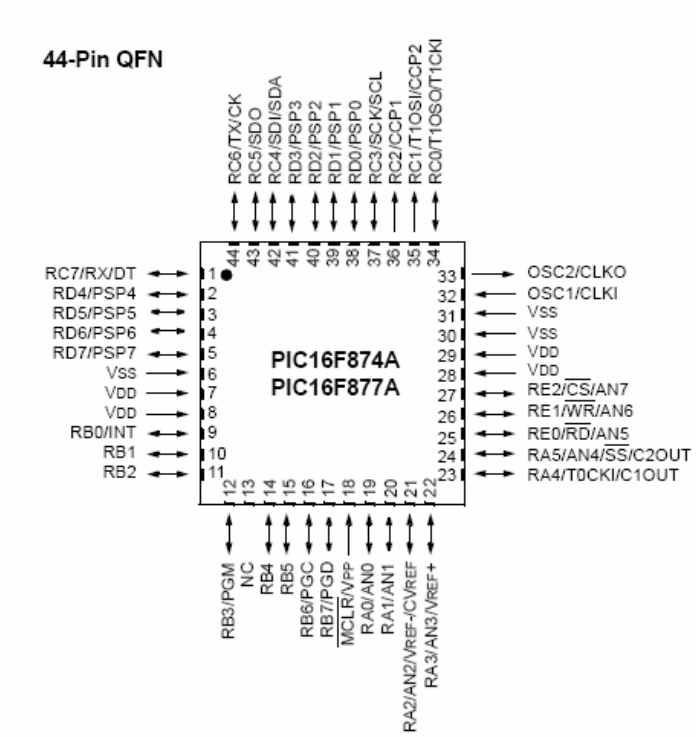

Figure 5-14 Pin configuration for the 44 pin QFN PIC16F877A microcontroller (Microchip Inc, 2003)

Several different examples of PIC chips were procured and tested. Sample programs were also investigated.

5.5.3 Issues raised with the PIC microcontroller

Through practical investigations, several lessons were learnt about the use of a PIC device.

- The chip itself requires additional oscillator and capacitor hardware in order to function. This will have to be included within the plan for the miniature sensor suite.
- The chip is programmed in Assembler code and then uploaded to the chip through a programmer. Assembler code comprises 35 instructions, however fewer are needed for even relatively complex operations. There is a range of well documented sample programs available for the ADC and I2C functions, so these chips can be programmed with very little specialist knowledge. Microchip provides programming environment software called MPLAB on their website which is designed for use with their microcontrollers. This is free of charge and does not require the use of other advanced programming tools or languages. This is very much an "off the shelf" product in that respect.
- All the required intersuite functions can be provided by the one chip, which reduces the number of components within the suite. This ultimately reduces the size and mass of the system.

- The microcontroller can supply 25mA to an output pin which can directly drive a device such as an LED (Smith, 2002) This can be used as an indicator or as part of the communications subsystem.
- The internal ADC uses the sensor analogue input voltages and converts them to an 8-bit number, where 0 is 0V and 255 is equivalent to 3V. This gives a reading of 85 per volt or 11.7mV per bit. Therefore a voltage reading of 0.9V equates to 77 (Smith, 2002). The I2C bus can transmit these 8-bit words directly to the Master suite.

The PIC microcontroller will be the central system of the sensor suite as it meets the overall requirements and provides the desired internal communications functions as well as processing the sensor data.

5.6 Conclusions drawn from the hardware investigations

Investigations using pieces of real hardware have provided a number of insights into the realities of designing a sensor suite system.

The whole sensor circuit has to be considered when constructing the suite, not just the sensor itself. Additional components such as capacitors or amplifiers may be required. Using sensors that require one standard voltage would mean that only one power source would be necessary. For the suite, this will be supplied by a battery, the capacity of which will be related to the application. The processing functions can be supplied by a single chip which includes an analogue to digital converter and I2C intersuite communications capability.

The overall criteria of MST COTS devices with low power requirements and low mass is achievable for many different devices including processors. The four sample sensors meet most of the criteria, however smaller MST devices are available and are discussed further in chapter 6.

6 Microsystems Technology

6.1 Introduction

The fourth objective of the project:

To investigate future full integration to "lab-on-a-chip", resulting in the eventual adaptation and miniaturisation of the suites to "matchbox" size

relates to two separate bodies of work within the overall project. This chapter discusses the possibility of future full integration and miniaturisation of the sensor suite system using Microsystems Technology (MST).

Although some discussion of the changes in the sensor suite design that will be necessary for full integration is made, the eventual "matchbox" concept is investigated further in chapter 8. The focus of this work is primarily on the applications of existing MST rather than the design and fabrication of the devices.

Sections 6.2 and 6.3 contain some background to the development of Microsystems Technology and the current state of its commercial availability. From this, specific MST sensors for the sensor suite concept will be investigated and the necessary changes to the conventional systems design will be discussed. This is covered in sections 6.4. The systems issues raised by this investigation will be addressed in section 6.5 and a further discussion on future full integration will be made in section 6.6.

6.2 Background – What is MST?

Microsystems Technology is a relatively new but fast growing part of the semiconductor industry. This section defines MST and provides examples of the current state of its development through both industrial initiatives and University research.

6.2.1 Definition

Although there has been much written on the topic of Microsystems, there does not appear to be a universally accepted definition of MST.

In general, MST refers to devices or systems that are on an equivalent micron scale to standard semiconductor devices, and in many cases, include microelectronics. The majority use the fabrication techniques established by the silicon semiconductor industry, such as micromachining, thin-film techniques and photolithography. MST refers to more than just components that have the same capability as their conventional counterparts, but at greatly reduced dimensions. This definition can be applied to the common American term, MEMS (Microelectromechanical Systems), whereas the European term, MST, has a broader meaning. Although the reduced dimensions of the

components is an important factor, the key to MST is the combination of these components to produce a “micro system” that provides a specific function.

For this study, it has been decided to adopt the definition given by “Microsystems in the 4th Framework IT” in September 1996 (Magan, 1996):

“In Europe, a microsystem (MST) is defined as an intelligent miniaturised system comprising sensing, processing and/or actuating functions. These would normally combine two or more of the following: electrical, mechanical, optical, chemical, biological, magnetic or other properties, integrated onto a single or multichip hybrid.”

Here the terms MST and MEMS will be used interchangeably depending on the type of systems and its origins.

6.2.2 Background and common use of MST

Since the first experiments into silicon etching techniques in the 1980s, the rate of production of MEMS and MST has grown substantially. As the fabrication techniques used in the semiconductor industry have become increasingly sophisticated, the range of MEMS components currently under development has broadened. Even over the duration of this project, the technology has progressed rapidly. However, the majority of these components are the results of university research programs and are not therefore commercially available. The most common components are accelerometers, pressure sensors and optical switches, as shown below.

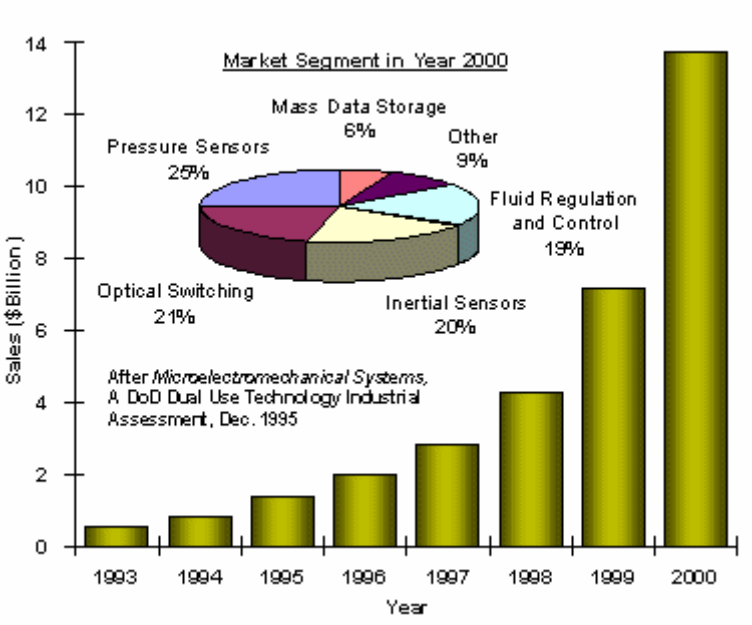

Figure 6-1 Market segments and Sales per year for the MEMS/MST industry (Michalicek, 2000).

The main industries that utilise this technology are the automotive and biomedical industries.

Common Automotive examples are:

- Accelerometers for Airbag deployment
- Tyre Pressure Sensors
- Inertial Navigation Sensors

In the biomedical industry, common uses include:

- Blood Pressure Sensors
- Accelerometers and Pressure Sensors in Pacemakers
- Sensors in Smart Prosthetic limbs

Other common uses include:

- Inertial Guidance Systems on Weaponry
- Optical Fibre systems
- Mass Data Storage devices
- Ink Jet sensors for printers
- Remote control vehicles

The future potential of these micron scale, highly integrated devices has been recognised by several other industries. These include Smart battlefield sensors for the Military, environmental control systems for housing and museums and for use in the Space industry to facilitate nanosatellites and planetary environment sensors.

6.2.3 European and Worldwide initiatives

As a relatively new technology, the need for collaboration between those engaged in research into MST, from both industry and academia, has been recognised. Information exchange and networking opportunities to promote advances in the field are key to having this technology adopted as the standard for many new applications. To this end, a number of initiatives have been founded in Europe and Worldwide.

NEXUS is a European non-profit association comprising over 1150 members from Europe and Worldwide. The aim of NEXUS is to promote Microsystems activities through conferences and report sharing. It also provides market analysis and strategic advice. Similarly, the European Society for Precision Engineering and Nanotechnology (Euspen) was founded in 1998 to raise awareness of emerging Micro and Nanotechnologies and provide opportunities for industry, universities and research institutes to meet through conferences and workshops. There are also several information exchange services available on the Internet. Minanet includes a searchable database of up to 1000 current MST projects. Other examples include MEMS Clearing House and MEMS Guide.

Europractice was established in 1995 to address the manufacturing needs for this emerging technology in Europe. Five MST Manufacturing Clusters were formed in the UK, France, Germany, Switzerland and Norway plus six additional Centres of Competence. Each Cluster is an association between companies and institutes in their

respective countries, each specialising in different techniques but all offering design and manufacturing for a range of products. (UK AMSTAP, 1999) There are also equivalent Clusters in the USA and Asia.

6.2.4 University research

Research into various aspects of MST is currently being carried out at institutions across the globe. A large number of universities worldwide have a micro-engineering department or are engaged in MST-based research activities to some extent. The list is extensive, however some notable examples follow:

- Berkeley Sensor and Actuator Centre, UC Berkeley, USA. – The centre was founded in 1986 and comprises a multidisciplinary team of 120 Graduate Students and Post-Docs under 10 Directors. The programmes undertaken all involve industrial collaboration in order to promote technology transfer between industry and academia. Research is conducted using many of the laboratories on the Berkeley and UC Davis sites and includes use of their own microfabrication facility. Projects have included:

    - Wireless Communicating microsensors
    - Biosensors and Biomanipulators
    - Adaptive Optical Micromirror arrays
    - Monolithic Self-Propelled Microbots
    - Silicon Germanium MEMS on CMOS process
    - CAD for MEMS
    - The Smart Dust project

- Research Centre of Intelligent Sensor Microsystems (DISens), TU Delft, Netherlands. – This centre was established in 2001 with the aim of promoting TU Delft as a major player in the MST research field. Their activities relate to medical instrumentation, environmental monitoring and transportation and have included a variety of intelligent sensor systems. One example is a smart wind sensor where the thermal flow sensor and related interface electronics have all been integrated onto one silicon chip. All aspects of the design and fabrication of these sensor systems are covered by work done at the Centre.

- Institute of Microelectronics, Tsinghua University, China. – The Institute is active in a variety of fields. It has focussed on many aspects of the development of various integrated circuits and their applications. Projects have included Information Microsystems for use in ID cards and public telephone cards, device design optimisation techniques and MEMS azimuth level detectors of use on miniaturised vehicles. In 2003, a proposal for research into a MEMS Satellite, including a payload of a micro imaging unit, was introduced at ESA's MNT for Space round table.

- Angstrom Space Technology Centre, Uppsala University, Sweden. – The ASTC has many current MST based space activities. Their main concept is called MMS – Multifunctional Microsystems, which comprises a single module design

that can be modified and updated using software. Proposed applications include an inflatable micro-rover and a balloon mission for Venus. They have also made advances in possible integration using techniques like thin film soldering and fusion bonding.

- Cranfield University has its own Nanotechnology group within the Department of Advanced Materials of the School of Industrial and Manufacturing Sciences. Research topics under investigation include Piezoelectric Ultrasonic motors and Thermal IR pyroelectric detectors for use in thermal imaging cameras. As with many departments at Cranfield, collaboration with industry is very important, as are the industrial applications of its research. The department also has its own fabrication facilities. Cranfield offers an MSc in Microsystems and Nanotechnology. The course covers all aspects of MST - the science that drives it, methods and processes, potential applications and the management of the technology. This course has received endorsement from many in the MST industry.

- The Central Microstructure Facility, Rutherford Appleton Laboratory, UK. – The CMF offers a neutral site for industry-academia or industry-industry collaborations in the form of fabrication services and R&D facilities. This encourages the technology transfer opportunities which will benefit those involved in this field.

6.3 Currently available components

Although there are many forms of MST devices and component currently under development at universities and research institutes, this project aims to take advantage of Commercial-off-the-shelf components that are readily available and can be acquired for a fraction of the cost of a bespoke or prototype component. The most common sensors are pressure sensors and inertia sensors such as gyroscopes and accelerometers, however other types are available.

Table 6-1 shows a selection of various types of COTS MST components with their power requirements, range and accuracy, operating temperature, physical dimensions and approximate cost. These reflect the selection criteria stated in section 5.2.3.

Accelerometers

Manufacturer	*Product*	*Voltage range*	*Current*	*Range*	*Accuracy*	*Temperature*	*Cost*	*Mass*	*dimensions mm*	
Analog Devices	ADXL250	4 - 6 V	3.5 mA	+/- 50g	2%	-40 to 85 C	£18.56	5g	9.9x10.6x5.4	dual axis
Analog Devices	ADXL202E	3 - 5.25 V	0.6 mA	+/- 2g	2%	-40 to 85 C	£32.70	<1g	5 x 5 x 2	2 axis
Colibrys	MS7000	2.4 - 5.5 Vdc	<200 uA	+/- 2g		40 to 125 C		3g	15 x 3.75x2.96	silicon flexure
Delphi (Angular)	G2RV	5 V	5 mA	+/- 500g	+/- 3%	-40 to 125 C			12.96x7.57x5	analog output
Endevco	35A	18 - 24 Vdc	3.5 - 4.5 mA	+/- 1000g	<5%	-55 to 125 C	£1,697	1.1g	6.35x7.62x6.35	integrated electronics
Endevco	65	22 - 30 Vdc	2 - 20 mA	+500g	<5%	-55 to 125 C	£1,199	5g	18.5x10x10	constant current
Kionix	KXM52	2.5 - 5.5 Vdc	1.5 mA	+/- 2g	1%	-40 to 125 C	NA		5x5x1.8	diff capacitance, ASIC
Kistler	8694MI	12 - 30 Vdc	2 - 20 mA	+/- 500g	+/- 1%	-55 to 135 C	NA	2.5 g	10.5x10.5x10.8	Quartz sensing element
SensoNor	SA50	4.5 - 5.5 Vdc	6 mA	+/- 50g	<5%		NA			ASIC, silicon sensor
ST (3 axis 2g)	LIS3L02	3 - 5.25 V	1 mA	2g per axis	10%	-40 to 85 C	£10.50		15.6x7.6x2.65	analog or I2C output

Gyroscopes

				(deg./s)						
Analog Devices	ADXRS300	5 Vdc	6 mA	+/- 300	0.1%	-40 to 85 C	$33	<0.5g	7x7x3	z axis+electronics
BAE Systems	SiVSG	5 Vdc	50 mA	+/- 100	0.5%	-40 to 85 C	~$1		29x18x29	resonance
BEI Gyrochip	QRS14	9 to 18 Vdc		+/- 50to1000	<0.05 d/s					solid state
Kionix	KGF01	5 Vdc	15 mA	+/- 75 to 300	1%	-40 to 125 C			7.7x15.5x3.2	capacitive based, x axis
MicroSensors	microring	4.75 to 5.25	15 mA	+/- 60	+/- 1 d	-40 to 85 C				force on diff capacitor, si
MicroStrain	3DM-DH	5.2 to 12 Vdc	50 mA	180/180/70 d	0.93/0.33/1	-25 to 70 C			2.8x6.7x0.8 cm	3 axis

Pressure

Manufacturer	*Product*	*Voltage*	*Current*	*Range*	*Accuracy*	*Temperature*	*Cost*	*Mass*	*dimensions*	*Other*
									mm	
acsensor	7290	5 Vdc	1mA	690 kPa	+/- 0.3%	-20 to 60 C	£3.50		17 x 10 x 3	chip on board, for tyres
Campus				70 - 150 kPa	+/- 15%	-10 to 80 C			0.8 x 2x2	flipchip. Capacitive
First Sensor	MPSi 012	5V		1200 kPa	0.3%	-40 to 125 C				
Honeywell	40PC	5 Vdc	10mA	103.4 kPa	0.2%	-45 to 125 C	£35.92		13.2x11.2x19	si piezoresistive,amplified
Honeywell	26PC	10 Vdc	1.33mA	103.4 kPa	0.5%	-40 to 85 C	£20.65	0.5g	7.1x10.4 x5	Surface mount.
Honeywell	180PC	7 - 16 Vdc	6 mA	103.4 kPa	0.5%	-40 to 85 C	£80.32	12g	29 x 16x10	absolute and differential
Melexis	MLX90210	5 V typ	0.4mA	100 kPa	22 mV/V/bar	0 to 70 C			1.9 x1.9 x 0.61	piezoresistive
Melexis	MLX90240	5 Vdc		35 kPa	58 mV/V/bar	-20 to 85 C	£8.00		7.5 x 7.5x3	can be unpackaged
MEMSCAP	SP82	7.5Vdc	1.5 mA	6000 kPa	0.20%	-55 to 125 C	£180	2.5g	12.6x12.6x4.5	piezoresistive
Motorola	MPX4080D	5.1 Vdc	7 mA	0 - 80 Kpa	+/- 3%	-40 to 105 C	£5.00		11.43x16x5.59	piezoresitive, analog
Novasensor	NPP-301	3.0 - 10Vdc	0.6 mA	100/200/700kPa	<0.20% FSO	-40 to125 C	£5.50	0.10 g	4x5x3	Surface mount.
Novasensor	NPD			up to 10000 PSI	4mV/V				1x0.7x0.175	piezoresistive
SensoNor	SP13	3 - 3.6V	2.8mA	50 - 637.5 kPa	+/- 10 kPa	-40 to 125C	£23.50		19x10x5	integrated T&P
Silicon Microstructures	SM5310	5V typ	1.5 mA	35 - 690 kPa	+/- 0.05 % FS	-40 to 85 C	£3.00		7.6x7.6x3.6	Surface mount.

Temperature

Analog Device	AD7418	2.7 - 5.5V	600 uA	-20 to 100 C	+/- 1C	-40 to 125 C	£1.40	0.1g	4x5x1.75	I2C compatible, analog in
Honeywell	TD	10 Vdc	0.1mA	-40 to 150 C	+/- 2.5C	-40 to 150 C	£18.50		4x3x1.5	thin film silicon resistor
Lake Shore Cryotron	DT670EBR	40 Vdc	10 um	-248 to 227 C			£527	72.7mg	0.4x0.43x0.04	Bare silicon die.
Melexis	MLX90247	no voltage		small heat rad	0.10%	-20 to 85 C			4x9	thermopile IR detector
National Semicond.	LM35	-0.2 to 35V	10 mA	-40 to 110 C	0.4C	-40 to 110 C	£5.30		4.5x4.5x3.5	semiconductor
National Semicond.	LM20	2.4-5.5 V	10 uA	-55 to 130 C	+/- 2.5	-55 to 130 C	£0.20		2x1.8x0.8	available unpackaged
Philips Semiconduct	KTY84-1	2V	2 mA	-40 to 300 C		-40 to 300 C	£0.34		3.4x1.5x1.5	resistance
Scientific Instrument	Si-410		10 mA	-271 to 177 C	0.5 K				23.6x63.5	silicon diode

Light / Radiation

Manufacturer	*Product*	*Voltage*	*Current*	*Range*	*Accuracy*	*Temperature*	*Cost*	*Mass*	*dimensions*	*Other*
				nm					mm	
Centronic	OSD5.8-7Q	5V	10 mA	400-950		0 to 70 C	£32.49		5.8 mm^2	hermetically sealed
Hero (UV)	EPD 150	10 V	100 uA	150-550		-40 to 125 C			2.5x2.5	photodiode
JIC	JIC117	2.7-5.5V	750 uA	210 - 390		-25 to 85			0.055 mm^2	in packaging
Photonic Detectors	PDB V601	25 V	13 uA	350 - 1100		-40 to 100 C			1.0 mm^2	Photovoltaic, blue
Twlux	TW30SX	3V	1 mA	215-387		0 to 60 C	£6.20		2.1x2.1	photodiode,TO18

Humidity

Honeywell	HIH-3610	4 to 5.8 Vd	200 uA	0 to 100%	2%	-40 to 85 C			4.3x9.5x2.0	
Hygrometrix	HMX2000	1.2 Vdc	0.7 mA	0 to 100%	3%	-40 to 85 C	£8.00		2 x 2	piezoresistive
MCB	si project			10 to 95%		20 to 300 C			2.5x2.5x0.5 m	porous silicon

Magnetometers

Melexis	MLX90215	5V	4 mA	prog	1%	-40 to 85 C	$10.12		5.3x3.5	programmable
NVE	AA002-02	2.7 - 5.25	650 uA	+/- 0.5 Gauss	2 mG	to 125 C			436x3370 um	SMT - analog
Xensor Integration	EMF-02	8-10V	4mA	0.1 - 0.1e-6 uT			€270 kit		1.6x1.8	3d sensor cube

Others

Rockwell Scientific	ProCamHD	3.3 V	60 mA	2/3",	68 db snr				12.5x8.5	iSOC imager
				1936x1086 pixel						
Tronics Geophones								1g	0.5 cm^3	seismic
									cm	
Indigo	Omega	<1.5 Watts power				0 to 40 C		<120g	3.4x3.7x4.8cm	bolometer camera

Table 6-1 Examples of COTS MST Sensors (listed alphabetically)

Examples for sensor suite design

The design for the basic environmental sensor suite proposed in chapter 5 includes four types of sensor: Accelerometer, Pressure, Temperature and Light/Radiation. In Table 6-1, further examples of these sensor types that utilise Microsystems Technology have been identified, and the specifications of several of these sensors are investigated further in the following sections. In order to compare the different designs and their suitability for use in a potential MST sensor suite, each sensor was evaluated and awarded a figure of merit based on common factors.

6.3.1 Figures of Merit and sensor comparison

Many factors could have been chosen as the basis of the figures of merit for each sensor type, for example thermal properties or reliability. It is recognised that each factor is important and provides useful information on the performance of the sensor. However, in this case each sensor design was evaluated in terms of its power requirements, dimensions, measurement range, minimum operating temperature and cost since these are relevant to the selection criteria discussed previously, were common to each of the designs and could be based on the data published by the manufacturers.

For inclusion in the sensor suite, each sensor should occupy as little physical space as possible. The first figure of merit therefore compares the volume of each sensor package. This is given in mm^3. As low power is also a requirement, the second figure of merit compares the power requirements of each sensor per unit volume. A third figure also relates the volume to measurement range of the sensor, in either per g, per kilopascal or per ˚C. Another requirement is for low cost COTS technology. Two figures involve a typical cost of each sensor; cost per unit volume and cost per unit measurement. Finally, since the survivability in extreme conditions is also a key factor, any sensor whose minimum operating temperature is above –20˚C is discounted.

The figures for each category of sensor are given below.

6.3.1.1 Accelerometers

The Figures of Merit for the Accelerometers are featured in Table 6-2

Product	Volume (mm^3)	Power / volume ($mWmm^{-3}$)	Volume per g (mm^3/ms^{-2})	Cost per mm^3 (£mm^{-3})	Cost per g (£/ms^{-2})
Analog Devices ADXL202E	50	0.036	25	0.65	16.35
Analog Devices ADXL250	566.7	0.03	11.33	0.03	0.37
Colibrys MS7000	166.5	0.006	83.25	NA	NA
Delphi G2RV	502.2	0.04	1.00		
Endevco 35A	307.3	0.26	0.31	5.52	1.70
Endevco 65	1850	0.14	3.7	0.65	2.40
Kionix KXM52	45	0.11	22.5	NA	NA
Kistler 8694MI	1190.7	0.17	2.38	NA	NA
ST LIS3L02	314.2	0.02	157.1	0.03	5.25

Table 6-2 Figure of Merit for MST Accelerometers (listed alphabetically)

The volume of the packages varies from 1850 to 45 mm^3, with the smallest being the ADXL202E and the KXM52. The accelerations measured by the sensors are ±2g, ±50g, ±500g or ±1000g and are designed for different applications. As such per g figures of merit should be compared for sensors with the same range. For tilt sensing and low g applications, the ±2g sensors are sufficient, although their cost per g is higher than that other types.

The Colibrys MS7000 series (formerly the Honeywell ASA7000) are MEMS silicon capacitive sensors and include their own interface electronics, such as an amplifier and its own microcontroller to store compensation values. Of the sensors analysed, these use the lowest power, drawing only 200μA at 3Vdc and has a relatively low power per unit volume. It has been designed for navigation and guidance for aerospace and defence applications and as such can withstand shocks of up to 10000g and 2000Hz vibration. They are available for ±2g and ±10g. They have a mass of 2.6 grams and are packaged in a low magnetic nickel housing. The latest capacitive accelerometer from Colibrys, the MS8000 series, has many of the same benefits as the earlier series. It also includes an integrated temperature sensor and is packaged into a chip of 14.2 x 14.2 x 3.3 mm, weighing 1.64 grams. However, the temperature sensor is only accurate to ±5°C, which may be insufficient for scientific environmental sensing. This model draws 250μA at 5Vdc, which is more than the previous model, but still compares favourably to the other types of accelerometers.

For measurement of more than one axis, Analog Device's dual axis model ADXL202E would be a preferred option. It can measure both dynamic and static acceleration in the x and y direction and can withstand shock of 1000g. Another benefit for the basic

sensor suite is that its readings can be read directly by a microcontroller without the need for an A/D converter. This reduces the amount of additional components required within the suite, and therefore its overall size and mass. It has a 5 x 5 x 2 mm hermetically sealed package, which is one of the lowest volumes recorded, and with its low power, this model would be well suited to the sensor suite.

Two types of three-axis accelerometer are featured in this study. The ST LIS3L02 incorporates a silicon capacitive sensing element and a CMOS IC interface for signal processing. The family of sensors includes the standard analogue output and a fully digitised I2C compatible output and are available in the SO-24 chip packaging. The Endevco 35A accelerometer utilises piezoelectric technology and include internal amplifiers. This unit weighs only 1.1grams and is powered by a constant current power source. However, the Endevco model retails for £1697, and has the highest cost per unit volume.

Given these options, the preferred accelerometer for the basic sensor suite would be the Analog Devices ADXL202E, for its low cost, small size and its direct to microcontroller capability.

6.3.1.2 Pressure Sensors

The Figures of Merit for a range of pressure sensors are listed in Table 6-3.

Product	Volume (mm^3)	Power / volume ($mWmm^{-3}$)	Volume per kPa (mm^3/kPa)	Cost per mm^3 (£mm^{-3})	Cost per kPa (£/kPa)
acsensor 7290	510	0.009	0.74	0.007	0.005
Honeywell 26PC	369.2	0.036	3.57	0.056	0.2
Honeywell 40PC	2809	0.018	27.17	0.013	0.35
Honeywell 180PC	4640	0.013	44.87	0.017	0.78
Melexis MLX90240	168.8	0.011	4.82	0.047	0.23
MEMSCAP SP82	714.4	0.015	0.12	0.25	0.03
Motorola MPX4080D	1022.3	0.035	12.78	0.0048	0.06
Novasensor NPP-301	60	0.03	0.6	0.09	0.055
SensoNor SP13	950	0.009	1.62	0.025	0.035
Silicon Microstructures SM5310	207.9	0.036	0.32	0.014	0.03

Table 6-3 Figures of Merit for MST Pressure Sensors (listed alphabetically)

The volumes range from 60 mm^3 to 2809mm^3, however both the cost per volume and cost per kPa are similar. There is also various pressure ranges available which can be chosen as the application requires.

The Melexis MLX90210 from Table 6-1 has the smallest dimensions when compared with the other sensor packages with a volume of 2.20mm^3. It is possible to order this sensor unpackaged, which could lead to easier full integration. This is a silicon piezoresistive bridge circuit fabricated through micromachining. This sensor would have to be interfaced with additional electronics to provide amplification and signal conditioning, although it is possible to interface it directly to another IC produced by the same manufacturer. Although this sensor has many advantages, it is unsuitable for the basic sensor suite due to its minimum operating temperature, given as 0°C. As stated previously, the maximum temperature on the Martian surface is 268K, or -5°C. Therefore this sensor is discounted in this case, as are others whose minimum operating temperature is above –20˚C.

The Novasensor NPP-301 series pressure sensor is also a silicon fusion bonded piezoresistive chip featuring a Wheatstone bridge circuit. The chip has plastic packaging and is designed to be surface mounted. As with the previous design, additional circuitry would be required to amplify the output. Although they have similar accuracy and design features, this sensor, unlike the Melexis model, can operate at temperatures as low as -40°C, however the overall package is twice the size.

The SensoNor SP13 is interesting because it includes an integrated temperature sensor in addition to the piezoresistive pressure sensor. However this sensor was designed for tyre pressure monitoring, and as such has an operating range of between 50 and 637.5 kPa. This would be too high for a generic sensor suite for use on Mars or other low pressure environments.

The Memscap SP82 has been designed for Aerospace and Defence applications, and so has been tested to withstand mechanical shock of 500g. It is available in a range of maximum pressures, from 0.5 bar (50 kPa) to 60 bar and can give absolute, relative or differential measurements. However, this is one of the largest of the packages investigated and, at £180 per item, one of the most expensive.

The Honeywell 40PC device discussed in chapter 5 is relatively large compared with the sensors discussed here. Also the attached funnel is unsuitable for the sensor suite concept. From the above, the sensor that is most suitable for this sensor suite would be the Novasensor NPP-301. Novasensor also have another piezoresistive sensor in development, the NPD, that has dimensions of 1mm x 0.7mm x 0.175 mm. If this sensor has similar features to the NPP, it could prove to be the preferred option for the suite. However, complete data on this sensor is currently unavailable.

6.3.1.3 Temperature Sensor

In chapter 5, the temperature sensor used a platinum Resistance temperature detector. Although it meets the size criteria, this is not an example of MST and is not made from a material such as silicon that could be fully integrated. The majority of the temperature sensors considered here are integrated circuit chips which will require less additional components than the RTD and are compatible with future integration.

The Figure of Merit for the temperature sensors is shown in Table 6-4.

Product	Volume (mm^3)	Power / volume ($mWmm^{-3}$)	Volume per ˚C (mm^3/˚C)	Cost per mm^3 (£mm^{-3})	Cost per ˚C (£/˚C)
Analog Devices AD7418	35	0.05	0.29	0.04	0.012
Honeywell TD	18	0.056	0.09	1.03	0.097
Lake Shore Cryotron DT670EBR	0.007	57	0.000015	75286	1.11
National Semiconductors LM20	2.88	0.01	0.016	0.07	0.001
National Semiconductors LM35	70.9	2.82	0.47	0.07	0.035
Phillips Semiconductor KTY84-1	7.65	0.52	0.023	0.04	0.001

Table 6-4 Figure of Merit for temperature sensors (listed alphabetically)

The Lake Shore Cryotron DT670EBR temperature sensor gives very different figures to the other sensors. The small dimensions are due to the fact that it is a bare silicon die with no packaging. This could simplify future full integration. This sensor is specifically designed for cryogenic conditions, so the temperature range would be ideal for measurements of the Martian surface conditions. On paper, this is the most suitable sensor, however it requires 40Vdc, which would need to be generated, and at $1000 per unit, the cost could prohibit its use in a low cost suite.

The National Semiconductors LM35 and the Analog Devices AD7418 are both semiconductor temperature sensors. They have similar dimensions and are both low cost. However, the AD7418 includes its own A/D converter and is I2C compatible. This type of sensor could be used as a stand-alone sensor on the I2C bus external to the sensor suite if additional temperature readings are required for the particular application. The National Semiconductors LM20 has the smallest physical dimensions of the packaged sensors and the lowest figures of merit overall. It's low power consumption and broad range means this is the preferred sensor for the suite.

6.3.1.4 Light/Radiation Sensor

Although a visible light sensor is discussed in chapter 5, the measurement of other types of radiation may be required for environmental sensing applications. Of the Radiation sensors investigated, the JIC177 Ultraviolet photodetector is the chosen model for the sensor suite. It can operate under low temperature and has acceptably small dimensions as well as requiring the lowest power. The others either cannot operate within the required temperature range or would require high voltage to be generated. The actual sensor choice would depend on the type of radiation to be measured.

6.3.2 Chosen MST sensors for sensor suite

From the COTS sensors investigated and based on the figures of merit derived, the sensors chosen for the final basic sensor suite are:

- Analog Devices ADXL202E 2 axis ±2g accelerometer
- Novasensor NPP301 100kPa pressure sensor
- National Semiconductor LM20 temperature sensor
- JIC117 UV radiation sensor

All of these sensors have the lowest figures of merit overall and will be appropriate for a wide range of applications. They also meet the selection criteria established in chapter 5.

6.4 MST issues raised and possible solutions

Although MST systems and components have obvious benefits, such as their low mass, size and power, further research will have to be undertaken in order to resolve the issues raised if they are to be used for sensing and Space applications. Three of the most common issues that would be associated with the use of these components in the planetary environmental sensor suite are discussed below.

6.4.1 Standardisation

As the table of commercially available components shows, there appears to be very little standardisation within this emerging industry. Whilst it is understandable that each component will have its own features to make it commercially attractive, in terms of a generic sensor suite, common input and output formats are desirable.

One example is that of the range of excitation voltages that the different sensors require. This can vary from 3Vdc to 40Vdc, even though the type of sensor may be the same. Many tend to use between 3 and 5 Vdc, however this is far from standard. If all the voltages were the same, it would mean that additional voltage regulators would not be needed, reducing the number of extra components. The format for the output also varies between sensors. Most give an analogue voltage, however some are amplified and others are in the range of millivolts. Other sensors include their own analogue to digital converters and some can be interfaced directly with microcontrollers. These differences could make interchangability problematic, since each sensor could require its own form of interface circuit or protocol. Without a universally agreed format, the choice of compatible sensors would be limited.

Initiatives such as the European Multifunctional Micro System Programme (EMMSP) proposed by the Angstrom Space Technology Centre of Uppsala University (Stenmark and Bruhn, 2003) start to address the need for some form of standardisation and cooperation in order to promote this technology. The aim of this programme is to bring together partners with systems that are in an advanced stage of development, and support the adaptation and integration of that system to fit a modular platform that will

eventually be launched as a Nanosatellite. The partners will benefit from the ability to flight qualify their systems and also from the combined quality assurance and feedback.

Another way in which some form of standardisation is required is in terms of quality assurance and reliability. As yet there is no widely accepted quality assurance programme for MST. Without sufficient reliability assurances, there is reluctance by the space industry to adopt this new technology for missions critical systems. Reliability studies and failure analysis is currently being undertaken by CNES (Schmitt, Esteve, Fourniols, Lafontan, Pons, Nicot, Pressecq, and Oudea, 2003; Barthe, Pressecq, and Marchand, 2003) amongst others with the aim of identifying and rectifying potential fatal errors.

The issue of standardisation can be addressed through the cooperation of the major players in the industry. The initiatives and knowledge transfer opportunities provided by bodies like ESA and those established specifically for the promotion of MST such as NEXUS should encourage the adoption of industry standards. However, since the space industry only comprises a small part of the overall MST industry, it is likely that these standards will be determined by other players and therefore will have to be adapted for use in Space.

6.4.2 Packaging

The issue of packaging is a significant one and as a result almost all meetings and conferences on Microsystems have a session devoted to this topic. The essential purpose for the packaging is to offer protection for the sensitive elements of the systems. However the methods used in traditional semiconductor manufacture may be inappropriate for Microsystems due to their unique and compact nature. The most common processes are that of injection moulding of a polymer to the circuit or attaching the chip to a lead frame (Ulvensoen, 1998).

MEMS components are extremely sensitive to the mechanical and thermal stresses experienced during traditional packaging methods, with the sensor elements being the most sensitive of all. In the injection moulding process, the sensor element is in direct contact with the moulding material. This can lead to problems involving shrinkage and structural transitions that occur as part of the hardening and cooling process. The most common solution to this problem is to cover the sensitive element with a soft material to absorb the stresses. Similarly a low stress adhesive must be used to bond the silicon dies to a lead frame.

The nature of many of the environmental sensors means that the sensing element must be exposed to the surroundings under investigation. This means that the sensor will interact with the gases, liquid and other particles present in that environment. Humidity can have severe effects on MEMS sensors. Surface tension causes a gluing effect on those with any moving parts, resulting in part failure. Humidity also reacts with the majority of adhesives used in the bonding process, causing changes in its effectiveness and additional liquid or gas content around the sensor. The common solution to this problem is to use a shielding membrane around the sensor element. However this adds to the complexity of the design, and as so would add to the cost per unit.

The principle concept behind MST is that of a device that incorporates multiple functions. Therefore it must be possible to integrate the different sensor elements and other functions such as a power source or transmitter onto a single chip. Close integration of the sensor with its associated electronics is also important. The low level of the output signal from each sensor means that the data handling circuits will have to be in close proximity in order to prevent excessive signal degradation (Val, 2003). Ideally, however, the entire system should be able to be packaged into the standard polymer chip packaging and be able to be mass produced on the same scale and at the same low cost as traditional semiconductor devices.

6.4.3 Space-related issues

There are specific issues that become important when considering MST for use in a Space and planetary environment.

The majority of the MST sensors that have been produced so far have been with a specific purpose in mind, such as tyre pressure monitoring or accelerometers for use on the guidance system of a missile. As such, the measurement range and accuracy required for these applications has determined the design limits of the sensor. Since there are some considerable differences between these terrestrial applications and those that an environmental sensor suite on the surface of Mars would encounter for example, the sensitivity of these sensors may not be sufficient. For example, the mean atmospheric pressure on Mars has been measured to be 675 Pa, compared to a mean of 101325 Pa on Earth. Those pressure sensors designed to measure 100 kPa and above are therefore unlikely to be sensitive enough for use in such as low pressure environment. This may limit the choice of commercially available sensors and may force the use of specially designed units.

In a similar way, the low temperatures experienced in Space may also require specialist equipment. As stated previously, the minimum operating temperature for most standard and MST components is -40°C. Observations of the Martian surface have recorded surface temperatures between -5°C and -90°C. This poses two possible problems. Firstly, any temperature sensor would have to be able to measure these ranges. This means that specialist cryogenic sensors would have to be used, which are commercially available but expensive. Secondly, all other components would need to be able to operate at these extremes. Although most components are not tested to this level, it is possible that they could still function, although low temperature experiments would have to be performed to investigate this further. However, if any component will not function properly at low temperatures, additional insulation and heating would be required. This adds to the packaging issues, and would increase the overall suite size and complexity.

The background radiation experienced by the sensor suite will have to be taken into account. This radiation is present on Earth and consists of alpha particles, neutrons and subatomic particles caused by cosmic rays and the decay of naturally occurring radioactive atoms. These particles pass through semiconductor material creating electron-hole pairs along their path, which can cause “soft errors” in the data being

collected. This means that the data retrieved is different to the data originally stored. These errors and their effects are unpredictable, and as a result, the effects could range from minor to catastrophic. The additional charge these particles create adds to that which builds up on the capacitor where the sensor is of a capacitive nature and causes erroneous readings. Since many MST sensors are capacitive, and the amount of charge required for a positive reading is being reduced, this could cause significant problems. The probability of one of these particles interacting with a sensor or another sensitive system is increased as the number of systems per area increases. As the goal of MST is to integrate as many systems into one chip as possible, this again increases the risk of soft errors.

The traditional answer to the problems posed by radiation is increased shielding. Current chip packaging will stop most alpha particles. However, it would require a 20cm layer of Aluminium to stop atmospheric neutrons from reaching the silicon chip (Electronic Design Europe, 2004). This is impractical given the scale of the chips in question, and even more so for those using MST. In order to address this, ST Microelectronics has devised a method of protecting their SRAM memory cells from soft error effects. They have integrated additional capacitors into the cell structure in the vertical dimension. Since the important factor in the fabrication of these silicon chips is the area that each chip covers on the silicon wafer rather than its depth, this will not significantly increase the area and therefore not increase the manufacture cost. The capacitors increase the amount of charge required to "flip" the cell, thus reducing the number of soft errors in a given time interval (Electronic Design Europe, 2004). Tests on these cells have shown that they are 250 times more resistant to soft errors than their traditional counterparts. This method could be used in MST chips, although it would add to the overall size. The affects described and their possible solutions are all based on observations made in terrestrial environments. The effects experienced in Space or in other planetary environments are very different. On Earth, most of the cosmic ray particles have lost much of their energy due to atmospheric collisions or are deflected by the magnetosphere. In an environment with little or no atmosphere, the energy remains, causing the effect to be more significant and dangerous for sensitive systems. Radiation effects in Space are more likely to require shielding from, and therefore additional packaging.

The sensor elements that require exposure to the external environment will be subject to contamination from the gases, liquids and other particles present in that environment. In the case of the Martian surface, this will also include the slightly magnetic dust that covers the surface of the planet. It has been observed that this dust settles on probes at a rate that covers 0.3% of the exposed surface area per day (Landis and Jenkins, 1997). Over long periods of time this would become significant, since it would cover solar panels, for example, and reduce power generation, or obstruct the sensor element so no further readings could be taken. More significantly for MST, the dust particles would have a considerable impact on the micron-scale elements of the sensors. Whilst macro sensors would develop a coating of the dust, micro sensors are more likely to be damaged or destroyed by the dust particles, due to their relative scale. This is likely to add to the packaging issues, so that sensitive areas are adequately protected.

There are other more general issues related to the use of sensor probes for planetary exploration. The suites themselves will of course be subject to the stresses of launch and spaceflight. Vibrations, extreme temperatures and vacuum conditions will all need to be taken into account when designing the suite and its launch housing. Once at its chosen destination, the suites will need to be deployed. Once again there will be shocks related to landing on a chosen surface that will need to be considered. Power generation will also be an issue, as with any space based probe. The most common forms of generation are solar panels and rechargeable batteries. In order to maintain the idea of a miniaturised suite, the power generators must be relatively small, as must their related electronics. This is one area where MST is ideal, since the majority of the sensors are designed to use low power.

A crucial issue regarding the use of MST for space is that of reliability. If an element fails, such as the primary sensor unit or the processor, the probe will be lost. This could result in mission failure, since fixing the problem would be highly unlikely. As previously discussed, the untested nature of this technology has so far hindered the adoption of MST by the industry. However, if the mass of the entire suite can be kept as low as possible, multiple suites could be used in the place of one larger probe. This adds redundancy to the overall sensing system, so that even the loss of a large number of the suites would not necessarily mean the end of the mission. This is one of the main benefits of the use of MST, and one of the principle reasons for the current interest in the technology by Space mission planners.

6.5 Full integration potential

The future goal of MST is for a fully integrated “lab-on-a-chip”, with as many functions as possible miniaturised and integrated into a single package. The traditional method of connecting different parts of the system together is the use of wires or some form of bonding. At the micro scale, wire bonding is no longer practical due to their relative size and resistive properties that would dominate the system and interfere with the signals being transferred.

Since the majority of MST components are silicon based and are fabricated on silicon wafers using techniques such as photolithography, it seems reasonable that these properties can be used to integrate several systems. The method which appears to be favoured in terms of research is that of using layering. The individual systems are formed by layering vertically, essentially stacking one on the top of another, reducing the necessary footprint area of the chip. It also means that no additional space is required on the circuit board of the final application, maintaining the same dimensions for increased functionality. Research is being undertaken at several institutions into system interconnections. One example is from Uppsala University (Kratz and Stenmark, 2003). They have used naked RF dies for a communications system, that is bare silicon chips with no packaging. Low temperature bonding has been used to stack the individual wafers and package them together. This is an example of a Multichip Module (MCM). These are not completely integrated since the dies are produced separately, but are more so than current technologies.

An investigation into the different integration technologies was conducted by Astrium Ltd. (Lecuyot, Snelling, and Tual, 2003). The three technologies investigated were the system-on-a-chip, the MCM and current hybrids. The hybrids use current MEMS chips and traditional bonding methods to integrate its related electronics onto a small printed circuit board. The published results of their investigation are summarised in Table 6-5.

Technology	System-on-a-chip	MCM	Hybrids
Integration levels	High Highest with current technologies	Medium Much better than current levels	Low Only the miniaturisation
Technology readiness	Development No working prototype	Prototype Some similar products	Product Flight proven
Technical hard points	Integrated design Complex project	Process compatibility	None
Industrial readiness	European Industry does not have capacity	MCM capacity Adaptation possible	Ready except for device procurement
Industrial hard points	Very large infrastructure required	Modification of MCM process and culture	None
Est. development cost	> 1 M£	~ 500 k£	~ 200 k£
Time to market	10 years	7 years	3 years
General pros	Ultimate in microtechnology, most efficient system	Good compromise, much better integration than current systems	Rapid development, easily integrated into current spacecraft
General cons	Very technical and still many hard point	Some development necessary	Not efficient Not easily industrialised

Table 6-5 Integration Technology Trade Off (Lecuyot et al, 2003)

This work concentrates on the different technologies with respect to use in the Space industry. At this time, the hybrid option appears to be the most accessible since it will not require vast amounts of further development and can be easily integrated into current spacecraft. As stated, however, this is not an efficient way to integrate this technology. MCMs are being developed and used in other industries, so their adaptation for use in Space should be possible. It will however require further development and changes in current processes to make them compatible with this type of technology. Chapter 8 discusses MCMs further as a possible packaging strategy for the sensor suite concept.

The system-on-a-chip for use in Space still has many obstacles to overcome before it is a reality. It is a highly complex project and as yet European industry does not have the

capacity to produce these systems. Worldwide collaboration may be required in order to optimise the available resources and produce a working solution.

A sensor suite could be a useful model for future integration. In its basic form, it would include sensing elements, signal conditioners, processor and communication unit. All these aspects have been produced using silicon micromachining technology and are available as commercially packaged MEMS chips. The designs of each need to be analysed and re-evaluated in terms of their combined inputs, outputs and common functions to produce a fully integrated system.

6.6 Conclusions

Microsystems technology is an emerging technology that has generated great interest and excitement in many different fields. Its benefits for the Space industry in terms of low mass and potential low cost have been well recognised.

An analysis of a range of commercially available MST sensors has shown that for the basic sensor suite described in previous chapters, the MST sensors of choice would be:

- Analog Devices ADXL202E 2 axis accelerometer
- Novasensor NPP-301 pressure sensor
- National Semiconductor LM20 temperature sensor
- JIC 117 UV photodetector

These sensors would provide the basis for an MST environmental sensor suite for use in a variety of applications including planetary surface exploration. The ultimate goal for this suite would be a fully integrated “lab-on-a-chip”. Current silicon wafer bonding techniques could be adapted to produce a Multichip Module version of the suite, however true full integration will require the re-evaluation of the design of all of the necessary parts of the suite, including its processor and communications unit.

7 Simulation of the Martian Surface Environment

7.1 Introduction

The fifth project objective is:

"To create a computer simulated environment and simulate deployment and search strategies for a range of scenarios to establish deployment patterns, communications architectures and the impact of performance parameters, such as reliability, on the overall system and the individual miniaturised suites."

By simulating various distribution patterns, the pattern that best meets the overall target requirements can be chosen. This investigation will focus on the likelihood of finding a given target, the pattern's impact on inter-suite communication and highlight the extent of any necessary design modifications.

7.2 Background

Simulation uses models to gather quantitative data on a real life situation. This section addresses why simulation is useful and what its purpose will be within this project.

7.2.1 Definition of Simulation

A model is a representation of the properties of a device, system or object. A simulation uses models to make conclusions that provide insight into the behaviour of a real world situation (McHaney, 1991). The simulations provide a quantitative way to understand the effects of system design decisions and measure the effectiveness of the key systems to increase confidence in that design.

Models can either be physical representation, such as a scale model for use in a wind tunnel, or a mathematical model, which uses algorithms and mathematical relationships to describe the system. A computer simulation uses mathematical models, and these can either be realistic or analytical. A realistic simulation generally involves animation and tends to be used for demonstration purposes by the end user. Analytical models are used in the design process. By gathering numerical data on how a system performs under different sets of conditions, statistical analysis can be performed and the probability of the system behaving in a certain way can be calculated.

In situations where testing of a system is vital, but a physical model is too expensive or complex, or the required environment is unavailable, a computer simulation is cost effective and can be applied at any stage in the design process rather than waiting until hardware can be supplied.

7.2.2 Why is it useful in this case?

A space mission tends to be the culmination of years of planning and design work. Most, especially planetary exploration missions are individual with bespoke pieces of hardware that have to function in a range of unique environments. There is usually only one chance to achieve a successful mission so each element is rigorously tested to reduce the risk of failure and predict the behaviour of the hardware. The simulation phase is therefore crucial in the design of space hardware. There is no way to test spacecraft in the actual space or planetary environment before the mission. Physical tests can be performed on Earth in analogous sites, however there are very few of these sites and hardware is made late in the mission cycle so test time is limited. In general, not many pieces of hardware are produced, so only a limited number of physical tests can be made. By this stage in the process, however, it would be very difficult to modify an earlier design decision so physical tests tend to be used to validate the results given by the computer simulations (Gaskell, Collier, Husman, and Chen, 2001).

With a computer simulation, the terrain can be specified for a wide range of tests. Monte Carlo probabilistic experiments can be performed in synthetic environments on a large number of design combinations in a variety of mission environments. For example, the dynamic behaviour of a rover can be tested over different surfaces, or the surface can be set and different rover or lander configurations can be tested. Surface phenomena such as rocks and craters can be generated within the simulation, and the environment can be tailored to the user's requirements.

In this project, simulation allows practical considerations for the design and potential use of the sensor suite concept to be investigated before the integration of the final design. The simulations should address questions regarding the reliability of the suites, the distribution patterns, deployment methods and the degree to which collaboration between the suites is required. Several deployment patterns will be considered. Assuming that the application involves locating a target on a planet surface, this simulation should answer the following:

- Which deployment pattern has the best survival rate given various size surface hazards?
- What effect does changing the pattern have on the ability to find a target?
- Which pattern finds that target most effectively?
- What effect does inter-suite collaboration have on the deployment and ability to find a target?
- Does the shape or size of the target influence the ability to locate it?
- How many sensors are required to ensure a given minimum number hitting the target?
- What is the effect of reduced suite reliability?
- What practical deployment and design issues do the simulations imply?

For the purposes of this simulation, the application is assumed to be locating a target resource or feature on the surface of Mars. Although this will be a relatively simple simulation, the key features of this environment will be addressed.

7.3 Martian Environment Simulation

One potential application for miniaturised environmental sensor suites is scattering them over the surface of Mars. Here they could be used for a variety of purposes. The exploration of the Martian surface has been the subject of several missions since the Viking Landers in the 1970s and further missions have been scheduled for the future.

In order to simulate the environment, assumptions are made concerning its features by analysing previously collected data, and a preliminary synthetic surface constructed. This surface was then converted to a numerical grid so that probabilistic simulations could be performed.

7.3.1 Why Martian Environment?

Here it is assumed that the sensor suites will be used to investigate the Martian surface. There are several potential applications for a network of sensors on the Mars surface including assessing suitability for landing sites or for future human colonies, performing a wide area search for areas of scientific interest or tracing the changes over time of areas visited by rovers. A simulation can investigate whether the suites are able to survive deployment and perform their designated tasks.

The surface of Mars has been of interest for many years, and Lander missions such as Viking, Pathfinder and the Mars Exploration Program have given detailed descriptions and images of their landing sites. This data means that the distributions of key features, such as rocks and craters are fairly well known, unlike when analysis of the landing dynamics for Viking was performed where the distribution of rocks was speculative and based on the Lunar surface (Muraca, Campbell, and Anderson King, 1975). Given the extent of data gathered since then, it is now possible to construct an accurate and sophisticated simulated model, such as the Synthetic Environment Package developed by NASA JPL that was used to test the flight code for 1997 Sojourner Rover (Gaskell et al, 2001) that could specify the surface gradient, distribution of rocks and diameters of craters.

As shown by the pictures from the NASA Mars Pathfinder mission from 1997 (Figure 7-1) and more recently from the Spirit and Opportunity Rovers of the NASA Mars Exploration Program (Figure 7-2), it becomes evident that the rocks and boulders are the significant feature of the Mars surface. They are therefore a major element of the simulated Martian environment.

Figure 7-1 Image of the Soujourner Rover and features of the Martian surface - from Pathfinder Image Archive (Goodall, 1998)

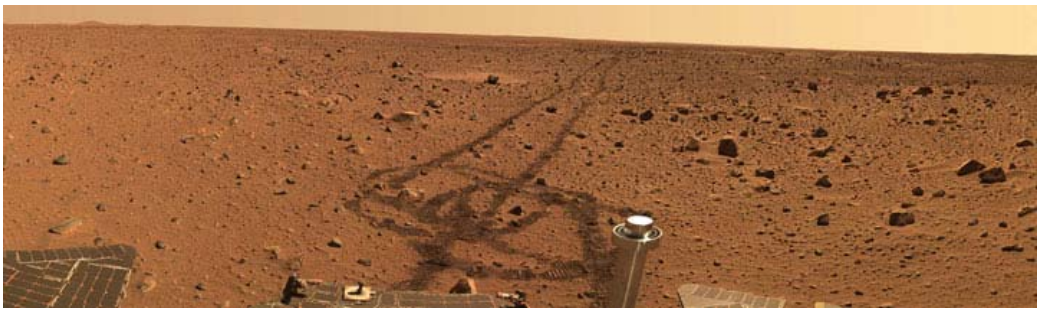

Figure 7-2 Image of Mars surface panorama taken by the Spirit Rover - From Spirit Image Archive 16/7/2004 (Viotti, 2004)

The simulation environment created for this project is relatively simplistic however it has the ability to specify the distribution of the surface rocks, since these will have the most significant influence on the deployment of the sensor suites.

7.3.2 Rock field creation

The first step in creating the simulation of the surface was to establish the distribution of the rocks of various sizes over a given area. Hauber *et al*. (1998) analysed the data for the rocks found at the Pathfinder landing site from the images taken of the area approximately 125m^2 around the lander, and this data has been used as the basis of this simulation.

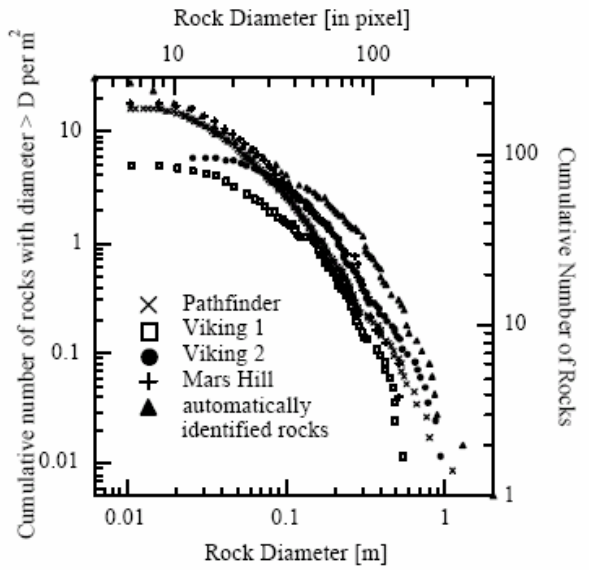

Figure 7-3 Rock diameter vs Cumulative number of rocks at the Pathfinder Landing (Figure 3 from Hauber *et al*.) (1998)

The diameters of the rocks were divided into categories. The corresponding cumulative rock distribution was taken from within the range of data discussed by Hauber. These cumulative numbers were then converted into the numbers of rocks per category. The values are shown in Table 7-1

Rock Diameters	Cumulative number of rocks	Numbers of rocks in given diameter range
>1m	2	2
1m – 50cm	7	5
50cm – 20cm	25	18
20cm – 10cm	60	35
10cm – 2cm	180	120

Table 7-1 Number of rocks within given diameter range

The paper states that the cumulative fraction area covered by rocks with a diameter of >2cm is 11.6%. This means that total area of rocks identified is 11.6% of the 125m^2 or 14.5 m^2. It is also noted by Hauber that the rocks are not uniformly distributed.

The fraction of the surface covered by rocks greater than a given diameter, *f*, can also be calculated using

$$f = f_0 \exp(-qD)$$

where f_0 is the fractional coverage by all rocks = 11.6%, D is the diameter in meters, and $q = 1.79 + \frac{0.152}{f_0}$ (Equation by Golombek and Rapp, cited in(Gaskell et al, 2001)).

Using this equation, the fraction of the surface covered by rocks with a diameter greater than 50cm is calculated as

$$f = 0.116 \exp\left[-\left(1.79 + \frac{0.152}{0.116} \right) \times 0.5 \right] = 0.0246$$

This fraction multiplied by the total area ($125m^2$) gives an area of $3.08m^2$. A circular rock with a 50cm diameter has an area of $0.196m^2$. If all the rocks in the calculated fractional area were equal, there would be a total of approximately 15 rocks. A similar calculation for a 1m diameter rock gives approximately 4 rocks in the corresponding fractional area. Assuming an average diameter between 1m and 50cm, this would mean that approximately 9 rocks in this category would be found in the area surrounding the lander. Although there are differences, the results given by the equation corroborate those taken from the graph.

The $125m^2$ subject area was assumed to be a square, which was divided into a 100 square grid, assuming each cell corresponded to a 1.12 x 1.12m square. Using a random number generator, "rocks" were placed on the grid according to their approximate diameter at random coordinates. Figure 7-4 is a visual representation of this "rock field".

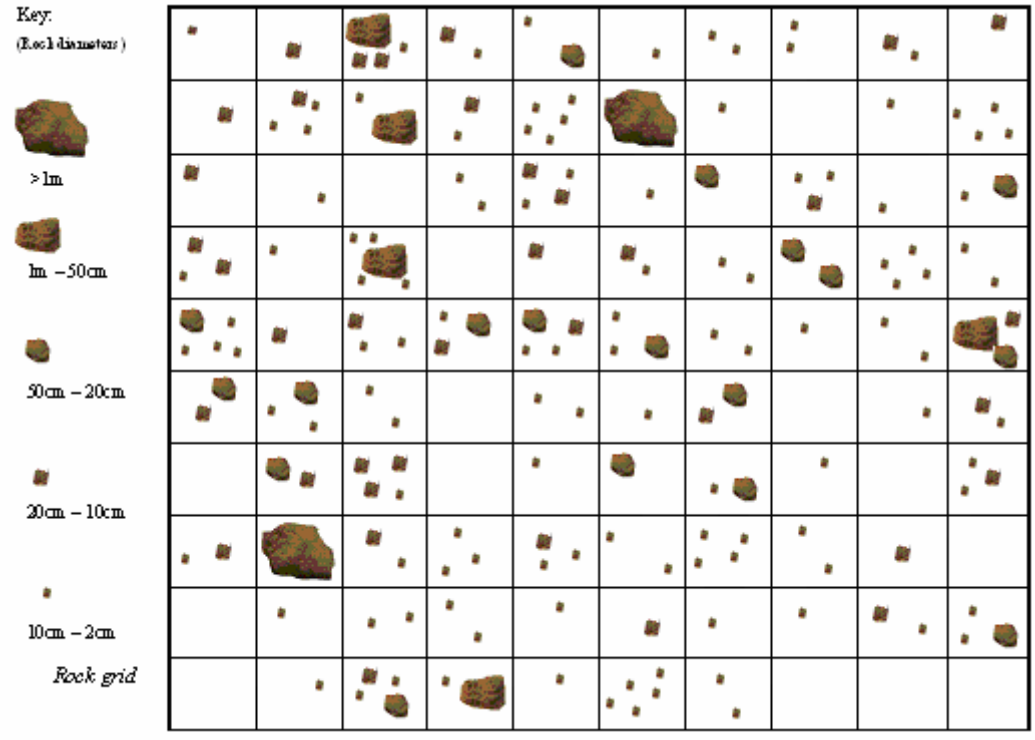

Figure 7-4 Randomly generated "Rock field" based on Pathfinder rock distribution data

It was assumed that only 1 of the >1m diameter rocks or 2 of the 1m – 50cm rocks could inhabit any one cell, since it would "fill" that square. Upon inspection of the actual images of the Martian surface, this appears to be an appropriate approximation of the rock distribution.

A similar random number generation exercise was performed to simulate the scattering of 100 individual sensor suites arbitrarily over the rock field. The crosses in Figure 7-5 represent the sensor suites. It can be seen that several of the "sensors" have landed on top of the "rocks". If this were to happen in reality, it is likely that the suite would break on impact, and would be considered a failure. As a greater percentage of the cell is filled with rock, the higher the probability of an unsuccessful deployment.

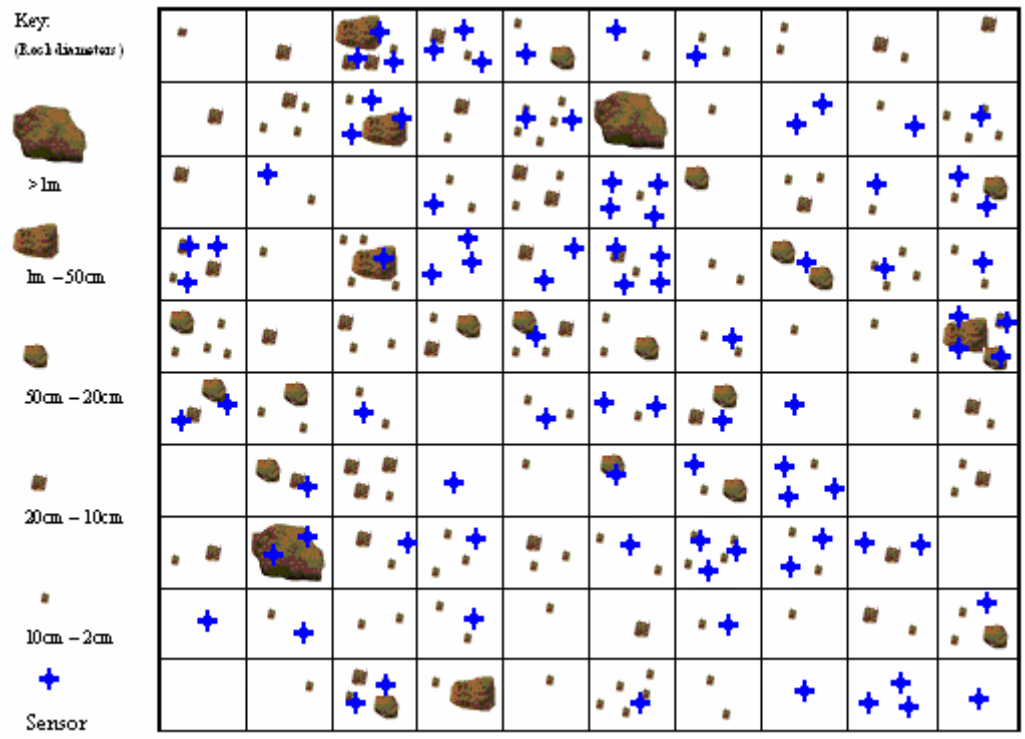

Figure 7-5 Representation of 100 sensor suites scattered randomly over the "Rock field"

This model was the basis for a computer simulation of the cells containing various diameters of rocks and corresponding sensor suite deployment.

7.3.3 Rock Field Visual Basic Subroutine

In order to run multiple iterations of the simulation, the rock field was converted into an Excel grid, containing the equivalent rock diameter values. Subsequent simulations will be produced using VBA subroutines.

Each rock is then assigned a random value corresponding to the area of a circular rock with a diameter within the specified range that is placed in a randomly chosen cell. The number of rocks is the number of iterations that are performed by the subroutine for that diameter range. For example, there will be 35 iterations placing a value between 95 (area of an 11cm diameter rock) and 315 (area of a 20 cm rock) on the grid. Since the minimum diameter that is specified by Hauber is 2cm with a corresponding area is $3cm^2$, hence 3 is the lowest value on the grid. The subroutine was also written so that if a cell was chosen more than once during the total number of iterations, the new value

would be added to the value already present in that cell. The resultant 10x10 grid is shown in Figure 7-6.

133		210		201	404	63	798	38	3
50	19		478	82	38		3	1711	1784
14	292	1116		50		47	57	70	261
22	229	132	113		113	283	268	123	1113
41	534	7	19	3	201	5709	683	38	
543	902	53		422	615	315		94	19
	15	69	153	4656	63	90	26	113	1787
1429	40	226	1520	104	45	48	66	7088	98
40		12	50	1067	50		12	1138	9855
354	6685	6349	3	285	9902	22	706		1477

Figure 7-6 Equivalent rock field represented by numbers, produced by VBA subroutine

The number contained in each grid cell corresponds to the total area of all of the "rocks" in that cell. If greater than 12500, it is assumed that the cell is "full", since the diameter of the rocks would be greater than the diameter of the square. In general, the higher the value, the greater the proportion of the square contains rocks. The blank squares are the equivalent to areas containing no rocks.

Once generated, this becomes the master surface terrain grid that is the base for the subsequent sensor deployment subroutines. An example of code used to generate this grid is contained in Appendix A.

7.4 Possible Deployment Patterns

The next phase of the simulation is to model the deployment of the individual sensor suites across the grid. This is achieved using colours corresponding the likelihood of a successful or unsuccessful landing based on the rock coverage within the chosen cell. Statistical analysis is performed on the data for each colour. This analysis is repeated for four different patterns of sensors; uniform, random, clusters and strings. The effect of reduced reliability is also discussed.

7.4.1 Visual Basic subroutine creation for simulation of varying deployment patterns

Since numbers represented the proportional rock coverage of each cell, another method had to be devised to represent the deployed sensor suites. This was achieved with a coloured cell meaning at least one sensor was present.

It is assumed that if a suite hit a rock it would be classed as a failed deployment. In cells where the area value was greater than 7854 (area of a 1m diameter circular rock), this is a likely occurrence. Therefore, it was decided that if a sensor were deployed onto these cells, they would be coloured red. If the cells are empty or contain an area value below that of 30cm diameter rock (707), these cells become green to represent a high probability of a successful landing where few or no rocks are present. Cells with values between 707 and 3748 (70cm diameter rock) are yellow, indicting a good chance of success from a medium coverage of rocks. Cells containing 3748 to 7854 are

orange, corresponding to a higher coverage of rocks and an increased likelihood of failure but still with a chance for a successful deployment. 30cm and 70cm diameters were arbitrarily chosen examples. The total number of each colour was recorded.

The sensors are deployed in four ways, each corresponding to a uniform deployment or random deployments of individual or groups of sensors. Where the choice of cells is different per distribution run, 100 runs were performed and the mean and standard deviation of each colour is calculated for comparison.

A VBA subroutine was written for each deployment pattern and is shown in Appendix A. Further descriptions of the patterns in relation to their programmes and the results obtained are covered in the following sections.

7.4.2 Uniform

A uniform distribution pattern corresponds to one sensor suite per square, or the idea of each sensor deliberately placed at equal distances across the subject area. This equates to the colouring of every square and is the equivalent of deploying 100 sensors. Also, as there is no random element to the distribution, the results will be the same every time for this particular grid meaning that only one iteration is required. The resulting grid pattern is shown in Figure 7-7.

133		210		201	404	63	798	38	3
50	19		478	82	38		3	1711	1784
14	292	1116		50		47	57	70	261
22	229	132	113		113	283	268	123	1113
41	534	7	19	3	201	5709	683	38	
543	902	53		422	615	315		94	19
	15	69	153	4656	63	90	26	113	1787
1429	40	226	1520	104	45	48	66	7088	98
40		12	50	1067	50		12	1138	9855
354	6685	6349	3	285	9902	22	706		1477

UNIFORM DISTRIBUTION – 1 PER SQUARE

Figure 7-7 Grid representing a uniform distribution of individual sensor suites

For this grid:

- red = 2
- orange = 5
- yellow = 12
- green = 81

This means that 81 of the 100 sensors would have a high probability of a successful landing and 2 of the sensors would almost certainly fail or break due to landing on a rock. 17 have varying probabilities of success.

7.4.3 Random sensors

This pattern represents 100 sensor suites deployed randomly across the grid. The program selects a cell on the master grid by choosing two random numbers as the x and y coordinates. A value of 10, representing an example sensor suite with a 10cm^2 footprint area, is then added to the value within the cell to recognise that a sensor has been placed and illustrate the effect on the proportional coverage of the square. Again the cell is coloured according to its value and the colour registered. This is repeated for 100 iterations. For example, if the cell's initial value is 690, the addition of a sensor will change the value to 700 and colour it green, adding 1 to the green total. If the cell is selected again and a second sensor is added, the value then becomes 710, which will change the cell colour to yellow, which in turn adds 1 to the yellow total. As with the uniform deployment, the total number of each colour at the end of the iterations is reported. It is possible that the final picture, as shown in Figure 7-8, may not match the numerical data, since some of the cells may have been randomly selected more than once therefore taking them into the next category.

133		220		211	404	63	828	58	23
70	29	10	498	92	58		13	1711	1784
24	302	1126	30	60	10	47	67	80	271
42	229	142	123		123	283	278	123	1133
41	554	17	29	3	201	5719	693	38	
553	912	53	20	422	635	335		124	29
	25	69	163	4666	73	90	36	133	1797
1449	40	246	1530	114	45	48	96	7108	98
70		12	80	1087	50	30	12	1138	9865
354	6685	6369	23	315	9912	62	716		1477

RANDOM DISTRIBUTION – 100 SENSORS PLACED RANDOMLY

Figure 7-8 Grid representing the random distribution of individual sensor suites across the master rock grid

As the random deployment will yield different results for every set of 100 sensors, the program is run 100 times and the mean total for each colour is calculated. This allows a fair comparison to be made with the data collected for the uniform deployment. The standard deviation of the data, σ, is also calculated within the program using a VBA conversion of the relationship:

$$\sigma = \sqrt{\frac{\sum_{i=1}^{n}\left(X_i - \overline{X}\right)^2}{n-1}}$$

where X is the value, $\overline{X}$ is the mean and n is the total number of runs (Sun, 1997).

The average values for the case above are:

- red = 2.13 (σ = 1.331)
- orange = 4.71 (σ = 2.162)
- yellow = 13.51 (σ = 2.911)

- green = 79.65 ($\sigma = 3.912$)

There are also 37 cells in the final grid that do not contain any sensors (white). This figure is expected as the probability of a square not being selected can be calculated as $P(0) = \left(\frac{99}{100}\right)^{100} = 0.366 = 36.6\%$.

7.4.4 Cluster

Another potential deployment strategy is using connected groups of sensor suites rather than individual ones. The "Cluster" pattern represents 9 interlinking suites randomly deployed as a single unit. To correspond with the other patterns, there will be 11 iterations of 9 suites per run.

As with the previous pattern, the program selects a set of random coordinates on the master grid, (i,j), which is added to and coloured. The 8 surrounding cells are then also selected, as illustrated in Figure 7-9, and their colours recorded. This means that there are only 11 random elements per 99 sensors deployed.

i-1, j-1	i-1, j	i-1, j+1
i, j-1	i,j	i. j+1
i+1, j-1	i+1, j	i+1, j+1

Figure 7-9 Illustration of cell selection in the Cluster pattern

Any square within the 10 x 10 grid can be randomly selected, however when an edge square is chosen, the remainder of the cluster will fall outside the specified grid. In order to compare similar 10 x 10 grids, only those within the grid are counted.

The method of recording the suite deployment using values of 10 and colours, and compiling statistical data over 100 runs is as with the random pattern. The final grid is shown in Figure 7-10.

133	10	220	30	221	424	73	808	48	3
60	39	10	508	102	58	10	13	1721	1784
24	312	1126	20	60	10	57	67	80	261
42	249	132	113		113	283	278	133	1123
51	544	7	19	3	211	5719	703	48	10
553	912	53		422	635	335	30	104	29
	15	69	153	4666	93	120	46	113	1787
1429	40	226	1520	114	65	68	76	7088	98
40		12	50	1077	60	20	22	1148	9855
354	6685	6349	3	285	9902	32	716	10	1477

RANDOM CLUSTERS – 11 CLUSTERS OF 9 SENSORS

Figure 7-10 Grid representing the random cluster distribution pattern of sensor suites over the master grid

The average values for the cluster pattern are:

- red = 1.28 (σ = 0.975)
- orange = 4.23 (σ = 1.841)
- yellow = 10.03 (σ = 2.646)
- green = 71.18 (σ = 6.378)

This gives a total number of deployed sensors within the grid of 86. This means that 13 of the sensors that were deployed as part of the clusters fell outside the 10 x 10 grid area and therefore were not counted. There are also 39 cells in the final grid that do not contain sensor suites.

7.4.5 Strings

The final distribution pattern that will be considered is randomly deployed strings of 5 sensor suites. There are 20 strings in total per run, 10 deployed vertically and 10 horizontally.

As with the clusters, the program randomly selects a set of coordinates, (i,j). The next four adjoining cells, as illustrated in Figure 7-11, are then automatically selected. The sensor recognition and colouration are performed as before. Again, if an edge square is selected, the remainder of the string may, depending on the orientation, fall outside the sample grid and therefore not counted.

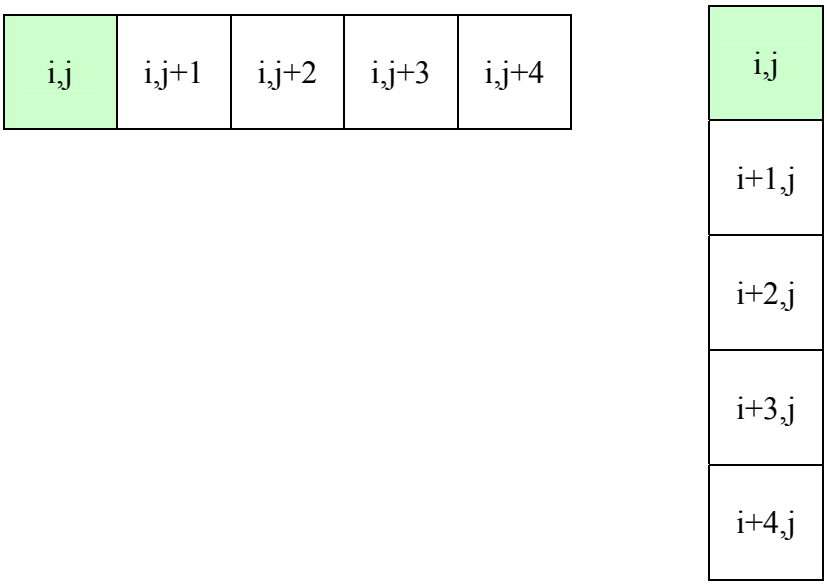

Figure 7-11 Illustration of cell selection for vertical and horizontal string patterns

The statistical data for 100 runs was calculated as per the previous random distribution patterns. This final grid is shown in Figure 7-12.

133		210		201	404	63	798	38	3
50	19	10	488	82	38		13	1731	1804
14	292	1136	20	50		47	57	70	261
22	229	152	133	10	123	303	278	133	1113
41	534	27	39	3	201	5719	683	38	
543	902	73	20	432	615	325	10	104	59
	15	89	163	4676	63	100	26	113	1787
1429	40	266	1550	154	75	88	66	7088	98
40		32	50	1097	50		12	1138	9855
364	6695	6379	13	325	9902	32	706		1497

RANDOM STRINGS – 20 STRINGS OF 5 SENSORS

Figure 7-12 Grid representing the random string distribution pattern of sensor suites over the master grid

The average totals of sensor suites in each colour category are:

- red = 2.1 (σ = 1.56)
- orange = 4.54 (σ = 2.134)
- yellow = 11.38 (σ = 2.95)
- green = 63.84 (σ = 7.051)

As with the clusters, there are 19 sensors that have been deployed outside the 10 x 10 grid and are not counted. There are 45 cells in the final grid that do not contain sensor suites.

7.4.6 Simulation of reduced reliability

The above simulations assume that the sensor suites have 100% reliability and that the only failures are due to impacts with rocks as they land. Other failures however may for example, occur due to faults in the suite electronics. To model the effect of these failures, the simulations were repeated to include an arbitrary 30% failure rate. 30% of the coordinates chosen at random were deemed to have "failed", removed from the overall sensor totals and coloured brown. In the case of the strings and clusters, if the coordinate cell was a failure, the whole string or cluster is considered a failure. The resulting grids are shown in Figure 7-13.

133		230	20	201	434	63	818	48	3
80	39	30	478	102	38	10	13	1721	1794
24	292	1146	10	50	20	57	77	70	271
52	249	132	113		113	283	278	123	1123
41	534	27	19	3	231	5719	683	48	20
553	902	53		432	625	325		114	49
	15	69	163	4656	63	90	26	123	1797
1449	40	246	1530	114	55	48	86	7108	108
50		22	60	1077	60	10	42	1168	9875
354	6685	6349	13	325	9912	62	706		1487

Random Distribution – 30% failure

163		210		211	414	63	798	48	13
50	19		478	82	38		3	1721	1804
14	292	1116		50		47	57	70	271
32	229	132	113		113	283	268	123	1113
41	534	17	19	3	201	5719	693	48	
553	902	63	10	422	615	315		104	19
	15	79	153	4666	63	90	26	113	1807
1429	50	226	1520	104	55	48	66	7088	98
40	10	12	50	1067	50		12	1138	9855
354	6695	6359	3	285	9902	22	706	10	1477

Uniform Distribution – random 30%

143	10	210		201	404	63	808	48	13
60	29		488	92	48		13	1731	1804
24	302	1126	20	70	10	47	67	90	281
22	229	142	143	30	133	283	268	133	1123
41	534	17	39	23	221	5739	713	68	10
543	902	53	10	432	635	345	40	134	39
	15	69	153	4656	73	120	66	153	1807
1429	40	226	1520	104	45	48	76	7098	108
40		12	50	1067	50		12	1138	9855
354	6685	6349	3	285	9902	22	706		1477

Random Clusters – 30% failure rate

133	10	220	10	211	414	63	798	38	3
50	19		488	102	58	30	33	1731	1794
14	292	1116		50		47	57	70	261
22	229	132	113		113	283	278	123	1113
41	534	7	19	3	201	5709	693	38	
543	902	63		432	625	335	20	104	29
	15	89	153	4666	63	110	46	133	1807
1439	40	246	1520	114	55	58	76	7088	108
50		32	50	1077	60	20	22	1148	9875
364	6685	6389	23	315	9932	62	706	10	1487

Random Strings – 30% failure rate

Figure 7-13 The four distribution pattern grids including a 30% failure rate

It can be seen from the grids above that the loss of the sensors can have a significant impact on the grid coverage and this becomes especially important to the patterns' ability to locate specific area of the surface.

The effects of sensor suite reliability will be discussed further in later sections.

7.4.7 Conclusions of sensor deployment patterns

The rock field from Section 7.3.2 was used to create a Visual Basic program to analyse the effect of the rock distribution on various sensor suite deployment patterns. Selected cells were coloured depending on the value representing the rock coverage in that cell.

The average totals from each colour category are shown in Table 7-2.

	Red (average/100)	Orange (average/100)	Yellow (average/100)	Green (average/100)	No sensor present	Sensors outside grid
Uniform	2	5	12	81	0	0
Random	2.13 (1.331)	4.71 (2.162)	13.51 (2.911)	79.65 (3.912)	37	0
Cluster	1.28 (0.975)	4.23 (1.841)	10.03 (2.646)	71.18 (6.378)	39	13
String	2.10 (1.56)	4.54 (2.134)	11.38 (2.95)	63.84 (7.051)	45	19

Table 7-2 Comparison of the average totals from each colour category for the different distribution patterns

For this particular distribution of rocks in the surface grid, the uniform distribution pattern has the greatest number of potentially successful sensor deployments, based on a comparison of the green totals. The number of failed deployments due to rock impacts is approximately equal for all four patterns.

The cluster and string distributions feature a lower overall number of sensors since those that represent parts of the sensor grid that have fallen outside the 10 x 10 grid are discounted. Additional sensors could be deployed to counteract this effect.

Due to the nature of random, cluster and string deployments, where cells can be selected multiple times, a high number of unselected squares are a feature of all 3 random patterns, which does not occur with a uniform distribution. For overall coverage, the uniform deployment appears to be preferable, however in reality, a random deployment would be less complicated to implement, since the suites do not have to be positioned exactly a certain distance apart. This is particularly significant for a planetary surface mission where the suites could be deployed during the descent of a Lander where there is no way of predetermining the sensor's landing positions.

7.5 Location of Target Resources

A potential application for the sensor suites is locating specific areas of interest on the planet's surface. The simulation can be modified to test the ability of each pattern to locate a desired target.

In this simulation model, the measure of successful target location will be defined as the number of sensor suites landing in any of 6 pre-selected squares. A variety of target shapes are considered, with four different arrangements of the six cells forming a large target or the six individual cells scattered over the grid to represent small targets. The average numbers of successes is compared for each of the four deployment patterns.

7.5.1 Visual Basic subroutine to simulate finding a specified target

Each of the four pattern subroutines was modified to locate a set of six chosen cells. The coordinates of the cells were specified to correspond to differing target shapes; a block, an L, horizontal and vertical lines and individual cells. The program was written to allow different coordinates to be specified without modification to the subroutine. An example of this code is shown in Appendix B. These targets are coloured blue in the figures below.

Over the course of the iterations, if the randomly chosen coordinates matched one of the targets, a "hit" was recorded. As before, the mean number of hits and the standard deviation were calculated for each of the random patterns.

In addition to this data, the results of the 100 runs were tabulated according to the number of hits per run. For each run, 1 was added to the 0-2, 3-5, 6, 7-11 or 12 or more category depending on the number of hits recorded. For the uniform case, this was always 6.

7.5.2 Target 1 – block

The first target investigated was a simple 3x2 block, highlighted in blue in Figure 7-14.

133		210		201	404	63	798	38	3
50	19		478	82	38		3	1711	1784
14	292	1116		50		47	57	70	261
22	229	132	113		113	283	268	123	1113
41	534	7	19	3	201	5709	683	38	
543	902	53		422	615	315		94	19
	15	69	153	4656	63	90	26	113	1787
1429	40	226	1520	104	45	48	66	7088	98
40		12	50	1067	50		12	1138	9855
354	6685	6349	3	285	9902	22	706		1477

Figure 7-14 Uniform sensor distribution grid showing the chosen block target

The modified programs were run for the other three deployment pattern, and the results are shown in Table 7-3 and Table 7-4.

	Average number of hits
Uniform	6
Random	5.98 (2.881)
Cluster	6.9 (5.546)
String	6.05 (2.973)

Table 7-3 Average number of sensors finding the block target

	Number of runs whose hit results were in the given ranges (/100)				
	0-2	3-5	6	7-11	12+
Uniform			100		
Random	10	37	13	35	5
Cluster	26	21	8	30	15
String	7	42	9	38	4

Table 7-4 Hit results for block target shown in specific ranges

These results show that the cluster pattern had the highest average number of sensors locating the desired target and a greater number of hits per iteration.

7.5.3 Target 2 – L

The coordinates chosen for the second target were three vertically connected cells and three horizontally connected cells, forming an L shape highlighted in Figure 7-15.

133		210		201	404	63	798	38	3
50	19		478	82	38		3	1711	1784
14	292	1116		50		47	57	70	261
22	229	132	113		113	283	268	123	1113
41	534	7	19	3	201	5709	683	38	
543	902	53		422	615	315		94	19
	15	69	153	4656	63	90	26	113	1787
1429	40	226	1520	104	45	48	66	7088	98
40		12	50	1067	50		12	1138	9855
354	6685	6349	3	285	9902	22	706		1477

Figure 7-15 Uniform sensor distribution grid showing chosen L shaped target

100 runs were performed for each pattern and the results are tabulated below.

	Average number of hits
Uniform	6
Random	6.36 (2.58)
Cluster	6.7 (4.275)
String	5.8 (3.015)

Table 7-5 Average number of sensors finding L shaped target

	Number of runs whose hit results were in the given ranges (/100)				
	0-2	3-5	6	7-11	12+
Uniform			100		
Random	5	39	12	40	4
Cluster	16	24	10	36	14
String	10	45	6	36	3

Table 7-6 Hit results for L shaped target shown in specific ranges

As with the block target, the cluster design has the highest hit rate.

7.5.4 Targets 3 and 4 – Horizontal and vertical lines

Target 3 and 4 are both straight lines; one horizontal, one vertical. From Figure 7-16 and Figure 7-17, it can be seen that both lines are located along the outside edges of the grid. 100 runs were performed for each deployment pattern and the results tabulated.

133		210		201	404	63	798	38	3
50	19		478	82	38		3	1711	1784
14	292	1116		50		47	57	70	261
22	229	132	113		113	283	268	123	1113
41	534	7	19	3	201	5709	683	38	
543	902	53		422	615	315		94	19
	15	69	153	4656	63	90	26	113	1787
1429	40	226	1520	104	45	48	66	7088	98
40		12	50	1067	50		12	1138	9855
354	6685	6349	3	285	9902	22	706		1477

Figure 7-16 Uniform sensor distribution grid showing chosen horizontal line target located at the outside edge of the grid

	Average number of hits
Uniform	6
Random	6.01 (2.038)
Cluster	4 (2.916)
String	3.39 (3.39)

Table 7-7 Average number of sensors finding a horizontal line target

	Number of runs whose hit results were in the given ranges (/100)				
	0-2	3-5	6	7-11	12+
Uniform			100		
Random	0	43	17	39	1
Cluster	33	36	11	20	0
String	46	32	6	13	3

Table 7-8 Hit results for a horizontal line target shown in specific ranges

The simulation was repeated for target 4. As before, the results of the 100 runs are tabulated below.

133		210		201	404	63	798	38	3
50	19		478	82	38		3	1711	1784
14	292	1116		50		47	57	70	261
22	229	132	113		113	283	268	123	1113
41	534	7	19	3	201	5709	683	38	
543	902	53		422	615	315		94	19
	15	69	153	4656	63	90	26	113	1787
1429	40	226	1520	104	45	48	66	7088	98
40		12	50	1067	50		12	1138	9855
354	6685	6349	3	285	9902	22	706		1477

Figure 7-17 Uniform sensor distribution grid showing chosen vertical line target located at the outside edge of the grid

	Average number of hits
Uniform	6
Random	6.3 (2.067)
Cluster	3.7 (2.946)
String	3.16 (2.751)

Table 7-9 Average number of sensors finding a vertical line target

	Number of runs whose hit results were in the given ranges (/100)				
	0-2	3-5	6	7-11	12+
Uniform			100		
Random	4	30	13	52	1
Cluster	32	44	6	17	1
String	48	33	12	6	1

Table 7-10 Hit results for a vertical line target shown in specific ranges

While the results for the random distribution are similar to the other target shapes, the cluster and string patterns show significantly less success. To test this result, the simulation was repeated with the horizontal and vertical line targets in different positions away from the grid boundaries. The results are shown in Table 7-11 and Table 7-12.

	Average number of hits
	Horizontal line
Cluster	6.44 (3.60)
String	5.02 (3.42)
	Vertical line
Cluster	6.5 (3.76)
String	5.09 (4.01)

Table 7-11 Average number of sensors in the cluster and string patterns finding line targets away from the inner grid

	Number of runs whose hit results were in the given ranges (/100)				
	0-2	3-5	6	7-11	12+
	Horizontal line				
Cluster	14	24	17	35	10
String	27	32	11	26	4
	Vertical line				
Cluster	12	37	7	31	13
String	35	27	6	24	8

Table 7-12 Hit results for line targets away from the inner grid, shown in specific ranges – Cluster and string distributions only.

These results are consistent with those obtained for the block and L shaped targets. The success of the cluster and string distributions appears to be dependant on the position of the target within the grid. However, this can be attributed to the function of the random number generator and initial conditions of the subroutine rather than being a feature of finding a straight-line target.

7.5.5 Target 5 – Individual cells

The final target consists of the six cells located individually on the grid rather than in a group. This represents the idea of the sensor suites finding six smaller targets across a larger area. The target cells are shown in Figure 7-18.

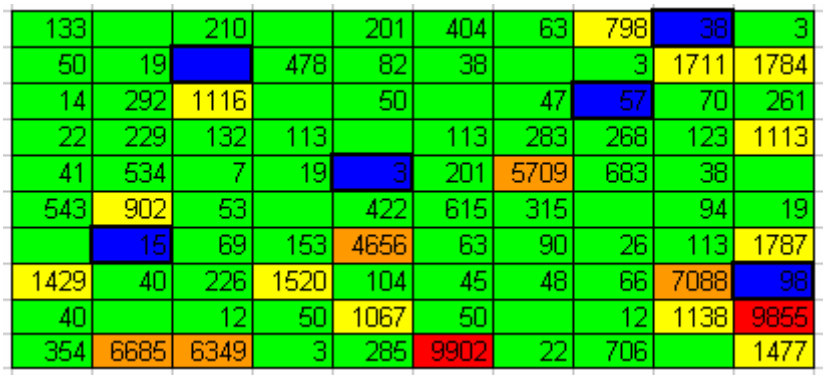

Figure 7-18 Uniform sensor distribution grid showing chosen individual targets

100 runs of the simulation were performed for each deployment pattern and the results tabulated.

	Average number of hits
Uniform	6
Random	6.08 (2.116)
Cluster	5.9 (1.957)
String	4.75 (1.94)

Table 7-13 Average number of sensors finding individual targets

	Number of runs whose hit results were in the given ranges (/100)				
	0-2	3-5	6	7-11	12+
Uniform			100		
Random	4	38	16	42	0
Cluster	3	40	21	36	0
String	12	54	15	19	0

Table 7-14 Hit results for individual targets shown in specific ranges

The averages for all four patterns are similar and the effect of the boundary targets is much less in this case, as this only applies to two of the target cells. Both the random and cluster distributions have a similar number of iterations where at least 6 sensors find the target. Therefore, for individual small targets there is not preference between these two distributions.

7.5.6 Conclusions for target location

The simulation program was modified to allow the location of six predetermined target cells in varying arrangements. The program was run 100 times for each of the deployment patterns. The mean number finding the target and the "hit rate" for each pattern and target shape were recorded.

In general, the cluster pattern had a higher success rate for all of the target shapes. An exception was when the target was located at the edge of the grid, however this was due to the description of the cluster pattern in the simulation program. However, there is not a significant difference in results between the random individual sensor deployment pattern and the random deployment of interconnected clusters of sensor suites.

7.6 Effect of reliability and quantity on the deployment patterns and target location

The above investigations were made assuming 100% reliability of the sensors. The effect of 70% sensor reliability on locating the target cells was also investigated. Using the hit rate tally, the minimum quantity of suites was addressed to ensure that at least 3 sensors found every target.

A further deployment option is proposed and discussed that uses both individual and clusters of sensors. Finally statistical analysis of the 70% reliability target location simulations is performed and conclusions made.

7.6.1 Runs with different reliabilities and quantities

Further simulations were carried out to investigate the effect of reduced reliability on the patterns' ability to locate the target cells. An arbitrary 30% of the suites in each run were assumed to fail due to electrical or mechanical errors rather than a failed deployment. Simulations for finding the block target and the six individual targets were compared and the results presented in Table 7-15.

	Large block target		Small individual targets	
	Mean number finding target	Mean number of failures	Mean number finding target	Mean number of failures
Uniform	6	1.94 (1.434)	6	1.8 (1.318)
Random	6.1 (2.646)	1.75 (1.381)	5.91 (2.437)	1.56 (1.225)
Cluster	6.79 (5.355)	1.57 (1.95)	5.64 (2.077)	1.52 (1.105)
String	6.08 (3.351)	1.59 (1.747)	4.73 (2.069)	1.31 (0.992)

Table 7-15 Average number of sensors finding the block and individual targets, and the mean number of failures assuming 70% reliability

With the larger target, the cluster pattern again has a marginally higher average number of suites locating the target. The expected value for the failure rate is 1.8 (30% of 6). The cluster pattern also has the lowest mean number of failures. However, the results are more even with the individual targets. In this case the random pattern has an average of 0.3 more successes than the cluster pattern. In either case, the reduced reliability has a significant impact on the number of successful deployments.

In each simulation, the number of sensor suites per deployment run has been 100. Further runs were made with an increased quantity of sensor suites to determine the minimum number required in order to achieve at least 3 target cells found in every deployment run. The results are for 100% reliability.

The uniform deployment is designed to always require 100 sensors for the 10x10 grid. For the random deployment, 140 sensor suites were necessary to ensure that the probability of reporting zero in the 0-2 hits category over multiple iterations was low, independent of the target pattern. The string pattern required 180 sensors, equating to 36 strings. However, the average number of sensors deployed that landed within the grid is recorded as 146, making the overall number similar to that recorded with the random distribution. Again this was independent of target shape. The cluster distribution required a greater number of individual sensors, 243, to meet the criteria. However this does equate to only 27 clusters, which would require a less complicated physical deployment strategy. If 16 clusters are deployed, equating to 144 sensors, the probability of reporting zero is 15%, which is still relatively low.

It can therefore be concluded that a minimum of approximately140 sensor suites is required to ensure a high probability that at least half of the number of target cells are found, regardless of deployment pattern or target shape. A greater number of sensors per deployment however will increase this success rate further.

7.6.2 Targeted deployment – the effect of 2 level deployment

All of the simulations so far performed have assumed that all of the sensor suites are deployed together. Another option is to have a two level, or targeted deployment.

A number of individual suites are deployed in the first instance. If the sensor registers that it has found the target, a cluster is then deployed which should locate the entire target. This should reduce the numbers of sensor suites required in each deployment.

The simulation model was modified and the results recorded. Whilst this is good concept, the simulation shows that this is a relatively inefficient way of deploying the sensor suites. For both the block target and individual targets, an initial deployment of 50 sensors resulted in an average of 3 sensors locating the target over 100 iterations. This can be seen as an “all or nothing” deployment pattern. Either all of the target cells are located, or none of the cells are found, hence the average of 50% of the number of targets located. A better average can be achieved by deploying a greater number of suites in the first level, however this increases the total number of suites that would have to be deployed making a single level deployment strategy preferable.

7.6.3 Histograms and Distribution plots

For each deployment run, statistical data on the number of sensor suites successfully locating the chosen target has been gathered. This data can be illustrated using a histogram, providing a graphical summary of the data collected thus far.

Figure 7-19 shows the distribution of sensor suites successfully locating the block target for the four deployment patterns.

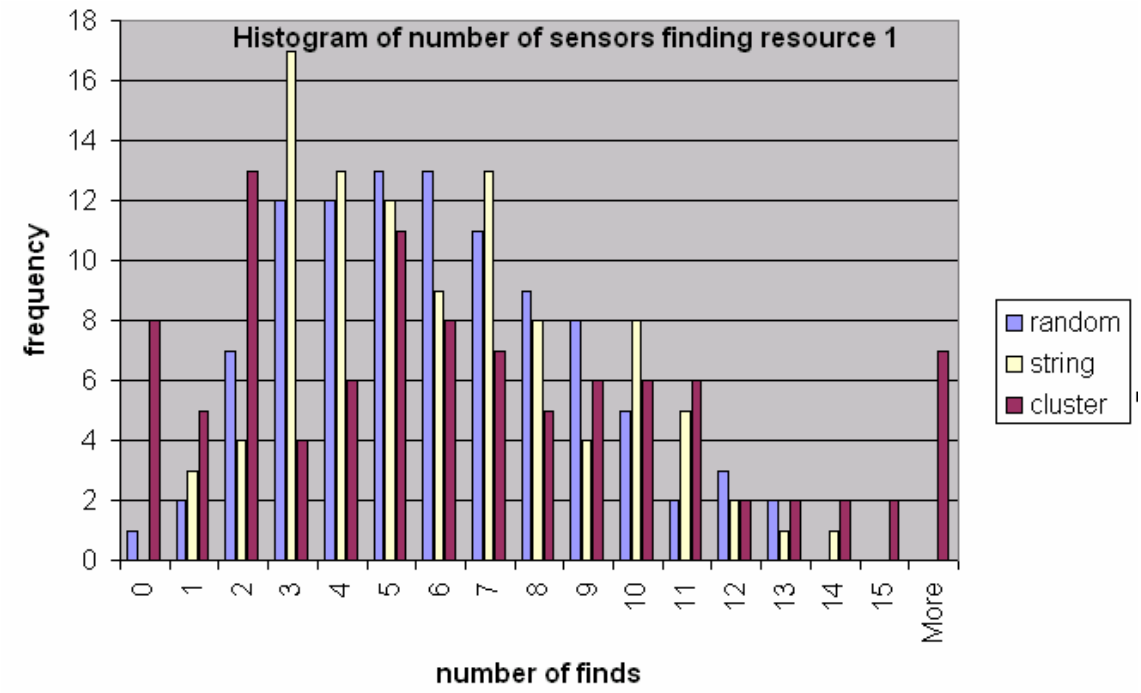

Figure 7-19 Histogram curves showing the number of sensors successfully finding the block target

This figure illustrates that the spread of the values for the cluster pattern is significantly wider than for the other patterns. From the data gathered, the mean success value is also shown to be higher for the cluster pattern than the other patterns.

The shape of the plotted data appears to be consistent with data that is normally distributed. The normal distribution curve (Figure 7-20) is a standard tool used to make statistical inferences, and it has been shown that many natural phenomena that relate to continuous variables conform to this distribution. As the sample size increases, the sample statistics such as the mean tend towards a normal distribution even if the population is not normally distributed (Fleming and Nellis, 2000) A feature of the distribution is that 68% of all sample values lie within 1 standard deviation on either side of the mean value, with 95% within 2 standard deviations. This can be used to determine the variability of the samples.

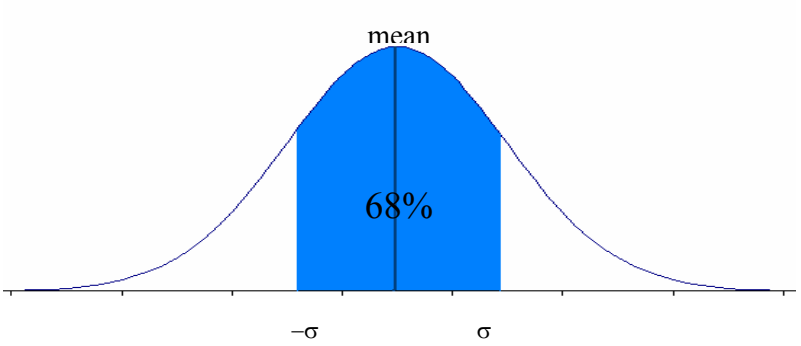

Figure 7-20 Standard Normal Distribution curve

Using the data from the simulations, 68% of runs (1 standard deviation) have a success rate of between 1.36 and 12.44 for the cluster pattern, compared to between 3.1 and 8.86 for the random pattern. On inspection, this can also be seen from the histogram data. It is therefore more likely to successfully locate a larger area of the target using the cluster pattern.

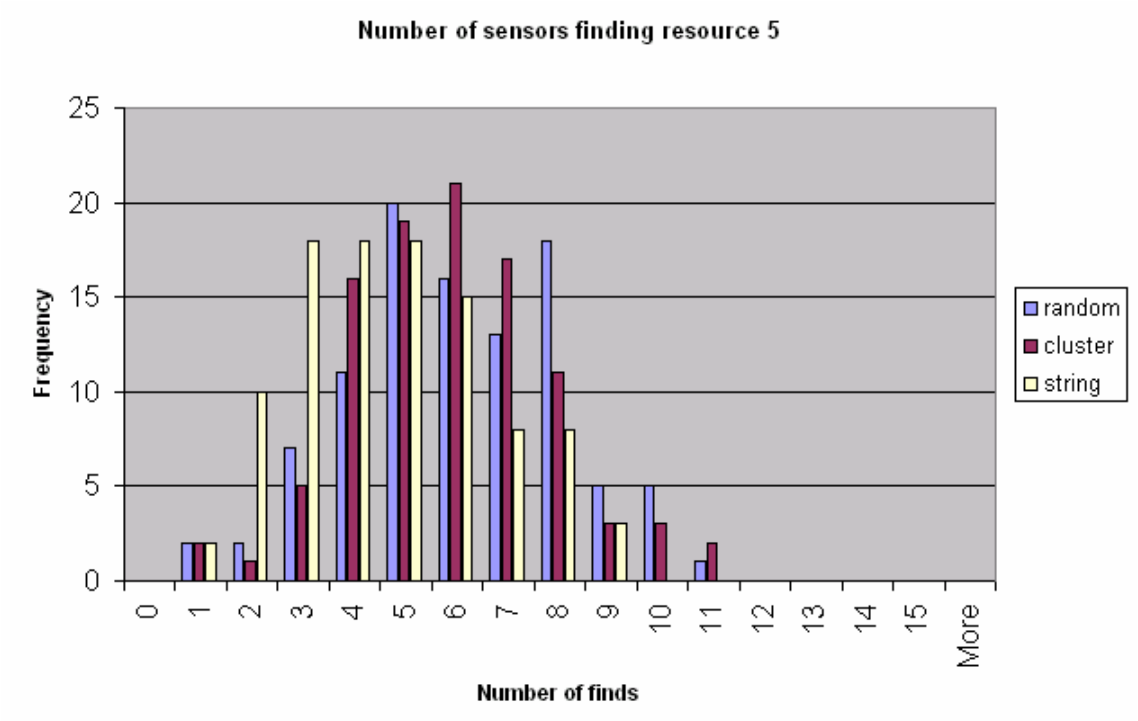

Figure 7-21 Histogram curves showing the number of sensors successfully finding the individual targets

In contrast, it can be seen that the spread of the data is much narrower for the successful location of the individual smaller targets, independent of the pattern. Comparing the data for the random and cluster patterns, 68% of the success values lie between 3.96 and 8.2 for the random and 3.94 and 7.86 for the cluster. On the diagram, this proportion of the data can also be seen to be between 4 and 8. In this case as the results are similar, there is no clearly preferred option.

Figures 7-22 to 7-24 show the histograms of the three random deployment patterns for the various target shapes. Figure 7-21 demonstrates that the spread of the data is for the random distribution relatively even for all five target shapes. The distribution of the uniform pattern data is expected to be the same regardless of the target shape.

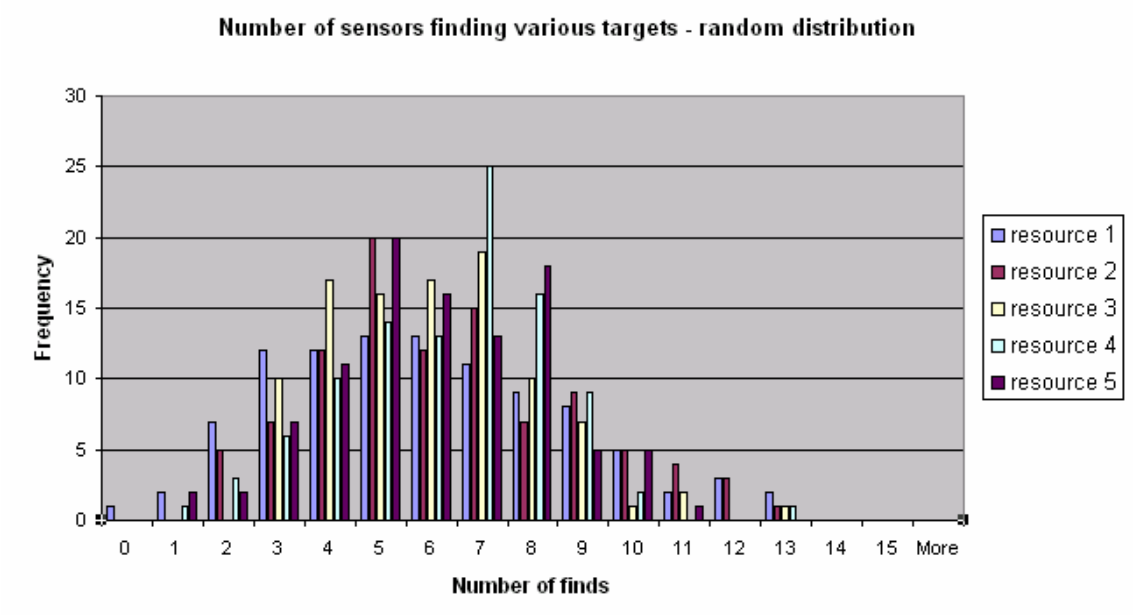

Figure 7-22 Normal distribution curves showing the number of sensors successfully finding the various targets using the random deployment pattern

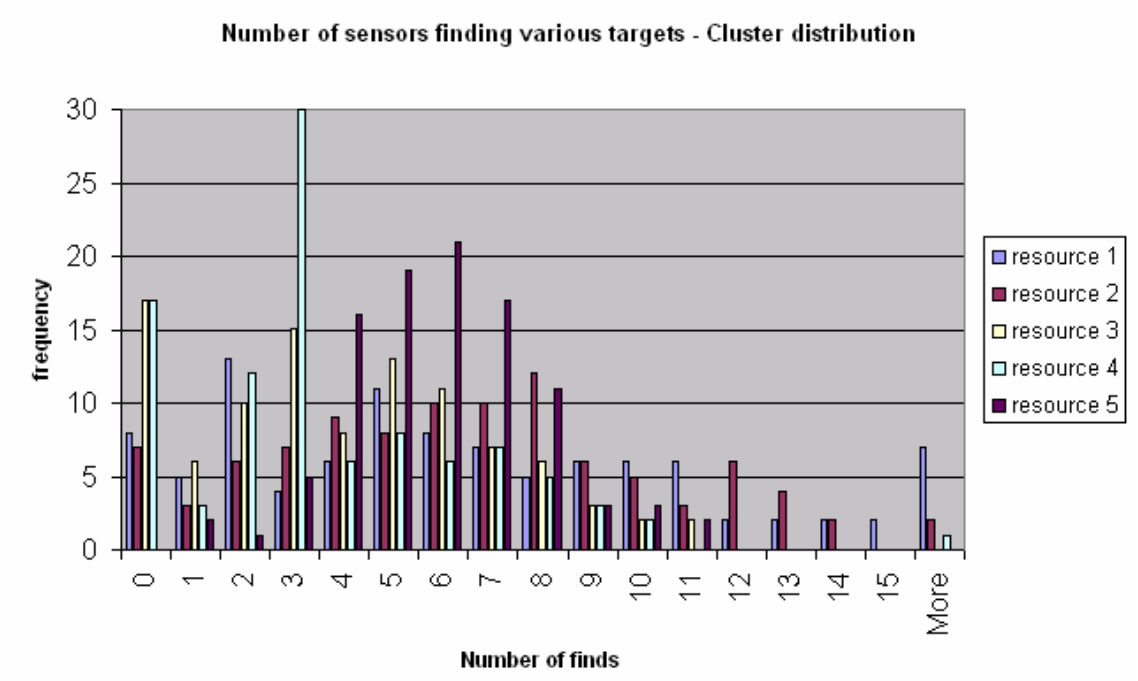

Figure 7-23 Histogram curves showing the number of sensors successfully finding the various targets using the cluster deployment pattern

The success of the cluster pattern appears to be the susceptible to changes in the position and shape of the desired target. As previously discussed the two charts with the lowest means are more likely to be related to the specifications of the simulation

rather than the effect of the pattern, however the means for the equivalent line targets away from the edges of the grid are still marginally lower than for the block patterns. The variability of the cluster data is shown to be much wider than for the other patterns consistently throughout the simulations, with the exception of the individual targets. With the larger targets, 68% of the number of successful landings can be calculated as ranging between 1.36 and 12.44 compared to between 3.94 and 7.86 for the smaller targets. This is verified by the graph, which illustrates that the spread for the larger target (resource 1) is greater than for smaller targets (resource 5). This means that although the number of successes is likely to be higher for the larger targets, the results are irregular.

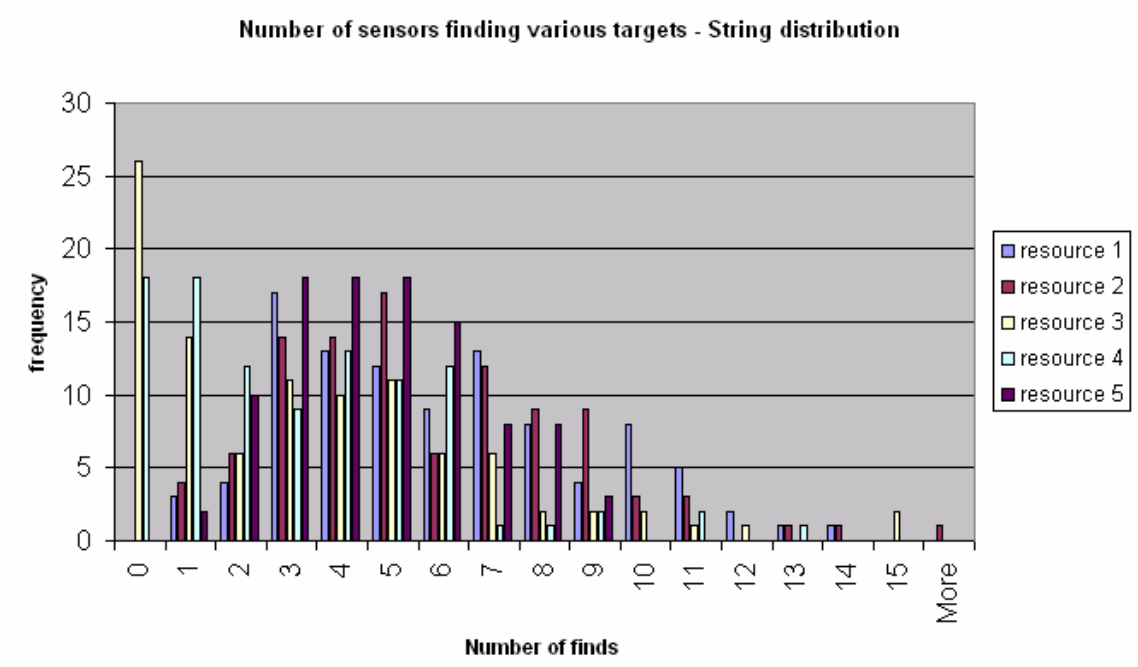

Figure 7-24 Histogram curves showing the number of sensors successfully finding the various targets using the string deployment pattern

The string distribution shows patterns similar to the cluster. However the mean success rate is lower and the spread of results is narrower.

From the data presented above it can be concluded that in spite of the irregularity of high success, the cluster pattern appears to be the most appropriate design to locate larger target areas. For smaller distributed targets, the random distribution of single suites appears to be the preferable option, however both designs yield similar results so either can be used effectively.

7.7 System Design issues raised by simulation

The results of the simulations will be used to influence the final design of the sensor suite system. In the case of any computer simulation, the features of the model should

reflect physical features of the system. With this simulation, those features predominantly model the interconnection of the suites and how this affects the systems ability to perform a given task.

The simulation has shown that a single level deployment is preferable, meaning using individual sensor suites to locate the target before deploying larger clusters of sensors adds additional complexity to the deployment strategy without significant gain in success.

Overall, similar results are reported with both the random individual distribution pattern and the cluster pattern. The cluster pattern can be regarded as a group of physically connected sensor suites that collaborate to report data, perhaps in the form of a grid or web, whilst the individual random pattern can be related to small wireless suites with no physical interconnection. The string pattern also yields successful results. This pattern relates to suites connected along a straight cable. Although the uniform pattern gives the most consistent results, in reality this could be a complex pattern to physically achieve. Placing the suites at regular intervals would be difficult if the suites were to be deployed from the air or ballistically from the ground. However if the application was for example tracing the path of a rover, the rover itself could deploy the suites uniformly as it travels. The pattern therefore is dependant on the method of deployment and the application.

Although there is no clear optimum pattern shown by the simulation, the cluster pattern is the recommended design. The mean number of target hits is marginally higher, however there are many other practical reasons for this recommendation relating to the physical connection of the suites. These include the possibility of sharing key systems, such as power, thereby reducing overall mass, and minimising the complexity of the communications system through a wired connection rather than a wireless ad-hoc network.

The reliability of the suites is shown to be an important factor in the success location of a target. As such the suite components should be chosen to have the highest possible reliability to reduce the risk of electrical and mechanical failure. With COTS components, the reliability factor should be available from the tests performed by the manufacturers.

In conclusion, the simulation has highlighted the preference of physical intersuite collaboration, high reliability and a randomly deployable cluster design, unless the application lends itself to a specific method of deployment.

7.8 Conclusions

A Visual Basic simulation for the deployment of sensor suites over the surface of Mars was produced based on the surface rock distributions recorded by the Mars Pathfinder Lander. This program was designed to allow several different patterns of sensor suites and be able to test the ability of the patterns to locate a target area on the grid.

The survival rate of the sensors was modelled based on the assumption that if a suite hit a heavily rock populated square it would be destroyed. For the example rock field created, the uniform pattern – based on one suite per grid cell, achieved the highest survival rate. Of the three random deployment based patterns, the cluster of 9 suites achieved the better results, however all three were similar. These rates assumed 100% reliability.

The principle effect of changing the deployment pattern is to increase the effectiveness of locating a target. More sensor suites and less reliance on random sensor placement generally equates to a higher fraction of the total number of suites achieving a successful hit. As such, the cluster pattern is the most effective overall, however the variability from the mean number of successful target hits is greater. The cluster represents a group of sensors that have physical intersuite communication. This option is preferred over the randomly deployed individual suites for larger target areas.

The shape of the target is generally insignificant in the ability for the sensor suites to locate them. The only exception is when the target consists of six smaller cells rather than one larger target. In this case both the random deployment and cluster pattern have a similar success rate.

The minimum quantity of sensor suites required to ensure a high probability of at least a 50% success rate is approximately 140, irrespective of the deployment pattern. Increasing this number further results in more target hits. However, the greater the number of suites, the increased risk of failure due to impacts in full squares.

The reliability of the sensors is paramount for the success of the deployment. A reduced reliability of 70% equates to an approximate 50% reduction in success rate. The components of the sensors therefore must be chosen and tested to ensure the lowest risk of failure due to electrical and mechanical factors.

The practical design issues raised by the simulation highlight the need for intersuite communication, either by wires or other means. As a random method of deployment gives greater results, the practical deployment strategy can be designed to exploit this, unless the application suggests a more appropriate alternative.

Overall the simulation has yielded a useful set of results that will shape the final system design.

8 Prototype System Design

8.1 Introduction

The second part of Objective 4 concerns the adaptation of the sensor suite design to fit into a "matchbox". Following on from initial hardware tests and MST paper study, This chapter outlines the full basic environmental sensor suite design, including a schematic and potential packaging design.

The final part of this chapter analyses the generic nature of the sensor suite system design further and suggests possible applications.

8.2 Sensor Suite Architecture Design

This section draws together the discussions from chapters 5,6 and 7 to give an outline of the generic sensor suite system including a schematic diagram of the circuit design. Although general discussion is given here, specific figures regarding subsystems such as power and data collection will be derived for a potential application in Chapter 9.

8.2.1 Final Component Choice

The principle components selected for the sensor suite design are shown in Table 8-1. The "other components" column refers to the additional hardware required for that sensor to operate effectively such as resistors or capacitors. These will have to be included in the final system circuit.

Component	Function	Power		size (mm)	Mass	Features	other components
		V (V)	I (mA)				
ADXL202E	Accelerometer	3	0.6	5 x 5 x 2	0.1g	±2g, 2 axis, digital	2 resistors, 3 capacitors
NPP 301	Pressure	3	0.6	4 x 5 x 3	0.1g	100kPa, for gases	amplifier and resistors
LM20	Temperature	3	0.01	2 x 1.8 x 0.8	0.01g	-55˚C to 130˚C	1 capacitor, 2 resistors
JIC117	UV	3	0.75	8.45 diameter x 6.5 height	0.1g	210 – 390 nm range, internal amplifer	in packaging
PIC16F877A	Microcontroller	3	0.6	8 x 8 x 0.65	0.1g	ADC, I2C, memory, timer	2 resistors, at least 1 capacitor, oscillator.

Table 8-1 Table of components selected for the final sensor suite

Each of these components is discussed further in the following subsections.

8.2.1.1 Accelerometer

The selected Accelerometer is the ADXL202E ±2g, 2 axis model from Analog Devices. A brief overview of this sensor and reasons for its selection are given in section 6.4.1.1 and in the table above. Figure 8-1 shows the internal block diagram and pin configuration as well as a picture of the device shown on a US penny for scale (Analog Devices, 2000).

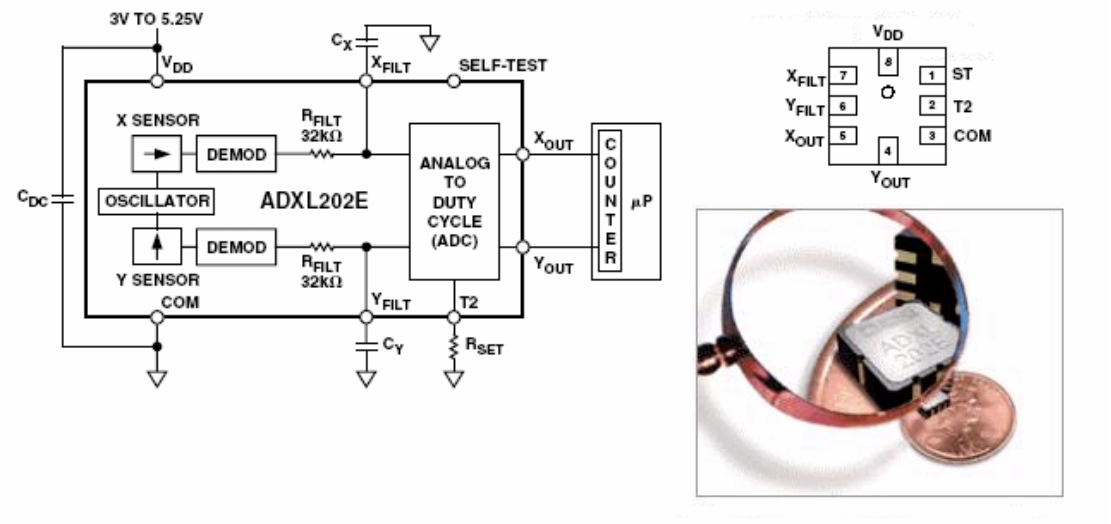

Figure 8-1 ADXL202E Accelerometer internal block diagram, pin configuration and scale photo

As featured in the block diagram, the devices includes an analogue to digital converter, hence the output pins can be connected directly to the microcontroller's digital input pins.

In addition to the power source, a set of resistors and capacitors are required in conjunction to this device. Their pin connections are shown in Figure 8.1. The capacitor C_{DC} allows decoupling of the signal to the noise on the power supply. A capacitor of 0.1µF is used, with an additional 100Ω resistor between the power supply and the power input pin V_{dd}. R_{set} sets the duty cycle modulation which the digital outputs are related to. Here, a 125kΩ resistor is used which sets the duty cycle rate to 1ms or 1kHz. This can be adjusted depending on the application. The capacitors labelled C_x and C_y set the bandwidth of the measurements, which determines the measurement resolution. The bandwidth has been set to 500Hz, resulting in $C_x = C_y = 0.01\mu F$.

The function of the accelerometer in the sensor suite is to measure the tilt angle or orientation. This provides information on whether the suite has deployed flat against the surface or if it has landed on an obstruction or on uneven ground. As with the ADXL150 model discussed in chapter 4, a full scale reading is given if the axis is perpendicular to the Earth's gravity, and zero if parallel to it. Once the output signal

has been converted to an acceleration, which can be calibrated experimentally, the tilt in degrees is calculated by(Analog Devices, 2000):

$$Pitch = \sin^{-1}\left(\frac{A_x}{1g}\right)$$

$$Roll = \sin^{-1}\left(\frac{A_y}{1g}\right)$$

This calculation can be performed in post-processing.

8.2.1.2 Pressure Sensor

An overview of the chosen NPP 301 pressure sensor by Novasensor appears in section 6.4.1.2 along with reasons for its selection. The version chosen measures 100kPa or 1 atmosphere since it is likely to used in standard or low pressure environments. A schematic of the sensor and an image of the package are shown in Figure 8-2.

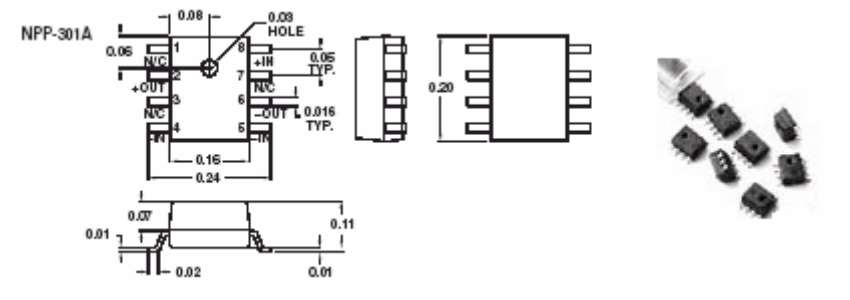

Figure 8-2 Schematic and image of the NPP301 pressure sensor (GE Novasensor, 2003)

The full scale output is given as 60mV (GE Novasensor, 2003), therefore an external amplifier circuit will be used before passing the data to one of the microcontroller's analogue input channels for conversion. The gain of this amplification will be set to 200 as previously demonstrated.

8.2.1.3 Temperature Sensor

The National Semiconductor LM20 temperature sensor is a precision CMOS integrated circuit sensor (National Semiconductors, 2002). It has a predominately linear output which will be connected directly to an analogue channel in the microcontroller. The range of the sensor is given as between –55˚C and 130˚C. The manufacturer's output curve is shown below.

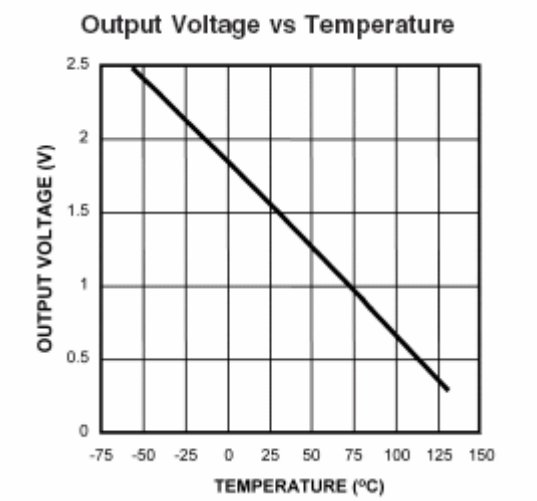

Figure 8-3 LM20 temperature sensor typical output curve

From this, the expected output at typical room temperature is approximately 1.6V.

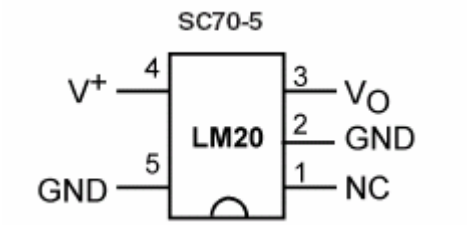

Figure 8-4 Pin connection diagram for the LM20 temperature sensor

The pin connection diagram in Figure 8-4 is for a packaged device, however this model is available as an unpackaged die, which makes it a useful candidate for future full integration.

8.2.1.4 UV Photodetector

As stated in section 6.4.1.4, the JIC117 Ultraviolet photodetector has been selected as a representative radiation sensor. The JIC117 has 1.2mV/nW responsivity and has an internal amplifier (IFW, 2002). The sensor is connected directly to an analogue channel.

This sensor has a hermetically sealed metal and glass package to protect the small active area. A schematic of the casing is shown in Figure 8-5.

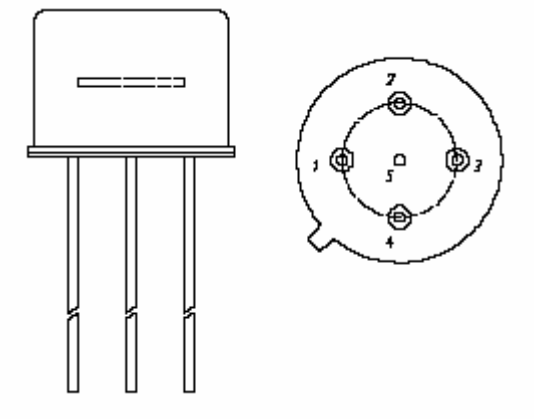

Figure 8-5 Schematic of the JIC117 UV photodetector package (IFW, 2002)

As this sensor will require access to the exterior of the sensor suite, the packaging will remain as protection.

8.2.2 Processing and communications

Details of the selected microcontroller, the PIC16LF877A from Microchip, are given in section 5.5.2. This model was selected for its functionality and relatively miniaturised packaging.

Depending on the application, data readings will be taken periodically. This will be controlled by the PIC's timer. The order in which data reading are taken is also specified within the PIC's programming. Several of the sensors will utilise the analogue input channels, which will then be processed by the PICs internal ADC. This means that additional ADC circuitry is not required. The internal EEPROM memory can store the digitised data before communicating the output at a predetermined time interval.

The microcontroller will also control the suite's communications. The output will be of two forms. Firstly an LED will be attached to one of the digital output channels. The microcontroller can be programmed to recognise when a reading from the ADC is above or below a user-defined value, such as when the temperature reading falls below 0˚C or 1.8V, which equates to an 8-bit value of 153. This triggers the output channel to illuminate the LED as an indicator. This can be used as part of the communication subsystem.

The main form of intersuite communication is performed via an I2C bus. Each bus has at least one Master, although several can be programmed with this capability as redundant Masters. The Master will call each Slave suite in turn to collect their data at regular intervals. This can be stored over a longer time than the amount of memory each individual suite permits, and then passed to additional suite that has the sole purpose of external communication. Again depending on the application, the Masters could process the collected data and only communicate the proportion that is deemed to be of the most interest.

The external communication suite will house only a microcontroller, memory, a transmitter and antenna, plus the appropriate power source. This suite will transmit the data at a predetermined time using a miniature RF transmitter to be collected by a central receiver.

The communications subsystem of the sensor suite concept is discussed further in chapter 9.

8.2.3 Power

Another selection criterion for the sensors and microcontroller is that can all by operated at the same voltage level. The voltage chosen here is 3V. This removes the need for additional voltage regulators and means that all the components can be powered from the same source.

Each suite will contain its own battery power source. The battery type is likely to be a coin battery, since this is available with appropriate dimensions. The limited surface area of the suite makes it unlikely that solar panels could be used to recharge the batteries, unless the required capacity is relatively small, hence non-rechargeable batteries are likely to be the preferred power source. The capacity of the battery will be related to the amount of power required and the length of time it is required to operate for. This again can be modified to the application specifications or can be given as a fixed limit to the duration of the mission.

The power subsystem is discussed in relation to an application in chapter 9.

8.2.4 Sensor Suite Circuit Diagram

A schematic of the final sensor suite circuit is shown in Figure 8-6. It shows the primary components with their passive components as well as their connections to the microcontroller and power source. The output LED is also featured.

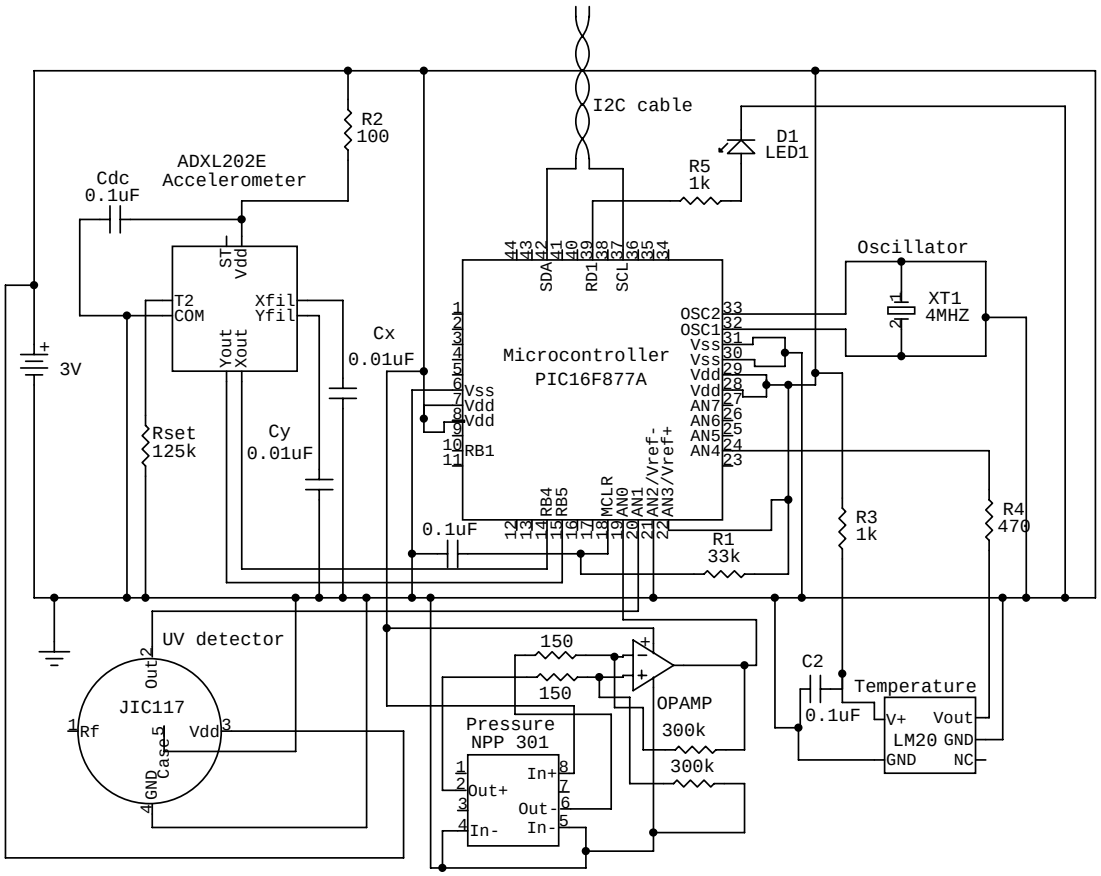

Figure 8-6 Schematic of the final sensor suite circuit

This diagram assumes that the circuit is printed on one flat circuit board. However in order for the sensor suite to have a miniaturised footprint area, other packaging options will have to be explored.

8.3 Demonstrator / MCMs

A brief discussion of Multichip Modules (MCMs) is given in section 6.6. This packaging format is the most appropriate for the sensor suite design.

A standard MCM comprises several bare dies bonded to a substrate then packaged into single chip. This a relatively common form of packaging and is similar to the QFN packaging used for the microcontroller. A typical example is shown in the figure below.

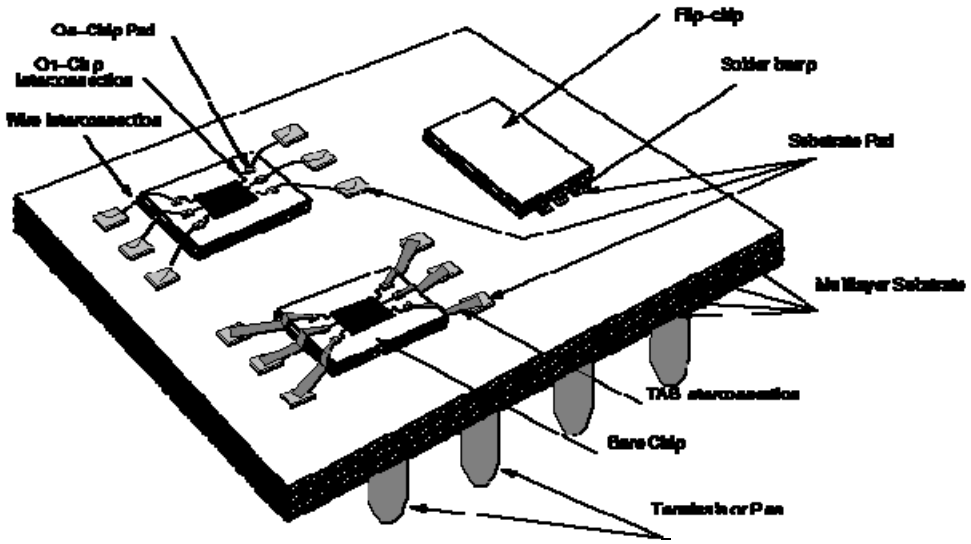

Figure 8-7 Standard 2D Multichip Module architecture (Al-Sarawi, 1997)

Due to the number of different chips within the sensor suite circuit, a 2D MCM would be unsuitable as the footprint area would be relatively large compared with the envisaged concept. Therefore a method of 3 dimensional or vertically stacked packaging would be preferable.

8.3.1 3D Multichip Modules

There are four recognised types of 3D MCM; Stacked packages, Stacked Chip-Scale package, Folded package and System-in-a-Cube (Goldstein, 2001).

The Stacked package is commonly used to connect several memory chips together for equipment such as mobile phones and computers. Each chip is separated by a thin layer of attach material and connected by wires to the package substrate.

The other three types bond the unpackaged dies instead of the chips. This makes for a more compact overall package. Examples of each type are shown below.

8.3.1.1 Stacked Chip-Scale package (CSP).

A Chip-Scale 3D stacking allows integration of different dies into the same footprint area, without having them fabricated from the same silicon wafer. If analogue and digital devices are to be part of the same system, they cannot easily be integrated together in the same fabrication process. The bare dies are stacked and wirebonded to the substrate. The bonds are attached to solder balls, which are used to attach the chip to the circuit board. An illustration of this is shown in Figure 8-8.

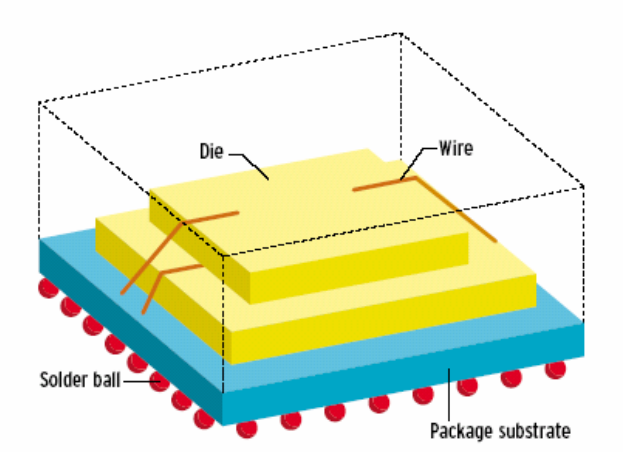

Figure 8-8 Illustration of a Stacked Chip-Scale package (Goldstein, 2001)

An example of this type of packaging is available in memory stacks from Amkor Technology (2002)

8.3.1.2 Folded Package.

The folded package, shown in Figure 8-9, has its dice attached via a metal layer to a strip of polyimide tape. The flexible tape is then folded. The strips can be straight as shown, or in a cross shape with the arms folded inwards.

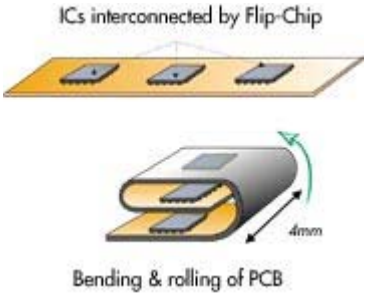

Figure 8-9 Illustration of a Folded Package (Valtronic, 2000)

Valtronic (2000) use this method in their 3D-CSP products. They also attach flip chips, or inverted bare dies, to the tape. After folding, passive components such as resistors or capacitors are surface mounted to the substrate. This additional bulk can determine the eventual size of the package rather than the active chips inside.

An example of a Valtronic system is a small hearing aid (Goldstein, 2001). This package included a processor, a digital signal processor, EEPROM and 18 passive components. The module dimensions measured 4.5 x 4 x 3 mm.

8.3.1.3 System-in-a-Cube.

This concept stacks layers of material embedded with chips (Goldstein, 2001). The layers are then connected together to form the package structure. An illustration is shown in Figure 8-10.

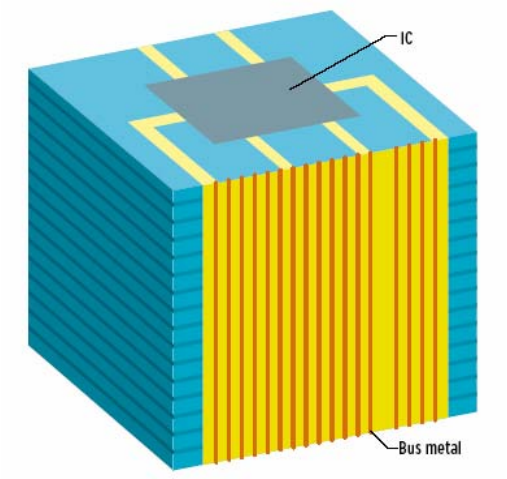

Figure 8-10 Illustration of a System-in-a-cube package

Three examples of this type of stacking technology are given below.

- Neostacking (Gann, 1999)

The Neostacking concept was developed by Irvine Sensors. Each layer is formed from a "Neo-die" in which the chips are embedded. Each Neo-die in the stack is of a standard size chosen to be slightly larger than the largest die. On layers where the dies are smaller, blank pieces of silicon are included. This silicon also aids thermal conduction. A thin layer of epoxy is used to bind the stack, then each layer is interconnected down each side using a metalisation process. A cap chip is attached to the top of the package. A "computer" was produced as a demonstration of the packaging concept. This comprised 52 chips in total, 10 different chip types and 48 layers. Unlike the Valtronics package, the passive components were integrated into the layers. The demonstration package measured 20 x 13 x 13mm.

This shows that systems such as the sensor suite are possible in miniaturised form using this type of technology.

- The BARMINT project

The BARMINT (Basic Research for Microsystems Integration) project developed a vertical MCM concept to house a micropump and multisensor chip (Siero, Morrissey, Carmona, Marco, Samitier, and Alderman,). Unlike the Neostack where each layer is fabricated for the specific purpose, this model used standard sized plastic leadless chip carriers (PLCC) and is based on off the shelf components. Each carrier contains a cavity that the chip is wirebonded in to. The carrier is then filled with globtop material.

The carriers are then glued together. As the carriers are preformed, the structure is already in place, and no additional cutting is required which could put unwanted stress on the components.

- Match X

Match X is a German collaboration. The chips required for a each subsystem are contained within a module similar to the carriers described above. These modules are then stacked together. This technology is being used for the Astrium Micropack (Eckersley et al., 2004).

The sensor suite concept will use a combination of these technologies. Each subsystem or sensor will have its own modular, however as this project prefers the use of COTS products, the modules should be similar to the carriers used in BARMINT.

8.3.2 Limitations to 3D stacking

Although the 3D stack packaging appears the best option for the sensor suite, there are disadvantages and limitations that should be considered (Al-Sarawi, 1997).

- The increased circuit density will lead to an increased power density, which will require dissipation. Therefore the thermal management of the device will have to be considered.
- There is currently a lack of design software available. This means that any modelling of the thermal design or mechanical stresses may not be accurate.
- The time it takes to fabricate an MCM is a function of its complexity. A 3D stack will require a longer lead time than a 2D MCM. This could be as long as 10 months, which may have an impact of the overall mission timeline if many suites have to be manufactured.
- This is an emergent complex technology and as such the cost will be higher than for a conventional 2D MCM.
- Few companies offer standard 3D products and very few offer general access to their technology. This will mean either the development of a suitable method by the designers or having an external party integrate the suites. A discussion of this issue is made in chapter 9.

8.3.3 3D Sensor Suite

In spite of the limitations mentioned above, the 3D stack is still the most appropriate technology for this sensor suite concept. As such, the illustration in Figure 8-11 shows a potential configuration for one sensor suite.

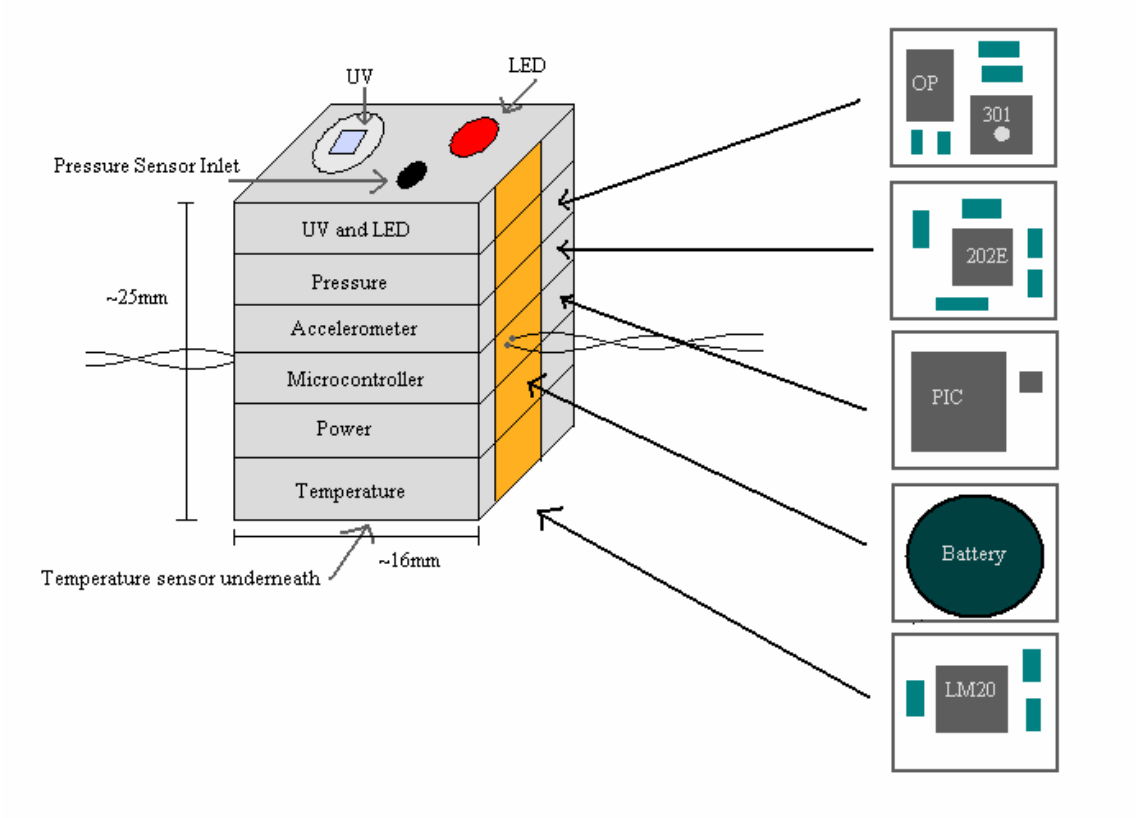

Figure 8-11 Illustration of the sensor suite module layer configuration (not to scale)

The position of the sensors depends on their function. For environmental monitoring, the temperature sensor element should be in contact with the medium it is measuring and the UV sensor should be open at the top of the suite. A hole is also needed for the pressure sensor inlet. All layers are connected to the processor layer and the power layer.

The sensor suite cubes will be attached to an I2C bus to form a collection or web of sensors. The configuration of these webs is discussed in chapter 9.

8.4 Can the design be made generic?

Part of the overall aim of this project is to design a generic MST sensing system. In this context, the generic term refers to a single design of suite system that can be used for a variety of applications with only slight modification. The modifications to the suite, for example, could include a higher capacity battery or additional sensors either integrated into the suite or attached to the I2C bus. The only limitation to the integrated components is that they have appropriate dimensions that will fit within the module structure.

As discussed in section 5.2.3, the temperature, pressure, accelerometer and radiation sensors form the basis of any environmental sensor suite, independent of its final destination or application. This is consistent with the base design in section 8.2.

The power subsystem of the suites will consist of a battery, since the limited size of the suite required by most applications would be incompatible with many other power systems. The long lifetime required by the scenarios also means that either the battery must have a high capacity or the components and design is energy efficient.

The requirements for the communications subsystem for each application indicate that the sensors should report to a central point preferably over several short distance sections, which reduces the amount of transmission energy required and reduces the likelihood for interference. These short distances can be achieved by intersuite collaboration and designated external communications hubs.

In conclusion, the baseline sensors, standardised power subsystem and intersuite communication ability are common to a range of applications making the sensor suite design generic in nature. However, some application-specific modifications may have to be made including additional sensors or insulation against extreme temperature or radiation environments. The sensors can be added using additional stacked layers and the insulation can be moulded to the outside of the suite, thereby leaving the core suite unchanged.

8.5 Conclusions

A schematic of the final sensor suite circuit design that incorporates the four chosen sensors and the selected microcontroller, first detailed in chapters 5 and 6, has been produced. This diagram also includes the necessary passive components, links to the appropriate analogue and digital channels of the microprocessor and output communication methods. A standardised voltage of 3V has been specified.

In spite of the limitations of complexity and time of delivery, the suite will be integrated as a form of 3D Multichip Module. The most appropriate design is the system-in-a-cube, which comprises a stack of standard size interconnected modules each containing subsystem components. These suites will be connected to the I2C bus to form a collection or cluster.

8 different space-related scenarios were proposed to highlight the generic nature of the baseline sensor suite. All of the scenarios were a form of environmental sensing application which confirmed that the baseline sensors and power subsystem could be used independent of final destination. However, the design should be able to be modified easily to include additional sensors and environment specific insulation.

Chapter 9 expands the Polar Region Cryoconite monitoring scenario and discusses various aspects of the system design in relation to this application. Of the previously discussed scenarios, this one was chosen because it was a terrestrial application with quantifiable limits and specifications which also is potentially relevant in a space context.

9 Synthesis and example system application

9.1 Introduction

The final objective of this project;

To bring together the theoretical limits, the practical hardware design and simulation results from the previous steps to refine the design and link it to the technological, industrial and future "bigger picture"

requires a synthesis of the findings from the different aspects of the project and demonstrate them through the use of a realistic mission case study.

Throughout this project, the emphasis has been on the potential use of the sensor suite concept on the Martian surface. However, in order to add validity to the concept, it was decided that actual data from a real mission scenario where this kind of sensor network would be beneficial should be used. Although there are likely to be future suitable Mars missions, a range of appropriate data does not appear to be available at this present time. Rather than use a fictitious example, it was decided to search for an analogous terrestrial scenario with similar objectives and challenges that would also have some relevance to the exploration of the Martian environment.

In Chapter 7, several possible applications were discussed, which included both terrestrial and space related examples. This chapter will discuss in further detail the example based on current research into Cryoconites that form in Arctic and Antarctic glaciers. Section 9.2 gives some background as to the nature of Cryoconites and how they relate to Space and this project.

Although much research has been done into Cryoconites – what they are and how they form, there has been little done on mapping their distribution and formation over the glacier surface. It is for this monitoring exercise that an *in-situ* sensor network will be most useful. This is discussed in section 9.3. This application is a novel use of the sensor suite concept.

The main objective of this chapter is to link work from previous chapters and relate it to the example. Section 9.4 covers the first of these "links" which relates the Fundamentals work to the hardware. This is done by assessing whether the sensor suites could be made to an appropriate size and still have the desired functionality. The second "link" is between the hardware and the simulation and is covered in section 9.5. The simulation shows the best search strategy for different shapes of target areas. Assuming these targets are the Cryoconites, the simulation shows whether clusters of sensors or individual suites would find the targets most effectively. This can be related to the design and distribution of the sensor suite system.

Section 9.6 examines the specific design issues relating to the Cryoconites example. These include the packaging and survivability of the suites in Arctic conditions, how the

data from the sensors will be collected and the deployment strategy. The final "link" section, section 9.7, looks at the link between the hardware and the broader industrial picture. This looks at the reality of the potential manufacturing of these sensor suites and also looks at the possible markets for a generic sensor network design such as this. Section 9.8 contains the baseline mission parameters revealed by this chapter and the conclusions drawn from it.

9.2 Background – What are Cryoconites?

The observation of Arctic cryoconites is one possible terrestrial application for the sensor suite concept. This section introduces cryoconites and describes their formation. It has also been proposed that cryoconites may be found on the surface of other planetary bodies not just the polar regions of Earth, which is discussed in section 9.2.2. As these will provide the conditions for the mission, section 9.2.3 examines and compares the Arctic and Martian environments.

9.2.1 What are Cryoconites?

Cryoconites are melt depressions that form on the surface of glaciers. Examples have been reported in the Arctic, Antarctic, Greenland, Canada and the Himalayas (Takeuchi, 2004). They generally occur in the ablation region of the glacier when dark organic and mineral material is deposited on the icy surface. This material is warmed by the sun and melts a small indentation into the glacier surface. This indentation then grows into a Cryoconite through a variety of processes. These include the absorption of solar radiation, either transmitted through the walls of the subsequent hole or a combination of direct and diffuse radiation being absorbed by the material at the bottom, and the downward convection of water warmed by solar radiation at the surface of the hole (Säwström, Mumford, Marshall, Hodson, and Laybourn-Parry, 2002). This is illustrated in Figure 9-1.

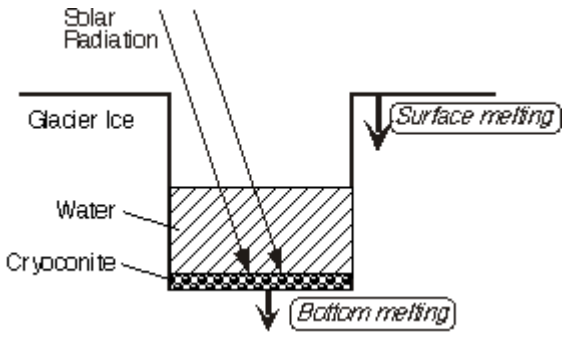

Figure 9-1 Processes for Cryoconite formation (Takeuchi, 2004)

The holes tend to be no more than 60cm deep and are cylindrical in shape. As the hole becomes deeper, the convection of energy from top to bottom becomes more difficult and eventually the downward growth will cease. The point at which the energy diminishes depends on the local climate, and therefore most Cryoconite holes in a given environment have the same depth. (Wharton, McKay, Simmons, and Parker, 1985)

Since they contain melt water, the holes freeze in winter then reform during the summer season as the solar radiation passes through the ice and reheats the dark sediment at the bottom of the hole. However in many examples, particularly those found in the Antarctic, a thick layer of ice remains over the hole forming a "lid". Because of this and the slow rate of sublimation, previously formed holes are unlikely to reopen to the atmosphere on an annual basis, but rather on a decadal one. (Tranter, Fountain, Fritsen, Lyons, Priscu, Statham, and Welch, 2004)

The layer of material at the bottom of the Cryoconite hole and the overlaying water has been shown to contain many forms of bacteria and other microbiota, with a greater concentration in the bottom material. Examples from Arctic Cryoconites have shown that the bottom material is dominated by cyanobacteria (mostly *Phormidium* sp.), while both the material and water contained some chlorophyte species. In general, the species found reflect those found in the local ecosystem, which suggests that that is the source of the material, and therefore varies from region to region. (Säwström et al, 2002) Biothermal processes such as photosynthesis caused by the bacteria present have also been recorded, although McIntyre's 1984 paper (cited in Säwström et al, 2002) reported that these biothermal effects were relatively small and so do not have a significant effect on the formation of the Cryoconite hole. Photosynthesis levels, and the resulting carbon levels, are however still of interest to those studying the microbial communities in Cryoconites and the capacity of the glacier to support such life.

Cryoconites appear to be able to form anywhere on the glacier surface, and that the smaller holes will tend to coalesce as they grow if formed close to each other. The following photographs were taken on the Midre Lovenbreen Glacier in the Arctic archipelago of Svalbard.

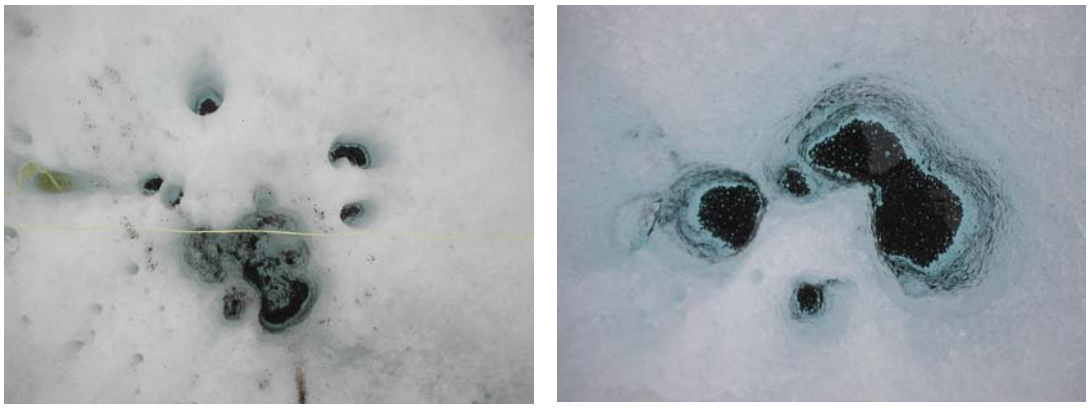

Figure 9-2 Cryoconites on Midre Lovenbreen Glacier (Courtesy of Prof. J Laybourn-Parry)

9.2.2 How do they relate to Space?

The ice-sealed environment of the Cryoconite is being considered as an analogue for the possible survival of life in the glacial surface environments of other planetary bodies (Tranter et al, 2004).

Various Microorganism colonies have been discovered in Earth environments that are subject to a wide range of physical and chemical conditions. Horneck (2000) presents several examples that demonstrate how life can survive providing there is an available energy source and that the environment is compatible with the chemistry of Carbon-Carbon bonds. These Extremophiles have evolved to ensure their survival under these conditions. Bacillus subtilis produce spores that protect their DNA structure against many hostile environmental features, such as high radiation and temperature extremes, by saturating the DNA with small proteins that alter its reactivity and produce a dormant, or anabiotic, state. In this state, these spores can survive for extended periods of time in the space environment, characterised by intense radiation, high vacuum and extreme temperatures. It is thought that microbiota could also have survived in a glacial environment in a similar dormant state. Cyanobacteria, similar to those found in Arctic Cryoconites mentioned previously, are the only prokaryote capable of oxygenic Photosynthesis. (Horneck, 2000) These have evolved to use sunlight as their energy source, but also had to protect themselves against the harmful short wavelength Ultraviolet radiation emitted by the Sun that the early Earth atmosphere offered no protection from. The thin Martian atmosphere, which like the Early Earth atmosphere, has very little Ozone (O_3) to absorb this short wavelength UV, and therefore any potential Martian biota would also have to adapt like the early Cyanobacteria.

Hoover and Pikuta (2004) proposed that the Cryoconite phenomenon may also occur on Comets, on Mars and on some of the Jovian moons. It is suggested that similar localised heating effects could occur around the dark rocks that are present within Comets and beneath the surface of the Polar ice caps and permafrost on Mars as those that create Cryoconite holes on terrestrial glaciers. The related dust, inoculi and solar energy that enable the liquid water to form underneath an icy surface may provide an environment where biological activity can adapt to utilise the gases, substrates and nutrients from the rocks and ice such that the activity can continue even in the most extreme hydrochemical conditions and sustain colonisation (Tranter et al, 2004).

Cryoconites are among the coldest polar microbial communities, (Säwström et al, 2002) and therefore these kinds of microorganisms might provide the best analogue for the type of life that may inhabit the Polar regions of Mars or be found beneath the icy crusts of Europa, Callisto or Ganymede. (Hoover and Pikuta, 2004)

9.2.3 Environmental conditions – similarities and differences.

Compared to Earth, Mars is a hostile environment. However, there are terrestrial analogues that are extremely cold and dry, called Endolithic habitats (Horneck, 2000), in the Earth's polar regions.

The following is a comparison of some of some key environmental conditions observed on Mars and those recorded at the Adventdalen Weather Station (78N 16E) (see Appendix C) – the closest weather station to the Midre Lovenbreen Glacier (79N 12E) in Spitzbergen, which will be the subject of this investigation. The data used for this comparison is taken for the period July 16 2003 to May 16 2004 (Hansen, 2004)

The similarities and differences will have to be taken into account when using the Cryoconite model as a sample mission for the sensor suites, and design modifications would have to be made accordingly for the two environments.

9.2.3.1 Temperature

The surface temperature range for Mars has been recorded to be between –123°C and 25°C, which are subject to seasonal and diurnal fluctuations. These diurnal fluctuations only affect the top layer of the surface, and at a depth of 15-20 cm the temperature converges to the diurnal mean – for example if the diurnal range is between –90°C and –10°C, the below-surface temperature will be approximately –50°C. (Horneck, 2000) The Polar regions of Mars have recorded temperatures below –50°C.

Temperatures observed at Adventdalen over the selected period range between –29°C and 8°C, and are subject to similar diurnal and seasonal fluctuations. Temperatures recorded above the surface also have the added "windchill factor" which creates an effective temperature of, for example, –50°C when the actual recorded temperature is –22°C.

9.2.3.2 Atmosphere composition

The Martian atmosphere is very thin and is mainly composed of Carbon Dioxide (CO_2). CO_2 constitutes 95.3% of the atmosphere, whilst the remainder consists of Nitrogen (N_2) (2.7%) and Oxygen (O_2) (0.13%). As previously mentioned, the atmosphere contains little if any Ozone (O_3), although there is the suggestion of a small amount in high-latitude winter conditions. (Horneck, 2000)

By contrast, Earth's atmosphere consists of 72% Nitrogen (N_2), 21% Oxygen and 1% comprising traces of Argon (Ar), Water, Carbon Dioxide (CO_2) and Ozone (O_3) and has a column thickness of approximately 10^4 kgm^{-2}. In areas above the Earth's poles, Ozone levels have been shown to be depleting over several years. (Newman, 1999)

9.2.3.3 Wind speed

The wind speeds measured by the Viking Landers in the early 1980s show seasonal variations. (Williams, 2004) Speeds of between $2ms^{-1}$ and $7ms^{-1}$ were recorded during the summer, while during the autumn months speeds of between 5 and 10 ms^{-1} were observed. Mars also experiences dust storms where winds can reach speeds of between 17 and 30 ms^{-1}.

Data gathered at Adventdalen shows that the range of recorded wind speeds remains fairly constant throughout the year, and speeds of anywhere between $1ms^{-1}$ and $12ms^{-1}$ can be recorded at any time. There are also periodic gusts of up to $20ms^{-1}$.

9.2.3.4 Pressure

The mean surface atmospheric pressure on Mars has been observed to be 5.6 mbar (or 560 Pa). This results in an extremely cold and dry climate. (Horneck, 2000) The

Standard Atmospheric Pressure on Earth is given as 1013 mbar (1.013×10^5 Pa). Readings taken at Adventdalen show the range of pressures to be between 998 and 1023 mbar for the selected period. These reading also fluctuate over the course of a day.

9.2.3.5 Radiation

Solar radiation is the main source of energy to a planet's surface. This is generally in the form of shortwave radiation with peaks in the Visible and Near Infrared regions, which reaches the planet surface either by being transmitted directly or diffusely through the atmosphere. A percentage of the solar radiation is reflected back into space and the remainder is absorbed by the planet's surface and reemitted as thermal infrared radiation.

The intensity of the solar radiation that reaches the Earth's surface in the Arctic varies over the course of the year from a maximum of 400 Wm^{-2} during the summer to zero in the winter. This variation is caused by the relative position of the sun – since during the winter the sun does not appear above the horizon and therefore the surface receives no solar radiation. (NSIDC, 2004) It is likely that a similar effect would be seen in the polar regions of Mars, even though Mars is further from the Sun.

Different wavelengths of solar radiation are absorbed by different parts of the atmosphere depending on its composition. On Earth, UVc radiation (200 to 280 nm) and the majority of UVb radiation (280 to 320 nm) are absorbed by the "Ozone layer". These are the two most harmful types of UV radiation to living organisms. As mentioned previously, the levels of Ozone above the Earth's poles has been decreasing over several decades, resulting in higher levels of UV radiation reaching the surface. (Newman, 1999) The Martian atmosphere is predominantly composed of CO_2, which absorbs all radiation with wavelengths below 200nm. During the Martian winter, the Ozone present in the Martian atmosphere absorbs the UV with wavelength between 200 and 250 nm, but during all other seasons nearly all of the UV radiation reaches the planet's surface. So, although the solar constant for Mars is much less than that of Earth and less solar radiation reaches the planet's atmosphere (Mars 589.2 Wm^{-2}, Earth 1367 Wm^{-2}), the fraction of radiation reaching the surface is far greater. (Horneck, 2000)

The planet surface reflectivity or Albedo determines the proportion of radiation that is absorbed by the surface. This changes depending on the type of surface terrain. Relevant examples for the Arctic are surfaces such as fresh snow that reflects 90% of radiation, compared to melting snow that only reflects 50% (NSIDC, 2004). The Albedo recorded in the Martian Polar regions has a maximum of approximately 40%, which means that a greater amount of the radiation is absorbed by that surface than by its terrestrial equivalent (Putzig, 2003).

9.2.3.6 Gravity

The acceleration due to gravity on Earth is recognised to be 9.81 ms^{-2}. On Mars, it has been recorded to be 3.69 ms^{-2}.

9.2.3.7 Humidity

Relative humidity compares the actual water vapour content of the air to the maximum water vapour that it could hold, or saturation level, and is given as a percentage. At Adventdalen, relative humidity of between 50% and 90% has been recorded.

The air on Mars is reported to be cold and dry, with a very low relative humidity during the day. However, it has also been observed that liquid vapour fog, or 100% humidity, can occur at night (Williams, 2001).

9.2.3.8 Surface type

The Martian surface comprises soil particles that have a grain size of less that 50μm. (Williams, 2001) The bulk density of this soil is estimated to be between 1.2 and 2.0 gcm^{-3}. (Golombek, Cook, Economou, Folkner, Haldemann, Kallemeyn, Knudsen, Manning, Moore, Parker, Rieder, Schofield, Smith, and Vaughan, 1997) The surface also features various sizes of rocks ranging from pebbles to boulders. (see chapter 7). Another feature is the slightly magnetic dust, with the consistency of flour, that covers the surface. This has been seen to coat equipment left on the surface.

The Arctic comprises frozen ocean surrounded by land masses and islands. The central Arctic Ocean is ice covered all year round, and there is snow and ice covering the land parts for most of the year.

9.2.3.9 Length of day

The Martian day is approximately 24.6 hours long, which is very similar to Earth, and like Earth, Mars also has seasons.

9.2.3.10 Summary of environmental conditions

	Mars	Earth (Arctic Region)
Temperature	-123˚C to 25˚C (Average –50˚C)	-29˚C to 8˚C
Atmospheric composition	CO_2 – 95.3% N_2 – 2.7% O_2 – 0.13%	N_2 – 72% O_2 – 21% 1% traces including CO_2, Ar and O_3
Wind Speed	2 – 7 ms^{-1} (summer) 5 – 10 ms^{-1} (autumn)	1 – 12 ms^{-1}
Pressure	5.6 mbar	1013 mbar
Radiation	Solar radiation – 589.2 Wm^{-2} All 3 types of UV	Solar radiation 1367 Wm^{-2} UVa and some UVb only
Gravity	3.69 ms^{-1}	9.81 ms^{-1}
Humidity	0%	50-90%
Surface Type	Grainy soil with rocks and boulders. Slightly magnetic dust.	Frozen ocean with ice and snow
Length of Day	24.6 hours	24 hours

Table 9-1 Summary of Martian and Arctic environmental conditions

There are differences between the two environments, however the Arctic has been used as a terrestrial analogue for the Martian surface for several Mars hardware tests.

In terms of the sensor suites, the most significant conditions will be those relating to the chosen sensors; the temperature, pressure, UV levels and vertical acceleration used to measure tilt. The wind speeds and gravity will also be important to the deployment of the system.

9.3 Application of the Sensor Suite concept.

This section discusses the potential benefits of using the sensor suite concept for monitoring cryoconites compared to traditional methods. It then introduces sample data from the Midre Lovenbreen Glacier that will be the environmental baseline for the sample mission.

9.3.1 Benefits of the Sensor Suite concept to Cryoconite Research

The research conducted regarding Cryoconites has mainly been focused on the organic and inorganic composition of samples taken from both the material and the water. Other data, such as local and hole temperature and light levels, have been gathered on site using standard sensor devices and probes, with most of the analysis performed in the laboratory. The readings taken tend to be discrete and taken at the time of sample retrieval rather than continuously taken over the entire season.

One of the principle benefits of using the Sensor Suite concept is that a network of sensors can be deployed and left to give continuous data readings. As these are *in-situ* sensors, and are therefore in constant contact with the medium under investigation, they should be able to detect subtle changes that may occur in the environment or within the Cryoconite over time, for example, fluctuations in temperature or radiation levels that may be missed by only taking occasional readings. The growth rate and growth patterns of the Cryoconites could be continuously monitored over a season which would provide additional data on their formation conditions. The network would have sensors at regular predetermined positions within it, and as such, the data received by the different suites would change as the Cryoconite grew around them. Since the distances between sensors would already be known, it would then be possible to determine the size, and possibly shape, of the hole. One of the challenges that must be addressed is that of ensuring that the sensors themselves do not unnaturally influence the environment they are monitoring. For example, in this case, it means that they must not melt the ice around them.

The distribution of the Cryoconites over a large area of the glacier surface has yet to be mapped. Those studied have tended to be those observed in one selected area of the glacier. By deploying small groups of sensors over a large area, a picture of the overall distribution can be developed. This would show whether their position on the glacier is random or if there is a pattern related to certain environmental conditions.

There are also potential miniaturisation benefits associated with the Sensor Suite concept. Säwström et al (2002) noted that during their investigation they were unable to measure photosynthetically active radiation levels within the Cryoconites because their light meter was too large to fit into the holes. A sufficiently miniaturised light meter included in the sensor suite would eliminate this problem and enable further readings and analysis to be performed.

The initial Sensor Suite concept includes relatively simple sensors, such as temperature, pressure and light meters. However, these are useful environmental indicators and are the types of measurements that are routinely made when taking samples on the glacier. In this case, the bacteria present have been fairly well researched using standard sampling methods. If this example were to be extended for extra-planetary use, other more sophisticated sensors may have to be incorporated into the suite in order to detect possible life, although it may be possible for comparisons to be made using the initial environmental sensors already present.

In this scenario, networks of sensors would be deployed both at the locations of preformed Cryoconites and randomly around the glacier to detect any later formations. These would then report their position, the current and subsequent size, growth rate and also return environmental information from both inside the hole and from the surrounding area.

9.3.2 Example data from Midre Lovenbreen Glacier

Data from a study of the Cryoconites on the Midre Lovenbreen Glacier will be used in order to provide realistic baseline parameters for the size and performance criteria of the

sensor suites. The study was made during the summers of 2000 and 2001. (Säwström et al, 2002)

Glacier:	
Air Temperature	-5.5°C to 10.3°C (mean = 2.5°C)
Ave. Daily Incident Radiation	7.2 x 10^2 µmol m^{-2} s^{-1}
Maximum Incident Radiation	2.5 x 10^3 µmol m^{-2} s^{-1}
Cryoconites:	
Diameter	5 cm to 50 cm
Depth	10cm to 30cm (mean = 20cm ± 5.9 cm)
Volume	0.59 l to 37.3 l
Water Temperature	0.1 °C[a]
Average Glacier Coverage	12 holes m^{-2}

[a] uniform with one exception. Largest hole = -0.1°C

Table 9-2 Data from Midre Lovenbreen Glacier 2000 (Säwström et al, 2002)

Other example data will be taken from the Adventdalen data mentioned previously.

9.4 Link 1 – Fundamentals and Hardware

Chapter 3 discussed some of the fundamental physical limits and relationships that govern the key components of the sensor suite. This section links these fundamentals to the practical example which has footprint maximum dimensions of 1cm^2.

9.4.1 Fundamentals related to sensor suite application

The smallest diameter of a cryoconite recorded in the study at Midre Lovenbreen was 5cm. Using this as a guide, the maximum size of the individual sensor suite should be 5cm. However, in order to ensure that even the earliest formation of a Cryoconite is detected, and minimise the environmental impact of a large number of suites, it has been decided that the suite should have an area in the order of 1cm. The depth of the sensor suite is less important.

The example discussed in chapter 3 showed that the theoretical size of a simple sensor system could be in the order of microns. (10^{-6}m) However the conclusion was made that it was user-defined requirements that limited the minimum size of a sensor suite, and these were likely to increase this size significantly. In addition, this example was also only for one sensor, whereas by definition any sensor suite will include several sensors plus their related electronics.

The sensors chosen for the suite are an accelerometer, temperature sensor, pressure sensor and light / radiation sensor. The following examines each sensor with regards to its fundamental equations and compares the theoretical limits to some user-defined requirements and currently available examples to confirm that the chosen sensors are compatible with the desired footprint dimensions.

9.4.1.1 Accelerometer

Following the discussion in section 3.3.1.1 and to show an example, typical target values of minimum acceleration a_{min}, damping coefficient ζ and bandwidth ω_c were selected that represent those commonly used in the microaccelerometers that are currently available. The minimum detectable acceleration should be less than 0.02g (g is the acceleration due to gravity and is taken as 9.81 ms^{-2}.) The bandwidth should be greater than 5 kHz to allow for different applications such as tilt sensing and vibration sensing. In order that the transient response has desirable characteristics, the damping ratio should be between 0.6 and 1.1.

When the lowest values in each of the ranges were substituted into the equations, ω_c = 4664 Hz, which is close to the desired limit, and a_{min} = 0.0014 ms^{-2}, which is acceptable. However the damping ratio ζ = 0.218, which would give a very underdamped response that is undesirable for this application.

Different combinations of a_1, l, b, h and d were substituted into the equations until the targets were met. It is likely that there are many different combinations that could produce the targets; the following is just one example:

a_1 = 2.4 mm	m = 4.31 μg	ω_c = 5086 Hz
h = 4.8 μm	k = 100.98	
l = 383 μm	x_{min} = 0.19 nm	a_{min} = 0.0004g
b = 270 μm		
d = 9.5 μm	β = 0.028	ζ = 0.671

Table 9-3 Typical values of accelerometer design parameters

These dimensions are consistent with microaccelerometers that are currently available on the market, such as the Analog Devices ADXL202E, which measures 5mm x 5mm and includes two accelerometers.

9.4.1.2 Pressure Sensor

A currently available piezoresistive pressure sensors, the diameter of the packaging of the Novasensor NPP 301 is approximately 4mm, including relevant internal electronics(GE Novasensor, 2003). Using the theory in section 3.3.1.2, for a pressure range of 100 kPa, the maximum diameter of the diaphragm would have to be 0.9mm. Since the hole has a diameter of approximately 0.8mm, it is likely that the diaphragm would be approximately the same size.

9.4.1.3 Temperature Sensor

There are several different types of temperature sensor with varying governing principles. The integrated circuit temperature sensor is produced using similar micromachining techniques to the MST components previously discussed and is essentially a transistor that includes a pn junction. This type of sensor uses the temperature characteristics of the silicon pn junction and has a temperature sensitivity

over the typical semiconductor operating range of –55°C to 150°C that is relatively predictable. Due to this operating range and its suitability for full integration, it is this sensor that is included in the final design.

The principle equation defines the forward voltage drop, $V_{F,}$ which equals the junction voltage $V_{BE,}$ that is produced by supplying a constant forward current I_F through the pn junction. (Webster, 1999) It is given by:

$$V_F = V_{BE} = \left(\frac{kT}{q}\right)\ln\left(\frac{I_F}{I_S}\right)$$

where k = Boltzmann's constant, q is the charge on the electron, I_s is the reverse saturation current of the junction and T is the temperature in Kelvin. This equation shows that the Temperature is proportional to the forward voltage drop. It can be shown that the forward voltage has an overall temperature coefficient of –2 $mV°C^{-1}$. Since the calculation relies on the thermal characteristics of the junction, the temperature can be calculated independently of the physical size of the junction itself. (Moore, 1998)

The minimum size of the sensor is then determined in the same way as any pn junction. An example of the minimum width of the junction was shown in chapter 3. The doping of the material sets a limit to the area of the junction. Typical dopant concentrations are in the order of 10^{16} cm^{-3} or 10^{18} cm^{-3}. The number of atoms in any area cannot be controlled precisely, however using a statistical distribution, the number can be estimated to within a given percentage. This percentage is user defined, and therefore sets the size limit. For example, if 100 dopant atoms are required at a density of 10^{16} cm^{-3}, the minimum volume needed would equate to a cube with sides measuring 215 nm. (Foll, 2001) If the volume is too small, there will not be enough atoms for the junction to function properly. However if the volume is too large, the doping precision needed assuming the statistical distribution of the atoms becomes impractical.

National Semiconductor's LM20 temperature sensor is available as an unpackaged die(National Semiconductors, 2002). The dimensions are given as 584 μm x 559 μm x 216 μm, although it is unclear as to what percentage of that is occupied by the actual pn junction. It is likely that the sensor constitutes an array of pn junctions rather than one individual larger cell. These dimensions are the result of current manufacturing and integration technologies, rather than those that are defined by fundamental limits.

9.4.1.4 Light sensor

Section 3.5.2.1 describes the fundamental equations that govern a photovoltaic cell photon detector. These principles are the basis for any photodiode or photodetector light sensor. It was concluded that the minimum dimensions for a diode measuring wavelengths of 400 nm, are 400 nm x 400 nm x 600 nm. This is dependant on the wavelength of the radiation being measured, the acceptable signal to noise ratio and the responsivity of the cell – the output current of the cell divided by the input optical

power, so a larger area, or array of cells, will be necessary to meet most user defined requirements.

Examples of microphotodiodes exist and are currently being investigated in the field of biotechnology. Optobionics (2004) have developed an Artificial Silicon Retina (ASR), which is designed to stimulate damaged retinal cells in the eye. The ASR is 2 mm in diameter and 25 μm thick and contains 5000 microphotodiodes, each connected to a microelectrode. These convert the light energy into electrochemical impulses to stimulate the cells and create visual signals to the brain. The photodiodes are also used as miniature solar cells to create their own power, which removes the need for additional batteries. Using the given dimensions, the linear dimensions of each cell can be estimated to be 25 μm x 25 μm. These devices are currently under patient trial. Figure 9-3 shows the ASR on a penny for scale and Figure 9-4 shows the individual microphotodiode. (Nighswonger, 1999)

2mm ASR® device lying on a penny

Figure 9-3 The Artificial Silcion Retina

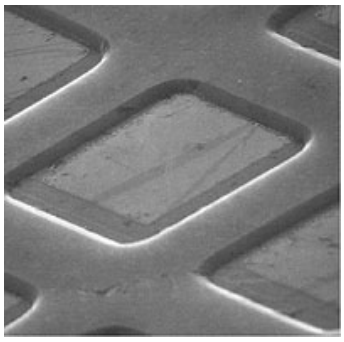

Figure 9-4 An individual microphotodiode

Other sensor network projects also include light sensors. Smart Dust contains a fully integrated light sensor that has an active area of 200 μm x 200 μm (Warneke, Scott, Liebowitz, Zhou, Bellew, Chediak, Kahn, Boser, and Pister,), however this is not a COTS device. Commercially available photodiodes are several orders of magnitude larger. The UDT sensors PIN-01-CJ photodiode (UDT Sensors , 2004) measures a range of wavelengths between 350 nm and 1100 nm, which includes optical and infrared wavelengths and has an active area of 400 μm x 400 μm. The depth of the active area is not specified, however using figure 3-13, it must be at least 140μm. This has a rise time of 11 ns and has a responsivity of between 0.1 and 0.35 A/W for optical wavelengths. (As the responsivity is an proportional efficiency, higher numbers are preferable.) Even including the packaging, this sensor only measures 3 mm x 3 mm, so is inside the 1 cm limit.

9.4.2 Other Considerations for the size of the sensor suite.

From the analysis above, it can be seen that all of the chosen sensors are available below the 1 cm diameter limit, even as "off the shelf" components. In most cases, however this does not include the packaging. The size and shape of the packaging for these sensors depend on the final users requirements and applications, and a variety of

styles are available. In general the choice appears to depend on the sophistication of the user's integration methods, such as using surface mounting, and now National Semiconductors are selling a range of components in unpackaged die format.

The other main components of the suite are the microprocessor, the power subsystem and communications

The size of the necessary power subsystem will ultimately depend on the required power for the other components of the suite. Currently, Lithium batteries have the highest available energy density, and therefore provide the most power for the smallest area. These are commercially available as "coin" batteries and are used to power watches and calculators. One example has a diameter of 12 mm and produces 29 mAh at 3V. Where space and mass are limited, other forms of lithium battery are being developed. Thin film lithium batteries are already being fabricated onto the back of Multichip Modules to provide their power, although the areas needed are in the order of 6.5 cm^2. (ORNL, 2001) Microscale lithium batteries are under development that will be even smaller. West *et al.* (2002) experimented with solid lithium electrolytes and produced cells with areas in the order of $(100\mu m)^2$ using microfabrication techniques. These discharged at 3.9V and approximately 1 nA h. Multiple cells would give higher currents or voltages.

As discussed in section 3.3.2, the minimum size of the information processing device depends on the number of operations, the desired speed and the ability to remove heat. These are user defined parameters. Currently, the smallest commercially available microcontroller is the PIC10F from Microchip, released in June 2004. (Microchip, 2004) They are an 8-bit controller with a 4 MHz internal Oscillator, 16 bytes of data memory and a watchdog timer. They operate at less than 350 μA at 2 V and have dimensions of 2.8 mm x 3 mm including packaging. It can control simple operations, however would need additional external components such as an ADC for use in a sensor suite. Other microcontrollers are available with internal ADCs and I2C buses, however these come in much larger packages. As a result the size of the microcontroller is determined by the function that is to be performed.

For the sensor suite, the microcontroller ideally should include ADC capability, at least 6 input/output channels and communications protocol capability such as an I^2C or USART. This limits the choice and size of the available chip. To stay within the desired $1cm^2$ area, an unpackaged version of a larger chip will be needed.

The limits to the size of the communications subsystem depend on the method of communication chosen. Examples used in this system include wire connections, optical and RF systems, each with their own limiting factors and equations. The limits for the wire are its area and capacitance. The minimum antenna size is determined by the wavelength, the desired gain and bandwidth. If an LED is to be used as a communication system, which would principally be as a device locating beacon, the main factors are size and brightness, which is related its power, and the distance that the signal must travel. The radiation received diminishes proportional to the square of the distance from the source. Therefore, either the LED must be very bright or the detector must be very sensitive.

9.4.3 Can the sensor suite have a 1cm^2 footprint?

Presently, the minimum size of the components, and therefore the sensor suite, is limited by current fabrication technology and the user's requirements. The fundamental physical laws discussed for each type of sensor and system relate only to that particular design. At extremely small dimensions, other factors such as quantum mechanics become significant, which means the design has to be reviewed. This is the basis of the research being carried out into nanotechnology.

The main requirement of this sensor suite is that is must be less than 1 cm^2 in footprint area. Other requirements, which will be discussed in detail in section 9.6, are related to the ability to function in extreme weather conditions, the method of data transfer and the required power. Certain COTS components will need to the integrated in their unpackaged state to reduce their size and a 3d stacking formation will enable the footprint requirement to be met. This does however bring about its own fabrication challenges. All these requirements affect the minimum size of the suite in some way, however both physics and current technology agree that this minimum is possible with the right configuration. As technology develops, further reductions in size will be possible and even smaller suites will be achievable

9.5 Link 2 – Hardware and Simulation

The simulations, discussed in chapter 7, showed that clusters of sensor suites yield a greater success rate for larger target areas. Locating single target squares, however, was better suited to a random deployment of individual suites. Both configurations are discussed in relation to the results of the hardware investigations.

9.5.1 Clusters of Sensor Suites

A cluster, or web, of sensor suites is defined here as several suites that are physically connected to each other and which share collected data with each other and a common hub. The overall size of the webs will be influenced by the reported size of the Cryoconites. This means that the diameter of the web will be approximately 50cm. This size assumes that accurate deployment of the web, landing at the centre of the target Cryoconite, is possible. Although this may not be the case in reality, a 50cm web should be able to detect part of the Cryoconite anywhere within an approximate area of 2.25 m^2 around the target, as illustrated in the figure below. This also determines a limit for the deployment accuracy.

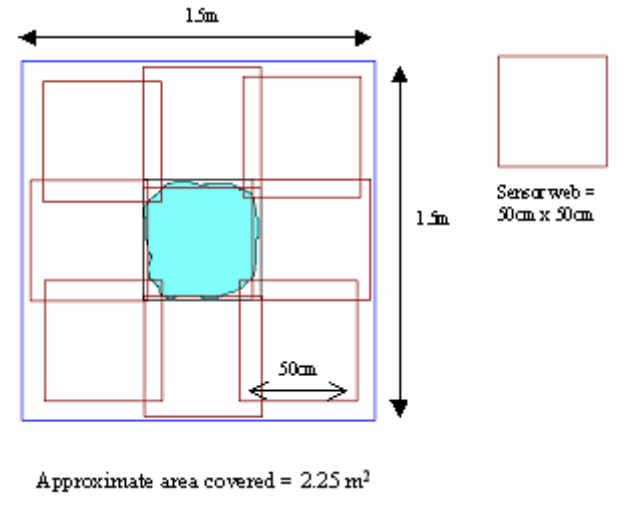

Figure 9-5 Illustration of the potential cryoconite detection area of one cluster.

During the hardware investigations it was decided to use the I2C bus architecture for intersuite communications. The three wires used for this bus would therefore be used to connect several suites together. The number of devices per bus is dictated by the capacitance of the wire and the device connectors, since the maximum allowable capacitance is 400pF. Since the sensors will be connected via the microcontroller, only the microcontroller from each suite will have a direct connection to the I2C bus, and therefore only the microcontroller's capacitance is taken into account when determining the total bus capacitance. Microchip (Bowling and Fischer, 2000) recommends 10pF as a good estimate for the capacitance of each device, however a value of 15pF will be used in this case to include a margin of error. The I2C specification also states that the amount of current on the bus must be no more than 3mA. For a 3V bus, a pull-up resistor of at least 1000Ω is required. Due to the number of available addresses, a maximum of 8 of any one type of device, such as a microcontroller, is permitted per bus. The number of suites and the length of the bus are therefore limited, which will influence the design of the webs. For example, if the design required 25 suites at 15pF each, then either the total wire capacitance must be less than 25pF, or the length must be limited to ensure that this value is not exceeded. Ideally the capacitance of the wire should be chosen that minimises its impact on the suite design. Possible configurations of sensor suites will be discussed in section 9.5.2.

As the chosen microcontrollers have I2C capability, a separate communications subsystem is not required on the suites within the web. This reduces the number of layers that will be required in the 3d stack and the number of components within the suite, which will reduce the complexity of fabrication, the mass of the suite and the power it consumes. There will however be the additional mass of the wire to consider, which therefore must be as lightweight as possible. The issue of the possible tangling of the wires will also have to be addressed when deciding on a configuration. It may be necessary to have a mechanism to ensure correct deployment.

Each I2C bus will have to have a Master suite as well as Slave suites to gather the data. A useful feature of the I2C bus is that any suite can be a Master, and a Slave can be changed to a Master if required. This gives the bus flexibility and also provides

redundancy in case any of the suites are damaged or the wires are broken. In addition, the Master suite will have some form of external communication system.

Although a wireless system could have been chosen, a system where there are wired connections is considered to be the preferred option for this application. A wireless network would have been simulated in a similar way to the individual squares, since they are essentially randomly distributed suites that form ad-hoc networks. The simulation shows that this is an effective strategy for locating smaller targets or random sensing over a large area. This particular application, however, involves finding larger target areas and monitoring the growth patterns of smaller targets over time. The simulation suggests that a cluster of sensor suites that collectively cover a greater area is preferable. The principle advantage of the web configuration is its spatial definition. With a wireless network, each suite must identify both its overall position and its position in relation to the other sensor suites in order to achieve accurate spatial measurements. This adds a further degree of complexity to the system. With the wired option, each suite is a predefined distance away from its neighbour, or within a finite range, so that only the central suite needs to recognise its location. There is some uncertainty as to whether the wires have deployed straight, however the relative position is still better defined than a completely random system.

Another advantage to using the I2C wired bus for this application is added system flexibility. The I2C protocol is a well established off-the-shelf protocol, and many pieces of hardware are commercially available that have been designed to use this software. If additional environmental characteristics were to be measured, a suite could be removed from the bus and replaced by an I2C compatible sensor that could report its data to the Master suite. This enhances the generic nature of the system design and increases its potential applications.

The next section investigates possible web configurations with regards to their shape and the number of sensor suites on each bus. The possibility of multiple buses will also be discussed.

9.5.2 Possible web formations

In order to maximise the capacity of the I2C bus, a wire a low capacitance must be used. Since part of the brief of this project is to use COTS components wherever possible, an example of commercially available low capacitance twisted pair cable, with a given capacitance of 41 pF per metre, has been used as a basis for this investigation into a variety of web formations. Since the bus uses 3 wires, or two pairs, the given capacitance should be doubled when calculating the capacitance of the bus at a certain length.

The Total Capacitance, C_{total}, of the bus can be modelled by the formula:

$$C_{total} = NC_{node} + 2lC_l$$

where N is the number of Sensor nodes, C_{node} is the capacitance of the individual Sensor node, l is the length of the bus and C_l is the Capacitance per unit length of the wire.

This can be rearranged to find the maximum number of nodes per bus for a given wire capacitance:

$$N = \frac{C_{total} - 2lC_l}{C_{node}}$$

and is plotted as a graph in Figure 9-6. The graph assumes that l = 0.5m, and C_{total} = 400pF. The two lines represent the assumed boundaries of the node capacitance, C_{node} = 15pF and C_{node}=10pF.

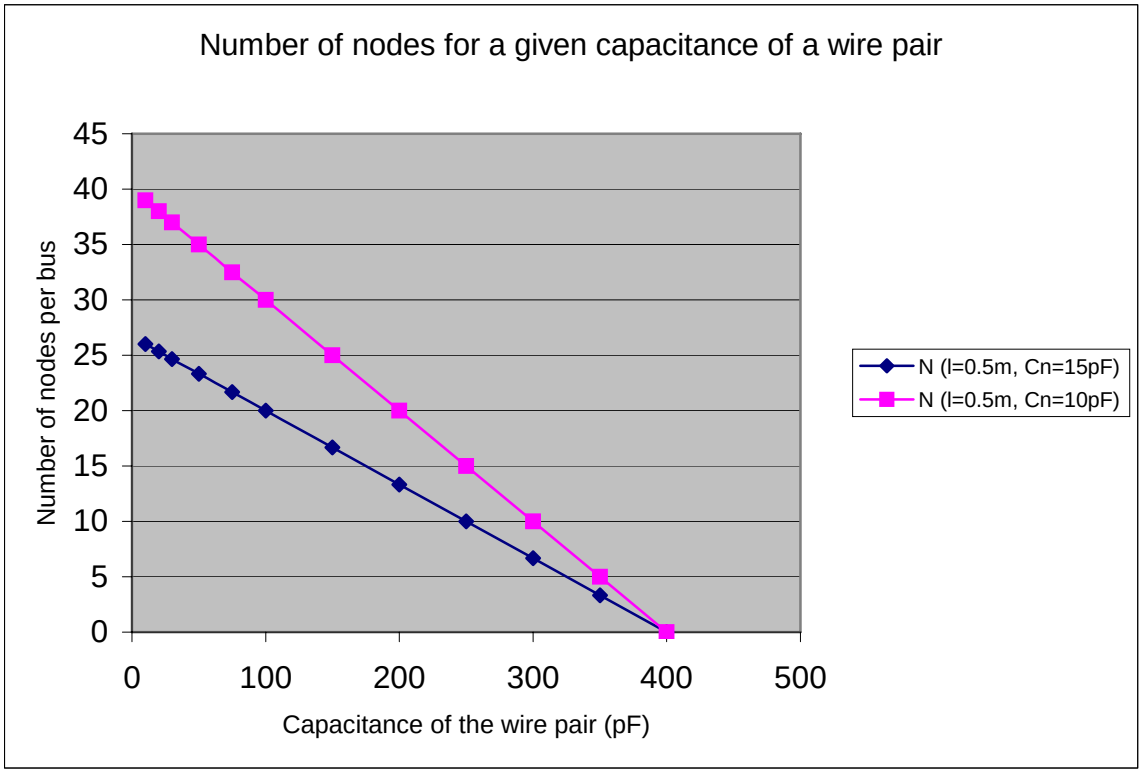

Figure 9-6 Graph showing the number of Sensor nodes per bus in relation to the capacitance of the wire.

The graph shows that the maximum number of nodes for the standard 41pF cable is between 24 and 36. The graph also shows that for the 15pF nodes, the difference between the number of nodes for a 10pF cable and a 50pF cable is only 3 nodes for a 50cm bus. This means that below 50pF, the reduction in the wire capacitance will not have a significant effect on the number of devices allowable by the I2C bus specifications, and therefore there will be little to gain from using an expensive specialist very low capacity wire when a standard 41pF wire may be sufficient.

9.5.2.1 Web Configurations

The following suite configurations are based on the higher node capacitance. Figure 9-7 shows a straight 50cm bus with even spacing between both 24 devices or 8 suites.

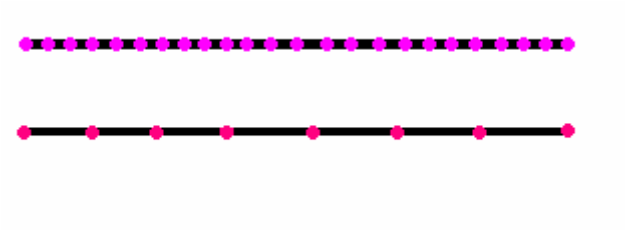

Figure 9-7 Straight 50 cm bus with either 24 devices or 8 sensor suites

Another option is to have a longer bus length with fewer devices in a "spiral" formation of diameter 50 cm. This design would require "spokes" in order to keep the wire in formation, as shown in Figure 9-8.

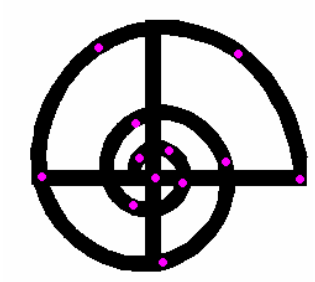

Figure 9-8 "Spiral" formation of sensor web

The diagram shows 12 devices attached to the bus. At a bus length of 2.5m, the total bus capacitance is 385 pF. The devices could either be evenly spaced at approximately 20 cm, or unevenly spaced with the suites in the centre closer together in order to give more coverage of the early growth of a Cryoconite. This assumes that the web can be deployed accurately onto the centre of the target.

One way to increase the number of suites in the web is to use multiple I2C buses. Each bus has its own Master, which is itself connected via a separate bus to a central suite with external communication capability. Two possible configurations for this are a square grid or concentric circles.

Figure 9-9 shows one possible grid configuration. This comprises 5 horizontal buses of 50 cm length with 5 sensors at regular intervals. The vertical wires are there for structure, apart from the central wire (yellow) that connects the 5 Master suites (blue) together. The "external" suite is in the centre coloured green.

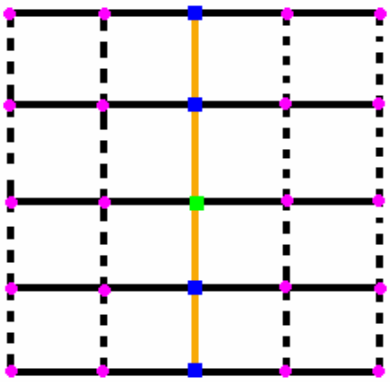

Figure 9-9 50 cm square grid configuration

Using standard low capacitance wire, each bus has a capacitance of 116 pF. A total of 5m of wire is used.

The concentric circle, or traditional "spider's web" approach is essentially 5 circular buses of 10cm, 20cm, 30cm, 40cm and 50cm diameter. These are then connected with 5 spokes of 25 cm length, one of which connects the Masters to the centre. The total amount of wire used is 6m. The length of each bus and its capacitance using the standard low capacitance wire is shown in the table below.

Diameter of Circle (cm)	Circumference of Circle (cm)	Capacitance (pF)
10	31.4	26
20	62.8	52
30	94.2	78
40	125.6	102
50	157.1	129

Table 9-4 Length of bus and capacitances for circles of varying diameter

The maximum number of devices on the largest circle can be 18, giving a total bus capacitance of 399 pF. There are several configurations of suites that can be used with this web concept. Two of the possible strategies are:

- a fixed number of suites per bus
- a fixed distance between each suite on each bus, and varying the number of suites accordingly.

For the fixed number of suites concept, two examples are discussed. The first uses 5 per bus and the second uses 8 per bus. These are shown in the diagrams below.

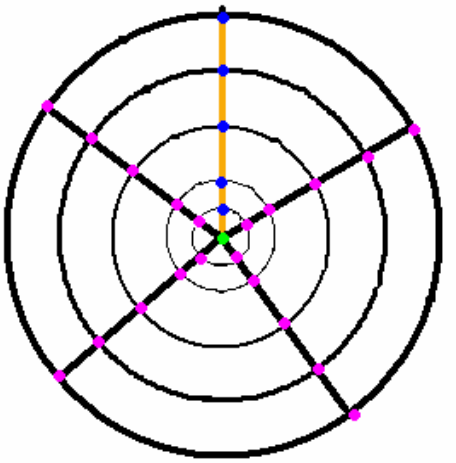

Figure 9-10 5 Suites per bus using circular web design

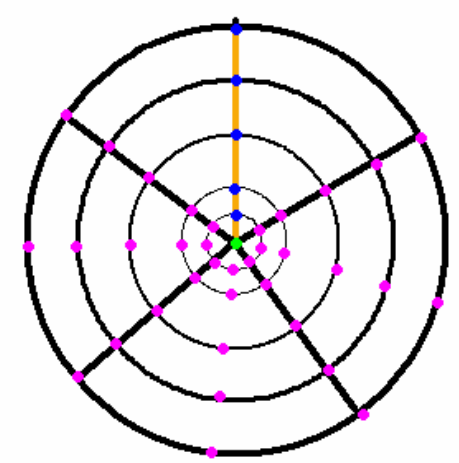

Figure 9-11 8 suites per bus using circular web design

Figure 9-10 shows 5 suites per bus, plus the central Master, positioned at the joins with the spokes. This uses a total of 26 suites. This particular design can be used in two ways; circular buses connected be structural spokes or straight buses connected by a structural circle. In the second way, fewer circles – one with 10 cm diameter and one with 50 cm diameter for example, and therefore less wire would be necessary, reducing the mass and complexity of the design Figure 9-11 shows the design with 8 suites per circular bus. This uses a total of 41 suites and has them positioned at the spokes and at equal distances between them. As this design has double the number of suites, it will give better sensor coverage of the area, however it will have more mass.

The other option for the circular bus is to have fixed distances between the suites. The example shown in Figure 9-1 has one suite approximately every 10 cm. This means that given the circumferences from Table 9-4, bus 1 would have 3 suites, bus 2 has 6 suites bus 3 has 9 suites, bus 4 has 12 suites and bus 5 has 15 suites. Where there are more than 8 suites, separate buses will be linked together via two masters to form the necessary circumference. These values have been rounded down, since the bus lengths

are not in multiples of 10 cm, so the extra length will have to be factored into any calculations. This configuration has a total of 47 sensor suites.

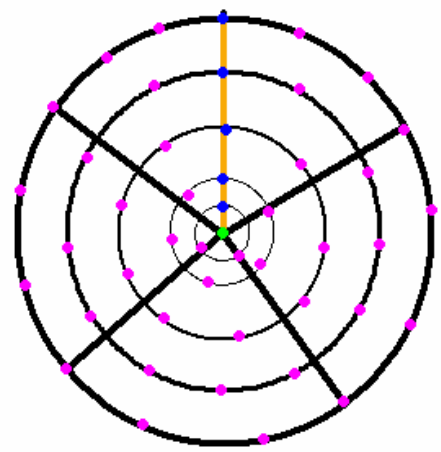

Figure 9-12. Circular bus with suites 10 cm apart

Table 9-5 compares the bus capacitance, the total number of sensors and the total length of wire required for all of the seven designed discussed.

Configuration	Bus length (m)	Area (m^2)	Capacitance of wire (pF)	Number of Sensor Suites	Total Bus Capacitance (pF)	Total length of wire (m)
String	0.50	0.005	41	24	401	0.5
Spiral	2.5	0.196	205	12	385	2.5
Grid	0.50	0.25	41	5	116	5
Circle (5)	1) 0.314	0.0079	26	5	101	
	2) 0.628	0.031	52	5	127	
	3) 0.942	0.071	78	5	153	5.96
	4) 1.256	0.126	102	5	177	
	5) 1.571	0.196	129	5	204	
Circle (10)	1) 0.314	0.0079	26	10	176	
	2) 0.628	0.031	52	10	202	
	3) 0.942	0.071	78	10	228	5.96
	4) 1.256	0.126	102	10	252	
	5) 1.571	0.196	129	10	279	
Circle (straight bus)	0.25	0.0025	21	5	96	3.135
Circle (10cm)	1) 0.314	0.0079	26	3	41	
	2) 0.628	0.031	52	6	142	
	3) 0.942	0.071	78	9	213	5.96
	4) 1.256	0.126	102	12	282	
	5) 1.571	0.196	129	15	354	

Table 9-5 Comparison of various web configurations

In addition to using this information, visual representations of the coverage over an example Cryoconite and practical simulations of the sensor suite configurations will be

used to select the preferred sensor web design. In each case, one suite within each web will have to become a devoted external communications suite.

9.5.2.2 Visual inspection of the web designs

The diagrams from this section have been superimposed over one of the photos of Arctic Cryoconites. It is assumed that the individual Cryoconites in the photo are relatively small but that the diameter of the group at the widest point is 50 cm. The largest of the group is considered to be Hole 1, with the other three smaller holes numbered clockwise. A comparison of the coverage and effectiveness of each configuration is then made.

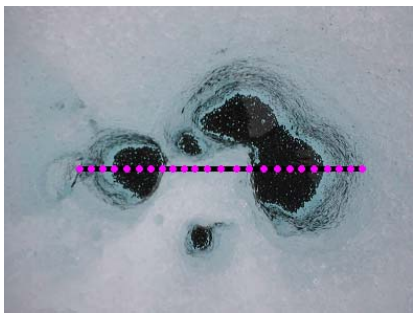

Figure 9-13a Straight 50 cm bus, 24 Suites

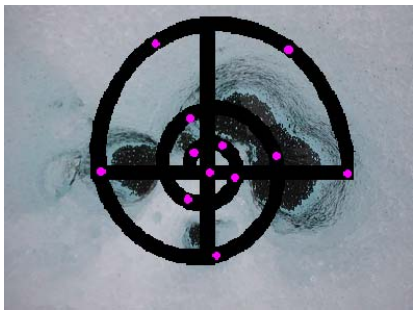

Figure 9-13b Spiral 2.5m bus, 12 Suites

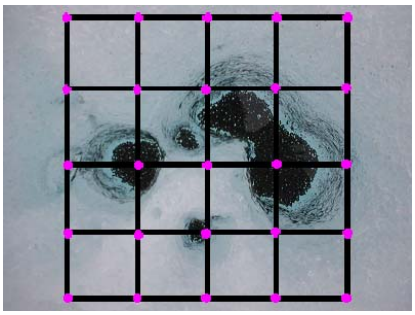

Figure 9-13c Grid of 5 50cm buses, 25 Suites

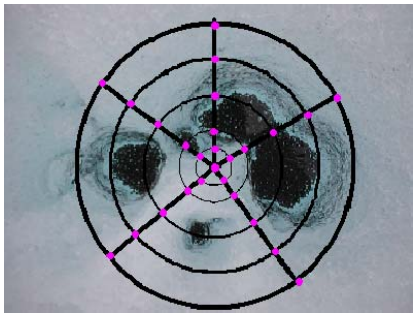

Figure 9-13d Web of 5 varying buses, 26 Suites

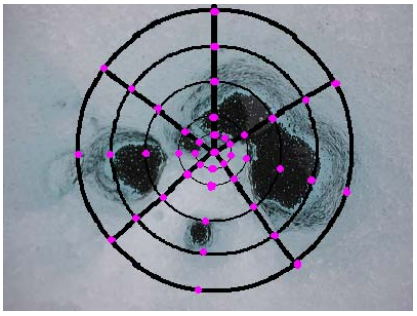

Figure 9-13e Web of 5 varying buses, 41 Suites

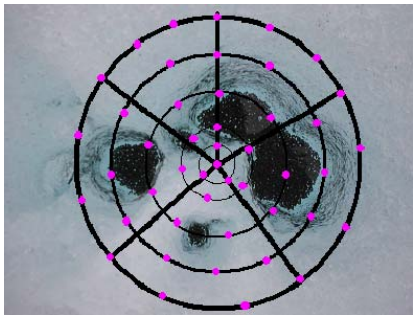

Figure 9-13f Web of 5 varying buses, 47 suites evenly spaced.

Formation	Hole 1	Hole 2	Hole 3	Hole 4
a	✓	X	✓	X
b	✓	✓	✓	✓
c	✓	✓	✓	X
d	✓	X	X	✓
e	✓	✓	✓	✓
f	✓	X	✓	✓

Table 9-6 Successful location of each example Cryoconite hole for each suite formation

Formation	Advantages	Disadvantages
a	❖ Highest percentage of suites finding target. ❖ Able to monitor growth in hole diameter over time.	❖ Unable to show shape of hole. ❖ Cannot detect off-axis holes.
b	❖ At least one suite in contact with or near to all four holes.	❖ Not enough suites to discern overall shape.
c	❖ Known spacing between suites gives indication of the size of the hole and the distance between smaller groups.	❖ Known spacing only if grid deploys with all the wires straight.
d	❖ Relatively low number of suites, which reduces overall mass.	❖ Lowest number of successful hits. ❖ Not enough suites to determine hole shape. ❖ Success dependant on landing orientation.
e	❖ All four holes are located	❖ Success dependant on landing orientation. ❖ Highest number of suites, therefore most mass
f	❖ Not dependant on orientation. ❖ Known space between suites for sizing holes.	❖ Relatively high number of suites.

Table 9-7 Advantages and Disadvantages of the web formations based on visual inspection.

Table 9-7 discusses the advantages and disadvantages of the different web configurations. Formation e. has suites on all four Cryoconites and appears to be the most successful configuration out of the six compared. However the final configuration, f, also has a good success rate and, due to the even spacing between the suites, is not dependant on the position in which it is deployed, unlike e. This formation can also give an indication of the size and growth of the hole as the distances

between the suites is known. This is a useful feature of this design. In this example, configuration f has the highest number of suites which is also an advantage over the other designs, however the even spacing is still the most significant benefit of the design, even if the number of suites is reduced. From the visual inspection, the evenly spaced suites on buses of varying lengths, figure 9-13f, is the preferred option.

9.5.2.3 Physical simulation of possible web designs

In order to do a physical simulation, models of three configurations were produced using Lego® bricks and flexible wire. The bricks are approximately the same size as the potential sensor suite, and the lengths of wire were cut to the same lengths as the buses discussed earlier. The three configurations produced were the evenly spaced web (Figure 9-14a), the grid (Figure 9-14b) and the spiral (Figure 9-14c). These pictures show the ideal deployed shape of the webs.

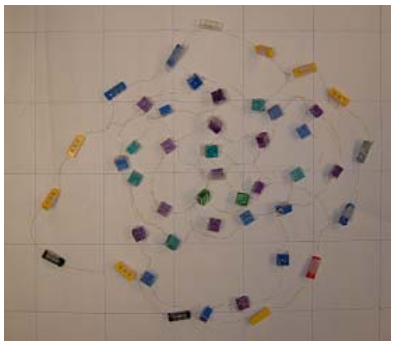

Figure 9-14a Lego® web

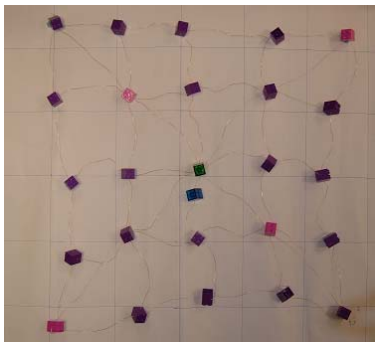

Figure 9-14b Lego® grid

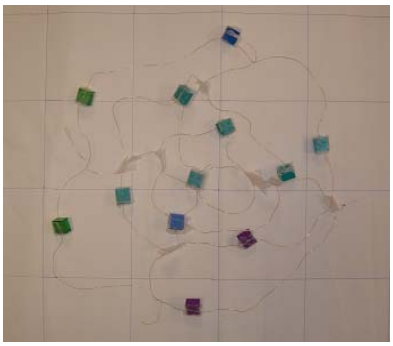

Figure 9-14c Lego® spiral

To simulate deployment, drop tests were done for each of the configurations from a height of 2m. Although not at deployment altitude, these drop tests are a simple way to identify and illustrate some of the basic issues related to aerial web deployment. All three designs were held by the centre suite then released. The spiral design maintained its shape well over the five consecutive drops. The web also retained its original shape, however care would have to be taken that the spokes were well secured and that the different layers did not become tangled and cross over. The grid configuration was the least successful of the drop tests. The wire was not rigid enough to deploy straight lines and the corners of the grid had a tendency to fold upon impact. The design also became tangled more frequently that the other two configurations. The wire used was more flexible than the low capacitance wire, however a mechanism would still need to be included to ensure that the lines of the grid deploy correctly. This adds to the complexity of the design and so is undesirable. Photographs were taken after each drop test, and examples of these are shown in figures 9-15a, 9-15b and 9-15c.

Figure 9-15a Dropped web

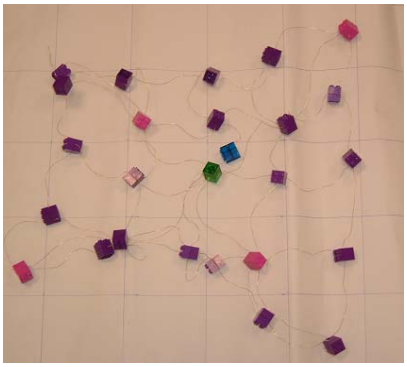

Figure 9-15b Dropped grid

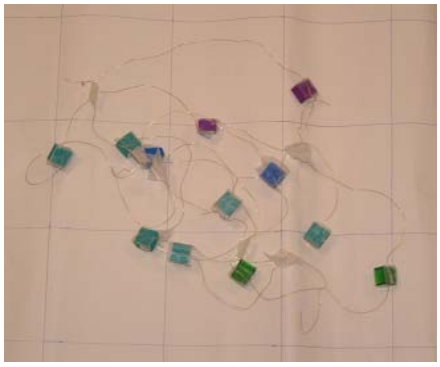

Figure 9-15c Dropped spiral

The results of both the visual inspection and the Lego® simulation conclude that the evenly spaced web is the optimum design for this application.

9.5.2.4 Wire capacitances, mass and resistance

The capacitance, mass and resistance of the bus wire are important parameters for the web. This section discusses the factors that influence the capacitance for a COTS low capacitance cable and for pairs of standard hook-up cable. The resistance and mass of the wires are calculated and a recommendation for the wire used in the sensor web is made.

When data is transmitted through a cable, the signal deteriorates. The amount of degradation depends on the data rate, the transmission distance, or length of cable, and the electrical characteristics of the cable, such as its impedance and its capacitance. The designers have specified that the most important characteristic for the I2C bus is its capacitance. The capacitance determines how much charge the cable is able to store, and can be calculated using the same principles as a parallel plate capacitor. The data is transmitted along the bus as a series of voltage pulses. If the bus cable consists of a twisted pair, as illustrated in Figure 9-16, the voltage charges the insulation surrounding the individual conductors. As in a capacitor, the cable takes time to reach saturation, which slows and interferes with the original voltage signal. This effect is particularly significant with higher frequency signals, and since the time taken is related to the capacitance, a low capacitance cable performs better. (Quabbin Wire & Cable, 1999)

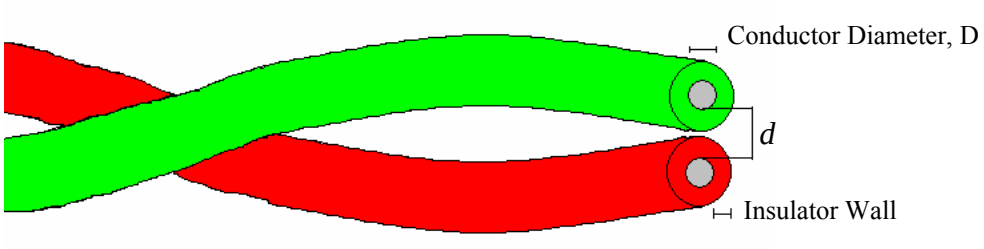

Figure 9-16 Representation of a Twisted Pair Cable

The equation for the capacitance of a parallel plate capacitor:

$$C = \frac{\varepsilon A}{d}$$

suggests three ways to minimise the capacitance of the cable, if it is assumed that the two conductors act as the two plates.

- Increase the insulation wall thickness, which increases the distance *d* between the two conductors
- Decrease the conductor diameter. The plate area, A, is approximately the product of the conductor's length and half its circumference ($\frac{\pi D}{2}$), as when calculating the area of a cylinder. Since the capacitance of wire is generally given per unit length, the diameter becomes the significant parameter and decreasing this will reduce the capacitance.
- Using an insulator with a low dielectric constant. The permittivity ε is given by $\varepsilon = K\varepsilon_0$ where ε_0 is the permittivity of free space and K is the dielectric constant. This varies according to the insulating material. Examples include PVC (K = 3.5 to 6.5), Polyethylene (K = 2.3) and Foam Polypropylene (K = 1.55). (Berk-Tek, 2002)

Whilst the parallel plate capacitance equation demonstrates the principles involved, a better approximation is given by the equation:

$$\frac{C}{L} = \pi\varepsilon\left[\cosh^{-1}\left(\frac{d}{D}\right)\right]^{-1}$$

This is the equation for the capacitance of an open-wire pair of transmission lines embedded in a material with dielectric constant ε. (Sander and Reed, 1978)
In this case:

$$\frac{C}{L} = \pi \times 4 \times 8.85 \times 10^{-12}\left[\cosh^{-1}\left(\frac{2\times(0.1524+0.511)\times10^{-3}}{0.511\times10^{-3}}\right)\right]^{-1} = 69.2\text{pFm}^{-1}$$

The given capacitance of 75.4 pFm^{-1} can be obtained if ε = 4.36 is used.

From the above equation, increasing the insulation thickness to 0.5mm gives a capacitance per meter of 54.2 pFm^{-1}. Similarly, if the calculation is made with a 28 AWG (= 0.321 mm) wire, the capacitance is reduced to 63.7 pFm^{-1}. If a Polyethylene insulator with a dielectric constant of 2.3 instead of the PVC insulator, the capacitance is reduced to 39.8 pFm^{-1}. The conductor diameter is generally dictated by the design of the circuit it is connected to, so its reduction potential is limited. Increasing the insulation thickness will increase the overall diameter of the cable, which in turn increases the mass, which is undesirable for this application. Therefore, the critical variable for a low capacitance cable is the insulation material.

Figure 9-17 shows another illustration of this finding. The capacitance was calculated for three different types of commercially available wire with varying conductor diameter. The first wire, available with conductors ranging from 24AWG to 30AWG, has a PVC insulator ($\varepsilon = 4.3$) of 0.41 mm thickness. The second has a 0.15mm thick Teflon ($\varepsilon = 2.1$) insulator, with conductors ranging from 24AWG to 32AWG. The final wire investigated had a 0.08mm Teflon insulator, with much thinner conductors ranging from 28AWG to 42AWG. The graph shows that the second wire exhibits the lowest range of capacitances. Although the conductor diameters are greater than the third wire, the additional distance between the conductors due to the thicker insulator, and the low dielectric constant reduces the capacitance by approximately $15pFm^{-1}$. This is equivalent to one extra suite per metre of cable.

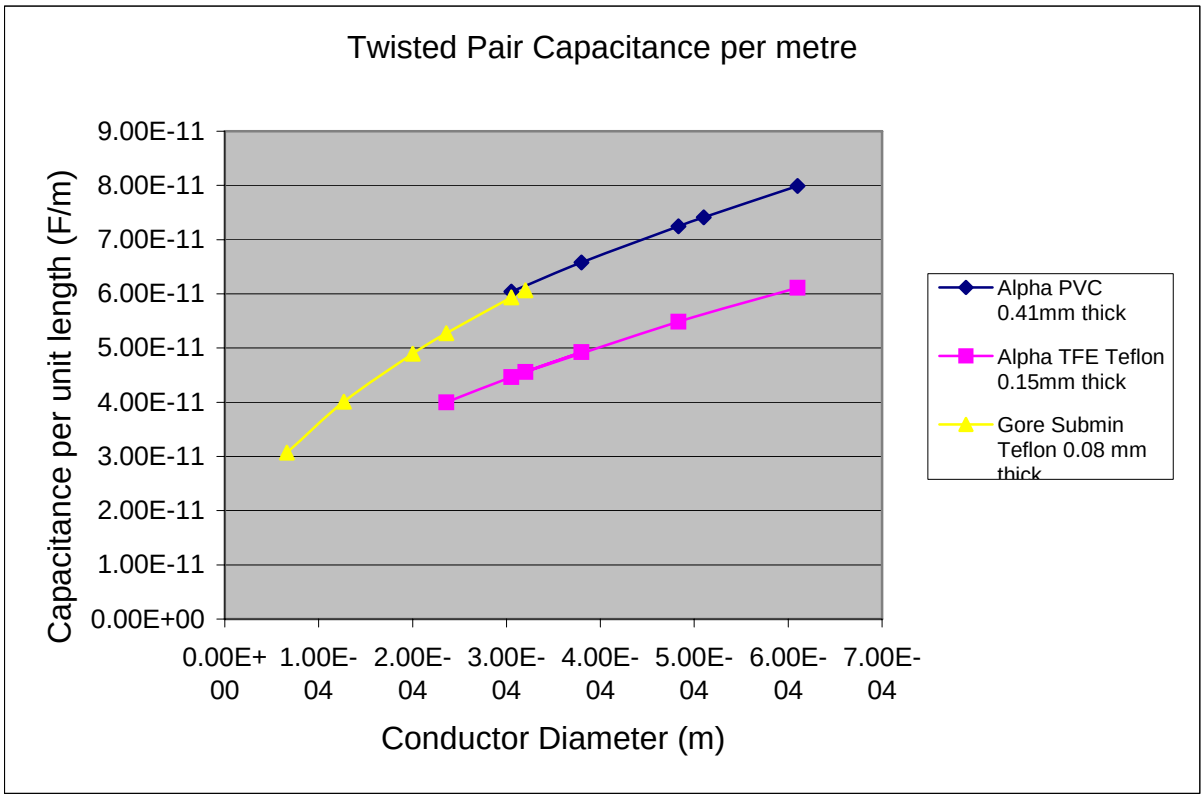

Figure 9-17 Graph of Twisted Pair capacitance per metre with respect to the conductor diameter.

The value for the capacitance of the wire used to investigate the possible web designs is based on low capacitance twisted pair computer cable. This type of cable is recommended for data transfer and digital audio applications. A specific example of cable with a nominal capacitance of 41pF/m (12.5 pF/ft) is Belden 9729 paired cable.(Belden Cable, 2003) The datasheet however raises other practical issues relating to the choice of wire, namely the diameter of the wire and its weight. The given overall diameter for a 2 twisted pair cable is 6.76mm. This is significant as the diameter of the suites is to be approximately 12mm. Most importantly the mass per unit length of the wire is calculated to be 51.3g/m. If the design requires 6m of wire, this will add an extra 308g to the overall mass of the system. As part of the system parameters are for a lightweight system, this is unacceptable. The additional mass of the wired system, as

opposed to a wireless one, must be minimised. Other types of cable were investigated and their capacitance, unit weight and diameter are listed in Table 9-8.

Manufacturer	Type	Capacitance (pF/m)	Weight (g/m)	Diameter (mm)	Weight of 6m (g)
ABE M13222[a]	4 conductor audio	108.2	32.7	4.60	196.2
ABE M39230[b]	2 pair foil shield	28.5	83.3	9.78	500
ABE 2424[c]	2 pair RS-232	39.4	34.2	5.33	205.2
Alpha Wire 58902[d]	2 pair Low capacitance	41 – 49.2	25.6	5.33	153.8
Belden 9729[e]	**2 twisted pairs**	**41**	**51.3**	**6.76**	**308**
Delco 30402[f]	2 Pair RS-422	41	87.8	8.51	526.8
Draka 21124[g]	2 twisted pairs	75.4	16.4	3.30	98.2
Quabbin 9604[h]	2 pair Cat 5 data cable	42.6	22.3	4.06	133.8
Quabbin 9464[h]	2 Pair Cat 5 data cable	50.8	23.8	4.45	142.8
Quabbin 5200[h]	2 Pair unshielded data cable	44.3	25.3	4.52	151.8
Quabbin 9304[h]	2 Pair Cat 3 data cable	62.3	14.9	3.38	89.4
Quabbin 9504[h]	2 Pair RS-422	50.8	41.7	4.85	250.2
Quabbin 8504[h]	2 Pair RS-232	45.9	40.2	5.94	241.2
Tensolite 26473[i]	4 conductor aerospace grade	29.5	41.7	4.95	250.2

[a] (Above Board Electronics, 1998a), [b] (Above Board Electronics, 1998b), [c] (Above Board Electronics, 1998c), [d](Alpha Wire , 2004) [e] (Belden Cable, 2003), [f] (Delcowire , 2004), [g] (Draka USA, 2004), [h] (Quabbin Wire & Cable Co., 1999), [i] (Tensolite, 2004).

Table 9-8 Characteristics of various cables (Listed Alphabetically)

The equation for the transmission lines is a good approximation for an unshielded cable. However many of the low capacitance cables investigated include a layer of shielding between the conductors and the jacket. The primary function of the shield is to limit signal interference from external sources. (Quabbin Wire & Cable, 1999) Repeating the calculation for the Shielded 24 AWG Alpha Wire cable (Alpha Wire , 2004) – with a Flourinated Ethylene Propylene (FEP, $\varepsilon = 2.1$ (Tillar Shugg, 1995)) insulator of diameter 0.3048 mm, gives a capacitance of:

$$\frac{C}{L} = \pi \times 8.85 \times 10^{-12} \times 2.1 \times \left[\cosh^{-1}\left(\frac{2 \times (0.511 + 0.3048) \times 10^{-3}}{0.511 \times 10^{-3}} \right) \right]^{-1} = 31.9 \text{pFm}^{-1}$$

Although the shield does not directly effect the areas between the two conductors, the results from using this equation with the data given for a shielded cable shows a discrepancy of approximately 10 pFm^{-1}. This is likely to be due to effects that the simple equation has not considered. A more accurate and complex method of calculating the mutual capacitance in a shielded twisted pair cable using conformal

mapping has been proposed by Gavrilakis *et al*. (2004) Their methods will not be analysed here, since the simple equation is adequate to demonstrate the principles.

The type of low capacitance cable considered so far has been designed for use in high speed data transmissions such as that used by Local Area Network cables. Therefore the design will have been optimised for that application. The speed of the data transmission between the suites will be much lower than that required in a standard computer network, and so ordinary electrical "hookup" wire may be sufficient to pass the data around the network.

The above theory can be applied to pairs of single wires in several ways. The capacitance of the uninsulated conductors with varying separation distances can be calculated. This assumes the dielectric constant of air, $\varepsilon = 1$. Also the capacitance of insulated wires can be calculated in the same way, assuming $\varepsilon = 1$ and that the effect of the insulation dielectric is negligible compared to the separation distance. This is illustrated in Figure 9-18. The smaller circles represent the conductors, and the larger circles represent the diameter of the conductor plus insulator. The capacitance of the bare conductors is shown in Figure 9-19, and the capacitance for different insulated wire is shown in Figure 9-20.

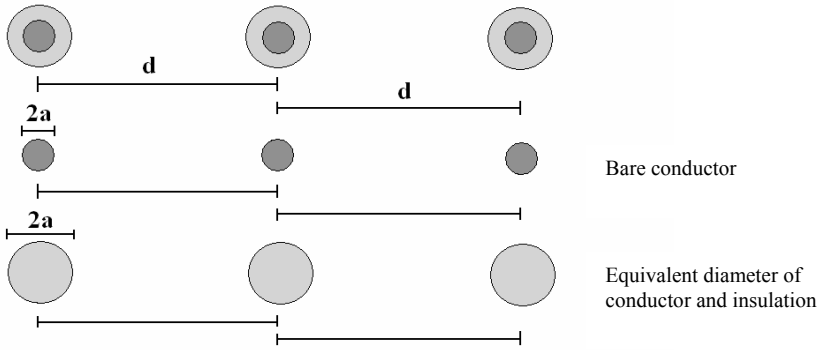

Figure 9-18 Illustration of the wire diameters used in an I2C bus, and the assumed diameters used to calculate the capacitance.

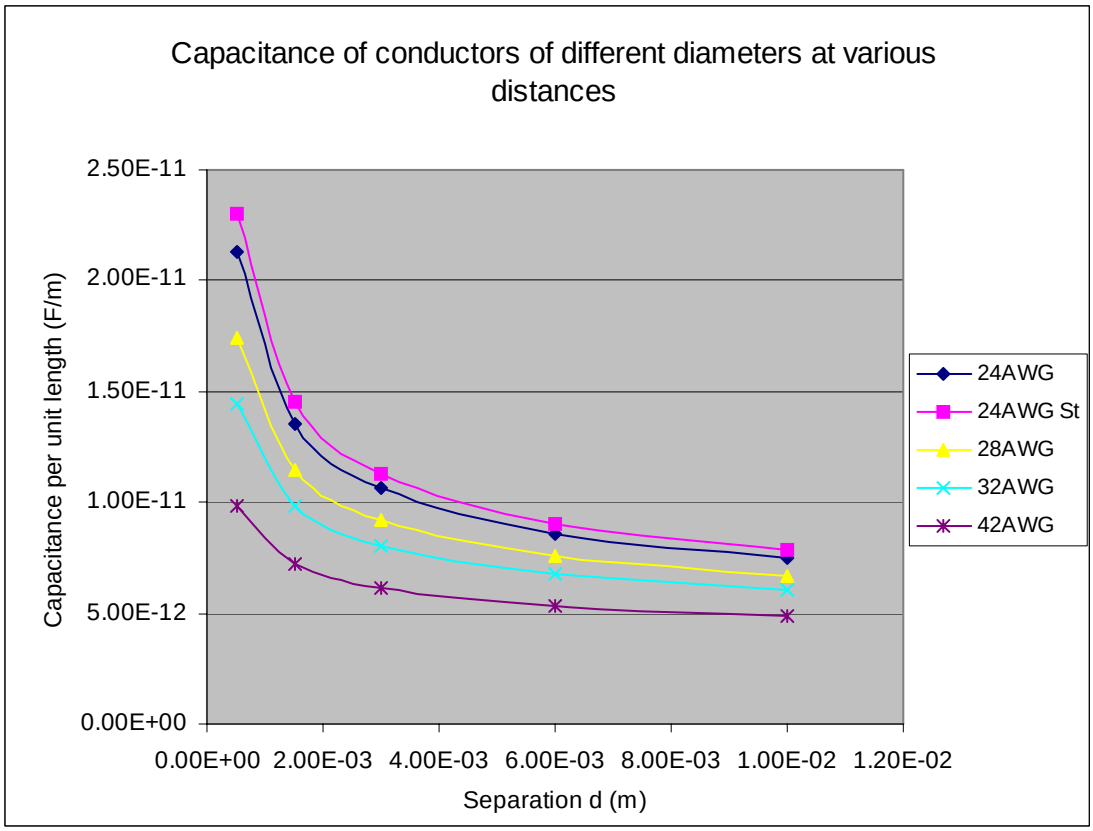

Figure 9-19 The capacitance of several bare conductors at various separation distances

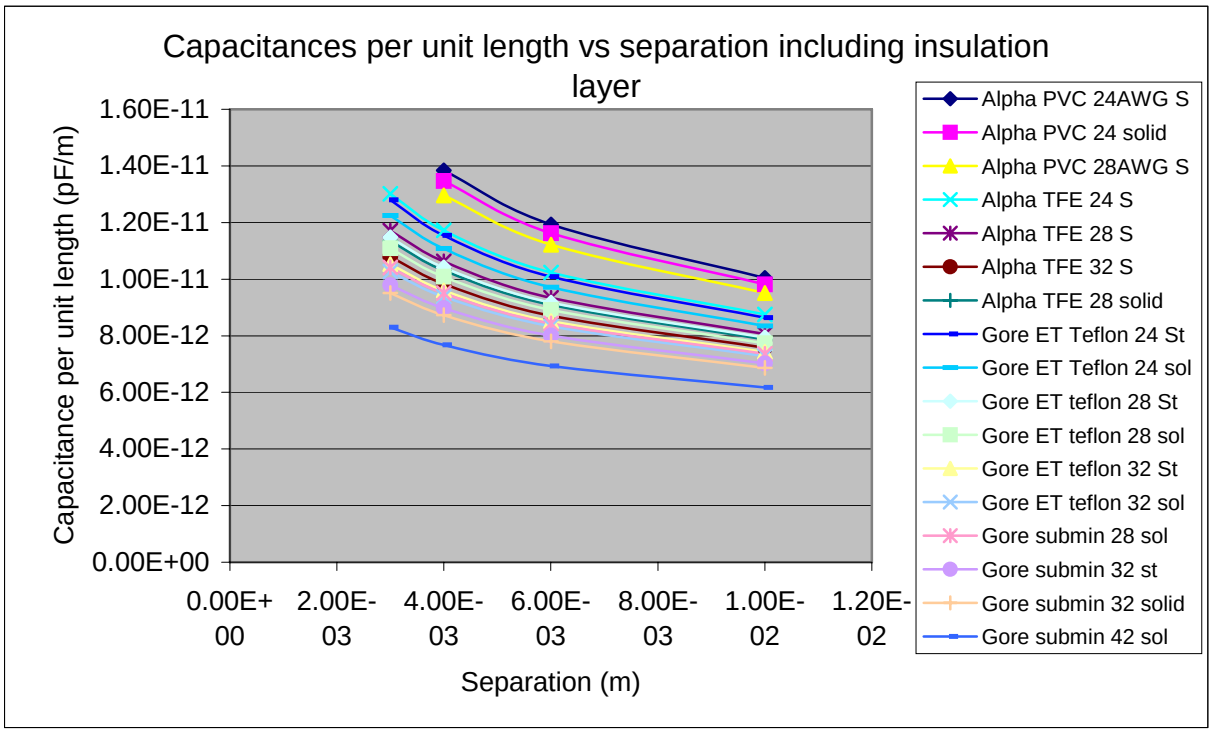

Figure 9-20 . Capacitance of insulated wires, assuming negligible insulation thickness in comparison with the separation distance.

In order to ascertain whether standard hookup wire could be used as an I2C bus, a test was performed using the I2C bus demonstrator connecting two desktop PCs, as described in chapter 5. The wires that connect the two boards are three 24AWG stranded wires with a PVC insulator that are approximately 85cm in length. The conductor diameter of the stranded wire was measured to be 0.61mm, and the insulator thickness was measured to be 0.41mm. The Dielectric constant for PVC is taken to be 4.3.

8 Bytes of data were successfully sent along this cable, where the clock speed of the bus was set to 90kHz. The cable was extended using 1m of identical cable and the test repeated. Again 8 bytes were successfully transmitted between the Master and Slave machines. Using the transmission line relationship, the capacitance of two pieces of this wire is calculated to be:

$$\frac{C}{L} = \pi \times 8.85 \times 10^{-12} \times 4.3 \left[\cosh^{-1} \left(\frac{\left(2 \times 0.41 \times 10^{-3}\right) + 0.61 \times 10^{-3}}{0.61 \times 10^{-3}} \right) \right]^{-1} = 79.9 \text{ pFm}^{-1}$$

This assumes the two wires are twisted together with no airgaps. Since there are three wires in this connection, the capacitance is assumed to be double that of the pair of wires, as shown in figure 9-17. This means that this 85cm bus would have a capacitance of 136pF if the three wires were tightly twisted together.

Theoretically, the maximum length of this bus should be 2.5m. However, a second test was made after extending the bus to 6m. The data was still successfully transmitted. This can be attributed to the fact that the wires are not tightly twisted, and there are gaps of up to 2cm between each pair of wires. The greater the distance between the wires, the lower the capacitance. Even when the 6m of wire were loosely twisted, there were still sufficient gaps to reduce the capacitance to an acceptable level.

The significance of the additional mass made to the system by the twisted pair cable was previously noted. A percentage of this can be attributed to the shielding and outside jacket. Simple calculations were made to determine the mass of the copper conductor and the insulation using their volumes and the density of the different materials, where:

$$Mass = Volume \times Density$$

Figure 9-21 shows the mass per metre with respect to the total diameter. The Total Mass line is a combination of the mass of the conductor and the mass of the insulation layer, and is plotted with respect to the total diameter.

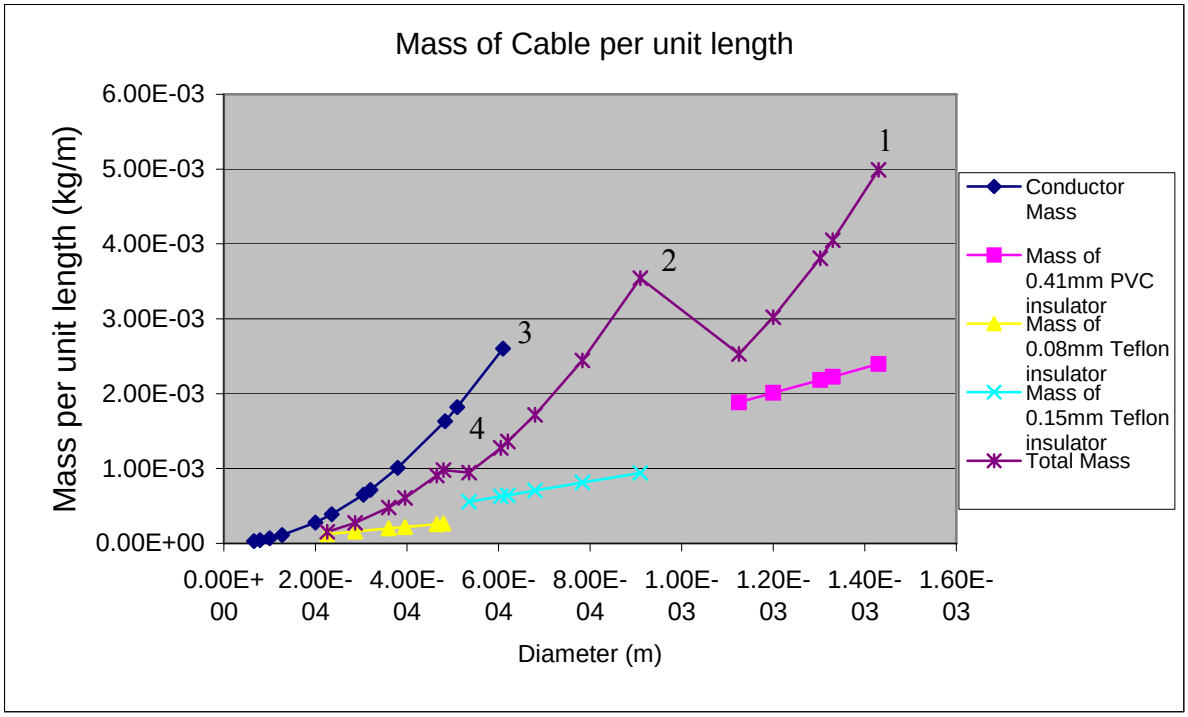

Figure 9-21 Graph showing the mass per unit length of wire with respect to its total diameter.

The calculations assume a copper conductor. Point 1 on the graph 1 corresponds to the mass of a 24AWG wire with a 0.41mm PVC insulation layer. This has a combined mass of 5g per metre. Although this appears to be low, when the mass of 6m of the three wires needed for the I2C bus, the wire adds an extra 90g to the system. The equivalent wire with a 0.15mm Teflon insulator adds 63g (point 2), whereas the bare conductor (point 3) adds 47g, which is approximately a factor of 2 less. The 32AWG 0.15mm Teflon insulated wire (point 4), which corresponds to the lowest twisted pair capacitance on Figure 9-20, has a mass of 0.945g per metre. This adds a total of 17g to the overall system. Although this is still significant in comparison with the ideal mass of the suites, this wire would be the preferred choice of those investigated, based on the mass. An Aluminium wire could also be used as a less massive alternative.

The other important factor to consider is the resistance of the wire. Ideally the resistance should be low so that the reduction in signal voltage, or noise level, is low and also that power dissipated as heat is as low as possible. Using the relationship:

$$R = \rho \frac{l}{A}$$

where ρ = resistivity of copper = 1.72 x 10-8 Ω, l is the length of the wire and A is the cross sectional area of the conductor.

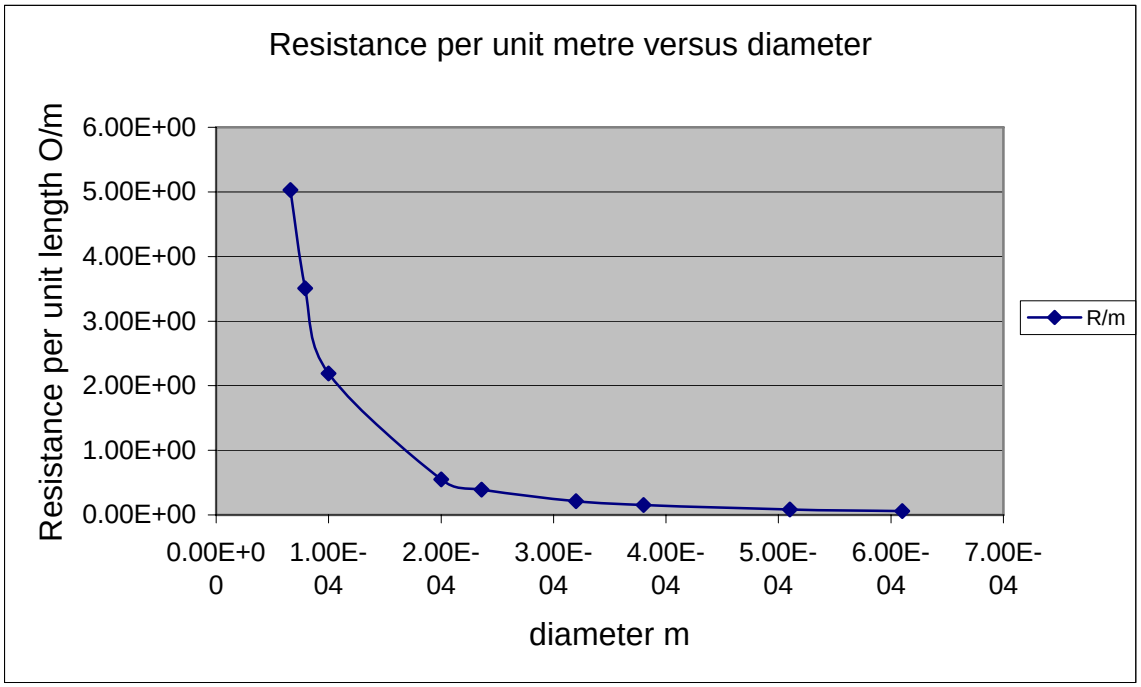

Figure 9-22 Graph showing resistance per metre of conductors with varying diameters

Figure 9-22 shows the Resistance per metre of copper conductors with varying diameters. It can be seen that conductors with a diameter less than 0.2mm have a much higher resistance than their larger counterparts. The resistance of the 0.2mm (or 32 AWG) copper conductor is 0.55 Ωm^{-1}. If the maximum current allowable by the bus is 3mA, the maximum signal voltage drop is 1.65mV. This compares with a resistance of $5\Omega m^{-1}$ for the 42AWG conductor, which gives a drop of 15mV. The power dissipated as heat from this conductor is also an order of magnitude higher than the 32 AWG wire.

9.5.3 Conclusions for the Sensor Clusters

Both visual inspections and physical simulations have shown that the best configuration of those considered for a cluster of sensor suites is web of 5 I2C buses with suites every 10cm along the bus, some of which may incorporate two linked I2C buses. This configuration:

- maintains its shape after deployment
- shows successful location of targets independent of orientation
- has a number of suites per bus which is independent of the capacitance since the length of the bus is predetermined.

The optimum cable type for this application has a diameter of 0.2mm (32AWG) and a 0.15mm Teflon insulation layer, or similar. This cable has a twisted pair capacitance of $40pFm^{-1}$, a resistance of $0.55\Omega m^{-1}$ and adds a total mass of 17g to the system. The use of single standard "hookup" wire is preferred to other commercially available data cables, since the high speed benefits of these types of cables is unnecessary for this application, and the shielding and outer jacket add extra mass to the system which can be omitted without loss to the internal communications.

9.5.4 Individual Sensor Suites

The simulation showed that randomly distributed single sensor suites were more successful at locating single cell targets. However, the hardware demonstrates that this would not be the case in this scenario.

The types of sensor included in the suite are most effective if in contact with the medium they are investigating. In this case, this means that to identify and monitor a cryoconite they would have to be deployed directly onto the target. This is due to the range of the sensors being insufficient to detect any subtle environmental changes over a larger distance. If the simulated single cell targets represent cryoconites that are less that 10 cm in diameter, there is very little margin of error in deployment, given the suite is designed to be 1 cm^2 in footprint area. These individual sensor suites are more suited to general surface sensing, however for the monitoring of specific targets in this application, the grid network of sensors is the more preferable option. Therefore this system will be solely comprised of the clusters of suites.

9.6 Specific Design Issues

This section describes the system overall design of the sensor suite web concept. The general overview of the system in terms of the Arctic Cryoconite monitoring application identifies several key areas, which are examined further in the subsequent subsections.

9.6.1 System design concept and identification of important factors

This system comprises two segments: the sensor suite webs and an airborne data gathering and deployment system. This is illustrated in Figure 9-23.

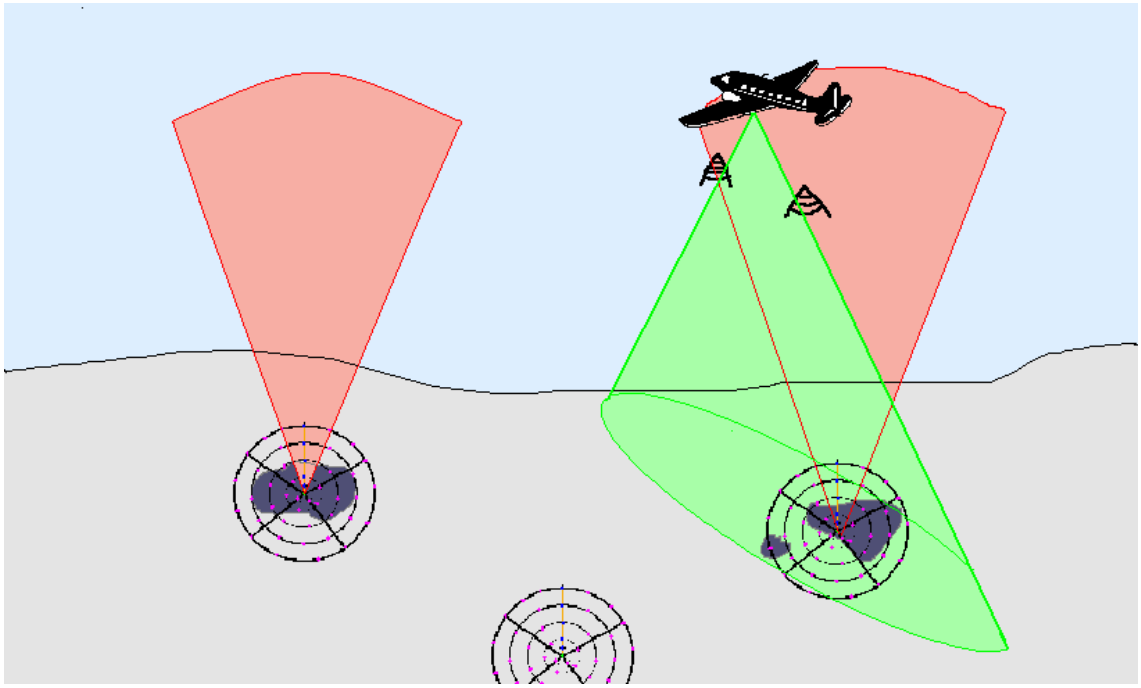

Figure 9-23 Sensor Suite Web system design concept

The sensor webs are of the concentric circle design with approximately 10cm between each sensor suite, as described in the previous section. Each sensor passes its data to a Master, which in turn passes the data to a central hub. Each sensor suite takes environmental data reading once every hour and passes a day's worth of data (24 hours) to the Master for processing. This central hub includes an external communications system comprising of a low power radio link to the data gatherer.

The airborne data gatherer is either an unmanned air vehicle (UAV) or a remote control aircraft. UAVs are already being used in the Polar regions for aerial environmental sensing. They offer established and complementary environmental measurement techniques to that of the proposed sensor web, as well as the ability to cover large areas.

This part of the system has two primary functions: to deploy the webs over the glacier and to collect the data. The aircraft will have to make several passes over the subject glacier, which will be in the order of square kilometres in area. The first will visually identify candidate Cryoconites where the webs will be dropped on the second pass.

Webs will also be dropped on clear areas to make control measurements and confirm that the webs themselves are not influencing the creation of Cryoconites. Since the cryoconites are formed by dark material heating areas of the ice, the webs should have a light colour to reduce the chance of creating a hole themselves. After the deployment, the aircraft will make further passes at weekly intervals, when the data from each central hub will be uploaded. At this time, aerial photographs of the subject glacier will also be taken to monitor the growth of the Cryoconites. Each suite will include an LED that will illuminate when the suite recognises that it is in contact with the Cryoconite. The periodic aerial photographs showing the illuminated sensors will provide a map of the field as well as monitor the growth over time of the holes as more LEDS are visible.

This system is effective in terms of both spatial and temporal measurements. The aerial segment will take global measurements of the glacial field and the *in-situ* sensor web will make local measurements. These measurements are also continuous to monitor small-scale developments, whereas the weekly aircraft pass records discrete changes over a longer period of time.

9.6.2 Data collection

The system requires two methods of data collection. Environmental data collected by the sensor suites is to be transmitted to a receiver located in the UAV using a radio link. The other method is a visual image of the field to compare discrete changes over time.

9.6.2.1 Environmental data collection

In order to select an appropriate external RF communications link, an estimate of the volume of data produced from each suite, and by each web, is required.

Each sensor reading produces 8 bits of data. The sensors make a total of 5 readings (Temperature, Pressure, Light, x-axis tilt and y-axis tilt) per cycle, plus an 8-bit identification tag. Therefore each cycle produces 48 bits of data. Since conditions will not be changing rapidly, a cycle of readings will be taken once an hour, resulting in 24 cycles per day, producing 1152 bits per sensor suite. If each web consists of 46 suites, each web produces 52992 bits per day. If data collection passes of the UAV are made once a week, each web will have collected 363 kbits of data, assuming that all of the raw data is transmitted and no data processing has been carried out.

If all of the web's data is passed to one Master suite, that will require additional memory to store each day's data. Microchip produce a range of serial EEPROM electronically erasable memory chips that can be included in the Master suite. The 24xx512 range (Microchip Inc, 2003a) can store up to 512 kbits and is I2C compatible, which means that the data can be passed directly from the bus to the memory. This chip will draw its own current from the system, however it does have a low power stand-by mode when it is not needed to be operational.

The rate that data can be transmitted and the width of the antenna beam must be compatible with the aerial collector. The typical speed of a UAV is approximately $20ms^{-1}$. This means that in 5 seconds the plane has travelled 100m. If the transmission data rate was such that it took 5 seconds for the 363 kbits to be transmitted, the beam of the antenna would have to be 100m wide so that the plane was in range of the signal for the required time. As with all the components, the transmitter module must be within the specified size limits, have low power consumption and be commercially available. Several miniature RF transmitters were analysed in terms of their data rate, range, electrical characteristics and physical size. These are illustrated in Table 9-9.

	Range	Data rate	Time to transmit 363 kbps	Equivalent distance covered by plane	Power		Frequency	Size mm
					V	I		
ABACOM AT-MT1-xxx[a]	91.44m (300ft)	2400 bps	155s	3000m	3.7V	7mA	418, 433.92, 916.5 MHz	14 x 10
ABACOM AM-TX1-4xx[b]	100m	2400 bps (1200 baud)	155s	3000m	2.5 – 12V	2.5mA	418 or 433 MHz	7.5 x 11.5
Linx TXM-xxx-LR[c]	914.4m (3000ft)	10000 bps	37s	740m	3V	5.1mA (5nA pd*)	315, 418, 433 MHz	9.15 x 12.7
Linx TXM-xxx-ES[d]	305m (1000ft)	56 kbps	6.5s	130m	3V	7mA (95μA pd)	916 MHz	16 x 13
BR-L-C30 Bluetooth[e]	10m	721 kbps	0.5s	10m	3.3V	60mA (2mA pd)	2.4 GHz	13.2 x 18.8
UltimateBlue SiW3000[f]	100m	721 kbps	0.5s	10m	3V	60mA (25μA pd)	2.4 GHz	6 x 6

* pd represents power down current

[a] (ABACOM Technologies, 2004b), [b] (ABACOM Technologies, 2004a), [c] (Linx Technologies, 2004), [d] (Linx Technologies, 2003), [e] (Blue Radios, 2004), [f] (RF Microdevices, 2004).

Table 9-9 Examples of miniature RF transmitter modules

Bluetooth (Bluetooth SIG, 2003) is currently a popular standard for wireless networking. As with the I2C bus, it is well documented and there are a wide variety of compatible components. The typical transmitted data rate is 720 kbps, but can transmit up to 1 Mbps. This standard was however designed for the wireless use of computer peripherals, and as such its initial specification had a range of only 10m. Transmitters are now available with a range of 100m, which would be more suited to this application. Although the data rate is considerably higher than any of the others featured in Table 9-9, the power drawn is an order of magnitude higher. Since the size of the suites makes them power-limited, this is a significant factor. Even though the higher draw

would only be for a fraction of the time, 10 seconds at 7mA is still more favourable than 3 seconds at 60mA. These time estimates include initialisation and response time between the transmitter and receiver.

Ideally, the transmitter should have a range in the order of kms, a data rate over 350 kbps and draw minimal power. It may be possible to specify these parameters and develop a bespoke transmitter module, however the design brief is to use COTS components. This therefore imposes limits on the system.

The Linx TXM-xxx-ES (Linx Technologies, 2003) is a frequency modulation FSK transmitter. It has a maximum data rate of 56 kbps and is capable of transmitting 1mW of signal power over 300m. The currently available module uses a frequency of 916.48 MHz and has an FM analogue bandwidth of 28 kHz. It is also a stand-alone chip, requiring no other external RF components except for an antenna. This reduces integration complexity. It is also has a range of compatible receivers. Like many of the transmitters, this model has a "power down" capability, essentially putting the chip into sleep mode until it is needed, which enables it to be used in low power situations. One drawback to this chip is that its given lowest operational temperature is 0˚C, meaning that in extreme temperatures the communications system will require extra insulation. Of those investigated, the Linx ES series is the most appropriate for this particular application.

An important part of the communications systems design is the choice of antenna. The recommended choice for transmissions at this frequency is the ¼ wave monopole antenna. The JJB Series from Antenna Factor (Antenna Factor, 2004) is a compact antenna designed for use at 916MHz. Although the overall length of the antenna is determined by its operational frequency, (Linx Technologies, 2003) in this case:

$$L = \frac{71.34}{F_{MHz}} = \frac{71.34}{916} = 0.078 \text{ m}$$

this type of antenna has been designed to have the same performance but in a 7mm diameter package, 16.6mm in length. A ¼ wave antenna has a half-power beam width typically between 45˚ and 360˚ (RF Cafe, 2004) and has a wide angled radiation pattern (Figure 9-23.), meaning that the beam angle can specified to enable the receiver to have maximum contact time with the data during its flyover.

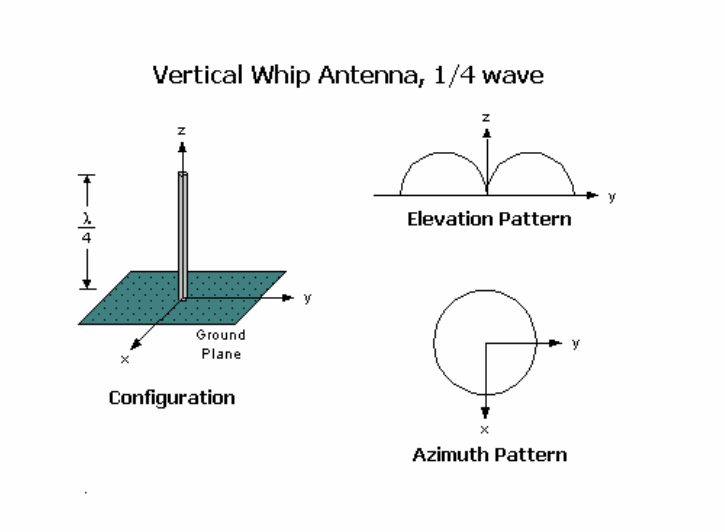

Figure 9-24 Radiation Pattern for a ¼ Wave Vertical Whip Antenna (RF Cafe, 2004)

Assuming that 10 seconds is required for a complete data transfer, if the receiver is travelling at 20ms^{-1} then the beam must have a width of at least 200m. As an approximate calculation, if the receiver is at a height of 300m, the beam angle must be at least 37˚. This is shown in figure 9-25. The wider angle of the antenna gives a margin for additional connection time, allow a higher velocity or enable the UAV to be flown at a lower altitude. A lower altitude would also reduce losses over distance.

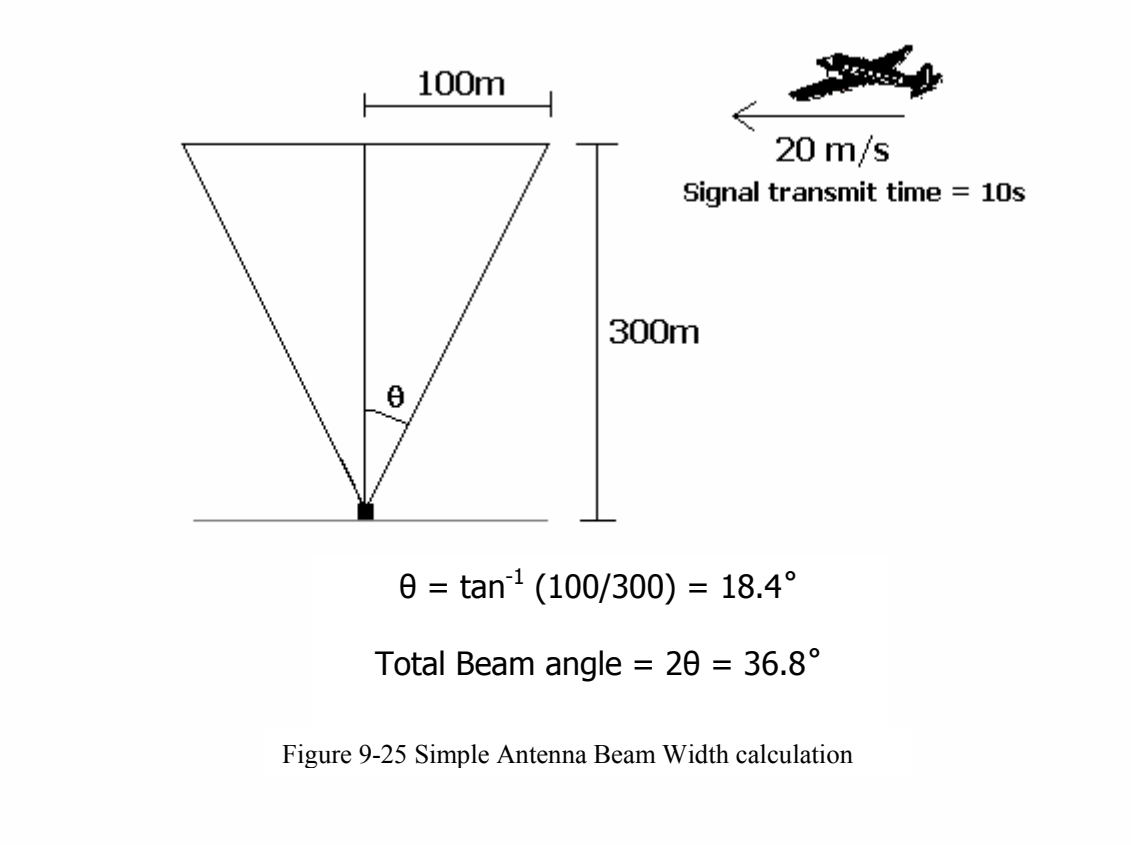

Figure 9-25 Simple Antenna Beam Width calculation

One feature of this type of antenna is that it must be deployed vertically compared to the ground plane. This will impact the overall of the system in that the suite housing the antenna must be vertical, or as near to vertical as the beam width will allow and still have adequate coverage.

9.6.2.2 Aerial platform

The aerial platform for the communication system is intended to be an Unmanned Aerial Vehicle (UAV). This platform will serve three key purposes:

- House the RF receiver to collect sensor data
- House an imager to take aerial photographs of the field
- Deploy the sensor webs to their chosen targets

There are many UAVs that are either in full commercial production or in the developmental phase. UAV forum (SRA International , 2005) provides a useful overview of current programmes, as well as descriptions of some of the aircraft and lists of vendors. The various specifications of these UAVs will not be discussed in detail here, however one example, Aerosonde (2000), will be taken as a representative vehicle of the type that would have to be used for this application.

The Aerosonde UAV (Figure 9-26) is a robotic aircraft that has been used for a range of meteorological observation purposes. It is a good example to use in this scenario, as it has been used successfully in Arctic conditions, and as such would not require modification to allow survival in extreme climates.

Figure 9-26 The Aerosonde UAV – a representative vehicle for the aerial communications subsystem (Aerosonde, 2000).

The vehicle has a wingspan of 2.9m and weighs 15kg. It has a cruising speed of between 80 and 150kph (22 and 42 ms^{-1}) and has a range of 3000km at an altitude of up to 7km. It is powered by a battery pack that provides enough power for approximately 1 hour. It also has the capacity to carry a payload of up to 5kg.

The vehicle is designed to make environmental observations, and as such houses its own air pressure, temperature and humidity sensors, and uses a UHF radio for communications. This means that is important to ensure that this signal operates on a different frequency to the sensor suite transmitters to avoid unnecessary interference. Its navigation utilises GPS, which would be useful in this case to reference where the subject glacier field is.

The 5kg payload would have to include the suite receiver, memory storage unit, antenna and associated electronics. The receiver module for the suites is assumed to be the equivalent Linx ES module connected to a microcontroller, battery and bank of memory. An omnidirectional antenna can be mounted horizontally onto the vehicle. The size of the antenna must be chosen and oriented as not to interfere with the aerodynamics of the vehicle. One possible example is a 2dBi antenna available from Phazar (2004) which is suitable for the 916MHz frequency range. This antenna is approximately 30cm long and weighs 227g. The camera for taking the aerial map and its relevant mechanisms also account for a proportion of the total payload mass. Miniature digital cameras are available commercially that weigh less than 50g, although at the expense of image resolution. From this it is reasonable to budget 500g for these aspects of the communications subsystem out of the total payload mass budget.

If the aerial platform is to be used to deploy the suites, the remaining payload mass budget will comprise the webs and the deployment system. The system will be discussed in section 9.6.3. Assuming that the deployment mechanism contributes no more than 500g to the mass total, this means that a total number of webs whose combined mass is no more than 4kg can be deployed. For example if each web has a mass of 200g, the total number of webs that can be deployed from this vehicle is 20. This places a limit on the number of webs in the overall system.

9.6.2.3 Aerial map

An aerial map of the glacier field taken once a week during the data collection fly-over will provide a discrete time-lapse view of the cryoconite growth as opposed to the continuous data collected by the *in-situ* sensors. Also an initial map is to be constructed to enable targeted deployment. Each suite is equipped with an LED, which is programmed to illuminate when the sensor data meets a predetermined criteria set to recognise that the suite is in contact with a cryoconite. The LEDs will aid visual recognition of the cryoconites and growth analysis of the digital images.

An optical system has been chosen for the imaging task over, for example a radar image, principally for ease of use. An optical image from a digital camera requires very little data processing and the data can be analysed quickly and simply. Also it is a cost effective system, since reasonably high resolution cameras are commercially available for relatively low cost. A radar system, especially an in-orbit system, would not be able to detect very small objects on the surface, whereas an optical system can resolve much smaller areas, such as those covered by the sensor webs, especially at the altitudes recommended by the transmitter ranges.

The key factors for this part of the system are:

- the area of the ground that the camera can see, which is related to the altitude of the vehicle.
- the image resolution and related camera choice.
- the number of pictures to be taken to enable coverage of the whole field.

9.6.2.3.1 Ground coverage area

The area of the ground that can be seen in one image is related to the camera's field of view angle and the altitude at which the images are being taken.

The field of view angle that has been assumed for this analysis is 73˚. This is a typical value, but is dependant on the type of lens. It is assumed that a circular lens produces a circular ground footprint, the diameter of which is related to the altitude as shown in figure 9-27.

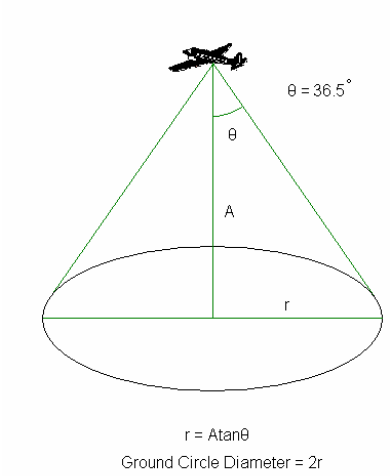

Figure 9-27 Ground circle diameter related to field of view angle and altitude.

For example, if the vehicle flys at an altitude of 300m, the radius of the ground circle is:

$$r = A\tan\theta = 300\tan 36.5 = 222\,\text{m}$$

This means that the ground circle has a diameter of 444m and covers an area of 0.15 km^2. Since the image itself is generally a rectangle of aspect ratio 4:3, it is assumed that to avoid any aberrations at the edges of the image, the image area is equivalent to the rectangle that fits inside the ground circle. This is illustrated in figure 9-28.

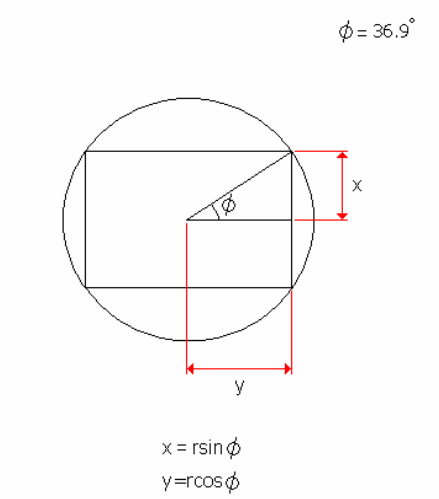

Figure 9-28 Calculation of size of the square area that fits inside the ground circle

In this example, r_{300} = 222m so:

$$x_{300} = r_{300} \sin 36.9 = 133.3\,\text{m}$$
$$y_{300} = r_{300} \cos 36.9 = 177.5\,\text{m}$$

This image therefore covers an area of 0.095km^2. The ground circle and image dimensions for various altitudes are shown in table 9-10.

Altitude A, (m)	Ground circle radius, r (m)	Image length, 2x (m)	Image length, 2y (m)
50	37	44.4	59.2
100	74	88.9	118.3
200	148	177.7	236.7
300	222	266.6	355.0
400	296	355.4	473.4
500	370	444.3	591.7
1000	740	888.6	1183.5

Table 9-10 Ground circle radius and image square length related to altitude.

This shows that, as expected, an image taken during a flyover at a higher altitude covers a larger area of the glacier field than those taken at a lower altitude. This area is significant when considering the minimum image resolution that is required to detect the cryoconites.

9.6.2.3.2 Image Quality and Pixel Number

The number of image pixels determines the size of object that can be distinctly seen by each pixel within the image area, assuming the field of view remains constant. An example of a camera with a low pixel number has an image area containing 640 x 480 pixels. This means that the image of a 20m x 15m area is divided in to 307200 pixels, each measuring an equivalent area of 3.125cm x 3.125cm. The same 20m x 15m area taken with a camera that has 3264 x 2448 pixels, gives an equivalent area per pixel of

0.61cm x 0.61cm. This means that the image is clearer and smaller objects can be clearly distinguished.

The specifications of several currently available digital cameras were investigated, with particular focus on the number of pixels, the mass of the camera and its dimensions. Images with a high number of pixels require a larger amount of memory to store them, since the file sizes are generally bigger. Whilst cameras with a lower number of pixels per image store the images on internal memory cards, which limits the number of images that can be taken, cameras with a higher number generally require additional memory cards. Those cards can store between 16MB and 1GB of data, which means the limit on the number of photos stored can be as high as is necessary. In general, the higher number of pixels per image, the larger and more massive the camera is. A camera whose images have a lower number of pixels can weigh as little as 36g, however the Canon 4992 x 3228 pixel camera weighs 1.5kg.

In this case, the image area is related to the altitude of the aerial vehicle, as described in the previous section. In order for the cryoconites to be seen on the initial pre-deployment flyover, and for a good visual image of the LEDs on the webs from subsequent passes, it is assumed that the equivalent pixel area must be approximately 10cm x 10cm. Figure 9-29 shows the relationship between the number of pixels and their equivalent length for varying altitudes. A line is also drawn at 10cm as the maximum desired length.

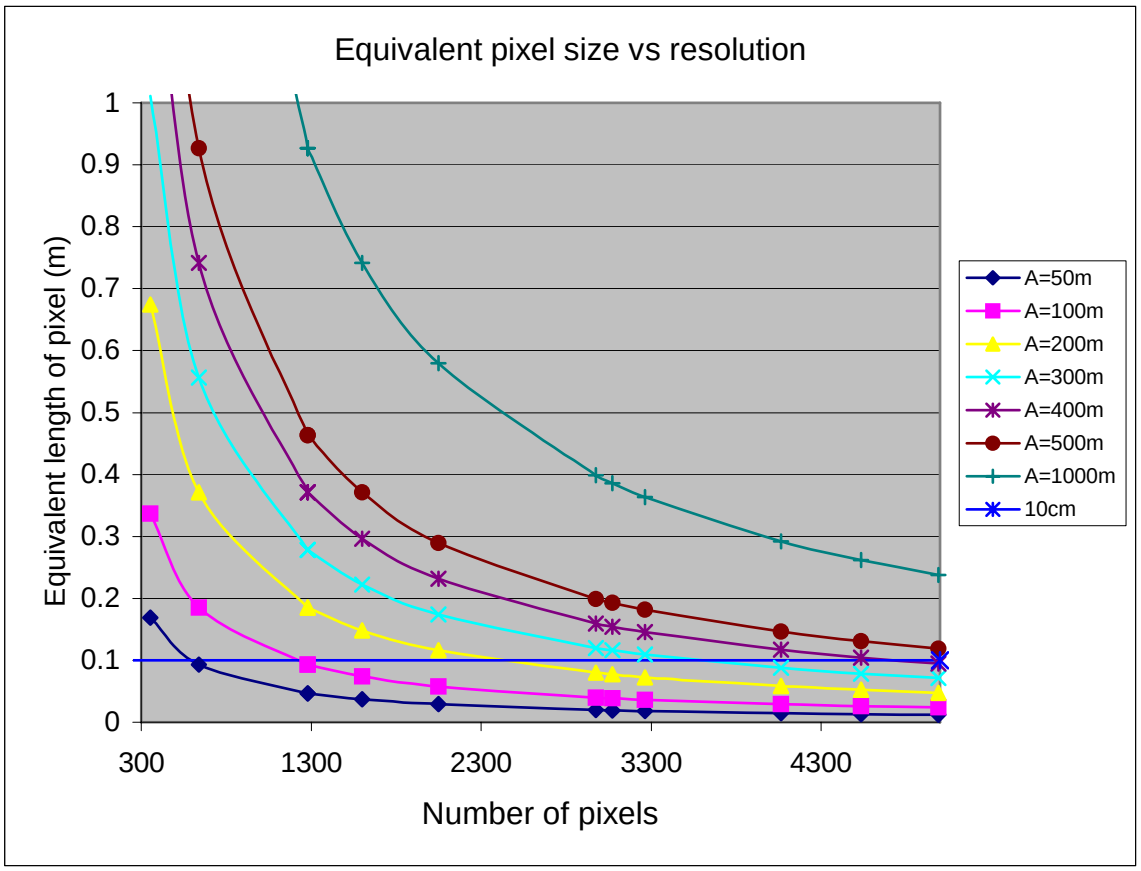

Figure 9-29 Graph showing the relationship between the equivalent pixel size and the number of image pixels for varying altitudes

It can be seen that in order to meet the minimum equivalent size criteria, a trade off has to be made between the altitude of the pass and number of pixels per image, and therefore mass, of the camera.

If the vehicle makes a data collection pass at 300m, or the maximum transmission range, the number of image pixels must be at least 3600 to be able to detect 10cm objects. This assumes a constant field of view of 266m x 355m as shown in Table 9-10. At this level, commercially available cameras tend to be designed for professional photographers, and therefore have many additional features, which in turn add mass to the camera. The Kodak DCS 14n for example, has a resolution of 4536 x 3024, which gives acceptable equivalent length (9cm x 9cm), has a mass of 1kg. This would constitute a considerable portion of the 5kg payload mass, without any additional mechanisms required to operate the camera. A smaller custom-made model with a high number of pixels per image would be possible, but this is not within the COTS remit.

At an altitude of 100m, this minimum becomes approximately 1200 pixels, however the field of view, and therefore the ground coverage per image, are reduced to 88m x 118m. The Casio Exilim EX-S20 has 1600x1200 pixels and has a mass of 100g. This would give a useful image at 100m (7cm), however at 300m the equivalent size becomes 22cm x 22cm, which would not give clear enough images of the cryoconites or the webs. At 200m, the requirement is 2400 pixels, which can be satisfied by the Pentax Optio S5i. This model has 2560x1920 (9.2cm equivalent length) and weighs 120g. Both of these models would be acceptable within the payload mass budget. It therefore appears that extract the maximum numbers of pixels per camera mass, the flyover altitude should be reduced to 200m or below. This would enable a clearer image of the field to be taken, as well as increasing the RF communications area, although the field of view captured by each image will be reduced. (All specifications are taken from Digital Photography Review (2005).)

9.6.2.3.3 Frequency of image capture

The frequency of which the images must be taken to ensure complete coverage of the subject field is also related to the altitude of the flyover.

At the assumed speed of $20ms^{-1}$, the air vehicle can cover a 1km distance in 50s. This does not change depending on the altitude. However, the camera will only see a 1km strip of the glacier. The width of that strip depends on the equivalent image area at the chosen altitude. This also determines to the number of images that are necessary to cover the whole glacier, and the number of passes, assuming that the first strip is covered by the first pass, the second strip is covered by the second pass, etc.

At an altitude of 200m, the shorter side of the image rectangle (2x) is of length 177.7m, therefore 5.6 (or 6 if rounded to the nearest whole image) photos would need to be taken

in order to image the whole 1km strip. This is illustrated in Figure 9-30.

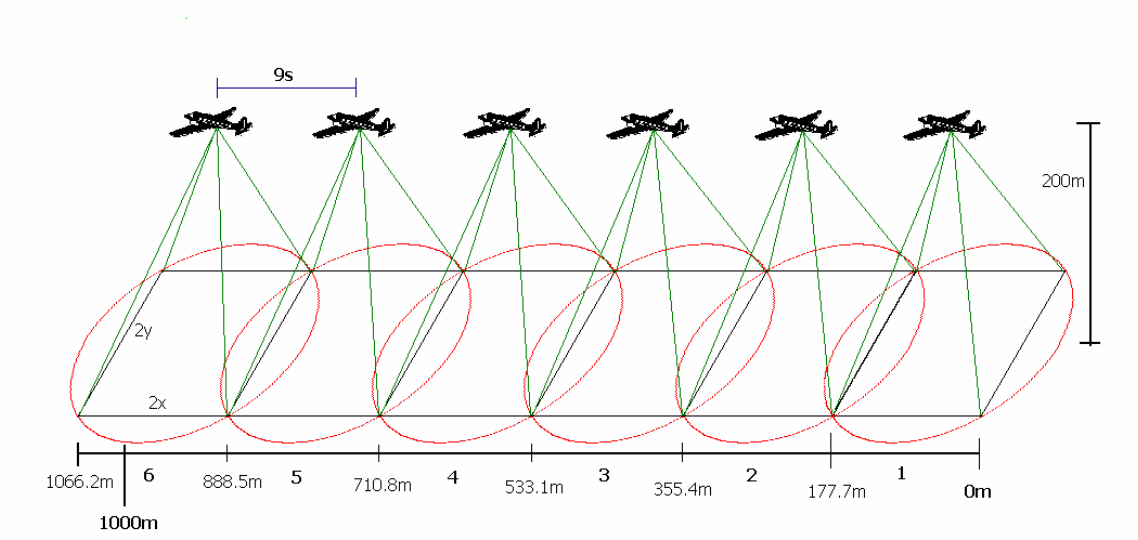

Figure 9-30 Representation of one flyover showing the number of images that would have to be taken to cover a 1km strip of glacier field.

Furthermore, 5 passes would have to be made to image the strips of length 2y = 236.7m that are needed to see the whole field. If the time taken to take 6 images is 53.3s, one picture would have to be taken every 9s. To cover the whole field, the flyover would need to last 266.5s, or 4 minutes 26s and at least 30 images would need to be taken. This is illustrated in Figure 9-31. The images would then be pieced together to form a map.

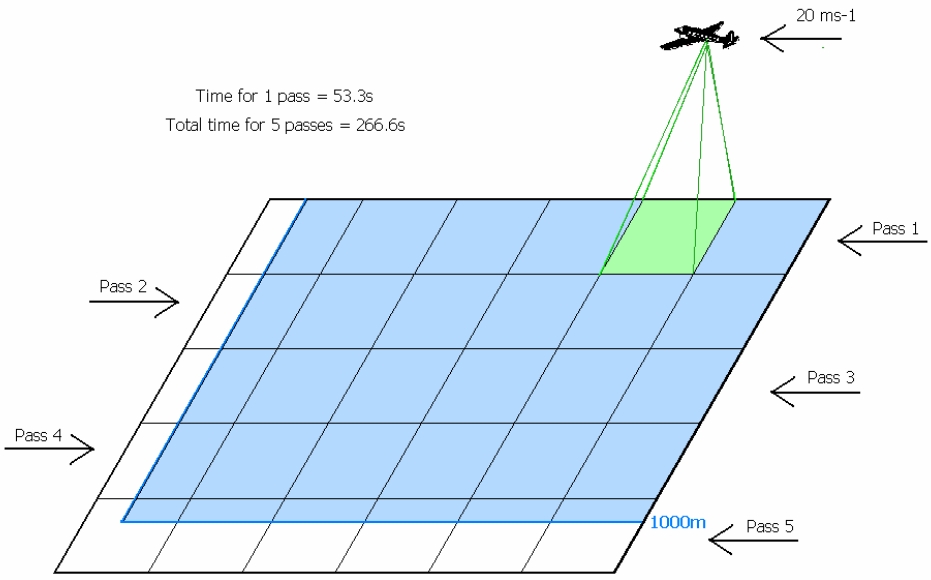

Figure 9-31 Illustration of the total number of passes and images required to image a 1km x 1km subject field.

At lower altitudes, although the equivalent pixel size is better, the image square is smaller. This means that more images are required per strip, and more passes are necessary to cover the field. For example, at 100m altitude, a 1km x 1km field would require 11.25 images per strip and 8.5 passes, this needs a total flight time of 480s, or 8 minutes and a minimum of 108 images. Therefore, a larger equivalent image area is preferred, which means the flyover altitude must be low enough to minimise the number of images, but high enough to have sufficient resolution.

9.6.2.4 Conclusions for communications subsystem

The baseline for the communications subsystem is shown in Table 9-11. This is information is divided into Ground section and Aerial section.

The results obtained in this section give an indication of the extent of the communications subsystem and the issues that will need to be addressed in its final design. The analysis done on the digital imaging system gives a good estimate for the type of camera system required, however further analysis would need to be done using the cameras specifics before integrating it into the aerial platform.

This specification assumes that no data processing is done within each suite, and that all the gathered data is transmitted to the receiver. This reduces the risk of missing a key finding due to having insufficient data. However, if each suite or web performed its own data processing, such as calculating average values between the suites or over the day, less data would need to be transmitted, therefore reducing the time taken per transmission and its related power input. Another possibility with data processing is programming the suite to transmit data only when the values are significantly different from a baseline. This would reduce the data stream, but at the expense of environmental data.

Ground Section			
		Specification	Comment
Number of bits of data produced per sensor suite		1152 bits per day	Based on 4 sensors reading at hourly intervals
Data produced per web in one data collection period		363 kbits per week	46 suites per web
External Communications Suite			
Transmitter		Linx TMX-xxx-ES	example
	Power	7mA @ 3V 95µA @ 3V (power down)	Full power if transmitting, or in a power down mode.
	Data Rate	56 kbps	
	Frequency	916MHz	Specified by transmitter
	Range	up to 300m	
	Transmission power	1mW	
	Transmission Time	6.5s + initialisation time	
Suite Antenna		JJB ¼ wave	example
	Gain	-1dBi	
	Dimensions	7mm diameter 16.6mm length	designed for compact applications

Aerial Section			
Unmanned Aerial Vehicle			example: Aerosonde
	Speed	$20ms^{-1}$ (assumed)	Aerosonde = $22\text{-}42ms^{-1}$
	Wingspan	2.9m	
	Battery capacity	1 hour at 20W	
	Payload	5kg	
Altitude		200m	
Number of passes to cover a $1km^2$ field		5	related to equivalent image area
Total time of flight		4 minutes 26s	assuming $20ms^{-1}$
Communications Payload			
RF Receiver module		Linx ES	example
	Frequency	916MHz	Must not interfere with UAVs comms. system
Antenna		Phazar AMR Omni	example
	Gain	2dBi	
	Mass	227g	
Digital Camera		Pentax Optio S5i	example
	Resolution	2560x1920	
	Mass	120g	
	Field of View	73˚	typical value
	Equiv. Image Area	177.7m x 237.7m	Assumed aspect ratio of 4:3
	Number of Images to cover a $1km^2$ field	30	6 images per pass

Table 9-11 Baseline for communications subsystem

9.6.3 Sensor Web system deployment

The sensor webs are envisaged to be deployed from the aerial data collection platform, the UAV. If each web weighs approximately 200g, it is assumed that the UAV payload budget can hold at least 20 webs that can be deployed in one flyover without reloading.

Using an aerial photograph taken from an initial flyover, any cryoconites present on the glacier field that are visible can be identified. It is assumed that a method of targeted deployment will be used, and as such the position of the cryoconites will be translated into deployment times. A mechanism will deploy the webs to correspond with the position and number of cryoconites, up to a maximum of 16. If more than 20 are identified, then 16 candidate holes will have to be selected. The other 4 webs, or however many are remaining, will be set to be deployed at random times to act as a control group. This group will take readings of a clear area to act as a comparison to the readings being taken from the holes, and also to confirm that the webs themselves are not influencing the environment. This deployment pattern is simulated in Figure 9-32.

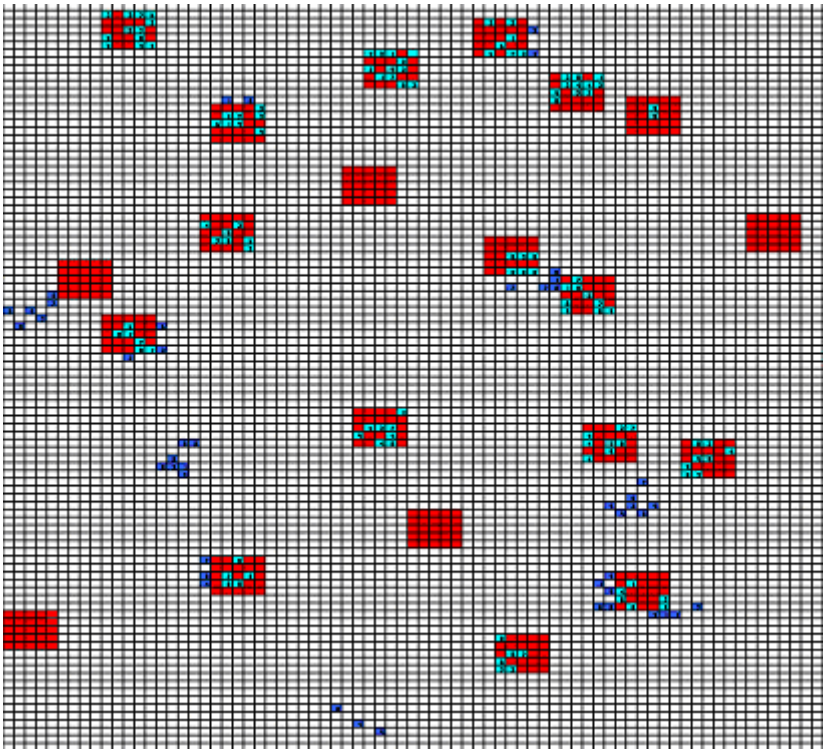

Figure 9-32 Simulation of the web deployment pattern used on the cryoconite field.

In this simulation, the red squares represent the webs, the light blue squares are the randomly grown cryoconites which are in contact with web. This is equivalent to the illuminated LEDs. The dark blue squares are other cryoconites that have either grown since the webs were deployed, or were not targeted on the initial pass.

The deployment mechanism will have a timer that can be set to release a web at a predetermined time. If the speed of flight is know, it should be possible to calculate using the photograph, after what period of time a cryoconite was directly below the

UAV. Using simple trajectory relationships, the time and distance when the web must be dropped in order to hit its target can be calculated.

If the UAV has a velocity v_{ox} = 20 ms^{-1} and deployment is made at a height y = 200m, the time taken for the web to reach the surface, t, is determined by

$$t = \sqrt{\frac{2y}{g}} = \sqrt{\frac{(2 \times 200)}{9.81}} = 6.39\,\text{s}$$

where g is the acceleration due to gravity = 9.81 ms^{-2}. The distance from the target, *x*, that the web has to be released is then calculated by

$$x = v_{0x}t = 20 \times 6.39 = 127.8\,\text{m}$$

This simple estimate does not allow for the effects of windspeed. Speeds of between 1ms^{-1} and 12ms^{-1} have been recorded in the subject area, so the deployment times will have to be adjusted according to the recorded value on the day of deployment. Assuming no wind, the web must be deployed 6.39s before the estimated time that the UAV reaches the target.

There are many external factors which will effect the accuracy and success of the deployment. Further analysis is required and it is likely that at the proposed altitudes, the potential level of accuracy that could be obtained may make it very difficult to ensure a successful find with this kind of targeted deployment. However if the desired deployment pattern is random, the required accuracy is reduced, which means this method of aerial deployment could be used successfully.

Possible deployment mechanisms include a rail or a ballistic launcher. The rail concept is to have two rails running along the length of the UAV. Each rail will house approximately 12 or 13 webs held by a claw device. At the designated time, the claw will open, releasing the web. This is illustrated in figure 9-33.

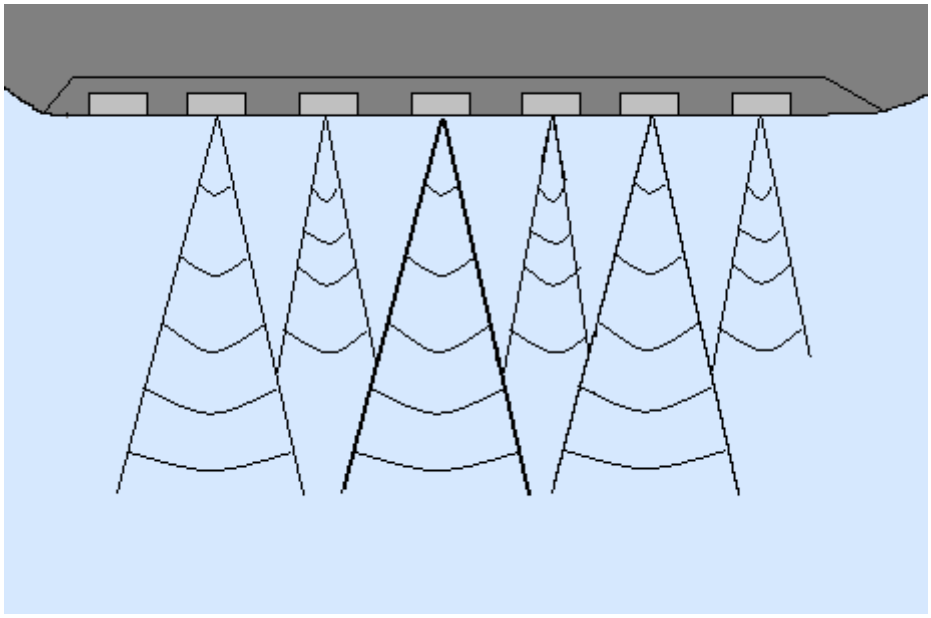

Figure 9-33 Representation of a rail deployment system

This method would add little to the mass budget, however having the webs hanging freely under the UAV increases the risk of interference with the plane's aerodynamics and also increases the likelihood of the webs becoming tangled together.

A second, and more complex, method would employ a system similar to the Foster-Miller "Webshot" (ALS Technologies, 2004). This is a system that deploys a net from a standard 37mm gas gun. It is designed to be used by law enforcement agencies to capture criminals. In this case, the Kevlar net is enclosed in a 37mm by 15cm casing which is fired from the gas gun. This then uses a small charge inside the casing to deploy the net. Here the net has a diameter of 3m. The system is shown in Figure 9-34.

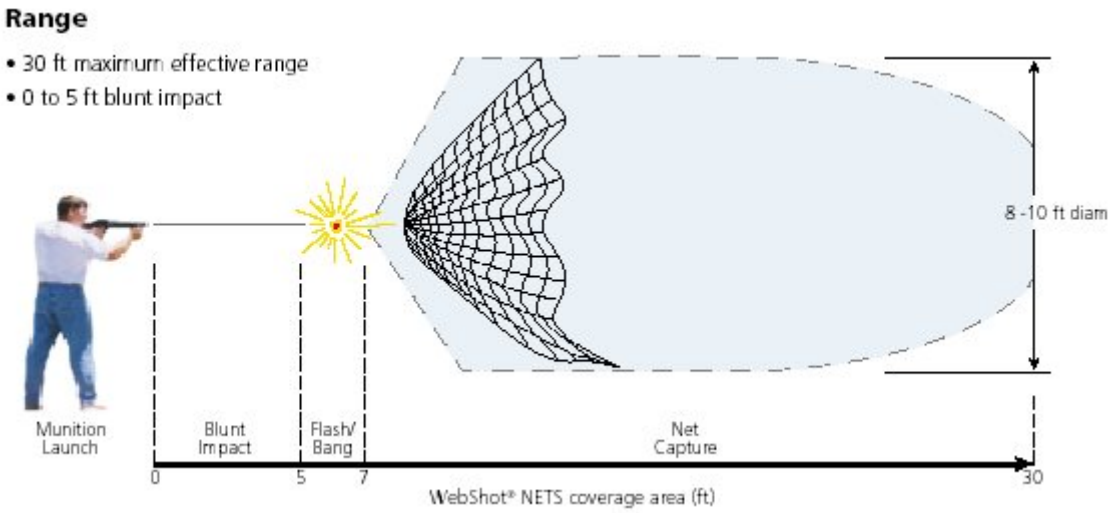

Figure 9-34 The Webshot net deployment system (ALS Technologies, 2004).

This is a more complex deployment system, however with modification it could be beneficial to this system. The firing mechanism would have to be controlled on a timer to allow for targeted deployment, and the casing sizes should be reduced to allow all the webs to fit into the system without reloading. The principal advantage of this idea is that the launcher could be directed to give better area coverage. The rail concept could only drop the webs to cryoconites directly below the flightpath. With a directional launcher, the angle could be changed to enable those off-axis to be reached. Also the casings reduce the likelihood of the webs tangling together, although they would have to be carefully packed into the cases to avoid the bus wires becoming knotted.

This deployment mechanism concept will require further analysis before a finalised design is implemented.

9.6.4 System Power Requirements

The power requirements of the system are important, as they will directly impact the size and capacity of the power subsystem. This section examines those requirements for each sensor suite over one cryoconite season of 90 days. Since batteries have been chosen as the primary power source, a comparison is then made between rechargeable and non-rechargeable varieties of battery.

The important electrical characteristics that are given in relation to a battery's performance are its nominal voltage and its capacity. In general, the capacity is given in Ampere-hours per unit mass (Ah/g), however the data given by the battery manufacturers generally is corrected for the mass of the battery, and is given in Ah. The parameter that will be used in this section to compare the performance and requirements of the battery is its energy. This is related to the power drawn by the system, and is given in Watt-hours (Wh). The energy is calculated as the product of the voltage and the capacity. This gives an indication of either how long a battery can run at a specified power, or how much power can be drawn over a specified time period. For example, a battery with a nominal voltage of 3V and a capacity of 25mAr would have an energy density of 75mWh. This means that it could either run a device requiring 75mW for 1 hour, or a device drawing 1mW for 75 hours. Alternatively if the battery had to be used for 24 hours, the maximum power that the device could need is 3.125mW. Therefore, the total power required by each device and the amount of time it has to be operational for must be established in order to correctly size the battery requirements.

9.6.4.1 Power drawn by the Sensor Suites

During one sensor measurement cycle, all four of the sensors and the Microcontroller are operational. Their individual power requirements have been drawn from their respective data sheets, and are summarised in Table 9-12.

	Voltage	Current	Power (P=VI)	Total power
PIC16F877[a]	3V	0.6 mA	1.8 mW	
ADXL202E[b] (accelerometer)	3V	0.6 mA	1.8 mW	
NPP301[c] (Pressure)	3V	0.6 mA	1.8 mW	7.68 mW
LM20[d] (Temperature)	3V	10 μA	0.03 mW	
JIC 117[e] (UV)	3V	750μA	2.25 mW	

[a] (Microchip Inc, 2003b), [b] (Analog Devices, 2000), [c] (GE Novasensor, 2003), [d] (National Semiconductors, 2002), [e] (IFW, 2002).

Table 9-12 Power Requirements for each sensor suite during one sensor measurement cycle

To provide this much power continuously for 1 day (24 hours), the chosen battery would have to have an energy of at least 184mWh. Over the 90 day season, the total energy per suite is 16.59Wh. This requires a very high capacity battery, and as a result would have a substantial mass in comparison with the individual suite. For example, a standard 6Whr battery has a given mass of 21g. If the required energy is 2.8 times larger, it can be assumed that the mass would also be 2.8 times larger, or 58g. If there are 46 suites in a web, that would add 2.67kg to the overall system. This is unacceptable for a low mass system, however, the measurements and power consumption can be cycled to reduce the drain on the battery.

9.6.4.2 Low Power operations

Two methods can be combined to reduce the power consumption per suite – power-down modes and power cycling.

The microcontroller has a power-down mode, or SLEEP function as part of its programming (Microchip Inc, 2003b). This means that the controller operates using a reduced current of 30μA, instead of the nominal 0.6mA, until it either receives a "wake-up" interrupt from the I2C bus Master or until the set time has elapsed by the on-board Watchdog Timer. Each time the controller goes into SLEEP mode, the timer is reset and another cycle begins. This mode reduces the power consumption from 1.8mW to 90μW, or from 3.89Wh to 0.19Wh over the season.

As part of the suite's communication system, an LED will be illuminated once a week during the data collection aerial pass if conditions are such that the suite recognises that it is in contact with a cryoconite. It is assumed that after the reading cycle has been completed on the appropriate day, the controller will continue to be active for a further 5 minutes (300s), to process whether the criteria have been met and the switch on the LED output for enough time to allow the fly-by. Assuming 12 passes in 90 days, this adds a further 1 hour at 1.8mW to the necessary energy.

Power cycling means turning off the sensors for the majority of the time, then reactivating them for a short period to take a reading. The sensors chosen are able to be

switch on and stabilise ready for a good reading in the order of ms. From this it is assumed that it is possible to switch on, take a set of readings from each sensor and send the data packet along the I2C bus in 1 second. This means that the full power mode would only be required for 2160s = 36 minutes = 0.6 hours over the 90 day season. 7.68mW over 0.6 hours equals a required energy of 4.6mWh.

The total required battery energy for low power operations then becomes:

$$(7.68\text{mW} \times 0.6\text{hr}) + (90 \times 10^{-3}\text{mW} \times 2160\text{hr}) + (1.8\text{mW} \times 1\text{hr}) = 200\ \text{mW h per suite}$$

This is a considerable saving which allows 90 days use instead of approximately 1 days use at full power. This is well within the range of many commercially available, small sized batteries.

This calculation also shows that although the timings are estimated, the high power mode only accounts for 3% of the total necessary energy. This means that the overall energy density is not particularly sensitive to these estimates. If the high power mode was run for 10s per cycle instead of 1s, this would add approximately 40 mWh to the requirements, however this is still only 19% of the total requirement. The power down mode requirement is still the significant factor. Since the timings are only estimates, the energy of the battery should therefore include at least an extra 10% margin, or be at least 220mWh. This would allow for an additional 4s per hour of high power mode.

9.6.4.3 Comparison of Rechargeable and Non-Rechargeable Batteries

There are many types of batteries available on the market in various sizes and with different chemistries. The chemistry of the battery and its main constituents determine the capacity of the battery. Chemistries containing Lithium are currently favoured for high capacity or long life applications, especially where a low mass solution is essential, such as digital cameras or mobile phones. These are available in both rechargeable and non-rechargeable formats. Both formats have their own relative merits. Other than the capacity, for this application the key factors for the power subsystem are the lifetime, the physical dimensions and the operating conditions

Naturally, a non-rechargeable battery has a finite operational lifetime. This then means that the capacity of the battery must be chosen according to the absolute amount of power required over the full operational period, in this case 90 days. Typically the voltage drawn remains constant until the capacity has fully diminished. Rechargeable batteries are not as constrained as this, as generally they can be recharged up to 1000 times. This means that even if the battery is not fully discharged every day, as in most cases the depth of discharge is not 100%, a smaller battery can be used that will be enough for one day's power. However, rechargeable batteries can lose up to 10% of their charge per month due to self-discharging, which would have to be factored into the capacity calculations.

Although a smaller rechargeable battery can be used, additional components are required in order to charge the battery. An obvious way to recharge the batteries in this

case would be to use solar panels. The solar panels would need to be sized according to the amount of energy required to charge the battery, the efficiency of the photovoltaic material and the number of sunlit hours per day. Even though for a mWh battery, the dimensions of the required panels are only in the order of millimetres, additional components would also be required to ensure correct charging and storage of the energy. Also, it would be important to ensure that the web was deployed with the solar panels orientated as to collect as much solar energy as possible. If the array were to land upside down, the power for that suite would fail after one day. This adds an extra degree of complexity to the system that is not necessary with a non-rechargeable cell. Although an individual rechargeable battery can be selected to have smaller dimensions than its non-rechargeable counterpart, it is often true that they have a lower nominal voltage. Since the devices determine this voltage, the correct voltage must be supplied. This is done by having more than one battery in series. However, any mass saving gained by using the smaller battery would be cancelled out.

As with the other components, the operational temperature of the battery is important due to the low temperatures experienced in this application. In general, due to the chemistry of the electrolyte, a battery works more effectively at higher temperatures. However each battery type has a minimum operational temperature where the electrolyte conductivity is reduced to such a level that the electrochemical reactions cannot take place. For rechargeable batteries, this level occurs at –20˚C. Depending on the chemistry, the level for non-rechargeable batteries is around –30˚C, however Tadiran have produced a range of Lithium batteries that could operate at levels as low as –55˚C (Tadiran Batteries, 2003b). The effects of temperature on the voltage and the capacity vary with each make of battery, so the selected battery would have to meet all the necessary criteria in the worse case temperature scenario. On the glacier fields, temperatures as low as –29˚C have been recorded, and although it cannot be guaranteed that temperatures will not fall below this over the season, a non-rechargeable battery should still be able to function. Since the limit on rechargeable batteries is higher, extra power would be required to provide some heating, and extra insulation would be required to keep the temperatures at an operational level. Most rechargeables require a minimum temperature of 0˚C whilst charging. Although this would be during the daytime where temperatures should be above 0˚C, again this cannot be guaranteed and heating would have to be provided. The thermal conditions of the system are discussed further in section 9.6.5.

One further consideration to be made is whether to have one battery per suite or one single battery with enough capacity to power all 46 suites in the web. For the 90 day duration, each suite requires an energy of 225mWh, or approximately 2.5mWhrs for 1 day if recharging. To power the whole web, 10.35Wh would be required for the whole season, or 0.115Wh for one day. This would require a significant battery size, as demonstrated in section 9.6.5.1, although the mass would be less than 46 individual 1g cells. In addition, all batteries have a maximum recommended continuous current. Although the total current drawn by the suites in power down mode is 1.3mA, which can be handled by many batteries, when all 46 are taking readings this would require a pulse of 1.15A. This would be too high for most batteries with the appropriate size dimensions. Another argument against a single battery is potential failure. If the connection to the battery is severed or the battery fails the entire web is lost. If each

suite has its own power, one faulty battery will only affect one suite and so is not a critical failure.

In terms of operational conditions and system simplicity, the non-rechargeable battery is the preferred option for this application, with each suite housing its own power supply. A suitable commercially available battery is a Lithium Manganese Dioxide CR1620 coin battery (Panasonic, 2005). These types of battery are generally found in calculators or watches. The CR1620 has a 3V nominal voltage and can provide energy of 225mWh. It has a mass of 1.3g, a diameter of 16mm and a height of 2.0mm. Although the diameter is above the $1cm^2$ footprint limit, the specification can be adjusted to accommodate it. The total mass added to the system by the suite batteries is 46 x 1.3g = 59.8g.

The above discussion does not include the power requirements of the external communications system, since this will be housed in a separate suite where all power can be concentrated on this task.

9.6.4.4 Communications system power requirements

As discussed in section 9.6.2.1, the chosen RF transmitter requires 7mA at 3V or, 21mW, for the given transmission period. Assuming a 10s period, this requires an energy of (21mW x 1/360 h) = 58μWh per transmission. Assuming 12 transmissions in 90 days, the total energy capacity of the battery must be at least 0.7mWh for the transmitter. A microcontroller must also be part of this suite. Assuming this must be at full power for 1 minute once a week and on power down mode for the remainder of the time, the total power requirement is:

$$(1.8 \times 0.2) + (90 \times 10\text{-}3 \times 2160) + 0.7 = 195.46\text{mWh}$$

Again, the CR1620 coin battery has a energy capacity of 225mWh, however it also has a recommended maximum continuous current drain of 0.1mA. The transmission current exceeds this, even though it would only be for 10s. The Tadiran TL-4935 battery (Tadiran Batteries, 2003a) however has a much higher capacity, 1.7Ah at 3.6V = 7.8Wh or approximately 35 times that of the CR1620, and has a maximum current of 10mA, which is above the required amount. This does however have a 33mm diameter and a mass of 21g, although there may be others available that better suit the size criteria. For the purposes of this example, this battery will be chosen for the external communications power subsystem.

This assumes that the full power of the communications suite is only required for the 10s transmission period. However, even if the full power mode is required for the total duration of the aerial data collector's flight, which is calculated in section 9.6.2.3.3 as approximately 4 ½ minutes, the battery discussed has a large enough capacity to provide the appropriate power levels for this length of time.

9.6.4.5 Conclusions

Each sensor suite will include its own non-rechargeable CR1620 Lithium coin battery, with a energy capacity of 225mWh which is enough to power the suites for a 90 day season, assuming the microcontroller uses its power-down mode and power cycling is used to lower the power consumed by the sensors. The coin battery does exceed the $1cm^2$ footprint area requirement, so the final suite design must accommodate this change. The battery can function at a minimum temperature of –30˚C, therefore for Arctic applications additional heating and insulation are not required. The batteries will add 59.8g to the system.

The external communications subsystem will have its own battery. Although the CR1620 battery has enough capacity, it cannot sustain the current needed to run the transmitter. Therefore a larger TL-4935 battery will be used for the purposes of this example, however in practice a smaller battery may be used instead. This battery will not require additional heating and will add 21g to the system.

The power subsystem will be distributed throughout the web rather than having one battery supplying all the power to the web. This will avoid the problem of critical power failure caused by the loss of the battery.

9.6.5 Thermal issues

The sensors and components have been chosen specifically because of their ability to function at low temperatures. This is an important feature for both the Arctic application and the eventual use on Mars. However, electronic components tend to work more efficiently at temperatures higher than the minimum. This is achieved by enclosing the sensor suite in a layer of insulation material.

Since the sensor suite draws power, that power will be dissipated as heat energy. This means that the suite will be warmer than its surroundings, however since these are low power devices, this heat difference will be small. An advantage of this is that even without insulation, the heat difference should be small enough not to significantly influence the cryoconite or the surrounding ice. Using insulation will keep the heat in and raise the internal operating temperature. The thickness of insulation is related to the heat transfer by conduction, and is analysed in section 9.6.5.2.

9.6.5.1 Relative temperature of the suite due to thermal resistance

The power output, or rate of heat transfer out of an IC chip is proportional to the difference between the chip's temperature and the ambient temperature. The proportionality constant, the thermal resistance r_{th}, depends on the size and shape of the chip and can vary from 30 to 70 K/W. If P is the power dissipated from the chip as heat, the temperature of the chip is given as:

$$T_{ic} = T_{amb} + r_{th} P$$

This means that the change in temperature caused by the power dissipation is equal to the product of the power and the thermal resistance (Young, 1992).

At peak usage times, the sensor suite will draw 7.68mW of power. This means that a maximum of 7.68mW is dissipated by the suite. If the thermal resistance of the suite is taken to be 70 K/W, the temperature difference between the suite and its surroundings is 0.54 K. In power down mode, the power is 90μW, giving a temperature rise of only 0.0063K. Although this is an estimate, since the true thermal resistance of the suite is unknown, the answer given is sufficiently small enough that it is unlikely to cause significant impact to the cryoconite region.

If the ambient temperature is at –29˚C, even at full power, the temperature of the suite would be –28.5˚C. Although the suites can operate at –40˚C, the performance is improved if operating at –20˚C or above. Insulation and additional heaters can provide this additional heat.

9.6.5.2 Heat dissipation through thermal conduction

The principle method of heat dissipation in this system is thermal conduction. This heat flux, Q, can be analysed in terms of the temperature difference and the thermal conductivity of the material used as insulation. The relationship assuming a spherical object encased in a ball of insulation is given as:

$$Q = -\frac{4\pi k r_1 r_2 (T_2 - T_1)}{r_2 - r_1}$$

Where the heat flux, Q, is constant, having reached steady-state equilibrium and the thermal conductivity, k, is given in units of $Wm^{-1}K^{-1}$. The definitions of r_1, r_2, T_1 and T_2 are shown in Figure 9-35.

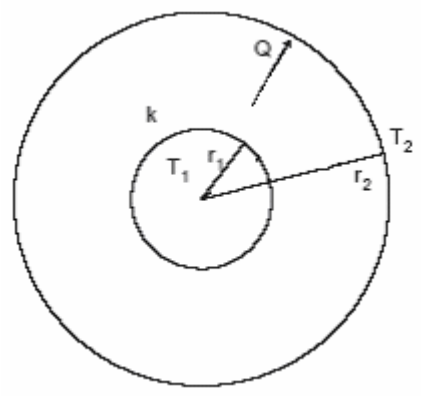

Figure 9-35 Diagram showing the notation used for heat flux analysis for spherical geometry (Hobbs, 2005).

Derivation of this relationship, and those for one-dimensional and cylindrical geometries are shown in Appendix D. (Hobbs, 2005).

It can be shown that as the outer surface radius r_2 tends to infinity,

$$Q_{\lim,r2\to\infty} = -4\pi k r_1 (T_2 - T_1)$$

This means that for a finite object, with radius r_1 and limited power Q, there is a maximum temperature difference that can be sustained which is independent of the insulation layer thickness (Hobbs, 2005). If the required temperature cannot be obtained from the natural amount of power drawn by the system, then additional heaters drawing extra power are required. The alternative is to increase the power available by increasing the size of the object.

The following section shows examples based on the idealised dimensions of the sensor suite.

9.6.5.3 Examples assuming the suite is a 1cm diameter sphere

A good insulating material has a low thermal conductivity. Values for example materials are given in Table 9-13.

	Thermal Conductivity, k ($Wm^{-1}K^{-1}$)
Aerogel	0.005
Air	0.024
Aluminium	205
Copper	385
Cork	0.04
Fibreglass	0.04
Glass	0.8
Ice	1.6
Styrofoam	0.01

Table 9-13 Typical values of thermal conductivity (Young, 1992).

Aerogel (Berkeley Lab, 2004) is a silica material that contains a very small fraction of solid silica. The structure of the material is such that the transportation of thermal energy is difficult, making this a good insulator.

For the purposes of this analysis, the sensor suite is assumed to be a sphere. The insulating material is assumed to be Aerogel, with k = 0.005 $Wm^{-1}K^{-1}$. Assume the ambient temperature to be –29˚C (244K), or a worse case Arctic scenario, and assume that the desired operating temperature is –20˚C (253K). This makes the desired temperature difference (ΔT) 9K. If the inner radius r_1 is taken to be 5mm and the heat flux, Q, is 7.68mW, assuming full power mode, the temperature difference calculated using the infinite insulation relationship is:

$$\Delta T_\infty = \frac{Q}{4\pi k r_1} = \frac{7.68\times10^{-3}}{4\pi\times0.005\times0.005} = 24.45\,\mathrm{K}$$

This means that there must be a value for r_2, or thickness of insulation, that will maintain the desired temperature. This also shows that the desired temperature of –20˚C cannot be maintained if the ambient temperature is below –44.5˚C, or that at –29˚C ambient temperature, a desired temperature higher than –4.5˚C cannot be maintained no matter how much insulation is used.

The value for r_2 can be found by plotting the relationship:

$$\Delta T = \frac{Q(r_1 - r_2)}{4\pi k r_1 r_2}$$

as shown in Figure 9-36.

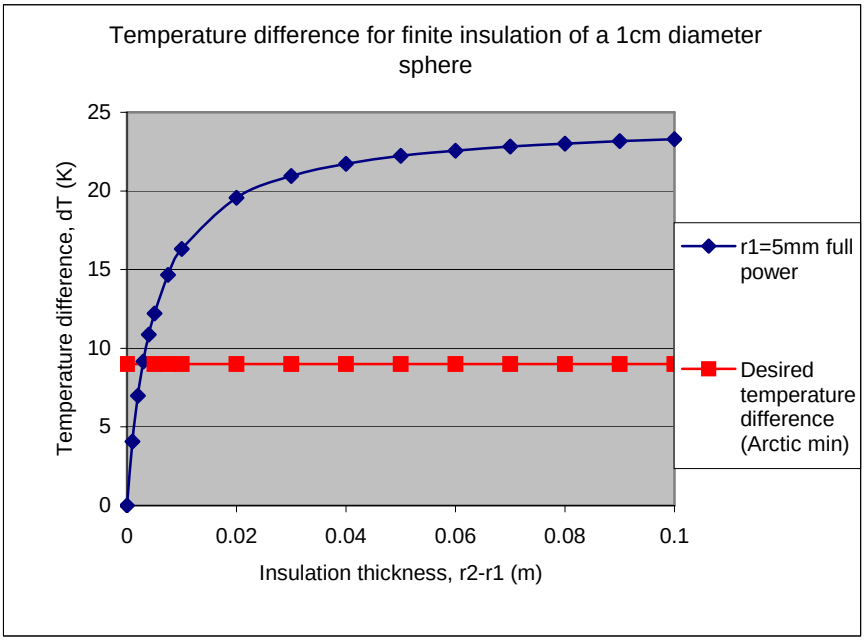

Figure 9-36 Graph showing the temperature difference of various insulation thicknesses surrounding a sphere of 1cm diameter.

This shows that the minimum insulation thickness required to maintain the desired temperature is 3mm. This would mean that each suite would have a diameter of 16mm.

This analysis assumes that the suite is continuously in full power mode. However, as shown in the previous section, the majority of the time the suite has been designed to be in power down mode. This means that the maximum Q will be reduced to 90µW.

Applying the infinite insulation equation for this value of Q,

$$\Delta T_\infty = \frac{90 \times 10^{-6}}{4\pi \times 0.005 \times 0.005} = 0.29\,\mathrm{K}$$

This shows that the heat flux is insufficient to maintain the desired temperature. The minimum power required to maintain a temperature difference, assuming infinite insulation, is 2.8mW. To achieve this the power must be increased, which in turn will

require a battery with greater capacity and mass, as discussed in the previous section. If the system is run continuously at at least 3mW, the desired 9K temperature difference if achievable. However, the total power drain in one day would require a battery capacity of 72mWh or for the 90 day season, 6.5Wh. In addition to the added mass of this battery, the insulation layer would have to be 8mm thick, giving an overall suite diameter of 26mm, assuming the battery itself did not have a diameter larger than 1cm.

9.6.5.4 Conclusions for thermal issues

In full power mode, a layer of Aerogel insulation 3mm thick would be required to maintain a temperature difference between the lowest recorded ambient temperature and the desired operating temperature of 9K. However, in power down mode, even an infinitely large layer of insulation would not be able to maintain a difference above 0.29K above ambient. This means that to raise the heat flux, additional power would have to be dissipated and so a larger battery and heaters would be required.

It, therefore, seems reasonable, in order to maintain a low power solution, to ensure that all the components are tolerant to the minimum ambient temperature conditions, and only use insulation as protection against other factors, such as moisture or radiation.

The thermal problem becomes more apparent when the environmental conditions on Mars are investigated. The minimum ambient temperature there is 183K or –90˚C. This means that even though the components are able to operate in low Terrestrial temperatures, the minimum temperature difference provided by the insulation must be at least 50K. Even at continuous full power and with infinite insulation, this is not achievable. Increasing the power input to 17mW and adding a layer of insulation at least 6mm thick will however give the desired temperature difference, but at the expense of a larger battery, larger footprint area and potentially more complex system.

The above findings are summarised in Figure 9-37.

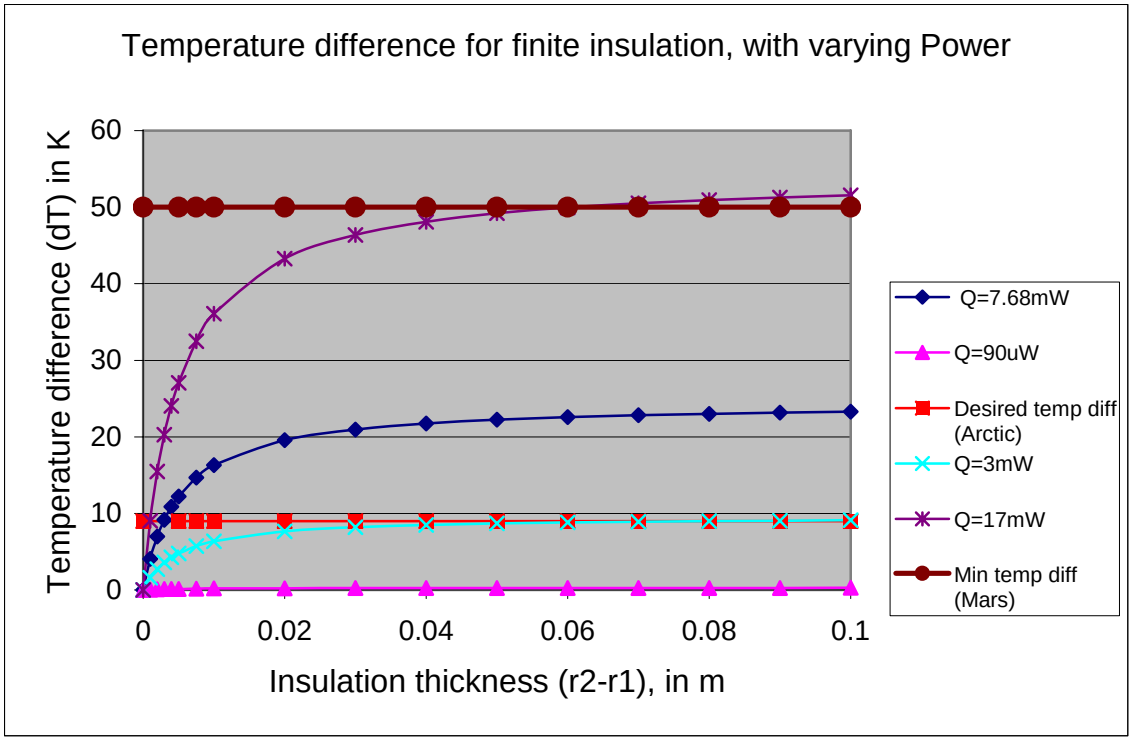

Figure 9-37 Graph showing the temperature differences achievable for varying power inputs and insulation thicknesses, all based on a 1cm diameter sphere.

The thermal subsystem of the sensor web is clearly an important one in terms of the affect on the suites' operating conditions and the external environment being measured. This area will require further investigation, especially for use on the Martian surface.

9.6.6 Survivability in extreme conditions

A key aspect of the sensor suite web design has to be its ability to survive, and be operational, in extreme conditions for extended time periods. Whilst traditional sensing equipment is exposed to the harsh temperatures, for example, for only a short amount of time during a data collection survey, the webs must be able to withstand these conditions continuously for a whole 90 day season.

In both Arctic and Martian environments, the low temperatures experienced by the suite will need to be considered. As the suites are in contact with the ground over long periods of time, the temperature of the suites will reach equilibrium with the environment, and as such has to have components designed to operate within these values, or be insulated against the cold, as discussed in the previous section. The bus wires will also be subject to these temperature extremes. If chosen incorrectly, the wires or insulation layer may freeze and become brittle. For example semi-rigid PVC becomes brittle at -10˚C, a temperature that is regularly experienced in Arctic conditions. However Teflon FEP has an embrittlement temperature of –73˚C and Teflon PFA becomes brittle at –267˚C (Tillar Shugg, 1995), making these types of wire insulation preferable for low temperature applications.

A cryoconite is, by definition, a pool of melted ice, so any sensor or electronics in contact with these areas would have to be protected against moisture penetration. As the hole grows, parts of the web will become immersed. The nature of the measurements that need to be taken, however, means that some of the sensors will need to be in direct contact with the liquid in order to give useful environmental information. The temperature sensor will need to be in contact to record the temperature within the cryoconite rather than the air temperature or the internal suite temperature. The UV sensor will need to be exposed to either the hole surface or to the hole water depending on the UV measurement required. The pressure sensor inlet will have to be above the surface to record the air pressure and to prevent moisture entering the internal structure via the inlet. The potential submersion of the suites has a direct impact on the position of the sensors and also highlights the need for either the suites to be able to float via their insulation or the need for some buoyancy aids to be added to the system.

The electronics and the accelerometer are housed within the suite, but will need to be protected against contact with any liquid caused by leakage. Traditionally hermetically sealed packages have been used to overcome this problem, however they are an expensive solution (Kelly, Alderman, Lyden, and Barrett, 1997). Of the properties of other possible encapsulating materials, the adhesion is important for moisture protection (Kelly et al, 1997). As liquid contacts the coating, the adhesion to the protected area can degrade causing voids in or delamination of the material, which allows access to the liquid. Silicone gels are commonly used to package sensors. Although they have a high permeability to water compared to other materials, they have better adhesion properties making these gels a useful packaging material (Dyrbye, Romedahl Brown, and Friis Eriksen, 1996). This is the kind of packaging used for pacemakers, however the gels offer little protection against a corrosive substance (Kelly et al, 1997). In the cryoconites case, these should provide sufficient protection. Other methods of protection are under investigation, and the field of Microsystems packaging is a growing area of research. In the case of the exposed sensors, the sensing areas may be coated with a passivation layer of material on the wafer scale (Dyrbye et al, 1996). This depends on the fabrication processes used by the manufacturer of the COTS component, and as such should be recognised as a possible additional sensor selection criterion.

The packaging of the suite may also be able to protect against undesirable radiation effects. This is particularly relevant in a Martian environment, however it is also a potential problem in some terrestrial environments, such as the polar regions. Stray cosmic radiation particles can cause single event logic upsets, which in turn may cause sensor reading errors or errors in the data transmission or storage. With the volume of data that is collected per day and a realistically chosen acceptable error rate however, the radiation effects can be minimised.

All the suites, independent of their final application, are subject to the deployment conditions. The system is designed to be deployed from altitude, and as such will have to withstand the impact on landing. Using the conservation of energy theorem, the final velocity of the web dropped from 200m is:

$$v_{final} = \sqrt{2gh} = \sqrt{2 \times 9.81 \times 200} = 62.64 \text{ ms}^{-1}$$

This assumes that the suites are dropped, rather than using a ballistic approach. The component most sensitive to impact shock is the accelerometer, however the device chosen can withstand shocks up to 1000g, as they have been designed for "dropping" applications. Providing deceleration occurs in a time greater than 6ms, the shock should not cause damage to the sensing element.

The deceleration can be estimated using the law of motion:

$$v^2 = u^2 + 2as$$

where v^2 is the final velocity, $u^2 = 0$, a is the deceleration and s is the distance of deceleration, or the thickness of the packaging between the sensor and the ground. Assuming a package thickness of 3mm, the deceleration can be estimated as approximately 65400g. This is considerably more than the sensor is designed to withstand. For a deceleration of 1000g, the packing needs to be approximately 20cm thick. The packaging design of the web must also be sufficiently robust not to break on contact with the ground. Relevant tests and extensive calculations would have to be carried out on a prototype suite to ensure that the design can withstand both shocks and vibrations, however the compact and lightweight nature of the suite reduces their susceptibility.

Although these specific conditions can be addressed, the inherent redundancy built into the system is a further enhancement to its survivability. The large number of suites on multiple buses with interchangeable masters means that if a small number of the suites fail due to landing on incompatible surfaces or degradation, the web is still able to function and the mission is not lost.

9.6.7 Additional functionality

So far, the sensor suite concept includes relatively basic sensors that provide relevant, but general environmental data. Whilst this is useful for this application, the generic nature of the suite concept means that modifications can be made to the design to provide the system with additional functionality, as measurement criteria change or as technology progresses.

The principal modification that can be made is to the sensors themselves. Providing that they met the selection criteria of low power, miniaturised dimensions and, ideally, commercial availability, any sensor can be integrated into the suite, either in addition to or in replacement of any of the existing sensors. This enhances the design to enable the collection of more specific data. For the cryoconite application, a sensor to analyse the chemical composition of the melted ice or of the bacteria present may be the next desired function of the continuously *in-situ* sensor suites. Also, slightly larger or more power intense sensors can be added to the webs independently of the suites provided they are compatible with the standard I2C bus. This further broadens the range of potential web functions.

A relatively simple modification can also be made to the communication system to enable inter-web coordination. By sending a general call, webs can recognise others within range, and with additional data processing, could compare data sets collected.

This would be useful to detect any anomalous readings or recognise any web failures. It could also reduce the volume of data transmitted to the external receiver by making comparisons and only sending the most relevant or unusual readings. This additional functionality however would come at the expense of some of the scientific data, so a trade-off would have to be made as to the sensitivity of the comparison.

Another modification to the sensors that would increase functionality is to choose sensors that provide long-distance measurements. If the suites on the outermost bus had long-range sensors, measurements could not only be taken *in-situ*, but also of the surrounding area. This could then detect any other cryoconites that may not have been covered by a sensor web, but also detect any other interesting features of the glacier.

This long-distance sensor modification could be used in conjunction with other technological advances to give the webs mobility. If the suites could be equipped with "legs", upon detection of a cryoconite within range, the web could move itself to the optimum position for gathering the most useful data. This would require a high level of autonomy and data processing. These "smart" webs could eventually be deployed in any position at random and then order themselves to cover the subjects most efficiently. Although this requires a much more complex sensor web, the deployment system itself would be much simplified. The suites themselves within the web could also have the ability to reposition themselves along the communications bus if there is one area of particular interest, or it is in contact with a small subject. A mobility function provides the system with the ability to perform targeted measurements to enable the maximum efficiency to the gained from the study period.

As technology becomes more advanced, the generic design of the suites and webs have the potential for further modification and increased functionality to meet the requirements for a range of applications and end-users.

9.6.8 Necessary modifications to use the sensor suite webs on Mars

The aim of this chapter has been to provide the overall sensor suite system concept with reasonable subsystem values from a realistic terrestrial scenario. This section applies the results from this exercise to a similar Martian mission, and discusses the major modifications that would need to be made.

A key feature of the terrestrial system is the use of a UAV for external data collection and aerial mapping. An equivalent system could also be used on Mars. Mars UAVs or planes have been previously proposed for missions, however none have been implemented so far. Two NASA UAV concepts that are currently under development are MATADOR (Mars Advanced Technology Airplane for Deployment, Operations and Recovery) from NASA Ames and ARES (Aerial Regional-scale Environmental Survey) from NASA Langley. These are both likely to be contestants in the second NASA Scout competition beginning in 2005. The Scout competition will chose a mission that will be launched in 2011. The MATADOR concept aims to fly over the surface for approximately 45 minutes, the land and relay the data collected (Morris, 2004). However, there is no guarantee that a UAV mission will be chosen in this competition. The main drawback of the Mars planes that have been proposed is that

they are usually designed to crash-land after one pass. Unless a reusable concept is proposed that can make multiple passes, either the deployment and mission duration time for the suites will have to be re-evaluated or an alternative communications system will have to be used.

An alternative is for the suites to be used in conjunction with a Lander mission. The webs could be deployed from the Lander before it reaches the surface, and the RF receiver could be housed within the Lander, assuming it is in range. This does limit the subject field area, however this may still be a useful subject field, or longer range transmitters could be substituted within the communications suite. Another option is to use a more powerful transmitter to communicate with a relay station or an Orbiter. The illumination of the LEDs could be captured with a visual camera onboard either the Lander or Orbiter. A suitable mission for this would be the winner of the first Scout competition, Phoenix, which is scheduled for launch in 2007 (Univ. of Arizona and NASA, 2005). This is a Lander mission to the Martian Polar regions where it will dig through the top soil and sample the ice below for onboard analysis. Whilst the Lander aims to give detailed results of one area, combining it with sensors placed over a wider field could further enhance the data collected. However, since the ice is below a surface layer, the suites would have to be modified with an additional probe for example to penetrate the top soil. In this case, the webs can be deployed randomly instead of targeted, making the deployment system less complex.

As an addition payload to a larger lander, an extra 4kg may be acceptable, assuming the mass of the suite, batteries and connecting wires is as previously described. However, since mass is usually at a premium for any Space mission, this may have to be reduced. The scale of the deployment, using perhaps half the number of webs, would make a considerable mass saving. If the number of webs remains constant, the number of suites per bus, or the number of buses per web could also be reduced. This would mean a reduction in the volume of data collected and increased likelihood of an area of interest being overlooked, so a trade off would have to be made between the value of increased local readings against the larger scale investigation a larger number of smaller webs would yield.

The webs would also have to be modified to face different environmental conditions on Mars, as described in section 9.2.3. The temperature has a recorded average of –50˚C in the Martian Polar regions, which is considerably below that experienced in the Arctic. The sensors have been chosen for their ability to operate at down to –40˚C, with typical batteries operating down to –30˚C. At the average temperature, an insulation layer similar to that described for the cryoconite application would be sufficient, however extra insulation or a heater would be required if lower temperatures were to be protected against. With a 6mm thick layer of Aerogel insulation, the internal temperature can be raised by 20˚C at a constant power dissipation of 7mW. With the capacity of the batteries previously described, this however would reduce the potential mission period to 30 hours. Replacing all the suite batteries with the Tadiran models would enable a 35 day mission at 7mW, and would also allow for the temperature to be raised by 50˚C by providing a dissipation of 17mW but for a mission duration of only 15 days. This would be at the expense of slightly larger and heavier suites, so in this case the number of suites per web may need to be reduced.

The other environmental factors that will have to be specifically designed against are radiation and dust. If the components chosen are not radiation-hardened, intense UV and cosmic radiation will have to be insulated against, which may require special insulation. Although it is unlikely that moisture will cause a problem in this application, the equivalent problem surrounds the dust in the atmosphere. A covering of the fine dust may hinder readings from exposed sensors, and internal components will also have to be protected.

The sensors chosen have ranges that are suitable for terrestrial applications. For example, since the acceleration due to gravity and the atmospheric pressure are considerably lower on Mars, it must be ensured that these sensors have an appropriate range and sensitivity. If the temperature sensor is unsuitable, sensors designed for cryogenic purposes are also available commercially and can be substituted into the design. Depending on the purpose of the mission, additional sensors can also be incorporated within the suites.

As shown, the Arctic scenario has provided a useful mission baseline for a realistic terrestrial application, and the generic nature of the design means that the suites can be adapted for a suitable Mars mission with only a few general modifications.

9.7 Link 3 – Hardware/MST and Management/Industrial

Chapter 4 examined the strategic issues faced by the Space industry as a whole. This section discusses the industrial issues linked with the sensor suite concept. The primary business issues are selection of target markets, and whether to contract integration of the suites to another company.

9.7.1 Manufacture and integration of the Sensor Suites and Webs.

One of the design briefs for this project was to use Commercial Off The Shelf (COTS) MST components. This is principally to enable the sensor suite concept to be a low cost solution to planetary surface exploration and other applications. Costs are reduced by utilising the expertise already available in MST design and fabrication and taking advantage of the wealth of mass-produced products in the market place. For example, Accelerometers and pressure sensors are widely used by large industries such as the automotive industry, where the sheer volume of units required has reduced the unit price to less than a dollar. COTS components are thus cost-effective avoiding the additional costs of designing and manufacturing a limited number of bespoke components.

There are drawbacks however to using commercial components. The main disadvantage is that the scope of the mission then becomes limited by the specifications of the components and by the manufacturers guidelines for their operation. This has been demonstrated in several instances during the sensor suite design discussion. Although in most cases a component can be found that will deliver the required parameters, if there is only one supplier of that component, the power of that supplier is increased. This then leaves the project open to the threat of increased unit price or

discontinued supply. This threat is relatively limited, so the advantages of using COTS components are greater than the disadvantages.

The main issue, however, is the integration of the suite. Although this will be a generic design, the production of the sensor suite will be limited to the quantities required for the specific application. In addition to the integration of the components into the individual suites, the suites must also be integrated into the webs. This adds a further level of complexity.

There are three levels of production quantity for an integrated MST sensor suite;

- prototype (<10) working models for test and demonstration. Likely to be done in the lab by the designers.
- mission level – approx 100 – 2000. Enough for one sample mission. Too many for research lab, not enough for own specialist equipment.

- Mass run > 100,000 as in automotive industry. Too many for Space applications, although quantity maybe possible if used in other markets too.

For the cryoconite monitoring application described above, each web has 46 sensors. If 25 webs had to be produced for a demonstration mission, this would require the integration of 1150 individual suites. This is neither a small prototype quantity nor does it have the volume to warrant a mass run. The question then becomes is it more cost effective to integrate in-house using specially purchased equipment or contract the integration out to an external party.

Four costs must be considered when deciding whether to make or buy. In this case, integrating the suites in-house is the "make" option, and having the suites integrated by another company is the "buy" option. These costs are transaction costs, specialisation costs, agency costs and asset specificity (Rickard, 2000).

Transaction costs relate to the fact that the important factors in the cost of a product is more than just its market price. With every transaction there is an element of uncertainty. This includes whether the product will perform to the necessary standard and whether delivery will be made to the specified schedule. In the case of the suites, these transaction costs will be related to whether the number of suites required can be produced and whether they can be produced to space-qualification standards of non-contamination and reliability. These costs increase with the complexity and the mission critical nature of the product, however they decrease as the number of transactions increases. If the supplier has been used previously, the uncertainty about the quality of their work is reduced and the transaction cost is lowered.

Specialisation costs are dependant on economies of scale and production learning curves. In general, expertise reduces production costs. This is because as a company's core competency, they will have perfected the processes needed for efficient production, and can therefore offer lower unit price than a company who does not specialise in this kind of production. A specialist company can also take advantage in economies of

scale to lower their costs. A company specialising in component integration would employ its expertise for many different applications, not just sensor suites. This cost is therefore limited by the size of the potential market, although as the popularity of the technology grows, more potential customers are created.

Agency costs are related to the internal organisational costs of a company producing products in-house. A new department may have to be created, which in turn requires functions such as Human Resources and Accounts to service the need for staffing and budgets.

Asset specificity is where an asset cannot be redeployed to another use without considerable cost (Rickard, 2000). There are three types of asset specificity: Site, Physical and Human. Site specificity is the cost advantage gained by locating asset in close proximity. Physical asset specificity relates to an item of equipment being purchased for one specific purpose. If in order for it to be used for another purpose that equipment has to undergo extensive reconfiguration, this will incur costs. Human asset specificity is the group of individuals with specialist knowledge. If these people leave, the training of new people would incur training costs.

These costs can be shown as curves relating the net cost of purchasing a fixed quantity from the market or by producing the same output in-house. This graph is shown in Figure 9-38.

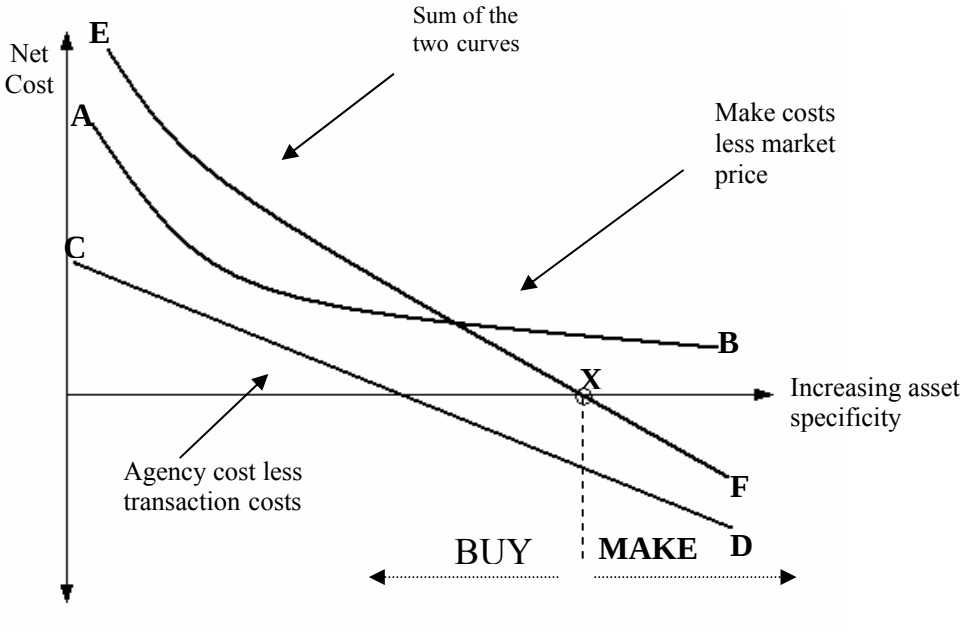

Figure 9-38 . Graph of asset specificity versus net cost used to evaluate whether to make or buy (Rickard, 2000)

The vertical axis represents the net cost of the unit. The horizontal axis shows production increasingly dependent on asset specificity, whilst keeping output constant. The line AB represents the cost difference between purchasing the item and producing it. This curve is based on the assumption that generally a specialist company can

produce a product cheaper than a non-specialist. However as the asset specificity costs increase, the cost advantages of a dedicated asset reduce the cost advantage of using a supplier. Curve CD shows the net difference between the transaction costs and agency costs. As the asset specificity increases, the transaction costs rise and eventually it becomes more cost effective to incur the agency costs in-house than the high transaction costs of purchasing the unit. The curve EF is the sum of the other two curves. Point X is the point where the two net costs are balanced. Therefore, to the right of this point it is more economical to produce in-house and to the left it is more cost effective to buy from the market. These curves depend on the market conditions at the time and can change as the market changes.

Although the exact costs would have to be evaluated, it appears to be more cost effective to contract the integration of the sensor suites to a third party. There are various companies that specialise in all aspects of MST design and manufacture including the final packaging. The main transaction cost in this case is the volume of production. In general these companies can integrate low volume orders and prototypes, however if the number of webs per mission is increased, or more than one mission is proposed, the volume required may become more than the supplier can provide. At this point, it may become necessary to invest in the equipment.

In the case of a company such as EADS Astrium (2004), the integration of MST components is outside their core skill set. However, the parent company EADS (2004) has many subsidiaries around Europe. To facilitate the needs of all of its individual companies and reduce the duplication of equipment in several places, they have a Corporate Research Laboratory. One of their core skills is integrating COTS components and they have experience of integrating similar products. This is a hybrid solution to the make-or-buy decision, since it is both procuring from outside the individual company, but producing from within the larger organisation.

The costs involved in the production of the sensor suites will be the development costs which will be one-off, followed by the subsequent steady state costs incurred by the user for each suite. The development costs will include the cost of the initial design work and the production of several prototypes, both simple breadboard models and more complex test models. A breadboard model can be produced relatively inexpensively. The example shown earlier was produced for under £10, however this was not using the final MST unpackaged components chosen later. The researchers usually produce one fully integrated prototype before approaching a third party to carry out the integration of subsequent suites. This stage will have a learning curve, which may mean that several prototypes fail before one is produced of the required standard. This stage also includes any new equipment that would need to be purchased and the related training in its use. In general the development costs are higher than the steady-state costs. These would usually comprise the cost of the components and hardware needed for each additional suite. In the example this would be approximately £100 per suite, although bulk orders of the components are usually at discounted rates. Labour costs are incurred at both stages. At this stage, these costs will be multiplied by the number of suites required for the application. Overall, this appears to be an inexpensive solution, however the cost of 3D integration is unknown and likely to

increase the cost significantly, and although the COTS components are cheaper than bespoke components, there are other costs to be taken into consideration.

9.7.2 Markets for the sensor suite concept

If the volume of potential sensor suite production can be increased, a dedicated mass run of suites, or the procurement of specialist equipment and staff will become more economically attractive. Generally, the more units that are produced, the lower the cost per unit, as per the economies of scale concept. However, Space is a small market.

For a sensor suite system specifically designed to investigate the Martian surface, there are a limited number of suitable missions. The generic nature of this design has the potential to broaden the possible applications to other planetary surface exploration missions or be incorporated into existing mission plans to land on bodies such as comets. As section 9.6 shows, the design can be adapted for terrestrial applications like Arctic cryoconite monitoring and would be suitable for many types of environmental sensing, particularly applications is extreme environments. Minimal changes to the design and included sensors will present even more possible applications, however any further penetration into the planetary and extreme environmental sensing market is still relatively limited.

A way to increase the number of potential customers to increase the number of units produced is to approach different markets with the existing sensor suite, known as market extension. In this case, the focus is shifted to include indoor environmental sensing as well as outdoor applications. The recent trend for "smart" buildings that can sense their own internal climates is another possible use for a sensor network, or in sensitive environments such as art galleries, where the exact temperature, humidity and light levels are monitored in order to preserve the paintings. A sensor network that included a visual communication system such as an LED that illuminates if undesirable conditions were detected, provides a simple warning system from the gallery floor, in addition to the remote computer monitoring. Another potential market extension is into internal housekeeping data monitoring within machinery. Large industrial machines where internal conditions are critical to avoid parts failure could have a sensor network fitted to monitor these conditions. Here the small size of the suites would be an advantage since they can be added discretely to the system without the need for extra housing. The internal communications wired bus would also reduce the likelihood of interference with key electromechanical systems, which may occur with a wireless system. This application could be extended for use in the aerospace and automotive industries, as well as increasing penetration into the space market with use inside satellites and launch vehicles.

Another way to increase the commercial potential is to change the suite into a wireless system. The communications design would have to be altered, but the overall generic sensor suite concept would remain. This could be considered as a new product, but would have potential uses in all the markets mentioned, as well as attract customers whose very low mass requirements or mission design requires a wireless solution.

If the sensor suite web concept can be established as a versatile product with many potential uses, demand for the product will increase. The key benefit of this product to be highlighted to potential users has to be its generic design, and the utilisation of standard COTS systems such as the I2C bus, which enables further customer-specific enhancements to be incorporated into the design with few changes to the fundamental concept. This opens the product to many potential markets, and therefore has the potential to increase demand. If the demand is high enough, it then may be a good investment to establish a dedicated integration laboratory, which in turn would open up a new market sector for an existing company.

For an existing Space company such as Astrium, the move into MST sensor suites represents a diversification from its core business of satellites. However, they do have extensive prior expertise in planetary exploration hardware, and a previous interest in the utilisation of MST in Spacecraft systems. Their reputation in their field adds another dimension to the features of the sensor suite concept, as well as lowering the transaction costs of the potential users.

9.7.3 Conclusion

The high availability and low cost of COTS components means that they are most cost-effective for the sensor suite concept, even though the manufacturer's specifications can limit the scope of the suite's capability.

For the integration of the suites, the net costs of using a third party specialist company are less than acquiring the equipment and expertise required to integrate in-house. However, many companies are only able to provide low volume production, which may become inadequate as the numbers of suites required increases. At this point it becomes more economical to invest in dedicated equipment.

The volume of suites depends on the number of potential applications and markets it can be used in. The initial target market of planetary surface exploration is relatively limited, so penetration into the market for monitoring other extreme environments and extension into the indoor environment, as well as internal housekeeping data markets will be the next step to increasing potential orders. Changing the design to become a wireless system will also increase the number of applications.

The features and benefits of the suite concept that should be highlighted are the generic nature of the design and the use of standard protocols, which enables further design enhancement. The reputation of a well established company also reduces customer transaction costs and makes the concept an attractive option for all environmental sensing requirements.

9.8 Overall Chapter Conclusions

The following is a proposed mission baseline for an Arctic cryoconite monitoring mission.

Mission Specific Conditions			
Mission duration		90 days	UAV pass every 7 days
Subject Glacier field area		1000m x 1000m	
Number of Sensor webs		20 (16 targeted, 4 control)	deployed from aerial platform
Relevant Environmental Conditions			
	Recorded Temperature Range	-29˚C to 8˚C	depending on season
	Atmospheric Pressure	998 – 1023 mbar	
	Solar Radiation	0 – 400 Wm^{-2}	depending on season
	Acceleration due to gravity	9.81 ms-2	1g vertical for tilt measurements
Cryoconite parameters			
	Diameter	5 – 50 cm	
	Depth	10 – 30 cm	
	Water Temperature	0.1˚C	

Sensor Suite Configuration – 3D stacked Multichip Module			
Sensors		Temperature, Pressure, UltraViolet radiation, 2 axis Accelerometer for tilt measurements.	Unpackaged COTS MST-based components
Volume of data collected per day		1152 bits	1 set of readings per hour
Processing		PIC16F877A Microcontroller	with internal ADC and I2C capability
Intersuite communications		I2C bus (3-wired)	1 Master suite per bus
External communications		LED	otherwise all data passed to separate communications suite.
Power			
	Voltage	3V	
	Power requirements	7.68 mW active 90 µW power down	Full active power only when taking measurements
Battery		CR1620 non-rechargeable Lithium coin	minimum operating temperature –30˚C
	Capacity	225mWh (75Ah @ 3V)	
	Mass	1.3g	
	Dimensions	16mm diameter 2.0mm depth	
General Specifications			
	Thermal insulation	3mm thick layer of Aerogel	raise temperature by 9˚C

	Moisture resistance	Silicone gel coating over internal components. Passivation layer over exposed sensors.	
	Capacitance per I2C bus	400pF	manufacturers specifications
	Capacitance per suite	15pF (assumed)	Only PIC connected to the bus
	Total Mass per suite	3.4g (1.3g battery + 2.1g components)	assumed unpackaged dies - estimates
	Dimensions	10mm x 10mm (battery layer 16mm x 16mm) 25mm depth (estimate)	excluding insulation

External Communications Suite			
Total mass		25g	includes microprocessor
Overall Dimensions		33mm x 33mm x 20mm	estimate
Transmitter		Linx TMX-xxx-ES	example
	Power	7mA @ 3V 95µA @ 3V (power down)	Full power if transmitting, else in power down mode.
	Data Rate	56 kbps	
	Frequency	916MHz	Specified by transmitter in this case
	Range	up to 300m	
	Transmission power	1mW	
	Transmission Time	6.5s + initialisation time	
Suite Antenna		JJB ¼ wave	example
	Gain	-1dBi	
	Dimensions	7mm diameter 16.6mm length	designed for compact applications
Battery		Tadiran TL-4935	
	Capacity	6.12Wh (1.7Ah @ 3.6V)	
	Mass	21g	min temperature –55˚C
	Dimensions	33mm diameter 10.2mm depth	

Web Configuration			
Web diameter		50cm	
Total number of suites		46 active suites + 1 external communications suite	~10cm between each suite
Number of I2C buses		5 buses, 10cm apart	3/6/9/12/15 suites per bus
I2C bus wire		0.2mm diameter wire with 0.15mm Teflon insulation	
	Total length of wire per web	5.96m	

	Twisted pair capacitance	40pFm^{-1}	
	Resistance	0.55 Ωm^{-1}	assume copper wire
	Total mass of wire per web	17g	assume copper wire
Volume of data per web		363 kbits per week	
Total mass of the web		200g	96.6g Suite components 59.8g Suite batteries 5.6g Comms suite components 21g Comms suite battery 17g wire (component values estimated)

Aerial Section			
Unmanned Aerial Vehicle			example: Aerosonde
	Speed	20ms^{-1}	Assumed value. Aerosonde speed given as 22-42ms^{-1}
	Wingspan	2.9m	
	Battery capacity	1 hour at 20W	
	Payload	5kg	
Altitude		200m	
Number of passes to cover a 1km^2 field		5	related to equivalent image area
Total time of flight		4 minutes 26s	assuming 20ms^{-1}
Communications Payload			
RF Receiver module		Linx ES	example
	Frequency	916MHz	Must not interfere with UAVs communication system
Antenna		Phazar AMR Omni	example
	Gain	2dBi	
	Mass	227g	
Digital Camera		Pentax Optio S5i	example
	Resolution	2560x1920	
	Mass	120g	
	Field of View	73˚	typical value
	Equivalent Image Area	177.7m x 237.7m	Assumed aspect ratio of 4:3
	Number of Images to cover a 1km^2 field	30	6 images per pass

Table 9-14 Baseline for Arctic cryoconite monitoring mission

Although a wireless system could have been proposed, for this application, the use of wires as the intersuite communication link has several advantages. Whereas individual sensor suites can detect small targets, the web is appropriate in detecting larger targets, as the physical network area coverage is wider. The predefined spatial definition of the suites results in a less complex position awareness system than with wireless suites, since all the suites are a known distance apart and do not have to locate each other to form a network. As this distance is known to within a fixed range, the webs can also monitor the growth of the target over time. A wired system also does not have the line-of-sight or interference issues of a wireless system, although the wires do add mass to the system.

One of the fundamental objectives of this project was to design a system that can be used for many different applications with only slight modification to the basic module. Although this discussion has been focused around the cryoconite model, a few basic changes can be made to enable the system to be used to survey the surface of Mars. The principle adaptations refer to the differences between the Martian climate and the terrestrial one. More thermal insulation will need to be added, since the average temperature on the surface is –50˚C. The components will also have to be treated against the increased radiation environment. Whilst moisture is unlikely to be an issue, protection against the fine surface dust will also have to be made. The web concept remains the same, however if a UAV cannot be used for data collection, the webs can be used by a Lander as an extension of its ground coverage, and the data collection module can be attached to the Lander instead.

The use of COTS components is beneficial because it reduces the overall cost of the system and shortens the development time, since all the components have all been designed and tested by their manufacturers. Each components, however, has its own specifications which impose limits on the ranges, sensitivities and operating conditions of each components and ultimately limits the scope of the mission parameters. For some components, such as the battery, alterations to the physical design of the suite will need to be made to accommodate the physical size of the piece. A prototype of the sensor suite can be fabricated in-house, however for the numbers required at mission level, it becomes more cost effective to have the system integrated by specialist contractors. The generic nature of the sensor web, where the core functions remain constant but specific sensors can be change or added to as required is a key part of the design. The use of standard protocols means that other devices can be added to the web as the user requires. This adaptability broadens the range of possible applications to become a cost-effective way of observing many different environments.

Conclusions

The overall aim of the project was given as:

To bring together current commercially available technology and relevant MST into small, standardised spacecraft "primary systems" architecture, multiple units of which can demonstrate collaboration…

This was achieved through the investigation and design of a system which comprises several webs of distributed sensor suites. All aspects of the system design were considered, including deployment strategies and the various required subsystems. The system concept is illustrated below.

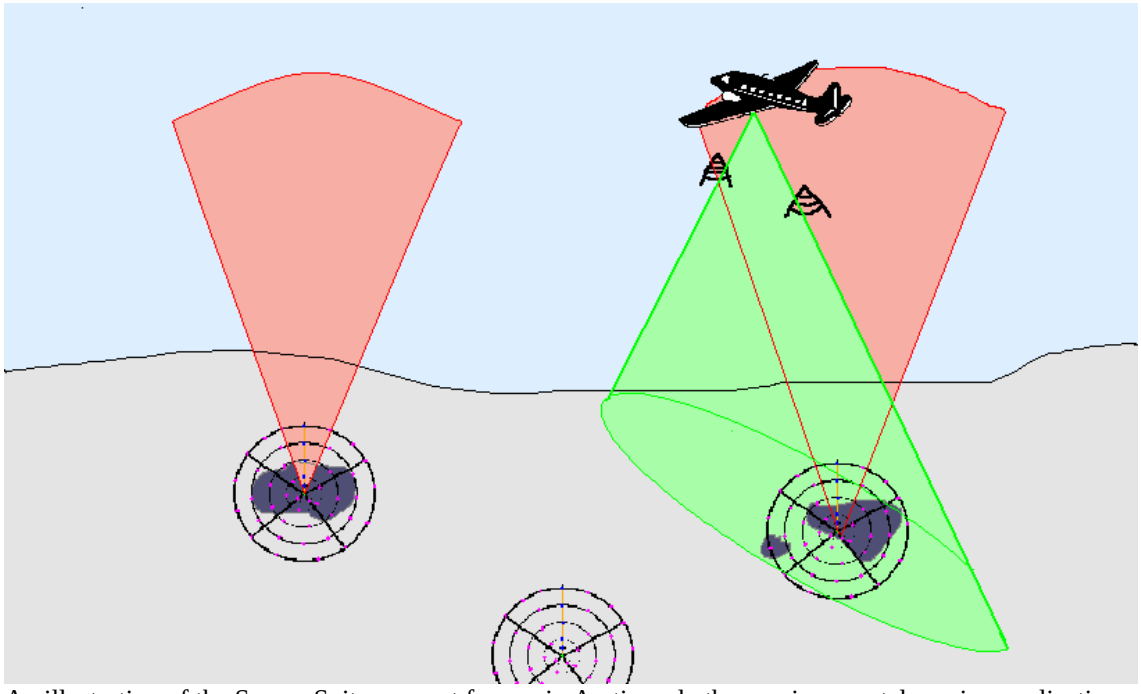

An illustration of the Sensor Suite concept for use in Arctic and other environmental sensing applications

COTS MST components were utilised where possible, thereby reducing the size, mass and overall cost of the sensor suites. Using these components, the proposed volume of each sensor suite is approximately 1.6 x 1.6 x 1.6cm. In addition to the miniaturised components, three-dimensional modular packaging was reviewed and selected. The required collaborative nature of the webs is achieved through the use of a standard I2C data bus between the suites, and a miniaturised RF link for each web to an aerial receiver such as a UAV

The standardisation aspect was addressed through the design of a sensor suite that could be used for a variety of applications with little modification. Existing Distributed Sensor Networks tend to have an application based architecture, however this system is designed to be more generic.

In order to focus the design, a realistic application was investigated. Cryoconites are small holes that form in glaciers. They contain bacteria and the monitoring of these

features is of interest to those studying extremophile life. If found in the polar regions of other planetary bodies, they could also contain biological material. The sensor suite networks have the potential to be deployed over a season and monitor the formation and growth of these holes. This is a novel application for a sensor web.

The systems design was the result of different investigations during this project. Breadboard demonstrators were produced to identify the issues raised by actual hardware, such as having a standard voltage rating for all the components enables a single power source to be used. Computer simulations were performed to establish a preferred deployment pattern for the suites which suggested that a cluster approach would have a number of benefits and could locate targets successfully. Not only could larger targets be found with the cluster, but the system overall had potential practical advantages such as possibly sharing core functions and an ease of intersuite communication. The web also offers redundancy which could increase the system reliability. Paper studies were also carried out on sensor networks and Microsystems Technology.

The use of MST for space was discussed in terms of the adoption of the technology by the industry and the related strategic issues. The overall space industry was examined, and although many have recognised MST as a beneficial technology, the industry as a whole is reluctant to adopt it without further proof.

The sensor suites were investigated from many angles, including from an industrial integration position. It was concluded that it was more economically efficient to contract the integration to a specialist source. A comprehensive mission baseline systems design for the sensor suites was finally produced.

Although the majority of the objectives have been met satisfactorily, the initial aim to demonstrate collaborative suites using hardware has not been fully met. The proposed solution uses the I2C bus and explores potential collaboration, however unfortunately technical difficulties arose when producing the hardware prototype, and as such this is not as advanced as initially envisaged. The web design however is inherently collaborative and several of the related issues have been raised and addressed.

Distributed Sensor Networks and MST for Space are both areas of current ongoing research. They have been acknowledged as a potential way forward, and innovations are being made to further this field. Most of the examples currently in existence are in the research or prototype stage and although there are many COTS sensors on the market, integration techniques will need to be developed further before this kind of the hardware is commonly used for the wider range of applications. In addition, further moves towards a standard for components and increased inter-disciplinary co-operation is needed before the sensor suite concept as described above could be a reality.

Recommendations and Further Work

Some of the key recommendations for further work are outlined below.

The systems design for the cryoconite monitoring application should be expanded further. Areas that would benefit from additional investigation would be:

- Power and Communications subsystems, with particular focus on energy harvesting and the completion of a comprehensive link budget.
- The Thermal subsystem and insulation issues, especially adaptation for use in extreme climates.
- Development of the deployment mechanisms
- Investigation into the benefits of data compression and aggregation for processing and communications.
- Expand the networking capabilities, for example wireless collaboration between webs.

Further, more sophisticated deployment simulations should be undertaken. These simulations could investigate the effects of different suite reliabilities on the system and simulate various environments based on broader applications.

A key recommendation is that this design should be developed and both a hardware and system prototype produced and tested in the field.

This is a concept has great potential for many different applications and the Author hopes that the initial groundwork presented here will be expanded beyond the boundaries of this project.

APPENDIX A

Example Visual Basic Code creating a simulated Martian rock field and simulating a uniform sensor suite deployment pattern

```
Sub rockgrid()

Dim a As Long, b As Long
Dim itover100 As Long, it100to50 As Long, it50to20 As Long, it20to10 As Long, it10to2 As Long

'a and b set axes of the grid  - 10 x 10 in this case
a = Range("a13").Value
b = Range("a14").Value

Dim pi As Double
pi = Cells(9, 1)

'use the table from the graph to get the number of rocks or number of iterations in each range
itover100 = Cells(25, 3)
it100to50 = Cells(26, 3)
it50to20 = Cells(27, 3)
it20to10 = Cells(28, 3)
it10to2 = Cells(29, 3)

'the following selects a random cell to place a value in for the iteration number of rocks

'Rocks with diameter over 100cm
Dim i1 As Long, j1 As Long, d1 As Long, k1 As Long
For k1 = 1 To itover100

i1 = Int(Rnd * a) + 4
j1 = Int(Rnd * b) + 3
'diameter of full square is 112cm so values over the equivalent area assume full
d1 = Int(pi * (112 / 2) ^ 2)
Cells(i1, j1) = d1
Next k1

'100cm to 50cm range
Dim i2 As Long, j2 As Long, d2 As Long, k2 As Long, r2 As Long, c2 As Long
For k2 = 1 To it100to50

i2 = Int(Rnd * a) + 4
j2 = Int(Rnd * b) + 3
c2 = Int((100 - 51) * Rnd + 51)
d2 = Int(pi * (c2 / 2) ^ 2)
'if cell is already assigned then add to it
r2 = Cells(i2, j2)
If r2 = 0 Then Cells(i2, j2) = d2
If r2 > 0 Then Cells(i2, j2) = r2 + d2
Next k2

'50cm to 20cm range
Dim i3 As Long, j3 As Long, d3 As Long, k3 As Long, r3 As Long, c3 As Long
```

```
For k3 = 1 To it50to20

i3 = Int(Rnd * a) + 4
j3 = Int(Rnd * b) + 3
c3 = Int((50 - 21) * Rnd + 21)
d3 = Int(pi * (c3 / 2) ^ 2)
'if cell is already assigned then add to it
r3 = Cells(i3, j3)
If r3 = 0 Then Cells(i3, j3) = d3
If r3 > 0 Then Cells(i3, j3) = r3 + d3
Next k3

'20cm to 10cm range
Dim i4 As Long, j4 As Long, d4 As Long, k4 As Long, r4 As Long, c4 As Long
For k4 = 1 To it20to10

i4 = Int(Rnd * a) + 4
j4 = Int(Rnd * b) + 3
c4 = Int((20 - 11) * Rnd + 11)
d4 = Int(pi * (c4 / 2) ^ 2)
'if cell is already assigned then add to it
r4 = Cells(i4, j4)
If r4 = 0 Then Cells(i4, j4) = d4
If r4 > 0 Then Cells(i4, j4) = r4 + d4
Next k4

'10cm to 2cm range
Dim i5 As Long, j5 As Long, d5 As Long, k5 As Long, r5 As Long, c5 As Long
For k5 = 1 To it10to2

i5 = Int(Rnd * a) + 4
j5 = Int(Rnd * b) + 3
c5 = Int((10 - 2) * Rnd + 2)
d5 = Int(pi * (c5 / 2) ^ 2)
'if cell is already assigned then add to it
r5 = Cells(i5, j5)
If r5 = 0 Then Cells(i5, j5) = d5
If r5 > 0 Then Cells(i5, j5) = r5 + d5
Next k5

End Sub
```

```
Sub uniformcolour()
'colour in the squares equivilent to a uniform distribution

Const limit1 As Integer = 7854
'7854 is the area of 100cm circle
Dim sumred As Double
sumred = 0
For Each c1 In Range("c4:l13")
If c1.Value > limit1 Or c1.Value = 7854 Then
   c1.Interior.ColorIndex = 3
   End If
```

```
 If c1.Value > limit1 Or c1.Value = 7854 Then sumred = sumred + 1
 Next c1
 Cells(19, 8) = sumred

Const limit2 As Integer = 3848
'70% of the area of 100cm circle
Dim sumor As Double
sumor = 0
For Each c2 In Range("c4:l13")
If c2.Value > limit2 And c2.Value < 7854 Then
    c2.Interior.ColorIndex = 45
    End If
 If c2.Value > limit2 And c2.Value < 7854 Then sumor = sumor + 1
 Next c2
 Cells(20, 8) = sumor

Const limit3 As Integer = 707
'the area of 30cm circle
Dim sumyel As Double
sumyel = 0
For Each c3 In Range("c4:l13")
If c3.Value > limit3 And c3.Value < 3848 Or c3.Value = 3848 Then
    c3.Interior.ColorIndex = 6
    End If
 If c3.Value > limit3 And c3.Value < 3848 Or c3.Value = 3848 Then sumyel = sumyel + 1
 Next c3
 Cells(21, 8) = sumyel

Const limit4 As Integer = 707
'the area of 30cm circle
Dim sumgr As Double
sumgr = 0
For Each c4 In Range("c4:l13")
If c4.Value < limit4 Or c4.Value = 707 Then
    c4.Interior.ColorIndex = 4
    End If
 If c4.Value < limit4 Or c4.Value = 707 Then sumgr = sumgr + 1
 Next c4
 Cells(22, 8) = sumgr

End Sub
```

APPENDIX B

Example Visual Basic code using the random distribution of sensor suites to locate a block target. (Includes mean, standard deviation and reliability adjustment)

```
Sub resource1randomfail()
Rem get the average number of each colour and adds a percentage of failed sensors
Dim i As Long, j As Long, k As Long
Dim iteration As Long
Dim a As Long, b As Long
Dim fa As Double, fail As Double

Dim r As Long
Rem simulates putting sensors randomly onto rock field.
Rem aveloop is the number of simulations
Dim aveloop As Long, v As Long
Dim red As Double, orange As Double, yellow As Double, green As Double
Dim loopred As Double, loopor As Double, loopyel As Double, loopgr As Double
Dim countdes As Long, count2 As Long, count5 As Long, count6 As Long, count11 As Long,
countmore As Long, countav As Long, countaverage As Long
Dim failave As Long

aveloop = Cells(21, 4)
red = 0
orange = 0
yellow = 0
green = 0

count2 = 0
count5 = 0
count6 = 0
count11 = 0
countmore = 0
countav = 0
countaverage = 0
failave = 0

 For v = 1 To aveloop

Rem first copy from first sheet and uncolour the grid and set resource squares to blue if not
picked they will stay blue
cpgridresf1
res1

Rem a and b set axes of grid
a = Range("a20").Value
b = Range("a21").Value

Rem iteration is the number of sensors
iteration = Cells(20, 4)

Dim c As Long
Dim sumred2 As Double, sumor2 As Double, sumyel2 As Double, sumgr2 As Double
```

```
Dim count As Long
count = 0
fail = 0

countdes = 0
sumred2 = 0
sumor2 = 0
sumyel2 = 0
sumgr2 = 0

Rem f = fraction that fail, ie 0.3 = 30% fail, or 70% reliability
fa = Cells(21, 7)
Rem selects a random cell to place a value in for iteration number of rocks for (1-f) sensors, the successful ones

For k = 1 To (iteration * (1 - fa))
i = Int(Rnd * a) + 5
j = Int(Rnd * b) + 5
Rem assign resource value to cells
i2 = Cells(21, 14)
j2 = Cells(21, 15)
i3 = Cells(22, 14)
j3 = Cells(22, 15)
i4 = Cells(23, 14)
j4 = Cells(23, 15)
i5 = Cells(24, 14)
j5 = Cells(24, 15)
i6 = Cells(25, 14)
j6 = Cells(25, 15)
i7 = Cells(26, 14)
j7 = Cells(26, 15)

c = 10

Rem if already assigned a value, then it adds to it
r = Cells(i, j)
If r = 0 Then Cells(i, j) = c
If r > 0 Then Cells(i, j) = r + c

Rem colours in the squares same as before, but only in selected squares

If Cells(i, j) > 7854 Then
   Cells(i, j).Select
   With Selection.Interior
      .ColorIndex = 3
      .Pattern = xlSolid
   End With

ElseIf Cells(i, j) > 3848 And Cells(i, j) < 7854 Then
   Cells(i, j).Select
   With Selection.Interior
      .ColorIndex = 45
      .Pattern = xlSolid
   End With
ElseIf Cells(i, j) > 707 And Cells(i, j) < 3848 Or Cells(i, j) = 3848 Then
```

```
    Cells(i, j).Select
    With Selection.Interior
        .ColorIndex = 6
        .Pattern = xlSolid
    End With
ElseIf Cells(i, j) < 707 Or Cells(i, j) = 707 Then
    Cells(i, j).Select
    With Selection.Interior
        .ColorIndex = 4
        .Pattern = xlSolid
    End With
End If

If Cells(i, j) > 7854 Then sumred2 = sumred2 + 1
If Cells(i, j) > 3848 And Cells(i, j) < 7854 Then sumor2 = sumor2 + 1
If Cells(i, j) > 707 And Cells(i, j) < 3848 Or Cells(i, j) = 3848 Then sumyel2 = sumyel2 + 1
If Cells(i, j) < 707 Or Cells(i, j) = 707 Then sumgr2 = sumgr2 + 1

Rem counts up number of sensors finding the target

If i = i2 And j = j2 Then count = count + 1
If i = i3 And j = j3 Then count = count + 1
If i = i4 And j = j4 Then count = count + 1
If i = i5 And j = j5 Then count = count + 1
If i = i6 And j = j6 Then count = count + 1
If i = i7 And j = j7 Then count = count + 1

Cells(30, 13) = count
Next k

Rem puts the number finding the target into categories

If count < 2 Or count = 2 Then count2 = count2 + 1
If count > 2 And count < 6 Then count5 = count5 + 1
If count = 6 Then count6 = count6 + 1
If count > 6 And count < 11 Or count = 11 Then count11 = count11 + 1
If count > 11 Then countmore = countmore + 1

Cells(20, 8) = count2
Cells(20, 9) = count5
Cells(20, 10) = count6
Cells(20, 11) = count11
Cells(20, 12) = countmore

Cells(24, 1) = sumred2
Cells(24, 2) = sumor2
Cells(24, 3) = sumyel2
Cells(24, 4) = sumgr2

loopred = Cells(24, 1)
Cells(26 + v, 1) = loopred
red = red + loopred
Cells(23, 9) = red

repeat for orange, yellow and green (not shown)
```

```
Rem for those that fail
Dim kf As Long
For kf = 1 To (iteration * fa)

i = Int(Rnd * a) + 5
j = Int(Rnd * b) + 5
Rem assign resource value to cells
i2 = Cells(21, 14)
j2 = Cells(21, 15)
i3 = Cells(22, 14)
j3 = Cells(22, 15)
i4 = Cells(23, 14)
j4 = Cells(23, 15)
i5 = Cells(24, 14)
j5 = Cells(24, 15)
i6 = Cells(25, 14)
j6 = Cells(25, 15)
i7 = Cells(26, 14)
j7 = Cells(26, 15)

c = 10
Rem if already assigned a value, then it adds to it
r = Cells(i, j)
If r = 0 Then Cells(i, j) = c
If r > 0 Then Cells(i, j) = r + c

Rem colour those that fail a different colour and do a separate count
Cells(i, j).Select
With Selection.Interior
    .ColorIndex = 30
    .Pattern = xlSolid
End With

If i = i2 And j = j2 Then fail = fail + 1
If i = i3 And j = j3 Then fail = fail + 1
If i = i4 And j = j4 Then fail = fail + 1
If i = i5 And j = j5 Then fail = fail + 1
If i = i6 And j = j6 Then fail = fail + 1
If i = i7 And j = j7 Then fail = fail + 1

Cells(22, 7) = kf
Next kf
Rem work out averages and sd for find and fail

countav = countav + count
Cells(29, 8) = countav
Cells(32 + v, 13) = count

failave = failave + fail
Cells(33, 8) = failave
Cells(32 + v, 14) = fail

Cells(32 + v, 15) = (count + fail)
```

```
Cells(20, 7) = v
Next v

Cells(30, 8) = countav / aveloop
' Cells(21, 6) = countaverage / aveloop
Cells(34, 8) = failave / aveloop
Cells(36, 8) = (countav + failave) / aveloop

Dim ifind As Long, tfind As Double, sumsqfind As Double, sdfind As Double, avefind As Double
Rem standard dev of finding target

avefind = Cells(30, 8)
For ifind = 1 To aveloop
tfind = Cells(32 + ifind, 13)
sumsqfind = sumsqfind + (tfind - avefind) ^ 2
Next ifind
sdfind = Sqr(sumsqfind / (aveloop - 1))
Cells(31, 8) = sdfind

Dim ifail As Long, tfail As Double, sumsqfail As Double, sdfail As Double, avefail As Double
Rem standard dev of fails

avefail = Cells(34, 8)
For ifail = 1 To aveloop
tfail = Cells(32 + ifail, 14)
sumsqfail = sumsqfail + (tfail - avefail) ^ 2
Next ifail
sdfail = Sqr(sumsqfail / (aveloop - 1))
Cells(35, 8) = sdfail

Dim iboth As Long, tboth As Double, sumsqboth As Double, sdboth As Double, aveboth As
Double
Rem standard dev of fails that find target

aveboth = Cells(36, 8)
For iboth = 1 To aveloop
tboth = Cells(32 + iboth, 15)
sumsqboth = sumsqboth + (tboth - aveboth) ^ 2
Next iboth
sdboth = Sqr(sumsqboth / (aveloop - 1))
Cells(37, 8) = sdboth


Dim ir As Long, io As Long, iy As Long, ig As Long
Rem average number of reds
Dim avered As Double, averagered As Double, tred As Double, sumsqred As Double, sdred As
Double
avered = Cells(23, 9)
Cells(24, 9) = avered / aveloop
averagered = Cells(24, 9)

For ir = 1 To aveloop
tred = Cells(26 + ir, 1)
sumsqred = sumsqred + (tred - averagered) ^ 2
```

```
Next ir
sdred = Sqr(sumsqred / (aveloop - 1))
Cells(26, 9) = sdred
repeat for orange, yellow and green

End Sub

Sub cpgridresf1()
copy grid and paste into sheet
Sheets("rock grid").Select
    ActiveWindow.ScrollRow = 1
    Range("C4:L13").Select
    Selection.Copy
    Sheets("failures resource1").Select
    Range("E5").Select
    ActiveSheet.Paste
    Application.CutCopyMode = False
    Range("E5:N14").Select
    Selection.Interior.ColorIndex = xlNone
End Sub

Sub res1()
' colours resources squares blue
    Range("J11:L12").Select
    Selection.Interior.ColorIndex = 41
' Put a border around
    Range("J11:L12").Select
    Selection.Borders(xlDiagonalDown).LineStyle = xlNone
    Selection.Borders(xlDiagonalUp).LineStyle = xlNone
    With Selection.Borders(xlEdgeLeft)
        .LineStyle = xlContinuous
        .Weight = xlThick
        .ColorIndex = xlAutomatic
    End With
    With Selection.Borders(xlEdgeTop)
        .LineStyle = xlContinuous
        .Weight = xlThick
        .ColorIndex = xlAutomatic
    End With
    With Selection.Borders(xlEdgeBottom)
        .LineStyle = xlContinuous
        .Weight = xlThick
        .ColorIndex = xlAutomatic
    End With
    With Selection.Borders(xlEdgeRight)
        .LineStyle = xlContinuous
        .Weight = xlThick
        .ColorIndex = xlAutomatic
    End With
    Selection.Borders(xlInsideVertical).LineStyle = xlNone
    Selection.Borders(xlInsideHorizontal).LineStyle = xlNone
End Sub
```

APPENDIX C

Weather in Adventdalen – 78N 16E (Glacier Midre Lovenbreen is 79N 12E)

May 16 2004

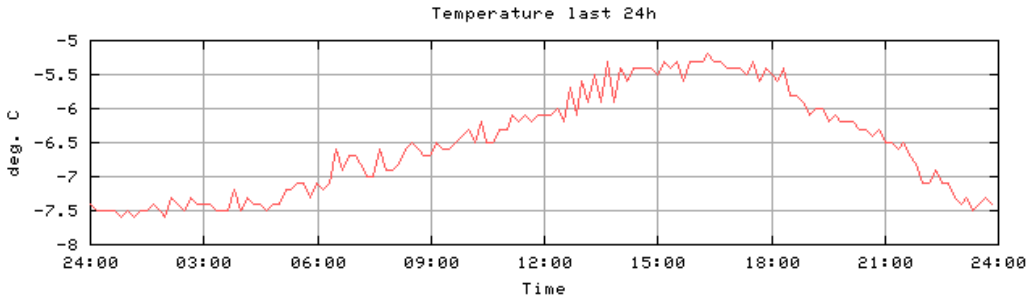

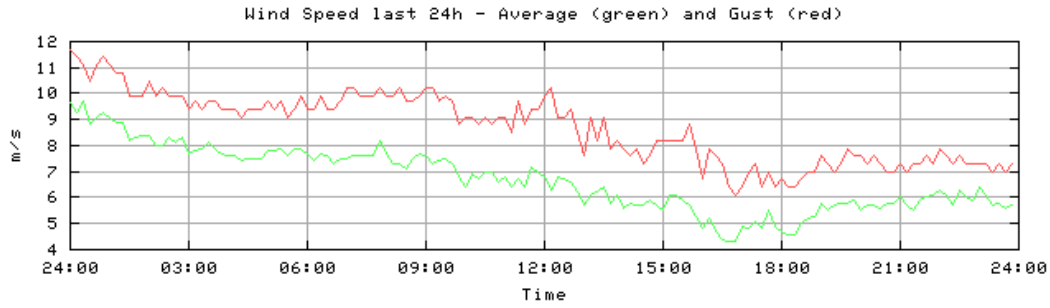

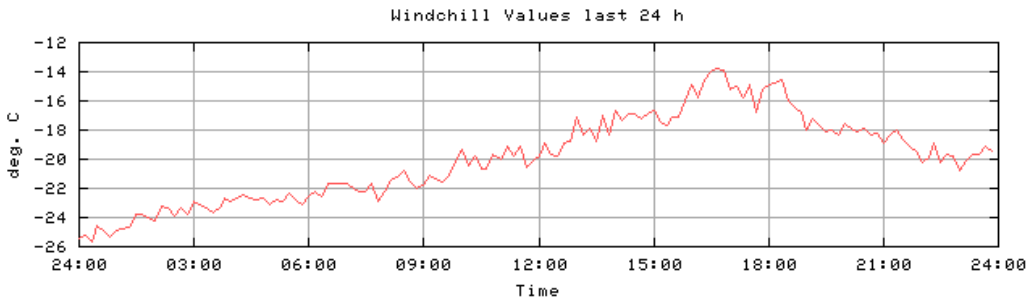

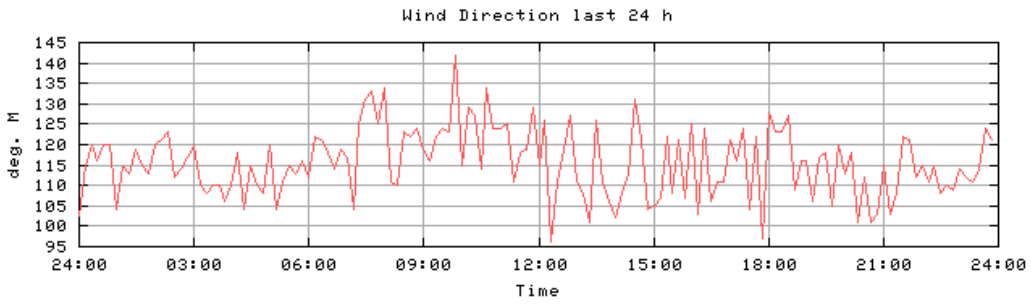

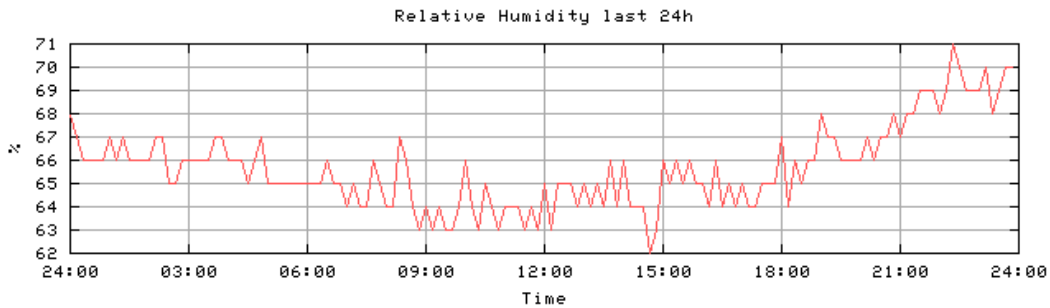

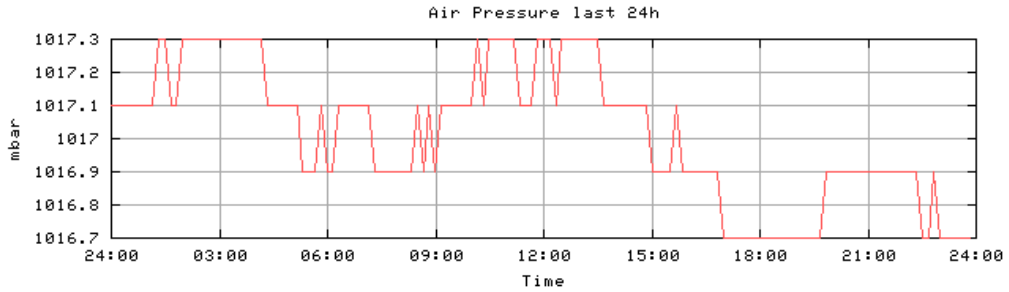

March 16 2004

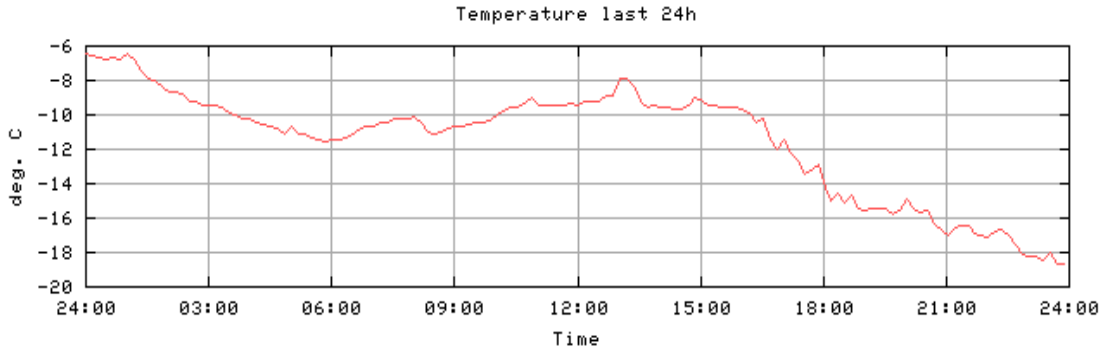

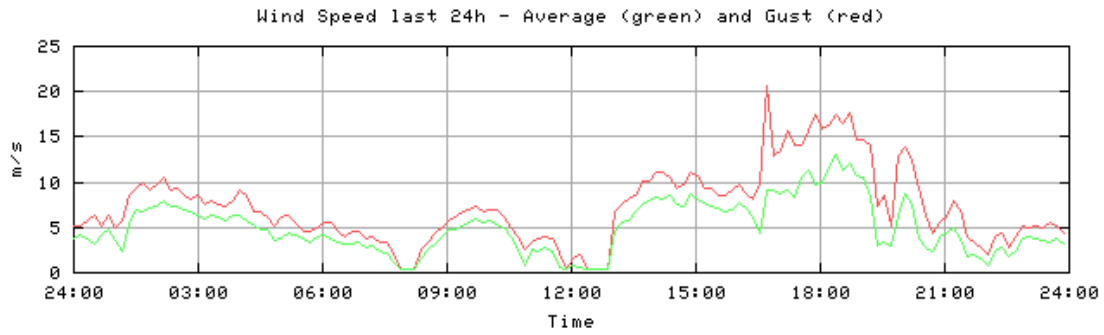

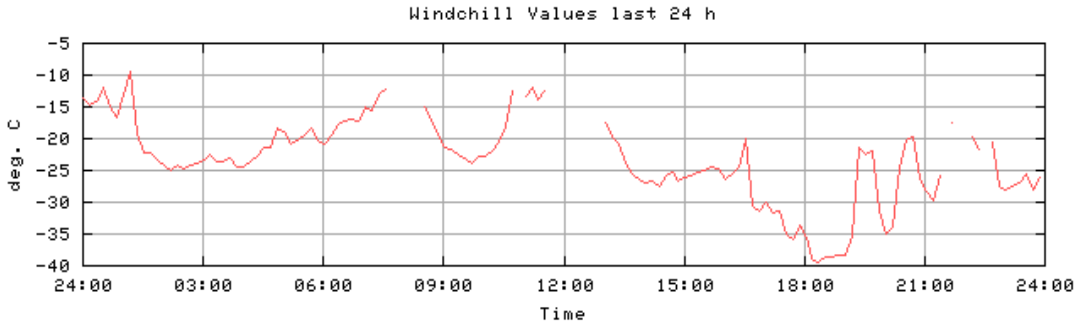

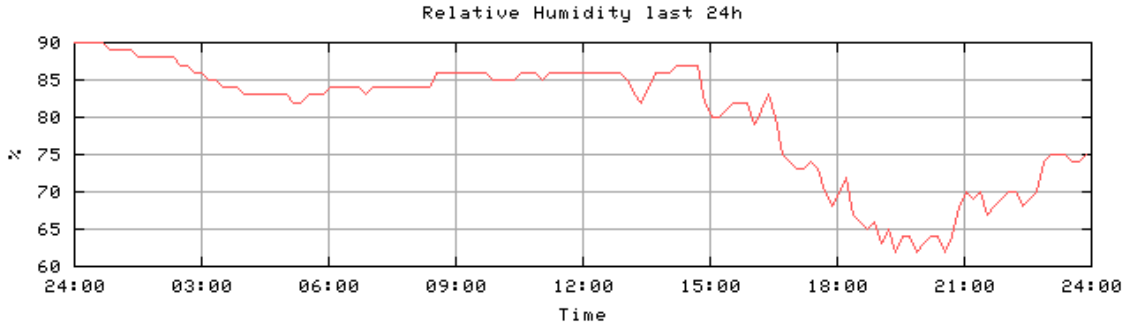

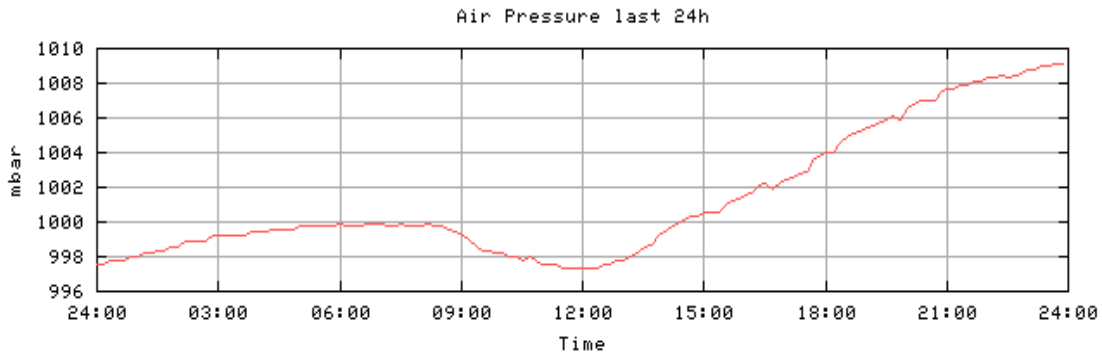

January 16 2004

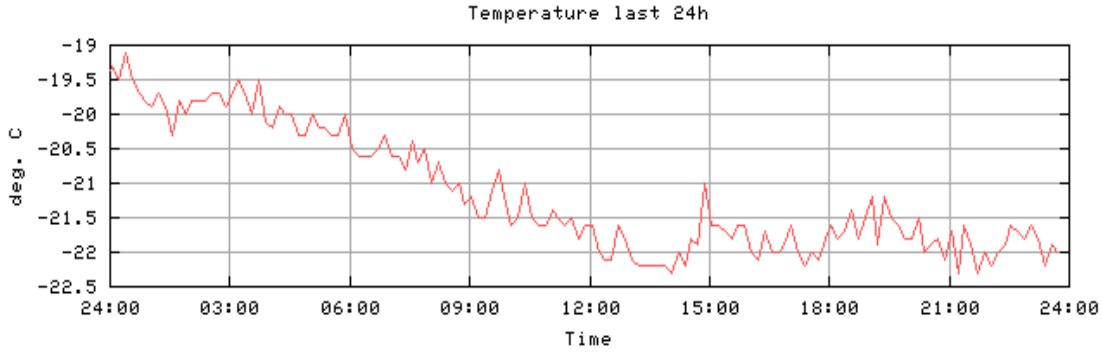

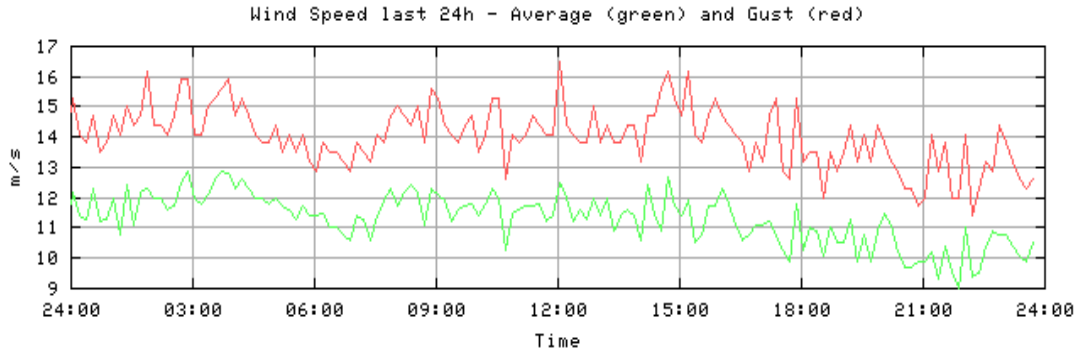

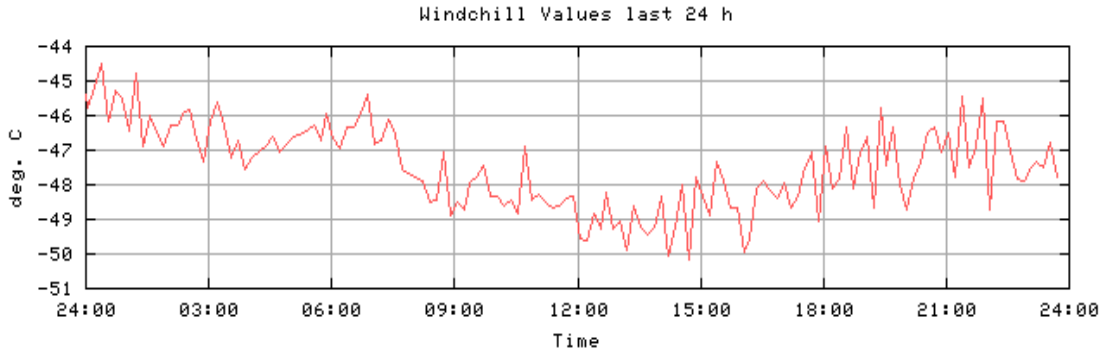

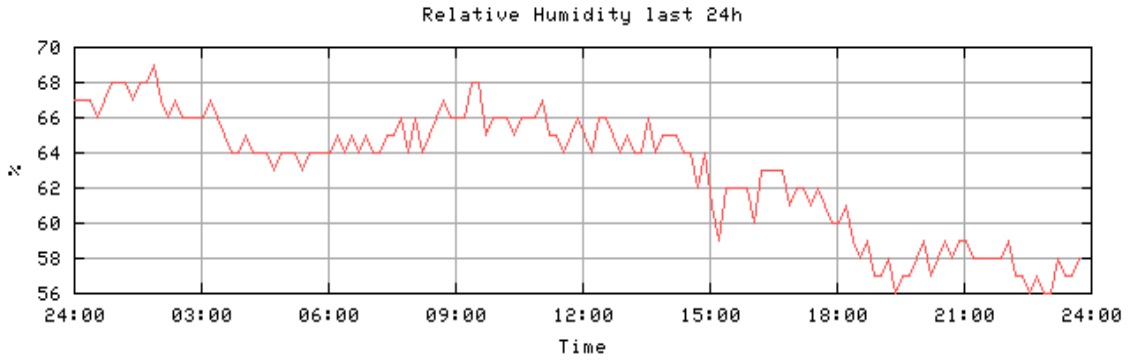

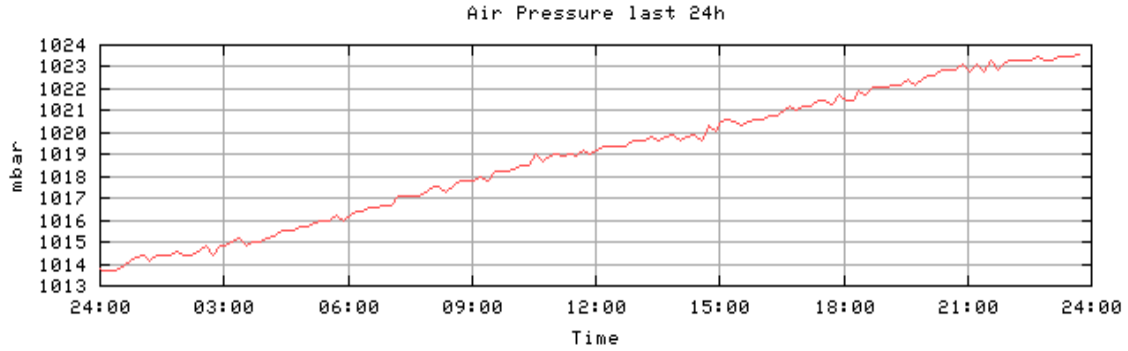

November 16 2003

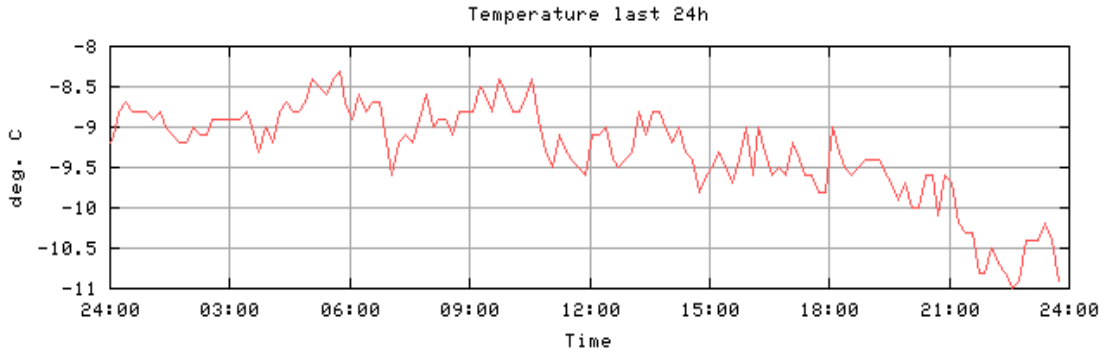

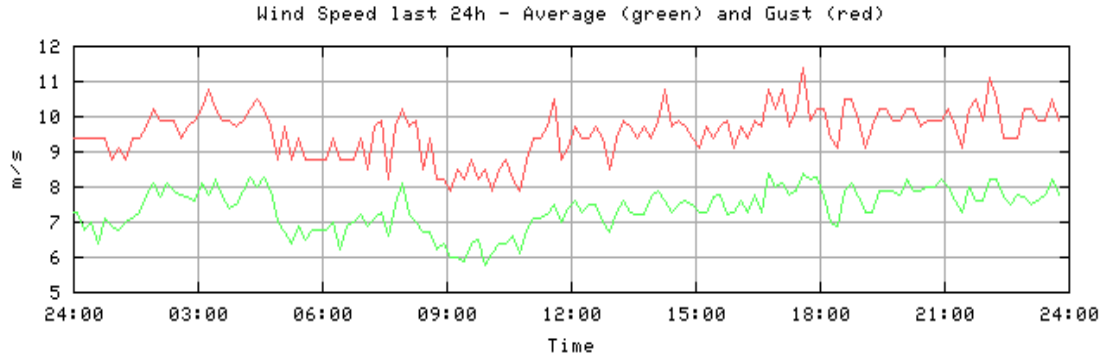

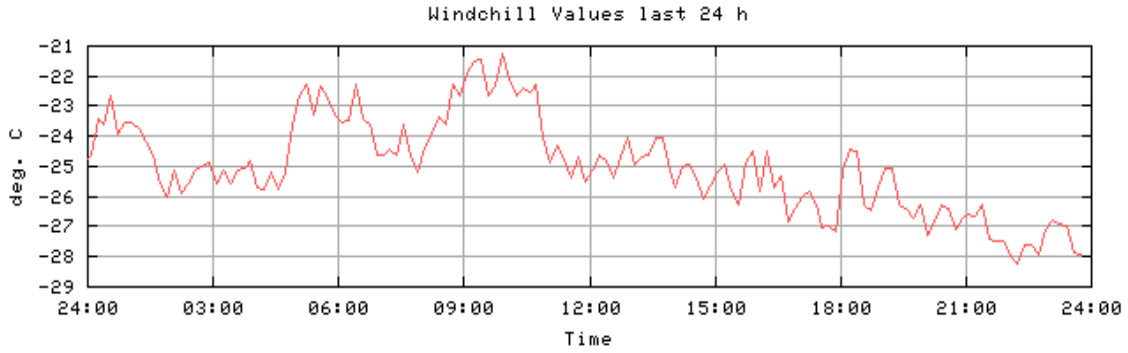

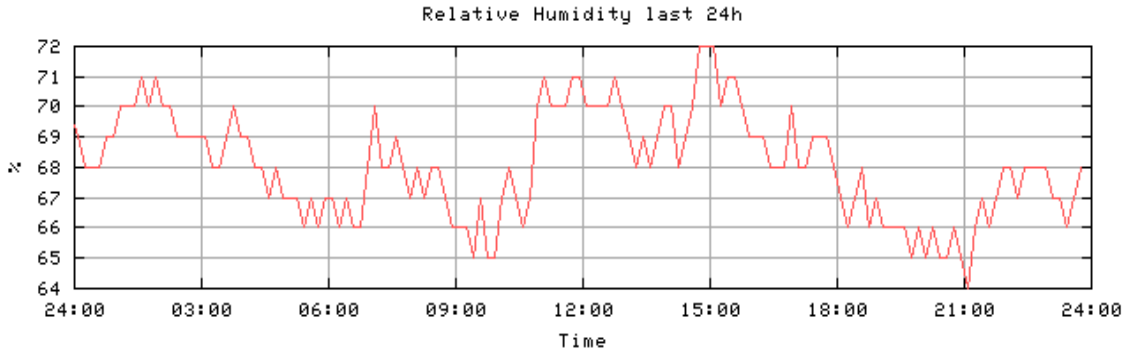

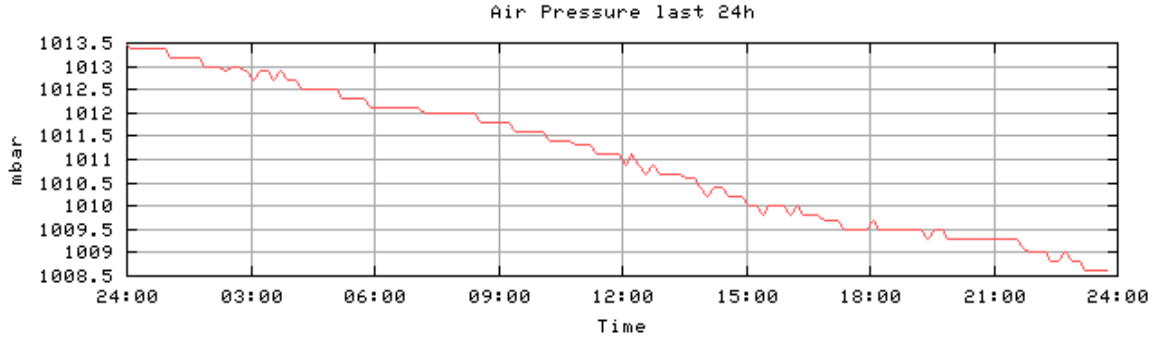

September 16 2003

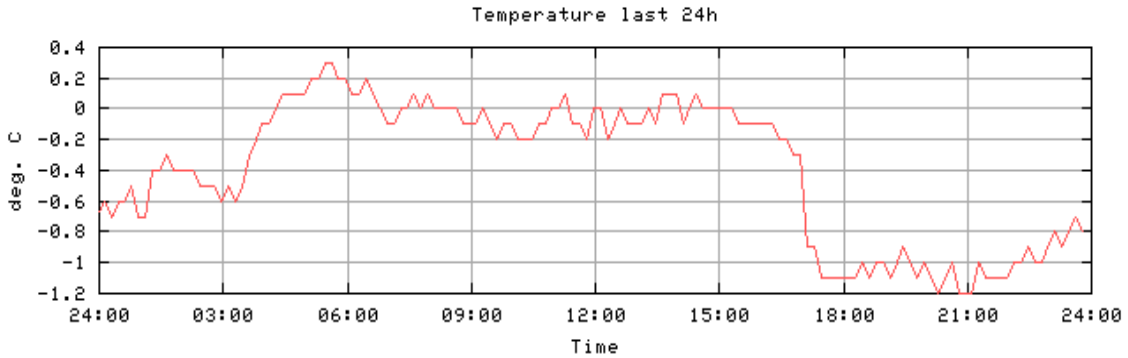

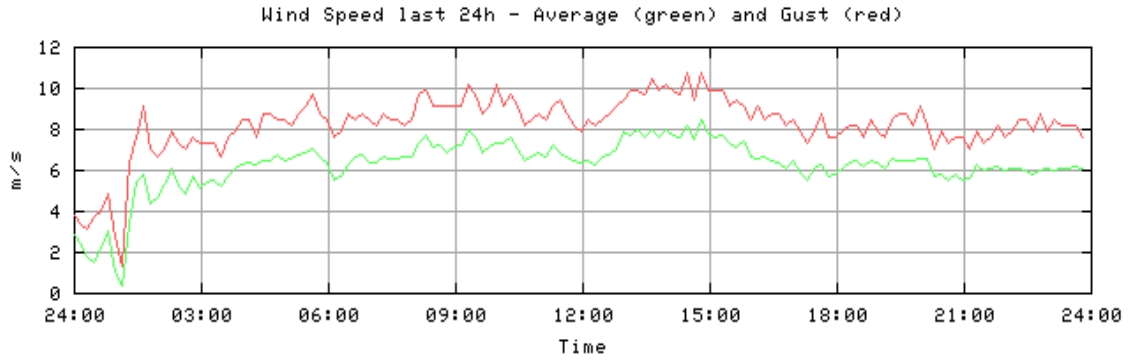
Wind Speed last 24h - Average (green) and Gust (red)
m/s
0
2
4
6
8
10
12
24:00
03:00
06:00
09:00
12:00
15:00
18:00
21:00
24:00
Time

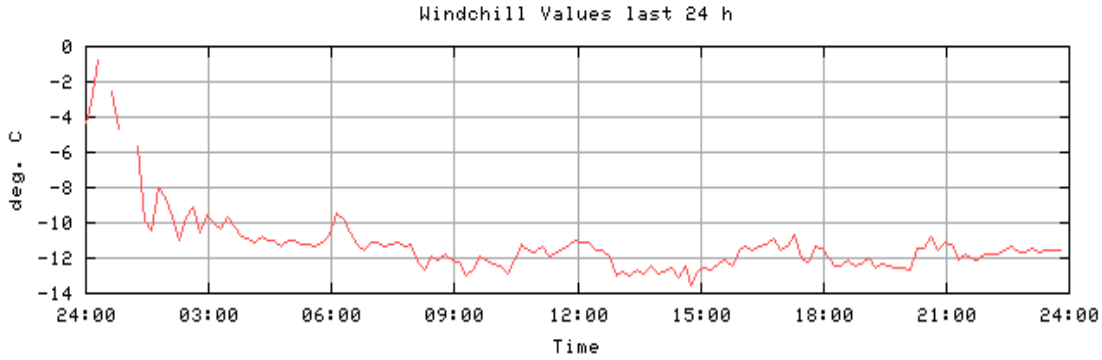
Windchill Values last 24 h
deg. C
0
-2
-4
-6
-8
-10
-12
-14
24:00
03:00
06:00
09:00
12:00
15:00
18:00
21:00
24:00
Time

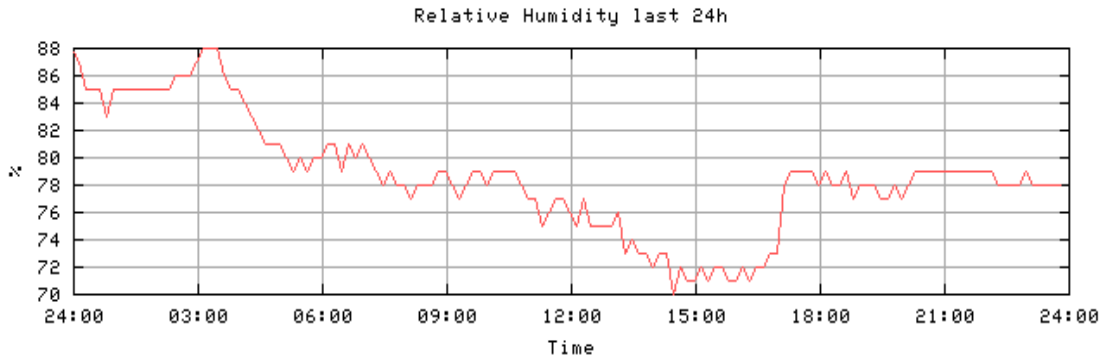
Relative Humidity last 24h
%
70
72
74
76
78
80
82
84
86
88
24:00
03:00
06:00
09:00
12:00
15:00
18:00
21:00
24:00
Time

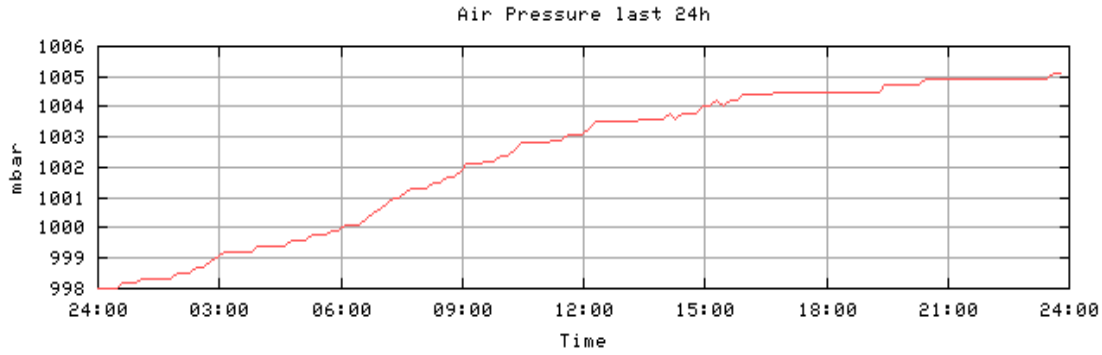
Air Pressure last 24h
mbar
998
999
1000
1001
1002
1003
1004
1005
1006
24:00
03:00
06:00
09:00
12:00
15:00
18:00
21:00
24:00
Time

July 16 2003

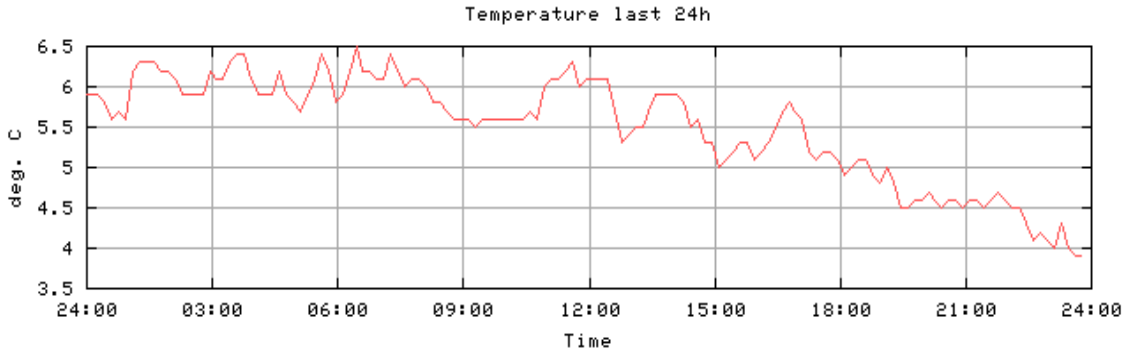
Temperature last 24h
deg. C
6.5
6
5.5
5
4.5
4
3.5
24:00
03:00
06:00
09:00
12:00
15:00
18:00
21:00
24:00
Time

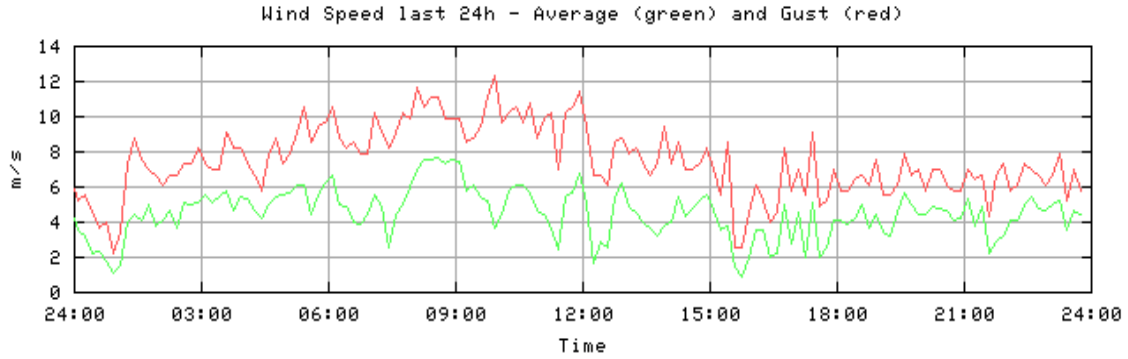
Wind Speed last 24h - Average (green) and Gust (red)
m/s
14
12
10
8
6
4
2
0
24:00
03:00
06:00
09:00
12:00
15:00
18:00
21:00
24:00
Time

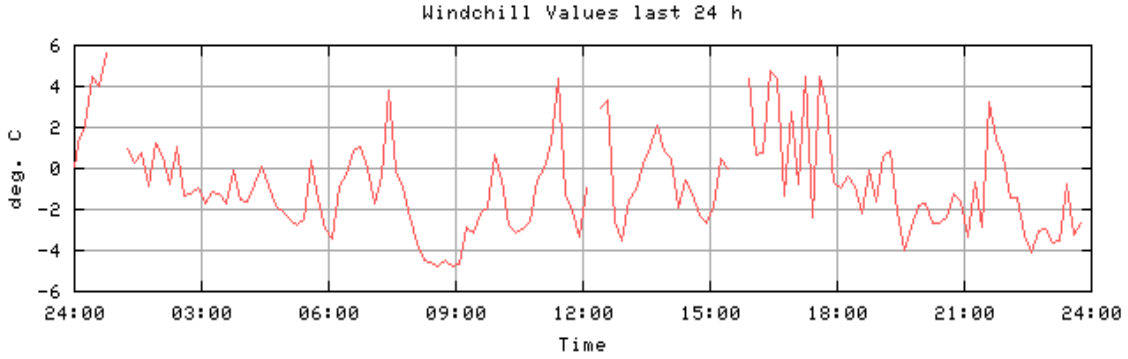
Windchill Values last 24 h
deg. C
6
4
2
0
-2
-4
-6
24:00
03:00
06:00
09:00
12:00
15:00
18:00
21:00
24:00
Time

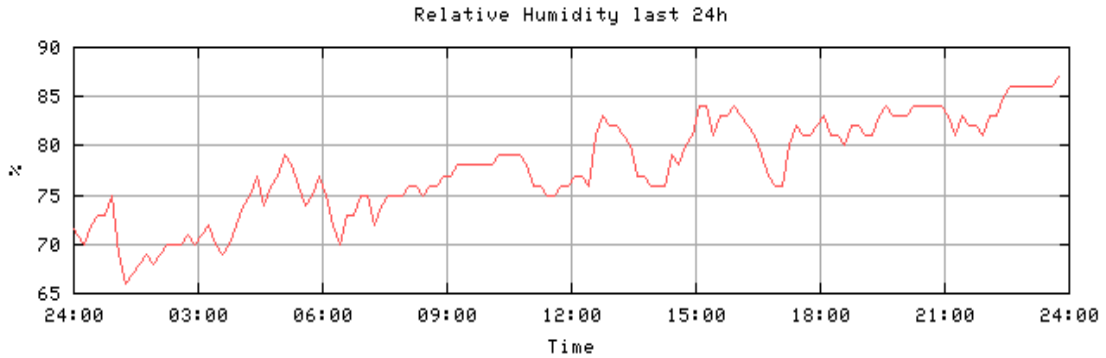
Relative Humidity last 24h
%
90
85
80
75
70
65
24:00
03:00
06:00
09:00
12:00
15:00
18:00
21:00
24:00
Time

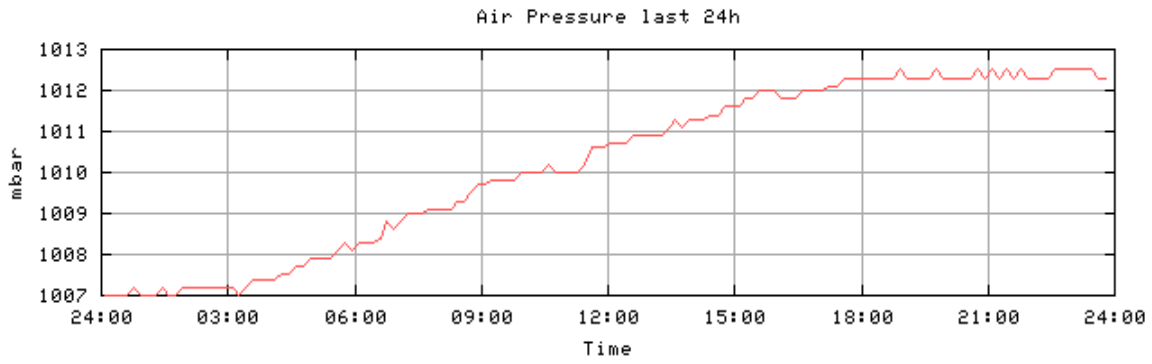

Additional temperature graphs

June 16 2003

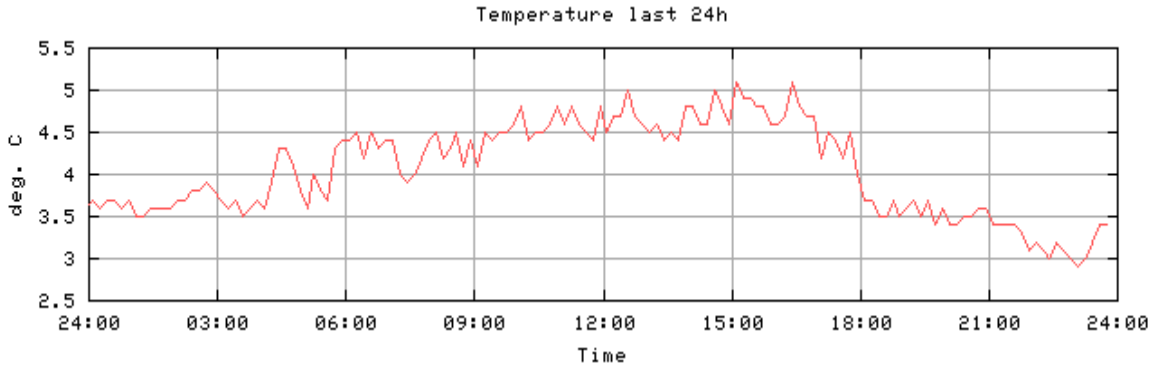

August 16 2003

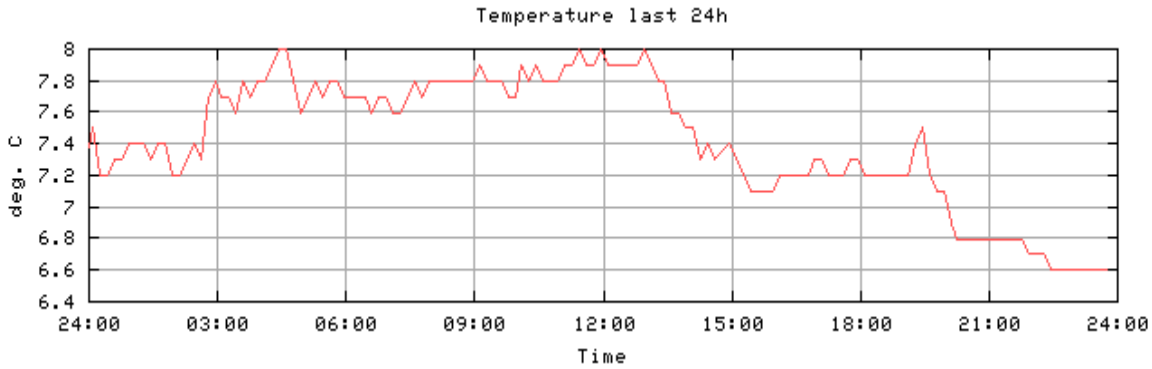

October 16 2003

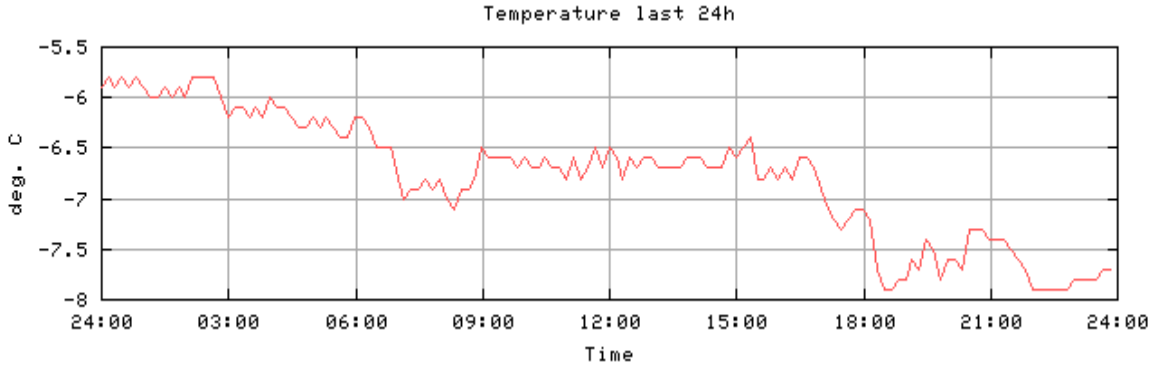

December 16 2003

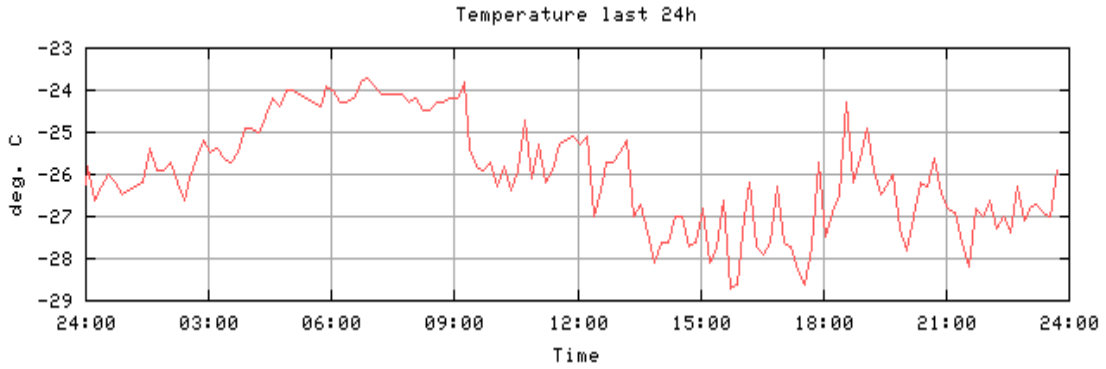

February 16 2004

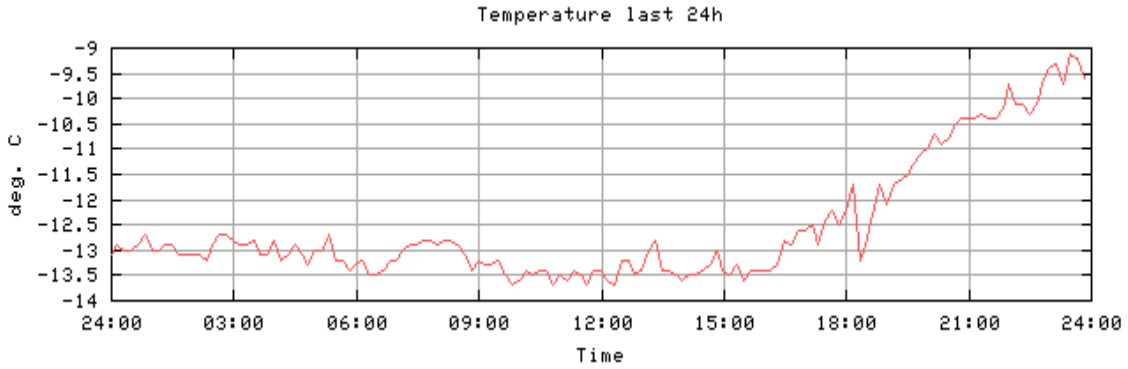

April 16 2004

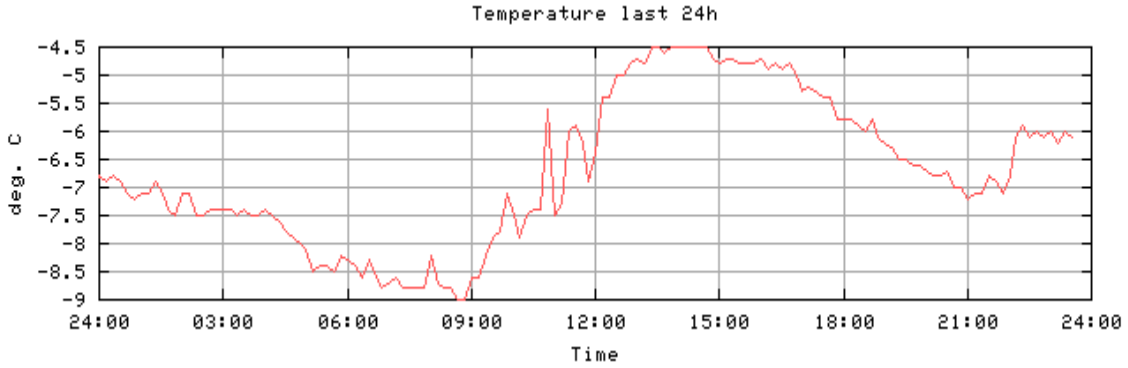

APPENDIX D

Thermal Conduction Notes

(courtesy of Dr. S.E.Hobbs)

$$\begin{aligned}
\text{area} &= \int mf(m)d(\log m) \\
&= \int mf(m)d(\log_{10} e \ln m) \\
&= \log e \int mf(m)d(\ln m) \\
&= \log e \int mf(m)\frac{dm}{m} \\
&= \log e \int f(m)dm
\end{aligned}$$

Thus the integrated area under the curve in the meteorological format is proportional to the contribution from the mass interval. The area should be divided by $\log e = 0.43429$ (or multiplied by 2.30259) to obtain the contribution correctly normalised when $\log_{10} m$ is used for the x-axis.

9.3.3 Area and Mass Fluxes

The number flux density as a function of mass derived above can be used to calculate area and mass fluxes by weighting the number flux by the cross-sectional area or mass of the impacting particles. Thus the area flux (F_A, typical units $\mathrm{m^2\ m^{-2}\ s^{-1}} = \mathrm{s^{-1}}$) between masses m_1 and m_2 is given by (assuming that the particles are spherical with known density ρ)

$$F_A(m_1, m_2) = \int_{m_1}^{m_2} A(m)f(m)dm \quad (9.24)$$

$$\simeq \int_{m_1}^{m_2} \pi r^2(m)f(m)dm \quad (9.25)$$

where $r(m) = \left(\frac{3m}{4\pi\rho}\right)^{1/3}$

The mass flux (F_M, typical units $\mathrm{g\ m^{-2}\ s^{-1}}$) is

$$F_M(m_1, m_2) = \int_{m_1}^{m_2} mf(m)dm \quad (9.26)$$

Other derived fluxes can be obtained as required. In broad terms, the area flux is used to estimate the area of holes made in an exposed surface, and the mass flux for momentum transfer. Rules which are a function of mass or size can be implemented with these expressions. Extensions to allow for angular and velocity distributions of the particles can be combined with these mass-dependent distributions to give a more complete description of the micrometeoroid fluxes (the simplest cases to implement are those where the distributions are independent).

S.E. Hobbs, Technote (from GAIA ref SEH.doc), 17/8/04

9.4 Thermal Conduction

Analytical relationships giving the heat (quasi-static) flux in terms of the temperature difference, geometry and thermal conductivity can be derived for some simple geometries. Figure 9.5 shows the notation for either a cylindrical or a spherical geometry.

It is assumed that the system has reached a steady-state equilibrium, i.e. Q is constant. In both cases (cylindrical and spherical) the symmetry means that the heat flow is radial (and is in the opposite sense to the temperature gradient).

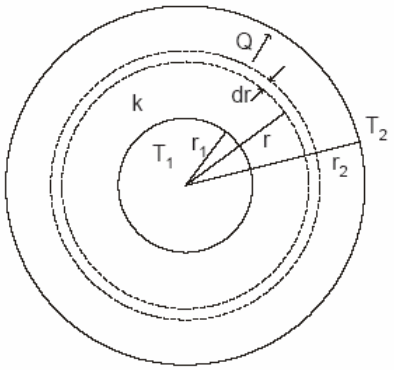

Figure 9.5: Diagram showing the notation used for heat flux analysis for cylindrical or spherical geometry. The flux Q is due to a temperature difference between an inner surface (radius r_1, temperature T_1) and an outer surface (radius r_2, temperature T_2). The homogeneous conducting medium has isotropic conductivity k. An elemental surface of radius r and thickness dr is shown.

9.4.1 One-dimensional Geometry

For a heat flow Q between parallel flat surfaces of area A distance d apart (ignoring edge effects) and temperature difference dT, the thermal conductivity k is defined such that

$$Q = \frac{kAdT}{d} \quad (9.27)$$

$$k = \frac{Qd}{AdT} \quad (9.28)$$

k has units of W m^{-1} K^{-1}. Note that this simple expression can be used for geometries which are effectively one-dimensional, e.g. parallel flat surfaces and struts.

9.4.2 Cylindrical geometry

Considering the elemental surface of thickness dr, the heat flux per unit length q is

$$q = -\frac{2\pi kr(T_{r+dr} - T_r)}{kdr} \quad (9.29)$$

$$dT = -\frac{q}{2\pi r}dr \quad (9.30)$$

This can be integrated to find the temperature difference

$$T_2 - T_1 = -\frac{q}{2\pi k}\int_{r_1}^{r_2}\frac{dr}{r} \quad (9.31)$$

$$= -\frac{q}{2\pi k}[\ln r_2 - \ln r_1] \quad (9.32)$$

$$= -\frac{q}{2\pi k}\ln(r_2/r_1) \quad (9.33)$$

$$q = -\frac{2\pi k\,(T_2 - T_1)}{\ln(r_2/r_1)} \quad (9.34)$$

Thus with cylindrical geometry, the heat flux for a given temperature difference depends only on the ratio of the inner and outer radii.

9.4.3 Spherical geometry

Considering the elemental surface of thickness dr, the heat flux for the whole sphere is

$$Q = -\frac{4\pi kr^2(T_{r+dr} - T_r)}{dr} \quad (9.35)$$

$$dT = -\frac{Q}{4\pi kr^2}dr \quad (9.36)$$

This can be integrated to find the temperature difference

$$T_2 - T_1 = -\frac{Q}{4\pi k}\int_{r_1}^{r_2}\frac{dr}{r^2} \quad (9.37)$$

$$= \frac{Q}{4\pi k}[1/r_2 - 1/r_1] \quad (9.38)$$

$$= -\frac{Q(r_2 - r_1)}{4\pi kr_1r_2} \quad (9.39)$$

$$Q = -\frac{4\pi kr_1r_2\,(T_2 - T_1)}{r_2 - r_1} \quad (9.40)$$

Note that in the limit as the inner and outer radii are almost equal, equation 9.39 simplifies to give 9.36 as it should.

Note that for this geometry there is a limit as r_2 tends to infinity.

$$Q = -\frac{4\pi kr_1r_2\,(T_2 - T_1)}{r_2 - r_1}$$

$$Q_{lim,r_2\to\infty} = -4\pi kr_1\,(T_2 - T_1) \quad (9.41)$$

A practical implication of this limit is that for a finite object (r_1) with a limited power budget (Q), there is a maximum temperature difference ($T_1 - T_2$) which can be sustained no matter how much insulation is used.

9.4.4 Practical materials

Thermal conductivities as low as 0.005 W m^{-1} K^{-1} can be achieved using silica aerogel [16]. Table 9.3 gives values for other materials.

Material	Thermal conductivity W m^{-1} K^{-1}
aerogel	0.005
air	0.024
aluminium	201
copper	385
cork	0.05
diamond	900
glass wool	0.04

Table 9.3: Typical values of thermal conductivity (data mainly from [7]).

[17] discusses how properties such as thermal conductivity change with physical parameters such as temperature and (for a gas) density.

9.4.5 Microsensor Package

Consider a microsensor package with a core size of 1 cm diameter including a battery. The core must be kept warm enough for the battery to remain in good condition (minimum temperature -20°C = 253 K), and the sensor is to be used on Mars (daily temperature range 190–240 K).

Assume the battery capacity is 80 W hr kg^{-1} (rechargeable Li-ion technology) and the package is insulated using aerogel (0.005 W m^{-1} K^{-1}). Assume also the battery density is twice that of water, i.e. battery density is 2000 kg m^{-3} (to convert from specific to volumetric capacity).

If almost all of the package is taken up with battery, then the battery volume is 0.5 ml, and its mass is therefore 1 g. The battery capacity is thus 80 mW hr. If the Mars night is taken as 16 hr (this allows for periods around sunset / sunrise when Sun is low in the sky) then the heating power available through the night assuming 100% depth of discharge is 5 mW.

For the limiting case of infinite insulation, the maximum temperature difference which 5 mW can maintain for a 1 cm sphere is

$$\begin{aligned} \Delta T_\infty &= \frac{Q}{4\pi k r_1} \qquad (9.42) \\ &= \frac{0.005}{4\pi\, 0.005\, 0.005} = \frac{1}{0.02\pi} \\ &= 15.9 \text{ K} \end{aligned}$$

Since the average temperature difference is greater than this, no amount of (aerogel) insulation can keep the battery warm. A solution to this is to change the size of the battery unit (it must be larger, since the capacity increases with size faster than the rate of heat loss).

S.E. Hobbs, 10/1/05

Alphabetical List of References

ABACOM Technologies (2004a), *AM-TX1-4xx Transmitter Module datasheet,* available at: http://www.abacom-tech.com/catalog/amtx1.PDF (accessed 2004a).

ABACOM Technologies (2004b), *AT-MT1-xxx Miniature AM RF Transmitter Module datasheet,* available at: http://www.abacom-tech.com/catalog/ATMT1.PDF (accessed 2004b).

Above Board Electronics (1998a), *Audio Cable - Multiconductor Small Diameter Foil Shield - Overall,* available at: http://www.aboveboardelectronics.com/manhattan/catalog/audio5.htm (accessed 2004a).

Above Board Electronics (1998b), *Computer Cable - 150 Ohm Super Low Cap Multipair Foil Shield - Overall RS-422,* available at: http://www.aboveboardelectronics.com/manhattan/catalog/computer82a.htm (accessed 2004b).

Above Board Electronics (1998c), *Computer Cable - Multiconductor Foil and Braid Shield - Overall, RS-232, RS-423, 28 AWG,* available at: http://www.aboveboardelectronics.com/manhattan/catalog/computer72.htm (accessed 2004c).

Aerosonde (2000), *Aerosonde - Global Robotic Observation System,* available at: http://www.aerosonde.com/aircraft/ (accessed 2005).

Agre, J. and Clare, L. (2000), 'An Integrated Architecture for Cooperative Sensing', *Computer,* Vol. 33, No. 5, pp. 106-108.

Akyildiz, I., Su, W., Sankarasubramaniam, Y. and Cayirci, R. (2002), 'Wireless Sensor Networks: A Survey', *Computer Networks,* Vol. 38, No. 4, pp. 393-422.

Alcatel Space (2004), *Alcatel Space ,* available at: http://www.alcatel.com/space (accessed 2004).

Alenia (2004), *Alenia Spazio,* available at: http://www.alespazio.it/ (accessed 2004).

Alpha Wire (2004), *Communication & Control Plenum-Rated Multipair Shielded (Low-Cap, Mid-Cap) FEP PVC cable,* available at: http://www.alphawire.com/pages/238.cfm (accessed 2004).

ALS Technologies (2004), *WebShot Nonlethal Entanglement Technology System,* available at: http://www.ozarkmtns.com/less-lethal/distract.htm (accessed 2005).

Al-Sarawi, S. (1997), *3D VLSI Packaging Technology,* available at: http://www.eleceng.adelaide.edu.au/Personal/alsarawi/node1.html (accessed 2005).

Amkor Technologies (2002), *3D Packaging,* available at: http://www.amkor.com

(accessed 2004).

Amos, J. (2004), *UK aims to be major space player - BBC News online article,* available at: http://news.bbc.co.uk/1/hi/sci/tech/3706646.stm (accessed 2004).

Analog Devices (1998), *ADXL150 ±5g to ±50g, Low noise, low power single axis iMEMS Accelerometer datasheet,* available at: http://www.analog.com/UploadedFiles/Data_Sheets/573918736ADXL150_250_0.pdf (accessed 2004).

Analog Devices (2000), *Low Cost ±2g Dual Axis Accelerometer with Duty Cycle Output (ADXL202E) datasheet,* available at: http://www.analog.com/UploadedFiles/Data_Sheets/53728567227477ADXL202E_a.pdf (accessed 2004).

Antenna Factor (2004), *JJB Series Ultra-Compact Antenna,* available at: http://www.antennafactor.com/documents/ant-xxx-jjb_data_guide.pdf (accessed 2005).

Arnon, S. (2000), 'Collaborative Network of Wireless Micro-Sensors', *Electronics Letters,* Vol. 36, No. 2, pp. 186-187.

Aziz, A. (2004), *Introduction to CMOS VLSI Design: Lecture 6 - Interconnect,* available at: http://www.ece.utexas.edu/~adnan/vlsi-04/lec6Interconnect.ppt (accessed 2004).
Notes: From lecture notes of EE360R Computer-aided IC Design, Fall 2004, University of Texas

Bancroft, R. (2004), *Fundamental Dimension Limits of Antennas,* available at: http://www.centurion.com/home/pdf/wp_dimension_limits.pdf (accessed 2004).
Notes: A Centurion Wireless Technologies White Paper

Barthe, S., Pressecq, F., and Marchand, L. (2003), 'MEMS for Space Applications: a Reliability Study', *4th ESA Round Table on Micro/Nano Technologies for Space,* ESTEC, The Netherlands, ESA, pp. 263-275.

Belden Cable (2003), *9729 Paired - Low Capacitance Computer Cable for EIA RS-422 Applications,* available at: http://bwccat.belden.com/ecat/pdf/9729.pdf (accessed 2004).

Berkeley Lab (2004), *Silica Aerogels - Thermal Properties,* available at: http://eande.lbl.gov/ECS/aerogels/satcond.htm (accessed 2005).

Berk-Tek (2002), *Technical Support: Product Characteristics and Performance Attributes: Insulation and Jacket Compounds,* available at: http://www.berktek.com/technical/gen102.asp (accessed 2004).

Blue Radios (2004), *BR-L-C30 Class 2 Bluetooth V1.2 module datasheet,* available at: http://www.blueradios.com/BR-L-C30.pdf (accessed 2004).

Bluetooth SIG (2003), *The Official Bluetooth Membership Site,* available at: https://www.bluetooth.org/ (accessed 2004).

Boeing (2004), *Boeing,* available at: http://www.boeing.com (accessed 2004).

Bowling, S. and Fischer, R.L. (2000), *AN736 An I2C Network Protocol for Environmental Monitoring,* available at: http://ww1.microchip.com/downloads/en/AppNotes/00736a.pdf (accessed 2005).

Calibre uk (2000), *WINI2C Typical Screenshot,* available at: http://www.calibreuk.com/i2c2000/pcixxscrn.htm (accessed 2005).

Calibre UK (2003), *PCI93LV 3-Volt compatible I2C Communications adapter PCI card for PCs datasheet,* available at: http://www.calibreuk.com/i2c2000/pci93.htm (accessed 2005).

Cass, S. (2001), 'MEMS in Space', *IEEE Spectrum,* Vol. 38, No. 7, pp. 56-61.

Davies, P.N. and Koza, M.P. (2001), 'Eating soup with a fork: How informal social networks influence innovation in high-technology firms', *Strategic Change,* Vol. 10, pp. 95-102.

Delcowire (2004), *Delcowire Low Capacitance Data,* available at: http://www.delcowire.com/pdf/29.pdf (accessed 2004).

Delin (2002), 'The Sensor Web: A Macro-Instrument for Coordinated Sensing', *Sensors,* Vol. 2, pp. 270-285.

Delin, K. (2005), 'Sensor Webs in the Wild', in Bulusu, N. and Jha, S. *Wireless Sensor Networks: A Systems Perspective*, Artech House, Norwood, MA, pp. 17-1 - 17-12.

Delin, K. and Jackson, S. (2001), 'The Sensor Web: A New Instrument Concept', *Proceedings of SPIE,* Vol. 4284, No. 1, pp. 1-9.

Delin, K., Harvey, R., Chabot, N., Jackson, S., Adams, M., Johnson, D., and Britton, J. (2003), 'Sensor Webs in Antarctica: Developing an Intelligent, Autonomous Platform for Locating Biological Flourishes in Cryogenic Environments', *34th Lunar and Planetary Science Conference,* pp. No. 1929.

Delin, K.A. and Jackson, S.P. (2000), 'Sensor Web for In Situ Exploration of Gaseous Biosignatures', *IEEE Aerospace Conference Proceedings,* Vol. 7, Big Sky, Montana, IEEE, pp. 465-472.

Dept of Trade and Industry (2004), *Micro and Nanotechnology Manufacturing Initiative - MNT Directory,* available at: http://www.mnt-directory.org (accessed 2005).

Dhillon, S., Chakrabarty, K., and Iyengar, S. (2002), 'Sensor Placement For Grid

Coverage Under Imprecise Detections', *International Conference of Information Fusion (FUSION),* Vol. 3, Annapolis, IEEE, pp. 1581-1587.

Digital Photography Review (2005), *Digital Camera Reviews,* available at: http://www.dpreview.com (accessed 2005).

Draka USA (2004), *24 AWG Unshielded Twisted Pair,* available at: http://www.drakausa.com/productDetail.aspx?productID=486&ID=8 (accessed 2004).
Notes: For Product Number EV24P0021124

Dyrbye, K., Romedahl Brown, T. and Friis Eriksen, G. (1996), 'Packaging of physical sensors for aggressive media applications', *Journal of Micromechanics and Microengineering,* Vol. 7, pp. 187-192.

EADS (2004), *European Aeronautic Defence and Space Company - Corporate Website,* available at: http://www.eads.net (accessed 2004).

EADS Astrium (2004), *EADS Astrium: Building for Space - Corporate Website,* available at: http://www.astrium.eads.net (accessed 2004).

Eckersley, S., Schalk, J., and Koppenhagen, K. (2005), 'The EADS Micropack Project: An Intelligent Microsystem Demonstrator for Small Mission Applications ', *The 4S Symposium: Small Satellite, Systems and Services,* La Rochelle, France, ESA, pp. N/A.

Electronic Design Europe (2004), 'Radiation Retreat', *Electronic Design Europe,* pp. 12-16.

Electronic Times (2001), *Intel Unveils World's Smallest Transistor,* available at: http://www.edtn.com/story/OEG20010611S0023 (accessed 2003).

Engineers Edge (2000), *Spring Constant K Calculator and Formula,* available at: http://www.engineersedge.com/spring_tension_calc_k.htm (accessed 2004).

Feng, J., Koushanfer, F. and Potkonjak, M. (2005), 'Sensor Network Architecture', in Ilyas, M. and Mahgoub, I. *Handbook of Sensor Networks: Compact Wireless and Wired Sensing Systems*, CRC Press, Boca Raton.

Feynman, R.P. (2001), *The Pleasure of Finding Things Out: The Best Short Works of Richard Feynman*, Penguin, London.

Fleming, M.C. and Nellis, J.G. (2000), *Principles of Applied Statistics* (2nd edition), Thomson, Salisbury, UK.

Foll, H. (2001), *Semiconductor Course Notes - 3.3.2 Scaling Laws,* available at: http://www.tf.uni-kiel.de/matwis/amat/semi_en/kap_3/backbone/r3_3_2.html (accessed 2004).
Notes: Given as lecture course notes from the Faculty of Engineering, University of Kiel, Germany

Frank, M.P. (2002), 'The Physical Limits of Computing', *Computing in Science and Engineering,* Vol. 4, No. 3, pp. 16-26.

Gad-el-Hak, M. (2002), *The MEMS Handbook*, CRC Press, Boca Raton, FL.

Gann, K. (1999), 'Neo-Stacking Technology', *High Density Interconnects Magazine,* Vol. December, pp. 1-4.

Gaskell, R.W., Collier, J.B., Husman, L.E., and Chen, R.L. (2001), 'Synthetic Environments for Simulated Missions', *IEEE Aerospace Conference,* Vol. 7, Big Sky, Montana, pp. 3556-3564.

Gavrilakis, A., Duffy, A.P., Hodge, K.G. and Willis, A.J. (2004), 'Partial Capacitance Calculation for Shielded Twisted Pair Cables', *IEEE Transactions on Electromagnetic Compatibility,* Vol. 46, No. 2, pp. 299-302.

GE Novasensor (2003), *NPP-301 Pressure Sensor Datasheet,* available at: http://www.gesensing.com/products/resources/datasheets/NPP_301_4_03.pdf (accessed 2004).

Goetz, R. (1997), 'Market Assessment for Space-Qualified MEMS', in Helvajian (Ed.), *Microengineering Technology for Space Systems*, The Aerospace Press, Los Angeles, CA, pp. 5-18.

Goldstein, H. (2001), 'Packages Go Vertical', *IEEE Spectrum,* Vol. 38, No. 8, pp. 46-51.

Golombek, M., Cook, R., Economou, T., Folkner, W., Haldemann, A.F.C., Kallemeyn, P., Knudsen, J., Manning, R., Moore, H., Parker, T., Rieder, R., Schofield, J., Smith, P. and Vaughan, R. (1997), 'Overview of the Mars Pathfinder Mission and Assessment of Landing Site Predictions', *Science,* Vol. 278, pp. 1743-1748.

Goodall, K. (1998), *Mars Pathfinder Image Archive,* available at: http://mars3.jpl.nasa.gov/MPF/mpf/image-arc.html (accessed 2004).

Greguras, F. (1998), *Systems-on-a-chip: Intellectual Property and Licensing Issues*, available at: http://www.bc.edu/bc_org/avp/law/iptf/articles/content/1998012002.html (accessed 2005).
Notes: This is from Boston College Law School's IP and Technology forum.

Hac, A. (2003), *Wireless Sensor Network Designs*, Wiley, Chicester.

Haenggi, M. (2005), 'Opportunities and Challenges in Wireless Sensor Networks', in Ilyas, M. and Mahgoub, I. *Handbook of Sensor Networks: Compact Wireless and Wired Sensing Systems*, CRC Press, Boca Raton.

Hansen, G.A. (2004), *The Weather in Adventdalen,* available at: http://haldde.unis.no/vaerdata/past_data/ (accessed 2004).

Hanson R.C. (1981), ‘Fundamental Limits in Antennas’, *Proceedings of the IEEE,* Vol. 69, No. 8, pp. 170-182.

Hauber, E., Jaumann, R., Mosangini, C., Russ, N., Trauthan, F., Matz, K.-D., and Fabel, O. (1998), 'Rocks at the Pathfinder Landing Site, Mars: Identification and Size Distribution', *29th Lunar and Planetary Science Conference,* Houston, TX, Abstract No. 1607.
Notes: Available at http://mars.jpl.nasa.gov/MPF/Science/lpsc98/1607.pdf

Helvajian, H. (Editor) (1999), *Microengineering Aerospace Systems*, Aerospace Press, El Segundo, California.

Hill, J., Szewczyk, R., Woo, A., Hollar, S., Culler, D. and Pister, K. (2000), 'System Architecture Directions for Networked Sensors', *ACM Sigplan Notices,* Vol. 35, No. 11, pp. 93-104.

Hobbs, S.E. (2005), *Technical Note 9.4 Thermal Conduction* , Unpublished.
Notes: This note is available in Appendix X

Honeywell (2002), *40PC Series Miniature Signal Conditioned Pressure Sensor datasheet,* available at: http://content.honeywell.com/sensing/prodinfo/pressure/catalog/c15_31.pdf (accessed 2005).

Hong, X., Gerla, M., Wang, H. and Clare, L. (2002), 'Load Balanced Energy-Aware Communications for Mars Sensor Networks', *Proceedings of IEEE Aerospace Conference,* Vol. 3, pp. 1109-1115.

Hoover, R.B. and Pikuta, E.V. (2004), 'Microorganisms on Comets, Europa and the Polar Ice Caps of Mars', *Proceedings of SPIE,* Vol. 5163, pp. 191-201.

Horneck, G. (2000), 'The Microbial World and the Case for Mars', *Planetary and Space Science,* Vol. 48, pp. 1053-1063.

IFW (2002), *UV - Photodetector with Integrated Amplifier (JIC 117/118/119) datasheet,* available at: http://www.eoc-inc.com/ifw/JIC_117_118_119.pdf (accessed 2004).

Jenkins, M. (2001), *Strategic Assets, Exploring the sources of success*, Unpublished.
Notes: Lecture notes from Cranfield School of Management Executive MBA "Strategic Management (SM)" course, taken by Author 2001

JPL (1996), *Sojourner Rover Homepage,* available at: http://mpfwww.jpl.nasa.gov/rover/sojourner.html (accessed 2004).

Kelly, G., Alderman, J., Lyden, C. and Barrett, J. (1997), 'Microsystem Packaging: lessons from coventional low cost IC packaging', *Journal of Micromechanics and Microengineering,* Vol. 7, pp. 99-103.

Kenny, T. (2002), *ME 117/220 Lecture #7: Pressure Sensors,* available at:

http://design.stanford.edu/Courses/me220/lectures/lect07/lect_7.html#lecture_7 (accessed 2004).
Notes: Taken from the lecture notes of course ME 117/220 Introduction to Sensors at Stanford University

Keyes, R.W. (2001), 'Fundamental Limits of Silicon Technology', *Proceedings of the IEEE,* Vol. 89, No. 3, pp. 227-239.

Kratz, H. and Stenmark, L. (2003), 'Communications Microsystems for Spacecraft - Current Research and Future Systems', *4th ESA Round Table on Micro/Nano Technologies for Space,* ESTEC, The Netherlands, ESA, pp. 209-220.

Labfacility Ltd (2004), *Pt100 thin film Platinum resistance temoerature detectors datasheet,* available at: http://rswww.com (accessed 2004).

Landis, G.A. and Jenkins, P.P. (1997), 'Dust on Mars: Material Adherence Experiment Results from Mars Pathfinder', *26th IEEE Photovoltaic Specialists Conference ,* Anaheim, CA, IEEE, pp. 865-869.

Lecuyot, A., Snelling, M., and Tual, J.-C. (2003), 'Microsystem Modules - a Roadmap of Space MST Integration Technologies', *4th ESA Round Table on Micro/Nano Technologies for Space,* ESTEC, The Netherlands, ESA, pp. 332-347.

Lin, Q. (2001), *24-351 Dynamics Course Project: Design of a Micro Accelerometer,* available at: http://www.andrew.cmu.edu/course/24-351/project/project.doc (accessed 2004).
Notes: Course notes from Junior Dynamics course in the Mechanical Engineering Dept of Carnegie Mellon University

Linx Technologies (2003), *ES Transmitter Module Design Guide,* available at: http://www.linxtechnologies.com/images/products_cat/rf_modules/es_series/es-txm_manual.pdf (accessed 2005).

Linx Technologies (2004), *LR Series Transmitter Module Data Guide,* available at: http://www.linxtechnologies.com/images/products_cat/rf_modules/lr_series/lr_txm_manual.pdf (accessed 2004).

Lockheed Martin (2004), *Lockheed Martin,* available at: http://www.lockheedmartin.com (accessed 2004).

Magan, J. (1996), *Esprit - TCS: Report on the TCS Microsystems Workshop,* available at: http://www.cordis.lu/esprit/src/tcsmsrpt.htm (accessed 2004).

Marion, J. and Thornton, S. (1995), *Classical Dynamics of Particles and Systems* (4 edition), Harcourt Brace, Orlando, FL.

Mason, A., Yazdi, N., Chavan, A., Najafi, K. and Wise, K. (1998), 'A Generic Multielement Microsystem for Portable Wireless Applications', *Proceedings of the IEEE,* Vol. 86, No. 8, pp. 1733-1746.

McHaney, R. (1991), *Computer Simulation: A Practical Perspective,* Academic Press, San Diego, CA.

McLean. J.S. (1996), 'An Re-examination of the Fundamental Limits on the Radiation Q of Electrically Small Antennas', *IEEE Transactions on Antennas and Propagation*, Vol. 44, No. 5, pp 672-676.

Meindl, J. (1995), 'Low Power Microelectronics: Retrospect and Prospect', *Proceedings of the IEEE,* Vol. 83, No. 4, pp. 619-635.

Messenger, R. and Ventre, J. (2000), *Photovoltaic Systems Engineering*, CRC Press, Boca Raton.

Michalicek, M.A. (2000), *Worldwide MEMS Growth,* available at: http://mems.colorado.edu/c1.res.ppt/ppt/g.tutorial/slide012.htm (accessed 2004).

Microchip (2000), *Microchip Technologies Home Page,* available at: http://www.microchip.com (accessed 2005).

Microchip (2004), *PIC10F200/202/204/206 Datasheet,* available at: http://ww1.microchip.com/downloads/en/DeviceDoc/41239A.pdf (accessed 2004).

Microchip Inc (2003), *PIC16F87xA Datasheet - 28/40/44-pin Enhanced Flash Microcontroller,* available at: http://ww1.microchip.com/downloads/en/DeviceDoc/39582b.pdf (accessed 2004).

Microchip Inc (2003a), *512K I2C CMOS Serial EEPROM Datasheet,* available at: http://ww1.microchip.com/downloads/en/DeviceDoc/21673c.pdf (accessed 2005a).

Microchip Inc (2003b), *PIC16F87xA Datasheet - 28/40/44-pin Enhanced Flash Microcontroller,* available at: http://ww1.microchip.com/downloads/en/DeviceDoc/39582b.pdf (accessed 2004b).

Min, R., Bhardwaj, M., Cho, S.-H., Sinha, A., Shih, E., Wang, A. and Chandrakasan, A. (2000), 'An Architecture for a Power-Aware Distributed Microsensor Node', *IEEE Workshop on Signal Processing Systems, SiPS: Design and Implementation,* pp. 581-590.

Min, R., Bhardwaj, M., Cho, S.-H., Sinha, A., Shih, E., Wang, A. and Chandrakasan, A. (2001), 'Low-Power Wireless Sensor Networks', *Proceedings of the IEEE International Conference on VLSI Design,* pp. 205-210.

Moini, A. (1997), *Quantum Efficiency of a Vertical Junction Diode,* available at: http://www.iee.et.tu-dresden.de/iee/eb/analog/papers/mirror/visionchips/vision_chips/analysis_photodiode.html (accessed 2004).

Moore, B. (1998), 'IC Temperature sensors find the hot spots', *EDN,* Vol. July 2 1998, pp. 99-110.
Notes: Also available as Application Note 689 from www.maxim-ic.com

Morris, J. (2004), *Multiple Mars UAV Proposals Likely in Next Scout Competition - Aerospace Daily and Defense Report,* available at: http://www.aviationnow.com/avnow/news/channel_aerospacedaily_story.jsp?id=news/MATADOR11174.xml (accessed 2005).

Muraca, R.J., Campbell, J.W., and Anderson King, C. (1975), *A Monte Carlo analysis of the Viking Lander dynamics at touchdown*, Report no. NASA TN D-7959, NASA, Washington, DC.

Myers, S. and Marquis, D.G. (1969), *Successful Industrial Innovations: A study of factors underlying innovation in selected firms*, National Science Foundation, Washington DC.
Notes: Quote used in lecture notes from Cranfield University "Technology Change and Environmental Assessment" course, taken by Author 2002

Nagel, D. (2002), 'Microsensor Cluster', *Microelectronics Journal,* Vol. 33, No. 1-2, pp. 107-119.

National Semiconductor (2001), *LP324 / LP2902 Micropower Quad Operational Amplifier datasheet,* available at: http://cache.national.com/ds/LP/LP2902.pdf (accessed 2004).

National Semiconductors (2002), *LM20 CI MDC MWC 2.4V 10µA Temperature Sensor Die Datasheet,* available at: http://www2.national.com/appinfo/die/die_dsheet.cgi/files/LM20CIMDCMWC.pdf

Newman, P. (1999), *SAGE III Ozone Loss and Validation Experiment (SOLVE) Home Page,* available at: http://cloud1.arc.nasa.gov/solve/ (accessed 2004).

Nicolau, D.E., Phillimore, J., Cross, R. and Nicolau, D.V. (2000), ' Nanotechology at the crossroads: The hard way or the soft way? ', *Microelectronics Journal,* Vol. 31, pp. 611-616.

Nighswonger, G. (1999), *Implantable Chips and Advanced Materials Stimulate Research Efforts to Restore Sight ,* available at: http://www.devicelink.com/mddi/archive/99/07/003.html (accessed 2004).

NSIDC (2004), *Arctic Climatology and Meteorology Primer ,* available at: http://nsidc.org/arcticmet/ (accessed 2004).

Open University (2002), *Beagle 2:System overview,* available at: http://www.beagle2.com/technology/overview.htm (accessed 2004).

Optobionics (2004), *ASR Device,* available at: http://www.optobionics.com/index.asp?pageid=13 (accessed 2004).

ORNL (2001), *Thin-Film Battery Applications,* available at: http://www.ssd.ornl.gov/Programs/BatteryWeb/Applications.html (accessed 2004).

Panasonic (2005), *Coin Type Lithium Batteries - MnO2.LI:Manganese Dioxide (CR type),* available at: http://www.panasonic.com/industrial/battery/oem/chem/lith/coin1.htm (accessed 2005).

Papavassiliou, S. and Zhu, J. (2005), 'Architecture and Modeling of Dynamic Wireless Sensor Networks', in Ilyas, M. and Mahgoub, I. *Handbook of Sensor Networks: Compact Wireless and Wired Sensing Systems*, CRC Press, Boca Raton,

Personick, S.D. (1981), 'Fundamental Limits in Optical Communication', *Proceedings of the IEEE,* Vol. 69, No. 2, pp. 262-266.

Phazar Wireless Antennas (2004), *2 dBi AMR Omni 916-957 MHz Antenna ,* available at: http://www.phazar.com/AMRunityomni.htm (accessed 2005).

Philips (2004), *About the I2C bus,* available at: http://www.semiconductors.philips.com/markets/mms/protocols/i2c/facts/index.html (accessed 2005).

Philips Semiconductors (2000), *The I2C bus Specification - version 2.1,* available at: http://www.semiconductors.philips.com/acrobat_download/literature/9398/39340011.pdf (accessed 2005).

Polastre, J., Szewczyk, R., Mainwaring, A., Culler, D. and Anderson, J. (2004), 'Analysis of Wireless Sensor Networks for Habitat Monitoring', in Raghavendra, C., Sivalingam, K., and Znati, T. *Wireless Sensor Networks*, Kluwer, Boston.

Porter, M.E. (1979), ' How Competitive Forces Shape Strategy', *Harvard Business Review,* Vol. 57, No. 2, pp. 137-145.

Porter, M.E. (1985), *Competitive Advantage: Creating and sustaining superior performance*, Free Press, New York.

Pottie, G. (1998), 'Wireless Sensor Networks', *Proceedings of IEEE ITW 1998,* pp. 139-140.

Putzig, T. (2003), *Mars Albedo Map,* available at: http://lasp.colorado.edu/~than/research/lpsc2003/talk/albedo.html (accessed 2004).

Qi, H., Iyengar, S. and Chakrabarty, K. (2001), 'Distributed Sensor Networks - A Review of Recent Research', *Journal of The Franklin Institute,* Vol. 338, No. 6, pp. 655-668.

Quabbin Wire & Cable (1999), *Technology Briefs: Why is Cable Capacitance Important for Electronic Applications,* available at:

http://www.quabbin.com/tech_briefs/tech5.html (accessed 2004).

Quabbin Wire & Cable Co. (1999), *Quabbin Cable Finder,* available at: http://www.quabbin.com/finder/index.html (accessed 2004).
Notes: General Cable Finder - Enter Product Number for specific datasheet

Quirke, C. (2003), *Data Handling Prototype for Small Spacecraft - MSc thesis* Cranfield University, UK.

RF Cafe (2004), *Antenna Patterns,* available at: http://www.rfcafe.com/references/electrical/antenna_patterns.htm (accessed 2005).

RF Microdevices (2004), *SiW3000 UltimateBlue SOC datasheet,* available at: http://www.rfmd.com/DataBooks/db97/SiW3000.pdf (accessed 2004).

Rickard, S. (2000), *The Firm's Vertical Boundaries*, Unpublished.
Notes: Lecture notes from Cranfield School of Management Executive MBA "The Economics of Organisations and Strategy (EOS)" course, taken by Author 2001

Roy, S., Gresham, E. and Bryce Christensen, C. (2000), 'The Complex Fabric of Public Opinion on Space', *Acta Astronautica,* Vol. 47, No. 2-9, pp. 665-675.

RS (1997), *NSL19-M51 Light Dependant Resistors datasheet,* available at: http://rswww.com (accessed 2005).

Sander, K.F. and Reed, G.A.L. (1978), *Transmission and propagation of electromagnetic waves*, Cambridge University Press, Cambridge.

Säwström, C., Mumford, P., Marshall, W., Hodson, A. and Laybourn-Parry, J. (2002), 'The Microbial Communities and Primary Productivity of Cryoconite Holes in an Arctic Glacier (Svalbard 79°N)', *Polar Biology,* Vol. 25, pp. 591-596.

Schmitt, P., Esteve, D., Fourniols, J.-Y., Lafontan, X., Pons, P., Nicot, J.-M., Pressecq, F., and Oudea, C. (2003), 'MEMS Behavioral Simulation: A Potential Use for Physics of Failure (PoF) Modeling', *4th ESA Round Table on Micro/Nano Technologies for Space,* ESTEC, The Netherlands, ESA, pp. 258-262.

Shackleford, J.F. and Alexander, W. (Editor) (2001), *CRC Materials Science and Engineering Handbook* (3 edition), CRC Press, Boca Raton, Florida.

Siero, J., Morrissey, A., Carmona, M., Marco, S., Samitier, J., and Alderman, J.'Thermal Behaviour of V-MCM Package Containing a Thermo-Pneumatic Micropump, Sensors and Integrated Electronics', *1st International Conference on Modeling and Simulation of Microsystems, Semiconductors, Sensors and Actuators,* Santa Clara, CA, pp. 168-173.

Smith, D.W. (2002), *PIC in Practice*, Newnes, Amsterdam.

SRA International (2005), *UAV Forum Vehicle Overview,* available at: http://www.uavforum.com/vehicles/overview.htm (accessed 2005).

SSTL (2000), *Snap Nanosatellite,* available at: http://zenit.sstl.co.uk/index.php?loc=47 (accessed 2004).

Stenmark, L. and Bruhn, F. (2003), 'A European Multifunctional Micro System Programme for Space ', *4th ESA Round Table on Micro/Nano Technologies for Space,* ESTEC, The Netherlands, ESA, pp. 410-414.

Streetman, B.G. (1980), *Solid State Electronic Devices* (2 edition), Prentice-Hall, Englewood Cliffs, NJ.

Su, W., Akan, O. and Cayirci, E. (2004), 'Communication Protocols for Sensor Networks', in Raghavendra, C., Sivalingam, K., and Znati, T. *Wireless Sensor Networks*, Kluwer, Boston,

Sun, A. (1997), *Antony's VBA page - Standard Deviation and Mean,* available at: http://www.anthony-vba.kefra.com/vba/vba1.htm (accessed 2004).

Tadiran Batteries (2003a), *Lithium Batteries - Model TL-4935 datasheet,* available at: http://www.tadiranbat.com/prodpdf/viewpdf.php?datasheet=TL-4935.pdf (accessed 2004a).

Tadiran Batteries (2003b), *Product Specs: Standard Lithium Cells. XOL Series - Wafer Cells,* available at: http://www.tadiranbat.com/tl49xxxolw.php (accessed 2004b).

Takeuchi, N. (2004), *Cryoconite Hole Information,* available at: http://www.chikyu.ac.jp/takeuchi/cryoconite.html (accessed 2004).

Tensolite (2004), *NETFLIGHT Lightweight Aerospace Grade Copper Fibre Channel Cables,* available at: http://www.tensolite.com/product_documents/netflightFCLW.pdf (accessed 2004).

The Space Foundation (2004), *Space Certification Program,* available at: http://www.spaceconnection.org/spacefoundation.cfm (accessed 2005).

Tilak, S., Abu-Ghazaleh, N., and Heinzelman, W. (2002), 'Infrastructure Trade-Offs for Sensor Networks', *WSNA'02,* Atlanta, GA, ACM, pp. 49-58.

Tillar Shugg, W. (1995), *Handbook of Electrical and Electronic Insulating Materials* (2 edition), IEEE Press, Piscataway, NJ.

Townsend, J., Palmintier, B., and Allison, E. (2000), 'Effects fo a Distributed Computing Architecture on the Emerald Nanosatellite Development Process', *14th Annual Small Satellites Conferece,* Vol. 14, Utah, AIAA, pp. 7-7.

Tranter, M., Fountain, A., Fritsen, C., Lyons, W.B., Priscu, J., Statham, P. and Welch,

K. (2004), 'Extreme Hydrochemical Conditions in Natural Microcosms Entombed within Antarctic Ice', *Hydrological Processes,* Vol. 18, pp. 379-387.

UDT Sensors (2004), *Plastic Encapsulated Series - Lead Frame Molded Photodiodes,* available at: http://www.udt.com/Datasheets/Products/PlasticEncapsulated.pdf (accessed 2004).

UK AMSTAP (1999), *The Role of Micro System Technology for Space in the UK*, Report no. TP 1421, UK AMSTAP, UK.

Ulvensoen, J.H. (1998), 'Challenges in MEMS Packaging', *Micro Structure Bulletin,* Vol. 4, pp. 3.

Univ. of Arizona and NASA (2005), *Phoenix Mars Lander,* available at: http://phoenix.lpl.arizona.edu (accessed 2005).

US department of State (1992), *International Traffic in Arms Regulations*, available at: http://www.epic.org/crypto/export_controls/itar.html (accessed 2005)
Notes: this website contains excerpts from the Federal Regulations

Val, C. (2003), '3-D Innovating Packaging MEMS Applications', *4th ESA Round Table on Micro/Nano Technologies for Space,* ESTEC, The Netherlands, ESA, pp. 325-331.

Valdez, A., Hu, C., Kitts, C., Breiling, M., Slaughterbeck, A., Ota, J., Hadi, D., Kuhlman, T., and Lyons, S. (1999), 'The Artemis Project: Picosatellites and the feasibility of the smaller, faster, cheaper approach', *IEEE Aerospace Conference,* Vol. 2, Snowmass, CO, IEEE, pp. 235-243.

Valtronic (2000), *3D-CSP: Flip Chip on flexible circuit,* available at: http://www.valtronic.ch/skills/3dcsp.html (accessed 2005).

Verity, J. (1999), 'Tools for understanding strategic environments', *Management Quarterly,* No. Part 5, pp. 1-8.
Notes: This article includes the traditional PEST analysis - a PESTLE analysis is a later version of this technique

Viotti, M. (2004), *Mars Exploration Rover Mission,* available at: http://marsrovers.jpl.nasa.gov/home/index.html (accessed 2005).

Wang, Q., Hassanein, H. and Xu, K. (2005), 'A Practical Perspective on Wireless Sensor Networks', in Ilyas, M. and Mahgoub, I. *Handbook of Sensor Networks: Compact Wireless and Wired Sensing Systems*, CRC Press, Boca Raton.

Warneke, B. (2005), 'Miniaturising Sensor Networks with MEMS', in Ilyas, M. and Mahgoub, I. *Handbook of Sensor Networks: Compact Wireless and Wired Sensing Systems*, CRC Press, Boca Raton.

Warneke, B., Scott, M., Liebowitz, B., Zhou, L., Bellew, C., Chediak, J., Kahn, J., Boser, B. , and Pister, K.'An Autonomous 16 mm3 Solar-Powered Node for

Distributed Wireless Sensor Networks', *IEEE Sensors 2002,* Orlando, FL, pp. 1510-1515.

Waser, R. (Editor) (2003), *Nanotechnology and Information Technology - Advanced Electronic Materials and Novel Devices*, Wiley-VCH, Weinheim.

Webster, J.G. (1999), *The Measurement, Instrumentation and Sensors Handbook*, CRC Press, Boca Raton, FL.

Wertz, J.R. and Larson, W.J. (Editor) (1999), *Space Mission Analysis and Design* (3 edition), Microcosm Press and Kluwer, El Segundo, California.

West, W., Whitacre, J., White, V. and Ratnakumar, B. (2002), 'Fabrication and testing of all solid-state microscale lithium batteries for microspacecraft applications', *Journal of Micromechanics and Microengineering,* Vol. 12, pp. 58-62.

Wharton, R., McKay, C., Simmons, G. and Parker, B. (1985), 'Cryoconite Holes on Glaciers', *Bioscience,* Vol. 35, pp. 499-503.

Williams, D. (2001), *Mars Pathfinder Preliminary Results,* available at: http://nssdc.gsfc.nasa.gov/planetary/marspath_results.html (accessed 2004).

Williams, D. (2004), *Mars Fact Sheet,* available at: http://nssdc.gsfc.nasa.gov/planetary/factsheet/marsfact.html (accessed 2004).

Yarvis, M. and Ye, W. (2005), 'Tiered Architectures in Sensor Networks', in Ilyas, M. and Mahgoub, I. *Handbook of Sensor Networks: Compact Wireless and Wired Sensing Systems*, CRC Press, Boca Raton.

Young, H.D. (1992), *University Physics* (8 edition), Addison-Wesley, Reading, MA.

Zhirnov, V., Cavin, R., Hutchby, J. and Bourianoff, G. (2003), 'Limits to Binary Logic Switch Scaling - A Gedanken Model', *Proceedings of the IEEE,* Vol. 91, No. 11, pp. 1934-1939.